School of Pharmacy

Cytokines in alphavirus induced arthritis as possible targets for novel treatments

Wolfgang Wimmer

This thesis is presented for the Degree of

Doctor of Philosophy

of

Curtin University

June 2015

Declaration

To the best of my knowledge and belief this thesis contains no material previously published by any other person except where due acknowledgment has been made.

This thesis contains no material which has been accepted for the award of any other degree or diploma in any university.

Signature: …….

Date: ……..

Acknowledgements

I would like to thank my supervisors for their contribution to this thesis: Prof Dr Crispin Dass for the assistance and guidance in the course of my PhD and for always providing support when needed. I am especially grateful for accepting me as a student in the late stages of my project. Thank you also to Dr Andrew McWilliam for the encouragement to work independently throughout the project.

Further I would like to thank Dr David Williams and his wife Dr Sinead Diviney for their supervisory role during the first year of my PhD. You have taught me more than just the basic techniques in virology and you both have been an inspiration and motivation for me.

I would like to express my gratitude to all the staff at Curtin University that have helped me along the way, especially Dr Simon Fox for training me in various PCR techniques and for always giving an honest opinion.

Many thanks also to Irma Cornwall, for taking the time to give me a hand with the flow cytometry analysis. Your support is greatly appreciated.

Thank you to all my lab colleagues who have joined me along the way during these last years. A special thank goes out to Martha Mungkaje, for the collaboration and encouragement in the lab; to Dave Chandler, for taking me on a short excursion into protein chemistry and always bringing great coffee; and up and foremost to Alex Richards, who has been a companion from the start of this long journey. I will greatly miss our lab discussions about oldtimers and dogs. Alex, your kindness and support will never be forgotten and I wish you all the best in your future endeavours.

My gratitude also goes to Evi Buerkle, who, together with my mother, unknowingly motivated me numerous times and kept me focused to finish what I started.

I would finally like to thank my family, my brothers and especially my mother and my father, for always supporting me, even when the journey brought me to the other side of the world. You have encouraged me to pursue my dreams and never lost faith in me. Because of you I am the person I am today.

Lastly I would like to thank my beloved wife Diana. No matter how hard it was you have always supported me during this long project. You have encouraged me, motivated me and you have always been there when in needed you. It is to you I dedicate this thesis.

Abstract

Infections with alphaviruses such as RRV or CHIKV often induce severe myalgia and arthritic joint conditions in affected patients. Currently, treatment of these infections is only symptomatic with NSAIDs and analgesic drugs that often cause side effects on long term use.

Macrophages and macrophage derived cytokines are thought to be major contributors to the inflammatory conditions during RRV infection and this study investigated the involvement of various cytokines, such as TNFα, MIF and NO. We could further establish a role of IL-6, IL-18, IL-33 and IL-10 and we were able to exclude the involvement of PGE_2 in the pathogenesis of RRVD. With this extended knowledge several inhibitors of cytokine production were tested for their ability to inhibit transcription or release of pro-inflammatory cytokines. These inhibitors included erythromycin, clarithromycin, roxithromycin, ethyl pyruvate, pentoxifylline and resveratrol. Varying inhibitory effects on cytokine production were detected for all tested compounds during RRV infection with erythromycin and ethyl pyruvate showing strongest inhibition on most pro-inflammatory cytokines.

The second part of the thesis highlights a possible role of muscle cells during alphavirus infections. We could show that RRV is able to undergo a cytolytic replication cycle in muscle cells, which likely contributes to the initial viraemia in the acute phase of the infection. We further investigated the role of muscle cell derived myokines as contributors to RRVD pathogenesis and we could show increased transcription or release of the inflammatory cytokines TNFα, IL-6, MIF, IL-18 and IL-33. The cytokine inhibitors from previous experiments were trialled on RRV-infected myoblast cells and we were able to show a small inhibitory effect on IL-6 for macrolides but not ethyl pyruvate or resveratrol.

The last set of experiments briefly investigated the role of adipocytes in RRV infection. We could show that unlike most cells RRV can infect adipocytes without causing immediate cytolysis. Furthermore we found the cytokines IL-6, IL-33 and MCP-1 to be increasingly expressed or released. No change in transcription or secretion of TNFα, NO, MIF or IL-18 was detected, whereas expression of HMGB3 mRNA was found to be down-regulated in RRV infected adipocytes.

In summary, these results add more knowledge to the understanding of the pathogenesis of RRV infections and possibly infections with other alphaviruses.

Several compounds have been tested and found to inhibit pro-inflammatory cytokine production at varying levels, with erythromycin and ethyl pyruvate showing the strongest effects, suggesting their use in clinical trials or animal models of alphavirus infections.

Abbreviations

%CV	coefficient variation in %
µg	micro gram
µL	micro litre
µM	micro molar
ADE	antibody-dependent enhancement
ANOVA	analysis of variance
ATCC	American Type Culture Collection
BFV	Barmah Forest virus
bp	base pair
BSA	bovine serum albumin
cDNA	copied deoxyribonucleic acid
CHIKV	Chikungunya virus
CHIKVD	Chikungunya virus disease
CIA	collagen induced arthritis
CLA	clarithromycin
CO_2	carbon dioxide
CPE	cytopathic effect
d	day/s
DMEM	Dulbecco's Modified Eagle Medium
DMSO	dimethyl sulphoxide
DNA	deoxyribonucleic acid
E.coli	*Escherichia coli*
EDTA	ethylenediaminetetraacetic acid
ELISA	enzyme linked immunosorbent assay
EP	ethyl pyruvate
EPA	epidemic polyarthritis
ERY	erythromycin
EtOH	ethanol
FBS	foetal bovine serum
FITC	fluorescein isothiocyanate
G3PDH	glyceraldehyde-3-phosphate dehydrogenase
HI-RRV	heat inactivated Ross River virus

HMGB	high mobility groub box
hr	hour/s
HRP	horseradish-peroxidase
IBMX	isobutylmethylxanthine
IFN	Interferon
IL	Interleukin
iNOS	inducible Nitric oxide sythase
KE	kino extract
LDH	lactate-dehydrogenase
LPS	lipopolysaccharide
MCP-1	monocyte chemoattractant protein-1
mg	milligram
$MgCl_2$	magnesium chloride
MH broth	Mueller-Hinton broth
MIF	macrophage migration inhibitory factor
min	minute/s
mL	millilitre
mM	millimolar
MOI	multiplicity of infection
mRNA	messenger RNA
MTT	3-(4,5-dimethylthiazol-2-yl)-2,5-diphenyl tetrazolium bromide
MyD88	myeloid differentiation primary response gene 88
NCBI	National Centre for Biotechnology Information
NF-KB	nuclear factor kappa-B
ng	nanogram
NO	nitric oxide
NO_2^-	nitrite
NSAID	nonsteroidal anti-inflammatory drug
nsP1	non-structural protein 1
p.i.	post-infection
p.s.	post stimulation
PBS	phosphate buffered saline, adjusted to pH 7.3
PCR	polymerase chain reaction
pE2	precursor to envelope 2 protein
pg	picogram

PGE_2	prostaglandin E_2
PI	propidium iodide
P/S	Penicillin and Streptomycin
PXF	pentoxifylline
RA	rheumatoid arthritis
RNA	ribonucleic acid
RPMI	Roswell Park Memorial Institute
R-10	RPMI medium with 10% (v/v) FBS and P/S
R-5	RPMI medium with 5% (v/v) FBS and P/S
R-2	RPMI medium with 2% (v/v) FBS and P/S
RRV	Ross River virus
RRVD	Ross River virus disease
RRV-E2	Ross River virus envelope 2 protein
RT	room temperature
RT-PCR	reverse transcription-polymerase chain reaction
RVT	resveratrol
RXM	roxithromycin
S.aureus	*Staphylococcus aureus*
sec	second/s
SEM	standard error of means
TCID50	tissue culture infective dose 50%
TLR	toll-like receptor
TNFα	tumour necrosis factor alpha
UV	ultraviolet
v/v	volume/volume
w/v	weight/volume
x g	times gravity

Table of contents

List of tables

List of figures

1. Literature Review

1.1 Rheumatoid arthritis and viral arthritis

Arthritis is an inflammatory condition of the joint that is associated with pain, heat, swelling and loss or limitation of function of the affected joint (Stein, 2003). Due to the rather broad definition, arthritic conditions are classified into several categories. Degenerative arthritis or osteoarthritis is a common form of joint abnormality characterised by loss of cartilage followed by mechanical degradation of the joint. This arthritic condition is commonly found in the elderly due to increased wear and tear of the joint cartilage. Rheumatoid arthritis (RA) in contrast is a chronic inflammatory autoimmune disorder affecting approximately 1% of the population in most countries. Although the aetiology of RA is still not fully understood, much progress has been made in understanding the mechanisms that lead to the characteristic symptoms. Inflammatory processes play a crucial role in disease pathogenesis, characterised by hypertrophy of the synovial lining and infiltration of inflammatory cells such as fibroblasts, lymphocytes and macrophages (Firestein, 2003; McInnes & Schett, 2011).

Similar pathological processes, namely the involvement of the synovium and infiltration of immune cells have been found to contribute to the inflammation in a form of infectious arthritis, triggered by a number of viruses, such as the human immunodeficiency virus or hepatitis virus B and C (Tarkowski, 2006), although manifestation of arthritis is not a predominant symptom of the infection with these pathogens (Holland et al., 2013). Other viruses however are classified as arthritogenic pathogens, with joint inflammation being one of the characteristic symptoms of infection. These viruses include parvovirus B19, dengue virus, rubella virus and members of the alphavirus genus such as Chikungunya virus or Ross River virus (Franssila & Hedman, 2006; Suhrbier & Mahalingam, 2009).

Current research on arthritis focuses mainly on autoimmune conditions and their treatments, while research in the field of infectious arthritis is still lagging (Tarkowski, 2006). Considering the economic burden and health impact of viral arthritis, with some localised virus outbreaks affecting more than 1 million people (Schwartz & Albert, 2010), it is important that effective and economical treatment options, including antiviral compounds or alternative treatments for the symptomatic management of the disease are investigated. Current treatment of viral induced

arthritis focuses primarily on symptomatic pain relief using analgesics and/or non-steroidal anti-inflammatory drugs, which do however often come with significant risks of adverse effects after prolonged administration (Suhrbier et al., 2012).

Although it is not believed that the occurrence of viral arthritis increases the likelihood of developing autoimmune arthritis, the acute disease symptoms have a significant impact on physical health. Considering the duration of inflammatory joint conditions in viral arthritis, which for most alphaviruses generally lasts more than 6 months, sometimes up to two years (Mylonas et al., 2002), it is possible that some lasting damage to joint and cartilage might occur, which may hasten the onset of osteoarthritis. A recent report (W. Chen et al., 2014) supports this idea, with results showing that significant bone loss can be present in joints of mice infected with Ross River virus, an arthritogenic virus. These findings further highlight the strong similarities between viral arthritis and RA (Ryman & Klimstra, 2014).

1.2 Alphavirus infections as a cause of arthritis and myalgia

Suhrbier and Mahalingam (Suhrbier & Mahalingam, 2009) have reviewed viral causes of arthritis and discussed the array of viruses inducing arthritic conditions. While the risk of developing arthralgia (joint pain) or arthritis is small for most viruses, it is almost always predominant in infections with certain members of the alphavirus genus, namely Ross River virus (RRV), Chikungunya virus (CHIKV), Barmah Forest virus (BFV), Mayaro virus, O'nyong-nyong virus and the Sindbis virus group. Due to the disease presentation, with inflammation generally affecting multiple joints, the symptoms of RRV infections were initially diagnosed as epidemic polyarthritis (EPA) and only after the discovery of alphaviruses as the causative agent the term viral arthritis was used (Jacups et al., 2008). Affected joints often show severe swelling with large numbers of macrophages found in the synovial lining. The infiltration of these immune cells and the subsequent release of inflammatory cytokines are believed to be the major contributor to the development of joint inflammation (Assuncao-Miranda et al., 2013). The resulting arthralgia and arthritis often last for several months and in some cases up to two years, despite the initial viraemia period of only 4-7 days.

Apart from the severe arthritic symptoms, alphaviruses frequently cause excruciating muscle pain during the acute phase of infection. This myalgia often resolves within 7-10 days after onset, but prolonged pain has been reported to persist for months after infection (Sane et al., 2012). The cause of the occurring

myalgia is still not fully understood and it has been suggested that infiltrating macrophages release inflammatory cytokines and thereby induce painful muscle inflammation (Lidbury et al., 2008). A more recent study (K. S. Burrack et al., 2015) found increasing numbers of activated T-cells in the muscle tissue of RRV infected mice, which may further contribute to the reported muscle pain. Apart from the involvement of immune cells, several studies have shown that alphaviruses can induce necrosis in muscle tissue of infected mice (Morrison et al., 2011; Morrison et al., 2006) and it is likely that all of these factors contribute to the severe muscle pain. Besides the discussed arthritis and myalgia, several other but less debilitating symptoms are commonly present in infections with alphaviruses, including fatigue, maculopapular rash and fever (Suhrbier et al., 2012).

Although disease symptoms are self-limiting in alphaviral infections, the impact on health and economy is considerable, with approximately 4400-4800 infections recorded per year in Australia. A financial estimate (Woodruff & Bambrick, 2008) has calculated an average annual cost of A$4.3 to A$4.9 million for the Australian health system caused by RRV alone. Considering the cost for such a relatively small patient group and given that previous alphavirus outbreaks have affected up to 1.5 million people, such as the 2006 Chikungunya epidemic in India (Schwartz & Albert, 2010), the potential cost and impact on the population's health in a large scale outbreak is substantial.

Treatment of alphavirus induced arthritis mainly focuses on symptomatic relief using analgesics and non-steroidal anti-inflammatory drugs (NSAIDs) such as paracetamol, naproxen or ibuprofen (Suhrbier & La Linn, 2004). Corticosteroids have previously been used, with patient recovery rates reportedly similar to other therapy options. Due to the immunosuppressive effect of steroids and possible gastrointestinal side effects however many prescribers are reluctant to use this therapy option (Mylonas et al., 2004; Suhrbier et al., 2012). Recent research efforts have focused on antiviral therapy or alternative treatment of symptoms. Various compounds such as chloroquine and ribavirin have been tested for the treatment of alphavirus infections *in vitro*, however most do not appear to be viable options for future treatments *in vivo* (Parashar & Cherian, 2014). Anti-TNFα therapy with etanercept has unsuccessfully been trialled in acute RRV infection as it has exacerbated disease progression in a mouse model (Zaid et al., 2011). It appears that TNFα is important in the initial antiviral response and an exhaustive anti-TNFα treatment therefore has a negative impact on the host's ability to control viral infection.

Apart from symptomatic or antiviral treatment of the infection some research efforts have targeted the control of mosquito vectors responsible for viral transmission. The natural cycle of alphaviruses occurs between susceptible vertebrate hosts and hematophageous arthropod vectors, hence these viruses are commonly referred to as arthropod-borne viruses or arboviruses (Suhrbier et al., 2012). Transmission cycles in the wild usually involve non-symptomatic vertebrates such kangaroos, wallabies, horses and possums acting as viral reservoirs in Australia (Atkins, 2013; Boyd & Kay, 2000), however direct transmission from human to human via mosquito vectors has been reported in large alphavirus outbreaks such as the 2004 CHIKV outbreak on La Reunion island or the 2006 outbreak in India (Pialoux et al., 2007).

1.2.1 Ross River virus (RRV)

Ross River virus (RRV), a single stranded positive sense RNA virus of the alphavirus genus, is endemic to Australia and the Pacific islands region and was first isolated in 1959 from *Aedes vigilax* (northern salt marsh mosquito) around the Ross River in northern Queensland (R. Doherty et al., 1963). *Aedes (Ochlerotatus) vigilax* is the most common vector of RRV in Australia, besides other mosquito species such as *Aedes (Ochlerotatus) camptorhynchus* and *Culex annulirostris* (Atkins, 2013). Further *Aedes* species have shown to be susceptible to virus transmission and the rather recent increase of *Aedes albopictus* populations within Australia has raised public health concerns of increased transmissions of RRV (C. R. Williams, 2012). So far, no human-mosquito-human transmission has been recorded for RRV yet, however a single case is known of RRV transmission through a contaminated blood transfusion (Hoad et al., 2015).

Early reports of infections with RRV or the similar Barmah Forest virus (BFV) refer to the condition as epidemic polyarthritis (EPA) since alphaviruses were initially not recognised as the causative agent and arthritic symptoms generally affect multiple joints of infected patients (R. Doherty et al., 1963). Diagnosis was based solely on clinical symptoms and therefore RRV infections were indistinguishable from BFV infections until the latter virus was first isolated from an infected patient (Phillips et al., 1990). RRV is by far the most common alphavirus in Australia and in the last decade, approximately 4400-4800 cases of infection have been recorded annually, however outbreaks in the South Pacific with more than 50,000 patients have been reported previously (Jacups et al., 2008).

A previous report (Sammels et al., 1995) described the geographic distribution of genomically differing RRV strains within Australia, but no evidence has been found for the genetic diversity of various RRV isolates to correlate with symptomatic manifestations of the infection (Suhrbier & Mahalingam, 2009). The influence of the RRV genome on disease development has been further investigated (Jupille et al., 2011) and it was reported that gene sequences encoding the viral replicase non-structural protein 1 (nsP1) and precursor to envelope 2 protein (pE2) determine the development of arthritic symptoms in infections. Mutations in the coding sequence of these proteins resulted in avirulent strains such as RRV DC5692 and fully virulent strains such as RRV T48 and substitution of the nsP1 and pE2 gene region in DC5692 with the corresponding sequence of T48 restored full virulence. A mutation in these genes may hence potentially increase virulence in current RRV strains and possibly lead to longer lasting and more severe symptomatic manifestations.

Even though trials into RRV vaccination appear promising in current clinical phase 3 studies (Wressnigg et al., 2014), it is important to continue research into treatment options for RRV disease (RRVD). The cost of vaccinations might likely only be viable for high risk personnel or people living in high risk areas. In addition, research into the pathogenesis of RRVD could potentially help to understand infections with other alphavirus, such as CHIKV (Srivastava et al., 2008).

1.2.2 Chikungunya virus (CHIKV)

Chikungunya virus (CHIKV) is a single-stranded positive-sense RNA virus and the most common alphavirus worldwide, with localised outbreaks affecting up to 1.5 million people, such as the 2006 outbreak in India, or up to 50% of the population, such as the 2004 outbreak on La Reunion island (Schwartz & Albert, 2010; Suhrbier et al., 2012).

CHIKV was initially discovered in Tanzania in 1952 with small outbreaks recorded in other parts of Africa and Asia in the following decades (Powers et al., 2000; Robinson, 1955). A more recent outbreak of CHIKV in 2004 in Kenya has spread globally, affecting several millions of people by 2011 (Caglioti et al., 2013). Disease manifestation is similar to other arthritogenic alphaviruses however symptom presentation is significantly more severe. The name ‘chikungunya’ is derived from the Makonde language and means ‘that which bends up’, referring to the often stooped posture of infected patients due to excruciating joint and muscle pain (Schwartz & Albert, 2010). The often incapacitating arthralgia in CHIKV infection is

frequently present in the joints of extremities but can affect almost any joint. Further symptoms of CHIKV disease (CHIKVD) include high fever, fatigue and severe myalgia. As with RRV, the initial acute phase of infection lasts for 7-10 days, after which most symptoms slowly subside. Relapsing joint stiffness and arthralgia however often last for months or even years (Caglioti et al., 2013). Although mortalities in CHIKV infections have been reported in some instances, it is believed that underlying conditions were contributory factors (Bandyopadhyay et al., 2009; Economopoulou et al., 2009).

The transmission vectors for CHIKV are mosquitoes of the *Aedes* family found throughout Africa, Asia and more recently also in the Americas and Australia (Higgs & Vanlandingham, 2015; C. R. Williams, 2012). Genetic comparison of various CHIKV isolates found a mutation in the viral envelope protein gene (E1-A226V), which led to increased infectivity for *Aedes albopictus* (Asian tiger mosquito) and *Aedes aegypti* (Yellow fever mosquito) (Schuffenecker et al., 2006). This contributed to the larger scale outbreak occurring on La Reunion island in 2004, since urban transmission cycles of CHIKV rely on the presence of these mosquito species for successful human-mosquito-human transmission without the need for a reservoir (Caglioti et al., 2013; Tsetsarkin et al., 2007). The mosquito species *Aedes albopictus* is geographically widespread, which has facilitated the expansion of CHIKV in the last decade (Higgs & Vanlandingham, 2015). Several Australian mosquito species have been investigated as possible vectors for CHIKV transmission and the populations of *Aedes aegypti* and *Aedes albopictus* were found to be highly susceptible to virus infection and transmission (van den Hurk et al., 2009). With ongoing reports of CHIKV infections in travellers returning from affected regions (Viennet et al., 2013) and suitable vectors within Australia, we believe it is only a matter of time before a CHIKV outbreak will occur in Australia. Very similar conditions have previously led to a small outbreak in Italy in 2007 (Bonilauri et al., 2008; Rezza et al., 2007).

1.3 Cellular response in alphavirus infection and inflammation

It has been known for some time that a number of different cells and cell types are susceptible to alphavirus infection and La Linn et al. (La Linn et al., 2005) identified the importance of the α1β1-integrin collagen receptor for successful cellular binding (Aaskov et al., 1994; Wahlfors et al., 2000). Alphaviruses appear to interact with this surface integrin receptor and are then internalised via clathrin-mediated endocytosis

(Leung et al., 2011). However, studies with other alphaviruses have also reported a less common, clathrin-independent pathway (Paredes et al., 2004).

After entering the blood stream the initial path of the virus is unknown. It has been suggested that alphaviruses may undergo an early replication cycle in leukocytes and are then distributed through the lymph system (Assuncao-Miranda et al., 2013). Although there is no evidence of their involvement as yet, thrombocytes or platelets could potentially be involved in initial replication or distribution of the virus. Platelets are found at the site of virus entry into the blood stream and they have previously been reported to bind various viruses such as adenoviruses or dengue virus among others (Shimony et al., 2009). Thrombocytes can also internalise and shelter viruses as has been shown for the human immunodeficiency virus 1 (Flaujac et al., 2010), which could potentially facilitate the transfer of the virus to various target tissues or organs. With more recent reports highlighting the role of platelets in immune responses and as a source of inflammatory cytokines such as MIF, thrombocytes may also contribute to the hosts immune response upon virus infection (Semple et al., 2011; Strüßmann et al., 2013). More research is however necessary to investigate a possible role of thrombocytes in the infection of alphaviruses such as RRV or CHIKV.

Although a variety of other cells may contribute to the pathogenesis of alphavirus induced arthritis and myalgia, this research project has focused on macrophages and myocytes and has briefly investigated a possible role of adipocytes in RRV infections.

1.3.1 Macrophages in alphavirus infections

The important role of macrophages and their secretory products in rheumatoid arthritis is well established (Kinne et al., 2000). A previous study (Linn et al., 1996) confirmed the susceptibility of macrophages to RRV and demonstrated the ability of the virus to infect RAW264.7 macrophages and induce production of active virus particles for a period of more than 60 days post infection *in vitro*. RRV has been shown to persist in another macrophage cell line for as long as 170 days and despite the virus concentration falling below detectable levels in culture, a spontaneous relapse of cytolytic replication could be observed (Way et al., 2002). Virus entry into macrophages is thought to occur via either an integrin receptor pathway or via antibody-dependent enhanced (ADE) infection, which is mediated by the cellular Fc receptor if virus specific antibody is present (Linn et al., 1996).

Following *in vivo* infection, viral titres reach high plasma levels initially but drop below the serological detection limit within approximately one week. In contrast, viral RNA is detectable in the macrophage infiltrated synovium of infected patients for up to 5 weeks post-infection (Soden et al., 2000). This persistent, non-cytolytic infection and the possibility of a spontaneous relapse strongly indicate that macrophages play a major role in the prolonged duration of the infection.

Another indication that macrophages are pivotal cells in RRV infection is their increased migration into tissues that exhibited pathological symptoms during infection, such as joints and muscles. Macrophages have previously been shown to accumulate in the synovial lining of affected joints in RRVD (J. R. Fraser, 1986). Depletion of those macrophage infiltrates *in vivo* with disodium clodronate liposome treatment resulted in decreased levels of TNFα and MCP-1 in the affected tissues and a reduction in necrotic damage and local inflammation (Lidbury et al., 2008; Rooijen & Sanders, 1994). In addition to the infiltration into the synovium, macrophage migration into the striated muscles of RRV-infected mice has been observed previously. A study of RRV-infected mice (Lidbury et al., 2000) confirmed the primary role of macrophages in the muscle damage and found the declining presence of macrophages in the muscle correlated with the disappearance of symptoms.

To our knowledge, apart from macrophage-depletion with clodronate no treatment options targeting these immune cells or their cytokine release have been investigated in RRV infection.

1.3.2 Involvement of muscle cells in RRV infection

Due to the myalgia present in most patients, some studies have focused on the involvement of muscle tissue in the pathogenesis of RRVD, however initial research into the role of muscle cells has produced contradictory results. Murphy et al. (Murphy et al., 1973) observed severe muscle fibre damage and cytolysis in infected mice whereas later studies (Eaton & Hapel, 1976) reported a non-cytolytic alphavirus infection in primary mouse muscle cell cultures. It was later suggested that infiltrating macrophages and subsequent cytokine release as well as other host specific processes appear to be responsible for the necrotic processes leading to the myalgia and myositis experienced by many patients during RRV infection (Lidbury et al., 2000; Rulli et al., 2005). This observation resulted in a shift of the

research focus towards macrophages thereafter and away from the possible involvement of myocytes in disease pathology (Lidbury et al., 2008).

Using a mouse model it was shown that RRV and CHIKV undergo cytolytic replication cycles in muscles after initial infection (Morrison et al., 2011; Morrison et al., 2006; Murphy et al., 1973). It has also been reported that CHIKV can persist in human satellite muscle cells for prolonged periods of time (Ozden et al., 2007) and more recent work (Sane et al., 2012) has confirmed the *in vitro* susceptibility of human myoblasts and myocytes to Sindbis Virus, another member of the arthritogenic alphavirus genus. Despite these advances in research, the role of muscle cells in alphavirus infections is still poorly understood. The apparent viral replication cycle as well as a possible prolonged dormant infection in muscle cells both indicate that muscle tissue may be involved in the pathogenesis of RRVD.

Myocytes possess the ability to produce and secrete an array of cytokines such as Interleukin 6, which are often referred to as myokines, and hence are known to contribute to inflammatory processes (Muñoz-Cánoves et al., 2013; Pedersen et al., 2007). As Frost et al. (Frost et al., 2002, 2004) have reported, the secretion of pro-inflammatory cytokines can be induced by various stimuli *in vitro*, but to our knowledge it has never been shown if RRV can induce a cytokine response from myocytes *in vivo* or *in vitro*. The possible production of pro-inflammatory mediators secreted by muscle cells could very well exacerbate the myopathy and myositis induced by macrophage infiltrates and therefore offer a possible target for future treatment regimens.

1.3.3 A possible role of adipocytes in alphavirus infection

Earlier studies (Murphy et al., 1973) examined tissue samples of RRV-infected mice and found the highest viral titres in adipose tissue at 36 hr post infection. The average viral load in adipose tissue in the first 7 days was similar to the virus concentration found in muscles and exceeded titres in the blood. Cytolytic foci were detectable by 3 days post-infection in adipose tissue and necrosis continued even after virus levels dropped below the detection level. Despite these early reports little data is available on the effect of alphaviruses on either primary adipose tissue or adipocyte cell lines. Piper et al. (Piper et al., 1994) only refer to their unpublished data and mention the possibility to use Sindbis virus as an alphavirus vector for differentiated 3T3-L1 adipocytes, which could indicate the susceptibility of 3T3-L1 adipocytes to alphavirus infections.

Considering the limited information available, the possibility exists that the virus may undergo replication cycles in adipocytes within the first week of infection.

Research on adipocytes has highlighted their important role in inflammatory processes as producers of cytokines, such as the pro-inflammatory mediators TNFα and IL-6. Various stimulants like lipopolysaccharide (LPS) or several cytokines have been shown to induce production and secretion of these adipokines, often initiating further signalling cascades (Berg & Scherer, 2005; Coppack, 2001). Adipocytes have previously been shown to secrete macrophage migration inhibitory factor (MIF), which is known to play a role in the pathogenesis of RRV infection (Herrero et al., 2011; Hirokawa et al., 1997). A review of the contributing role of adipocytokines in rheumatic arthritis has however also highlighted the importance of considering other non-adipocyte cells present in adipose tissue as sources of inflammatory mediators, such as infiltrated immune cells (Schäffler et al., 2006).

A more recent focus on adipocyte biology has demonstrated their important role in the immune system as producers of various complement factors, such as C1 and C3a (Pattrick et al., 2009; Schaffler & Scholmerich, 2010). This is interesting and warrants further investigations, since both RRV as well as CHIKV have been shown to trigger immune reactions in which complement component C3 contributes to the destructive phase of the inflammation (Morrison et al., 2007; Morrison et al., 2008).

1.4 Cytokines in viral arthritis

Elevation of inflammatory cytokine levels such as TNFα and IL-6 are known to contribute to both the inflammation and pain in the joints of patients with rheumatoid arthritis (RA) (McInnes & Schett, 2011). Research into alphavirus induced arthritis has shown the pathological processes to be similar in RA and EPA, with cytokines thought to be the main contributors to disease progression in both conditions (Lidbury & Mahalingam, 2000a). A more recent study (Nakaya et al., 2012) confirmed this similarity by comparing the inflammatory processes of CHIKV induced arthritis with those present in RA. A significant overlap in the gene expression profile of numerous cytokines was apparent for both arthritic conditions and it was concluded that current RA treatments targeting cytokines may be beneficial for the treatment of alphavirus induced arthritis.

Besides cytokines, other factors are known to contribute to arbovirus induced disease development and the manifestation of symptoms. As mentioned previously,

Morrison et al. (Morrison et al., 2011; Morrison et al., 2008) have shown the involvement of complement factors, such as C3, in disease progression and pathogenesis of alphavirus induced arthritis and more recently the influence of myeloid differentiation primary response gene 88 (Myd88)-dependent TLR7 signalling on symptom manifestation and protection from disease was confirmed (Neighbours et al., 2012). These reports highlight the complex pathology in alphaviral arthritis. We believe however that pro-inflammatory cytokines secreted by various cells upon infection remain the major contributors to disease progression. The experiments described in this thesis focused on the involvement of following cytokines and may suggest future therapy options for EPA, based on inhibition of cytokine production.

1.4.1 Tumor necrosis factor alpha (TNFα)

TNFα is recognised as a major pro-inflammatory cytokine and numerous treatments for inflammatory diseases currently target the TNFα pathway. TNFα can be released by a variety of cells, in most inflammatory conditions however the main TNFα producers are thought to be monocytes and macrophages (Oppenheim et al., 2001). TNFα production is regulated by a complex network of cytokines and adipokines and as such presents many possible targets for treatment of rheumatoid arthritis (Tarner et al., 2007). The contribution of TNFα to disease progression in alphavirus infections has previously been confirmed (Lidbury et al., 2008). Elevated TNFα levels were detected in the synovial fluid of patients with RRV induced arthritis as well as in the serum of RRV infected mice. Infection of mice pre-treated with disodium clodronate liposomes to deplete macrophages resulted in lower serum levels of TNFα, MCP-1 and IL-1b, which indicates the macrophage origin of these cytokines in RRV infection.

The importance of TNFα as a key regulator in the production of further inflammatory cytokines is well established (Brennan & McInnes, 2008; Oppenheim et al., 2001), and since anti-TNFα treatments are successfully used in the management of RA it was concluded that they may be beneficial in the treatment of alphavirus infections (Suhrbier & Mahalingam, 2009). Exhaustive anti-TNFα therapies with etanercept or monoclonal antibodies such as infliximab however are expensive and may not be considered economical in a self-limiting disease with moderate sequaele. Patients often also experience adverse effects such as increased susceptibility to infections (van Dartel et al., 2012), which may make these treatment options less suitable for the management of alphavirus induced arthritis. The involvement of TNFα in

immune responses during viral infection has been reported previously and excessive anti-TNFα therapy was suggested to negatively influence the host's ability to counteract such infections (Suhrbier & Mahalingam, 2009). This concept was later confirmed when TNFα inhibition with etanercept exacerbated disease symptoms in RRV-infected mice (Zaid et al., 2011).

Our investigations focused on compounds that are known to reduce but not completely halt TNFα secretion in macrophages, thereby inhibiting excessive inflammatory processes without supressing basic immune reactions. Table 1 shows a list of compounds that have been tested in various macrophage cells or animal models. The list is not exhaustive and focused on inhibitors that were initially considered for our experiments due to availability and affordability.

1.4.2 Nitric oxide (NO) and inducible Nitric oxide synthase (iNOS)

Nitric oxide (NO) is a gaseous signalling molecule with crucial roles in immune responses, the regulation of inflammatory processes, neuronal communication and vasoregulation (Bogdan, 2015). It can be produced in most cell types via activation of one of three different NO-synthases (NOS): neuronal NOS (nNOS, NOS-1), inducible NOS (iNOS, NOS-2) and endothelial NOS (eNOS, NOS-3) (Pautz et al., 2010). Both nNOS and eNOS are pre-formed enzymes that produce NO depending on intracellular calcium levels with generally slow production rate. In contrast, iNOS is synthesized *de-novo* upon stimulation and output of NO is calcium-independent with higher production rates as compared to eNOS or nNOS. It appears that the NO produced during inflammatory and host defence mechanisms is almost exclusively derived from iNOS (Nagy et al., 2010; Schmitz et al., 2005). Expression of iNOS can be induced by various cytokines or other mediators in a wide range of cell types including macrophages (Kobayashi, 2010).

The central role of NO in the pathogenesis of rheumatoid arthritis has been established with increased levels of NO found in the serum and synovial fluid of patients with rheumatoid arthritis (RA) as compared to patients with osteoarthritis or healthy individuals (Ueki et al., 1996). It was later suggested that elevated systemic NO levels in inflammatory arthritis are likely due to increased iNOS expression in macrophages (Pham et al., 2003).

Table 1: TNFα inhibitors in macrophages or macrophage cell lines

Inhibitor	Cells / animal model	References
Thalidomide	RAW264.7 macrophages	(Noman et al., 2009)
Pentoxifyline	RAW264.7 macrophages, human alveolar macrophages	(Loftis et al., 1997), (Marques et al., 1999)
Erythromycin	Human monocytes (PBMCs)	(Bailly et al., 1991; Iino et al., 1992)
Clarithromycin	Mouse model	(Tkalcevic et al., 2008)
Roxithromycin	Human monocytes (PBMCs)	(Bailly et al., 1991)
SM905 (artemisinin derivative)	RAW264.7 macrophages	(J. Wang, 2009)
Pyrrolidine dithiocarbamate	Rat model	(Z. Zhang et al., 2009)
Ethyl pyruvate	RAW264.7 macrophages, mouse model	(Shang et al., 2009), (Ulloa et al., 2002)
Gabexate mesilate	Rat model, human monocytes	(Yuksel et al., 2003)
Dasatinib	RAW264.7 macrophages, mouse model	(C. Fraser et al., 2009)
Curcumin	RAW264.7 macrophages, rat model	(D. Chen et al., 2008), (Xiao et al., 2012)
Plant derived polyphenols	RAW264.7 macrophages	(Chandler et al., 2010)
Flavocoxid (baicalin and catechin)	Rat peritoneal macrophages	(Altavilla et al., 2009)
Resveratrol	Murine microglial cell line N9	(Bi et al., 2005; Lu et al., 2010)

A review on the role of NO in viral infections concluded that NO participates in the antiviral host response by interfering with the replication of DNA and RNA viruses (Reiss & Komatsu, 1998). Double stranded RNA is produced during virus synthesis in infected cells and is thought to induce iNOS and thus trigger antiviral responses (Steer & Corbett, 2003). A study investigating the expression of iNOS in RRV infection found that RRV is able to suppress important antiviral genes such as TNFα and iNOS in LPS-stimulated macrophages when infection occurred through an antibody-dependent enhanced pathway (Lidbury & Mahalingam, 2000b).

Considering the role of NO as both a pro-inflammatory molecule as well as a mediator in antiviral responses, a limiting however not exhaustive inhibition may be preferred in the treatment of RRVD. This would avoid excessive inflammatory processes but still allow basic antiviral immune responses.

1.4.3 Interleukin 6 (IL-6)

Interleukin 6 (IL-6) is involved in many metabolic and regulatory processes and acts as an important activator of immune responses. As a cytokine, it can have both pro-inflammatory as well as anti-inflammatory functions. Similar to TNFα, IL-6 is involved in most inflammatory processes and has been investigated as a target for anti-inflammatory intervention (Scheller et al., 2011). Although numerous cell types have the ability to produce IL-6, the primary source in inflammatory processes are monocytes and macrophages. The release of IL-6 can be induced by a variety of inflammatory stimuli, including TNFα, Interleukin-1 (IL-1), LPS or viruses. In the latter two cases toll-like receptor (TLR) activation appears to be involved in the activation of the cell to release IL-6 (Naugler & Karin, 2008).

After secretion IL-6 may initiate further responses via two pathways. The *classic* signalling pathway involves interaction with the membrane-bound IL-6 receptor and membrane glycoprotein 130, leading to the activation of the target cell. *Trans-signalling* involves a soluble IL-6 receptor that forms a complex with IL-6 which then activates glycoprotein 130 and induces further signalling cascades. This pathway can be utilized in an autocrine or paracrine manner by cells lacking the membrane-bound IL-6 receptor, but still produce glycoprotein 130 (Scheller et al., 2011).

The role of IL-6 as a myokine – a cytokine released by muscle cells – is usually associated with anti-inflammatory processes. Increased IL-6 concentrations are found in skeletal muscle and plasma during and after prolonged exercise and it appears that IL-6 induces other well-known anti-inflammatory cytokines like IL-1ra

and IL-10 (Pedersen et al., 2007). Apart from exercise induced release, myoblasts are however also known to release IL-6 upon inflammatory stimulation, which in turn can induce the release of further chemokines and other pro-inflammatory mediators (Gallucci et al., 1998; Scheller et al., 2011). Increased monocyte infiltration into muscles during RRV-infection has been reported previously (Lidbury et al., 2000) and IL-6 released from muscles during infection could possibly contribute to the characteristic myopathy as well as arthritic symptoms observed in RRVD.

IL-6 plays an important role in the inflammatory processes in RA, with elevated levels found in synovial fluids and plasma of affected patients. Targeted anti-IL-6 therapy, such as treatment with IL-6 antibodies has been trialled successfully to reduce disease progression and symptom manifestation in patients with RA (Brennan & McInnes, 2008; McInnes & Schett, 2007). Increased IL-6 levels have also been found in viral arthritides such as parvovirus B19 induced arthritis (Kerr et al., 2004) and a correlation between peripheral blood IL-6 concentration and CHIKVD symptom severity in patients was observed (Ng et al., 2009). Elevated IL-6 levels were detected in patients with severe arthritic symptoms while reduced levels related to mild symptom presentation. IL-6 was therefore suggested as a suitable biomarker for the prediction of disease manifestation in CHIKVD.

IL-6 inhibitors such as the monoclonal antibody tocilizumab have been successfully trialled for the treatment of RA (Hennigan & Kavanaugh, 2008), however to our knowledge no compound has so far been investigated for a potential IL-6 lowering effect in alphavirus infection.

1.4.4 Macrophage migration inhibitory factor (MIF)

Macrophage migration inhibitory factor (MIF) was the first cytokine to be discovered, and has been found to play a seminal role in the pathogenesis of several diseases including rheumatoid arthritis (H. R. Kim et al., 2007; Santos & Morand, 2006). MIF is produced by activated macrophages and is able to maintain macrophage activation by inhibiting p53 through interaction with CD74. This results in an autocrine loop which leads to continued macrophage activation and secretion of pro-inflammatory products, thereby maintaining the inflammatory response. MIF plays an important role in RA and it therefore warrants to be investigated as a possible target in the therapeutic treatment of RA (Morand, 2005). Apart from its role as a cytokine MIF is known to possess enzyme activity as a keto-enol-tautomerase (Bucala, 2012). It appears this feature is important for MIF to act as a cytokine and

potential anti-inflammatory agents could therefore either reduce MIF secretion or inhibit its enzyme activity (Garai & Lorand, 2009).

Herrero et al. (Herrero et al., 2011) established the critical role of MIF in RRV infection and showed that MIF-/- mice developed less severe disease symptoms with reduced transcription of several pro-inflammatory cytokines, despite reaching plasma viral titres similar to those found in infected wild type mice. Reconstitution of MIF in MIF-/- mice increased symptom presentation whereas treatment of infected wild type mice with ISO-1, a MIF inhibitor, reduced disease progression. With this recent evidence of MIF contributing to the symptoms in RRV infection it might be possible to find cheap and effective agents to relieve both the joint and muscle symptoms and hence reduce the impact of infection on patients. Recent findings have highlighted the importance of MIF in dengue virus infections (Chuang et al., 2015) which could indicate a possible role of MIF inhibitors in the treatment of other viral infections.

A number of small molecules and plant derived anti-inflammatory compounds such as caffeic acid, curcumin, and resveratrol have been investigated for potential anti-MIF activity (Molnar & Garai, 2005). These non-toxic constituents of fruits and vegetables are present in the diet, it is however not known if they are active when administered *in vivo* at these concentrations. Besides these naturally occurring molecules there is continuing research for synthetic agents such as ISO-1 (Al-Abed et al., 2005) and other synthetic compounds (L. Xu et al., 2013) capable of inhibiting MIF.

Table 2 shows a list of MIF inhibitors that were initially considered for our experiments. The list is not exhaustive and focused on inhibitors in regards to availability or affordability.

1.4.5 High mobility group box (HMGB) protein family

The high mobility group box (HMGB) protein family contains four members (HMGB1-4) of abundant non-histone proteins conserved across species which bind double stranded DNA without sequence specifity (Stros, 2010; Stros et al., 2007). They have previously been recognized as important effectors in nucleic-acid mediated innate immune responses by activating various toll-like receptors (TLRs), however most work in this field has focused on HMGB1 (Yanai et al., 2009). HMGB1 is known to act as an extracellular mediator that can be secreted to function as a cytokine in various inflammatory conditions (Huang et al., 2010) and it has been

suggested that HMGB2 may possess similar functions (Stros, 2010). Due to the limited data available on HMGB2 and HMGB3 our research project has focused on the role of HMGB1 in alphavirus infections and only briefly investigated the involvement of HMGB2 and HMGB3.

Within the nucleus, HMGB1 is responsible for stabilizing nucleosomes and presenting DNA to enable gene transcription. Constitutively present in most nuclei, it can be passively released by necrotic cells or actively secreted by monocytes, macrophages or neutrophils and further stimulate the release of pro-inflammatory cytokines (Andersson et al., 2014). In monocytes, HMGB1 is secreted via a non-classical vesicle mediated secretory pathway that may differ from the method of secretion by other cells (Gardella et al., 2002).

There are numerous reports highlighting the pivotal role of HMGB1 in the pathogenesis of RA as a possible target for directed therapy (Ulloa et al., 2003). HMGB1 is found in higher levels in synovial fluid of RA patients and when applied to synovial macrophages is able to stimulate production of TNFα, IL-6 and IL-1β (Taniguchi et al., 2003). Administration of HMGB1 into normal joints causes development of inflammation and arthritis, inhibition of HMGB1 prevents the progress of the arthritis (Andersson & Erlandsson-Harris, 2004).

Besides its function as pro-inflammatory mediator, a pathogenic role in viral infections has been suggested for HMGB1 previously (H. Wang et al., 2006). Active HMGB1 secretion has been reported for herpes simplex virus-2 infected epithelial HEC-1 cells (Borde et al., 2011) and increased HMGB1 levels were found in the lungs of H5N1 influenza-infected mice (Hou et al., 2014), which likely contributes to pulmonary inflammation. Human dendritic cells actively release HMGB1 in dengue virus infection, which initiates release of pro-inflammatory cytokines and modulates virus replication *in vitro* (Kamau et al., 2009). More recent data showed comparable HMGB1-release from dengue virus infected peripheral blood mononuclear cells (Ong et al., 2012) and HMGB1 has therefore been suggested as auxiliary biomarker for the diagnosis of dengue virus infections (Allonso et al., 2013). Given the importance of HMGB1 in RA it is surprising that no work has attempted to relate it to arthritogenic virus infections.

Much of the work on HMGB1 inhibitors has focused on possible treatment options of inflammatory processes and sepsis (Nogueira-Machado & de Oliveira Volpe, 2012; H. Wang, M. F. Ward, et al., 2009). No study has however considered the use of any of these inhibitors in the treatment of viral arthritis. Many HMGB1 inhibitors are

inexpensive, readily available and non-toxic and may therefore potentially offer economic and effective therapy options. Table 3 shows inhibitors that were initially considered for our experiments. The list is not exhaustive and the main selection criteria were availability and affordability.

Table 2: MIF inhibitors

Inhibitor	Cell line/ animal	References
Curcumin	Rat model	(Molnar & Garai, 2005; Xiao et al., 2012)
Umbelliferon	Rat model	(Molnar & Garai, 2005)
Resveratrol	Rat model	(Molnar & Garai, 2005)
Caffeic acid	Rat model	(Molnar & Garai, 2005)
ISO-1	RAW264.7 macrophages, Mouse model	(Al-Abed et al., 2005; Cho et al., 2010; Herrero et al., 2011)
Benzylisothiocyanate	*	(Ouertatani-Sakouhi et al., 2009)
AV411 (Ibudilast)	*	(Cho et al., 2010)
Epoxy-azadiradione	RAW264.7 macrophages	(Alam et al., 2012)

*Inhibitor only tested in enzyme assays

Table 3: Inhibitors of HMGB1 release

Inhibitor	Cell line/ animal	References
Ethyl pyruvate	Mouse model	(Hollenbach et al., 2008; Shang et al., 2009; H. Wang et al., 2008; Q. Wang et al., 2009)
Ethyl lactate	Mouse model	(Hollenbach et al., 2008)
Glycyrrhizin	RAW264.7, Mouse model	(Girard, 2007; Vitali et al., 2013; Wu et al., 2014)
Telmisartan	Mouse model	(Haraguchi et al., 2009)
Quercetin	RAW264.7, Mouse model	(Tang et al., 2009)
Rosmarinic acid	RAW264.7, Rat model	(Jiang et al., 2009)
Glutamine	Rat model	(Kwon et al., 2010)
Nicotine	RAW264.7, Mouse model	(H. Wang et al., 2004)
Chinese medicinal herbs: Danggui (*Angelica sinensis*), Green tea (*Camellia sinensis*), Danshen (*Salvia miltorrhiza*)	Mouse models	(H. Wang, M. F. Ward, et al., 2009; H. Wang, T. Xu, et al., 2009; H. Wang et al., 2008)
Curcumin	HUVECs	(D. C. Kim et al., 2011)
Minocycline	Rat phaeochromo-cytoma (PC12) cells	(Kikuchi et al., 2009)
Gabexate mesilate	RAW264.7, Rat model	(Hidaka et al., 2011)
Ketamine	RAW264.7, Rat model	(Z. Zhang et al., 2014)

1.4.6 Interleukin 18 (IL-18)

Interleukin 18 (IL-18) is a member of the IL-1 cytokine superfamily initially discovered in endotoxemic mice as interferon gamma inducing factor and later renamed to IL-18 (Okamura et al., 1995). It is widely recognised as a pro-inflammatory mediator and regulator of immune responses amongst other physiological and pathological roles. IL-18 is constitutively synthesized as an inactive precursor by a wide variety of cells and requires enzymatic cleaving by caspase-1 to transform into its active form. Macrophages and dendritic cells have been identified as the main sources for active IL-18, although cleavage can also occur in other cells (Dinarello et al., 2013) .

Once activated, IL-18 can form a trimeric complex with the two subunits of the IL-18 receptor (IL-18Rα and IL18Rβ) to initiate signalling pathways similar to IL-1, hence resulting in similar molecular responses, such as activation of NFκB, JNK or p38 MAP kinase pathways. This ultimately leads to increased production of nitric oxide, interferon gamma (IFNγ) and further chemokines (Arend et al., 2008). IL-18 binding protein (IL-18 BP) is an endogenous regulator of IL-18 that binds IL-18 with high affinity thus inhibiting its biological activity. IL-18BP secretion is upregulated by IFNγ and therefore provides a regulatory feedback loop for IL-18 (Arend et al., 2008).

The role of IL-18 as pro-inflammatory mediator in rheumatoid arthritis was reported previously (Gracie et al., 1999), with increased concentrations of both IL-18 mRNA and protein found in synovial tissues of patients with rheumatoid arthritis as compared to osteoarthritis controls. IL-18 has since been shown to independently induce NO and TNFα secretion by macrophages and contribute to the inflammatory processes present in RA (Arend et al., 2008).

IL-18 is involved in the immune response to viral infections, partly due to the activation of cytotoxic T cells that clear the virus (Gracie et al., 2003). A more recent investigation (Chirathaworn et al., 2010) has found increased IL-18 and IL-18BP serum levels in Chikungunya virus infections which promote the T helper-1 immune response. Both IL-18 and IL-18BP have thus been suggested as potential therapeutic targets for the treatment of CHIKVD. It is likely that IL-18 and IL-18BP concentrations are also elevated in other alphavirus infections such as RRVD and potential treatment options targeting the IL-18 signalling chain might therefore extend to a variety of virus infections or other arthritic conditions.

1.4.7 Interleukin-33 (IL-33)

Interleukin-33 (IL-33) was identified as a new member of the IL-1 cytokine family (Schmitz et al., 2005) and similar to other IL-1 cytokines it was found to activate NF-kB and MAP kinase pathways thereby triggering further inflammatory responses via the T1/ST2 receptor (also referred to as ST2L). This receptor is commonly found on mast cells and lymphocytes and activation initiates expression and secretion of pro-inflammatory cytokines and chemokines. IL-33 can be synthesized in a variety of cells including macrophages, mast cells and endothelial cells in which it is stored as a nuclear bound IL-33 precursor that can be cleaved and secreted as the active IL-33 upon exposure to stimuli (Arend et al., 2008). Cleavage is thought to be catalysed by caspase-1 or caspase-1-activated proteases, however the exact mechanism is still not fully understood. More recent data has shown that nuclear IL-33 itself possesses biological activity and can act as transcriptional regulator. Activation of epithelial and endothelial cells with pro-inflammatory stimuli results in inhibited expression of nuclear IL-33 (Kuchler et al., 2008). This indicates a pro- as well as anti-inflammatory role of IL-33, depending on the physiological and pathological processes.

The nuclear rather than cytoplasmic storage of IL-33 and the active secretion upon stimulation remind of the previously discussed HMGB1 (Haraldsen et al., 2009). Similar to HMGB1, IL-33 can act as an 'alarmin' when released from necrotic cells and alert or activate the immune system (Miller, 2011).

IL-33 has been investigated for its role in RA and increased IL-33 expression as well as secretion has been found in synovial tissues during RA, promoting local inflammation through mast cell activation (D. Xu et al., 2008). *In vitro* tests with fibroblasts showed increased expression upon exposure to inflammatory cytokines (Matsuyama et al., 2010). IL-33 has been shown to exacerbate symptoms in CIA, whereas blockage of its ST2 receptor reduced inflammation in CIA (Liew et al., 2010), which makes both molecules potential targets for future treatments.

IL-33 was referred to as T1 prior to its classification as interleukin and early reports suggested a role of T1 in the defence against viral infection. Respiratory syncytial virus-infected mice showed reduced lung inflammation when treated with monoclonal ST2−specific antibody and TH2−associated immunopathology was observed to be less severe (Walzl et al., 2001). To our knowledge, this is the only study to have investigated the involvement of IL-33 in viral infections.

1.4.8 Interleukin 10 (IL-10)

Interleukin-10 (IL-10) is, in contrast to the previously reviewed cytokines, an anti-inflammatory cytokine with a crucial role in infection and inflammation. IL-10 has a limiting effect on the host's immune response in infections in order to avert tissue or cell damage (Saraiva & O'Garra, 2010). Similarly, it is an important regulator that prevents overshooting inflammatory reactions and autoimmune pathologies by down-regulating pro-inflammatory cytokine production. IL-10 was initially thought to be exclusively expressed in TH2 and T regulator cells, however more recent data has confirmed its expression in a variety of other cells including macrophages, mast cells and myeloid dendritic cells upon stimulation (Saraiva & O'Garra, 2010).

The induction of IL-10 is a complex network of cell signalling pathways that can greatly differ from cell to cell. In macrophages its transcription is induced by pathogen derived products through pattern recognition receptors (PPRs) which generally involve TLR activation followed by activation of the MyD88 pathway. Once released, IL-10 can interact with the IL-10 receptor (IL-10R) which in turn activates the signal transducer and activator of transcription 3 (STAT3) pathway. Since the IL-10R is also expressed by macrophages and dendritic cells, IL-10 can act as an autocrine inhibitor on these cells and inhibit the synthesis of various pro-inflammatory cytokines (Mosmann, 1994). In general, IL-10 is released after secretion of pro-inflammatory cytokines to prevent an overshooting reaction (Trinchieri, 1997). Macrophages have been identified as the main producers of circulating IL-10 in LPS challenged mice (Haskó et al., 1996).

The involvement of IL-10 in the immune response to viral infection is widely acknowledged (Saraiva & O'Garra, 2010). Analysis of patient sera during dengue virus infection found a clear correlation between IL-10 plasma levels and disease severity with highest IL-10 levels detected on day 0 of fever onset (S. Green et al., 1999). Analysis of cytokine expression during RRV-ADE infection of macrophage cultures showed increased transcription of IL-10 as well as elevated IL-10 concentrations in the supernatant of infected cells as compared to controls (Mahalingam & Lidbury, 2002). Due to its regulatory effect in inflammation as well as its potent immunosuppressive properties IL-10 has been considered as a potential target for the treatment of RA (Keystone et al., 1998) and it was suggested that reduction of IL-10 levels in alphavirus infections might potentially lead to better treatment outcomes (Rulli et al., 2005).

1.5 Cytokine inhibitors for the treatment of RRV induced arthritis

As previously discussed, current treatment options for alphavirus infections are limited and usually target symptomatic relief with aspirin, paracetamol or non-steroidal anti-inflammatory drugs (Rulli et al., 2005). Corticosteroids have been used in the treatment of RRVD without significant disease exacerbation, however due to concerns in regards to their immunomodulatory effects they are used cautiously (Mylonas et al., 2004).

To this date there is no antiviral treatment available for RRV or CHIKV infections. Research projects have investigated several compounds, however none has successfully completed clinical trials (Parashar & Cherian, 2014). A recently developed RRV vaccine has entered phase 3 clinical trials and outcomes so far look very promising (Wressnigg et al., 2014). Considering the early stages of vaccine development and the likelihood that vaccination will only be used in high risk areas or by high risk personnel, we believe it is important to continue research into alternative treatment options for alphavirus infections.

The role of various cytokines has been investigated in alphavirus infection and offers many possible targets for future treatments. Our experiments have focused on the possible inhibition of several of these cytokines with inexpensive and readily available compounds. As previously mentioned, it was suggested that current treatment options for RA may be applicable for use in alphaviral athritides (Nakaya et al., 2012). We believe that, *vice versa*, agents with promising results in the treatment of EPA could potentially open the door for alternative treatment options in patients with RA.

The drug bindarit has previously been trialled in a RRV mouse model and treatment significantly reduced levels of monocyte chemoattractant protein 1 and TNFα in infected mice (Rulli et al., 2009). Similarly, macrophage infiltration into synovial tissues and muscles as well as disease severity was reduced, without affecting viraemia. This once more suggests that macrophages and macrophage derived cytokines are major contributors to RRVD progression and could be targeted for alternative treatment options.

Potential inhibitors of TNFα, (Table 1), HMGB1 (Table 3) and MIF (Table 2) were initially screened for affordability and availability. Following is a brief review on compounds that were tested in inhibitory assays.

1.5.1 Macrolide antibiotics

The anti-inflammatory effect of macrolide antibiotics has been investigated extensively in the last decades. Early investigations (Bailly et al., 1991) reported of an IL-6-inhibiting effect of erythromycin (ERY) and spiramycin on LPS-stimulated monocytes and similarly ERY was found to inhibit TNFα secretion from stimulated monocytes (Iino et al., 1992). Further studies (Ianaro et al., 2000) showed reduced production of TNFα, IL-1b, IL-6 and NO in LPS-challenged macrophages when treated with macrolide antibiotics such as ERY, clarithromycin (CLA) and roxithromycin (RXM). ERY as well as CLA also inhibited NO secretion in stimulated rat pulmonary alveolar macrophages (Kohri et al., 2000). An inhibitory effect on chemotaxis and infiltration of neutrophils into the airways *in vivo* has been reported for ERY, CLA, RXM and azithromycin (Tamaoki et al., 2004). The use of RXM as an anti-inflammatory agent in collagen induced arthritis (CIA) has been investigated previously and an inhibitory effect on T-cell and macrophage cytokine production was reported (Urasaki et al., 2005).

Recent drug development has therefore started to focus on macrolide molecules without antibiotic properties for the treatment of various non-infectious inflammatory conditions (Mencarelli et al., 2011). A recent review (Ogrendik, 2014) has summarised the potential benefit of macrolide antibiotics in the treatment of RA and we believe that macrolides may also exert their anti-inflammatory properties in alphavirus induced arthritis. To our knowledge, no macrolide has previously been investigated for the treatment of arthritogenic alphavirus infections.

Erythromycin (ERY), clarithromycin (CLA) and roxithromycin (RXM) are all 14-membered ring macrolides with very similar antibiotic profiles (Hardy et al., 1988). They are readily available and generally very well tolerated, even when given long term for prophylactic treatment (Rubinstein, 2001). To our knowledge, no direct antiviral properties have been reported for any of these macrolides.

1.5.2 Ethyl pyruvate (EP)

The anti-inflammatory properties of ethyl pyruvate (EP) were firstly reported by Yang et al. (Yang et al., 2002), who found modulated cytokine production in EP treated mice with haemorrhagic shock. Further investigations (Ulloa et al., 2002) analysed the potential use of EP as anti-inflammatory treatment in sepsis and systemic inflammation and found, that EP inhibited the release of both TNFα as well as HMGB1 through inhibition of the p38 MAP kinase and NFkB pathways in septic

mice. Even when administered up to 24 hr after the immediate response EP showed significant efficacy and reduced expression of late-phase cytokines.

EP has been tested in numerous models of septic shock with mostly positive outcomes, possibly due to the inhibitory effect on HMGB1 secretion (Dave et al., 2009; Fink, 2007). HMGB1 has also been suggested as a potential target in arthritic conditions (Ulloa et al., 2003) and it is rather surprising that EP has so far not been trialled in models of RA. No direct antiviral properties are reported for EP. A more recent study (Ong et al., 2012) investigated the effect of EP on dengue virus-infected monocytes *in vitro* and found dose-dependent decrease of HMGB1 release.

As previously outlined, we suggested that HMGB1 may be involved in RRV disease as a pro-inflammatory cytokine and therefore investigated EP as a possible therapeutic agent.

1.5.3 Pentoxifylline (PXF)

Pentoxifylline (PXF) or oxpentifylline is a xanthine derivative with various therapeutic effects. It has been shown to decrease blood viscosity and increase blood microcirculation and has been approved in Australia for the treatment of intermittent claudication caused by peripheral artery disease (Salhiyyah et al., 2012).

Early investigations into its biological effects have shown that PXF is also a strong anti-inflammatory compound, decreasing TNFα production in LPS-stimulated macrophages by inhibiting TNFα mRNA accumulation (Han et al., 1990). The TNFα inhibitory effect was confirmed for monocytes, however PXF did not reduce but rather increase IL-6 production in monocytes exposed to LPS (Schandené et al., 1992). Further investigations (D'Hellencourt et al., 1996) extended these findings to numerous other inflammatory mediators (namely IL-1b, IL-6, IL-8, IL-10 and TNFb) and reported that PXF interferes with cytokine production in a rather complex manner, strongly depending on type of stimulation and cellular environment.

Due to the initial reports of TNFα inhibition, PXF was investigated as treatment option in rheumatoid arthritis (Maksymowych et al., 1995). PXF decreased the number of swollen joints significantly in treated individuals, despite the clinical response not consistent with TNFα levels measured in patient blood samples. A more recent study however found reduced serum TNFα concentrations in a mouse model of rheumatoid arthritis when treated with PXF (Queiroz-Junior et al., 2013).

Previous reports have also highlighted the antiviral properties of PXF and found inhibition of viral replication in numerous DNA and RNA virus strains, including herpes simplex virus, vaccinia virus and rotavirus (Amvros'eva et al., 1993). More recent work has confirmed the antiviral properties for Japanese encephalitis virus (Sebastian et al., 2009) and reduced symptom manifestation in PXF-treated children with dengue virus infection was reported (Salgado et al., 2012). So far no study has been published on the effects of pentoxifylline in alphavirus infections.

1.5.4 Resveratrol (RVT)

Resveratrol (RVT) has long been known as a cardioprotective constituent in red wine and was later associated with prevention of cancer, cardiovascular diseases and ischaemic conditions. The molecular processes in which RVT exerts these properties are still not fully understood, it is however thought that its cyclooxygenase (COX)-inhibiting properties are at least contributing to some of the biological activities of RVT (Baur & Sinclair, 2006). COX is an enzyme that catalyses the synthesis of pro-inflammatory mediators which may partly explain the anti-inflammatory properties of RVT.

Apart from these properties RVT has been investigated for its influence on cytokine production in macrophages with inconclusive results. A previous study (Wadsworth & Koop, 1999) investigated the effects of resveratrol on LPS-stimulated RAW264.7 macrophages and found decreased nitrite (NO) release, but increased TNFα mRNA expression and induced TNFα secretion. Later investigations with LPS-treated RAW264.7 macrophages (Qureshi et al., 2012) showed decreased NO release as well as decreased levels of inflammatory cytokines, such as TNFα, IL-1b and IL-6, when treated with RVT. An inhibitory effect on IL-6 release from stimulated mouse peritoneal macrophages was reported previously (Zhong et al., 1999). These anti-inflammatory properties were further investigated in a rabbit model of inflammatory arthritis (Elmali et al., 2007), which showed significantly decreased cartilage destruction in RVT treated animals.

Previous reports also suggest antiviral activity for RVT, which has been shown to inhibit viral replication of most members of the *Herpesviridae* family, including Herpes Simplex virus 1 and 2, Varicella Zoster virus and Eppstein-Barr virus amongst others (Campagna & Rivas, 2010). The molecular mechanism in which RVT exerts its antiviral properties remains unclear, but may involve inhibition of the NFkB-pathway. While activation of the NFkB signalling cascade is often part of a

hosts antiviral response, previous research has also demonstrated that certain viruses such as Influenza A and Herpes Simplex virus 1 require activation of that same pathway for efficient replication (Santoro et al., 2003).

More recent work has reported of RVT's inhibitory effect on respiratory syncytial virus replication as well as virus induced IL-6 production in airway epithelial cells (Xie et al., 2012).

Both the antiviral as well as anti-inflammatory properties suggest a suitable role of RVT in the treatment of alphavirus infections. To our knowledge, no work has been done investigating RVT in the treatment of infections with arthritiogenic viruses.

1.5.5 Kino extract (KE)

Kino is a plant exudate formed by some trees upon infections or mechanical injury to the bark. In Australia several Eucalyptus species are known to produce this dark resin and indigenous people have traditionally used it in aqueous concoctions to treat various gastro-intestinal conditions and infections (Locher & Currie, 2010). The high tannin content makes kino a strong astringent with possible antimicrobial effects (von Martius et al., 2012). Traditional use of kino used as a tea includes the treatment of common colds, which could also indicate possible antiviral properties of the extract (Clarke, 2011). Little else is known of the biochemical and pharmacological effects of kino, however it has been shown that kino derived from *Corymbia calophylla* may possess anti-inflammatory properties (Martha Y Mungkaje, Curtin University, personal communication). *Corymbia calophylla* or *Eucalyptus calophylla* is commonly referred to as Marri and is a red gum tree native to Western Australia (Lim, 2014). So far, no reports have been published regarding the possible antiviral effect of its kino exudate.

Given the potential anti-inflammatory effect of aqueous kino extract we decided to investigate the possibility to use kino in the treatment of RRV-induced inflammatory processes.

2. Methods and Materials

2.1 Cell culture

All cell lines were purchased directly from the American Type Culture Collection (ATCC) unless stated otherwise.

2.1.1 Culture conditions

Cell culture media was purchased from Thermo Scientific (HyClone Laboratories, USA) and supplemented with 1% (v/v) Penicillin-Streptomycin solution (P/S) (Thermo Scientific, HyClone, 10000 units/ml Penicillin, 10000 µg/ml Streptomycin) , unless stated otherwise. For cell line propagation, 5 or 10% (v/v) foetal bovine serum (FBS; Serana, Australia) was added to the media. Cells were cultured in a humidified incubator (Quantum Scientific, Australia) in 5% (v/v) CO_2 at 37°C in T-75 flasks (NalgeNunc International; Denmark) and subcultured according to ATCC protocols. Cells were either manually scraped or detached using 0.25% (v/v) trypsin-EDTA (Thermo Scientific, HyClone Laboratories, USA) after rinsing twice with sterile normal saline (Baxter, Australia).

2.1.2 Test for mycoplasma

All cell lines were tested six-monthly for mycoplasma contamination as follows.

A T75 flask was passaged with 1 ml of 0.25% (v/v) trypsin-EDTA and a 50 µl aliquot of this cell suspension was centrifuged at 500 x g for 30 sec (Centrifuge 5417C, Eppendorf, Germany). The supernatant was discarded and the cell pellet lysed with Easy DNA High Speed Extraction kit (Fisher Biotec, Australia). In brief, 64 µL of Solution 1A and 16 µL of Solution 1B were added to each sample and the mixture was incubated at 95°C for 20 min. Then 20 µL of Solution 2 was added and this mixture containing the extracted DNA was diluted 1/100 (v/v) in PCR grade water (Fisher Biotech, Australia) for PCR analysis as usual using primers specific for mycoplasma (see 2.5.4). Mycoplasma positive sample cDNA was included as assay control. Experimental results were only included in this study when the cell lines tested negative for mycoplasma.

2.1.3 Culture of RAW264.7 mouse macrophages

RAW264.7 macrophages (ATCC, TIB-71) were cultured in R-5. At 80-90% confluency the cells were manually scraped and split 1/10 for subculture.

2.1.4 Culture of C2C12 mouse myoblasts

C2C12 mouse myoblasts (ATCC, CRL-1772; kindly donated by Erin Bolitho, School of Pharmacy) were cultured in R-5 or R-10. Cells were grown to a maximum 80% confluency to avoid differentiation into myotubes and passaged 1/10 using 0.25% (v/v) Trypsin-EDTA.

2.1.5 Culture and differentiation of 3T3-L1 mouse fibroblasts

2.1.5.1 Culture of 3T3-L1 mouse fibroblasts

3T3-L1 fibroblast cells (ATCC, CL-173) were cultured in Dulbecco's Modified Eagle's Medium containing 4500 mg/l glucose (DMEM, HyClone), 10% (v/v) FBS, Glutamax (Gibco, Life Technologies, USA) and antibiotics. Cells were subcultured with 0.25% (v/v) trypsin-EDTA before reaching the maximum density of $6x10^4$ cells per cm^2 as recommended by the ATCC. For differentiation and infection experiments, 3T3-L1 pre-adipocytes were only used up to passage number 12.

2.1.5.2 Differentiation of 3T3-L1 fibroblasts into adipocytes

Differentiation of 3T3-L1 pre-adipocytes into adipocytes was induced as per method of Shepherd et al. (Shepherd et al., 1995) and modified by Zebisch et al. (Zebisch et al., 2012). 3T3-L1 cells were cultured to confluence in 6-well plates (Nunclon delta, Nalge, UK) in DMEM containing 4500 mg/L glucose, 10% (v/v) FBS, Glutamax and P/S. Two days after confluence was reached, the medium was changed to additionally contain 0.25 µM dexamethasone (Sigma, Australia), 0.5 µM isobutyl-methylxanthine (IBMX, Sigma, Australia), 5 µg/mL bovine insulin (Sigma, Australia) and 2 µM rosiglitazone (Sigma, Australia). After an additional 2 d in culture, the medium was replaced and the cells were maintained in culture medium substituted with 5 µg/mL insulin for a further 3 d. After these differentiation steps, the cells were maintained in DMEM with 4500mg/L glucose, 10% (v/v) FBS, Glutamax and P/S as previously described until the cells fully differentiated into adipocytes. Prior to each experiment successful differentiation was confirmed by morphological examination of the cells under light microscopy and oil red O (Sigma, Australia) staining to visualise lipid droplets. Cells were only used for further experiments when differentiation rates of 60% or higher were achieved.

2.1.5.3 Staining of 3T3-L1 adipocytes with oil red O

Oil red O staining solution was prepared freshly by mixing 3 parts of 0.5 % (v/v) oil red O in isopropanol (Sigma, Australia) with 2 parts of normal saline and filtering through a 0.2 µm filter (Minisart, Sartorius, USA). Adipocytes were fixed in oil red O staining solution for 20 min, washed twice with normal saline and examined under a light microscope. Adipocytes could be recognised easily by characteristically red coloured lipid droplet inclusions whereas pre-adipocytes do not contain lipid droplets and hence did not stain (see Figure 1).

2.1.6 Culture of Vero (African green monkey kidney epithelial) cells

Vero cells (ATCC, CCL-81, kindly donated by David Williams, School of Pharmacy) were cultured in R-5 and grown to around 90% confluency before being passaged 1/10 using 0.25% trypsin-EDTA.

2.1.7 Culture of L929 mouse fibroblasts

L929 cells (ATCC, CCL-81) were cultured in R-10 to around 90% confluency and passaged 1/10 using 0.25% (v/v) trypsin-EDTA.

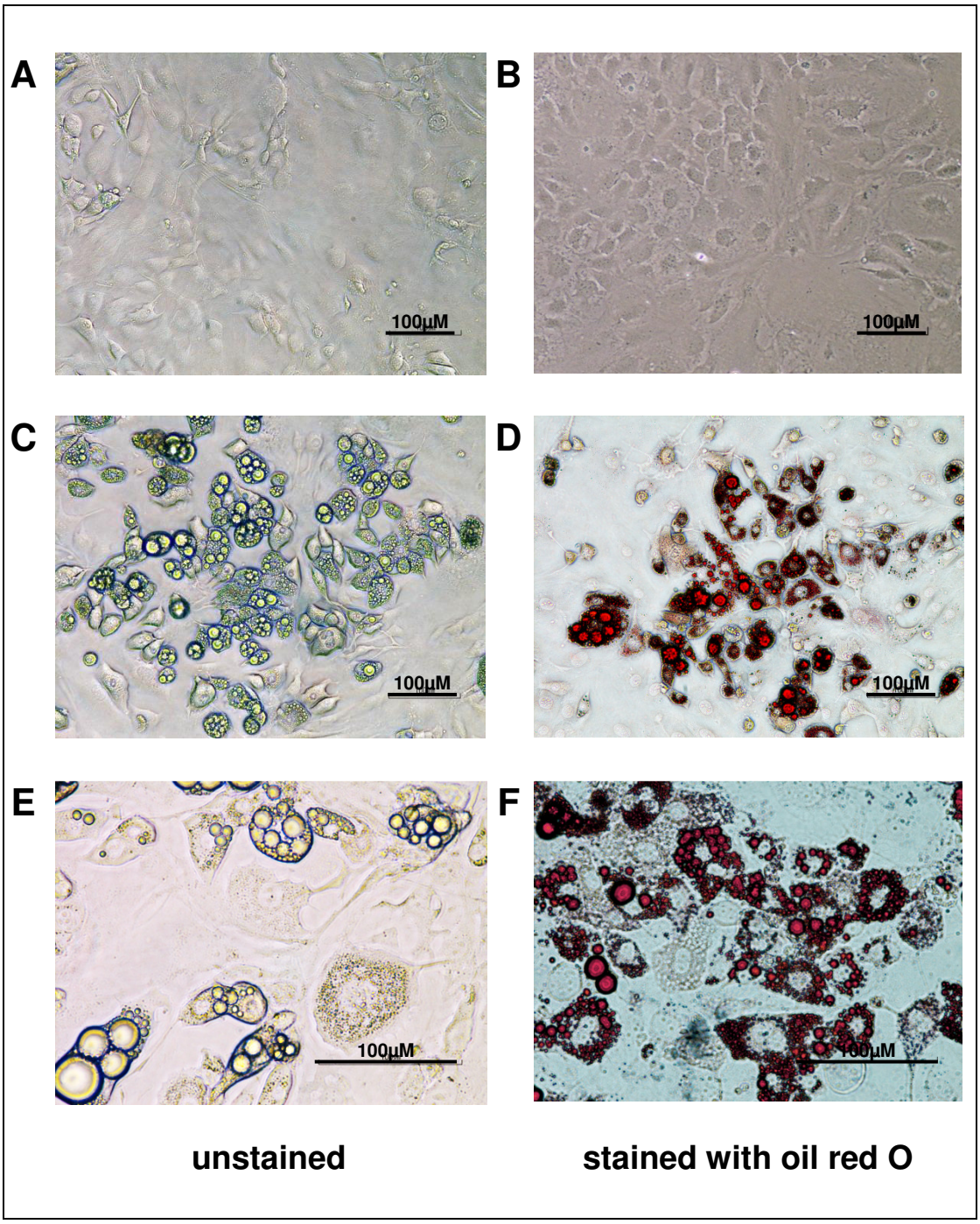

Figure 1: Differentiation of 3T3-L1 cells into adipocytes

Representative photomicrographs of 3T3-L1 pre-adipocytes prior to differentiation (A and B) and at day 10 of differentiation (C to F). (C) and (E) show characteristic morphology of unstained adipocytes with visible lipid droplets in the cytosol. Treatment with Oil Red O stain coloured the lipids droplets red (D and F). All monolayer photographs were taken with an inverse phase contrast microscope at 25x (A to D) or 40x magnification (E and F).

2.2 Virus culture

2.2.1 Ross River Virus strains

Ross River Virus (RRV) strains DC5692 and DC7194 were sourced from the Arbovirus Surveillance group at the Microbiology Department, University of Western Australia. RRV DC5692 is one of the early strains derived from *Aedes vigilax* in Western Australia, whereas RRV DC7194 was initially isolated in Queensland but is now found throughout Australia (Table 4). Virus was propagated as stated below and stocks were kept at -80˚C and thawed immediately before propagation or infection assays as needed.

RRV strain T48 was sourced from Dr David Williams (Curtin University, Western Australia). Stocks were grown as described and used for subsequent experiments. Early literature suggests to generate the T48 strain RRV by *in vitro* transcription of the plasmid pRR64 which encodes the full-length T48 cDNA clone (Kuhn et al., 1991), but considering the low divergence of RRV strains over large periods of time this was not deemed necessary (Sammels et al., 1995). The strain donated by Dr David Williams had initially been derived from the pRR64 plasmid and was passaged only few times in Vero cells.

Table 4: Virus strains

Virus strain	Area of initial isolation	Source
RRV DC5692	Western Australia (Faragher et al., 1988)	Arbovirus Surveillance group (Microbiology Department, University of Western Australia)
RRV DC7194	Southwest Australia (Faragher et al., 1988)	Arbovirus Surveillance group (Microbiology Department, University of Western Australia)
RRV T48	Townsville, Queensland (R. Doherty et al., 1963)	Dr David Williams (Curtin University)

2.2.2 Propagation of Ross River Virus

For virus propagation, Vero cells were grown in T75 flasks with R-10 until fully confluent. The supernatant was removed and 1000 µL of RRV stock with a $TCID_{50}$ of 10^6 or above was added to each tissue culture flask (MOI = 1). The flasks were kept at 37°C and gently rocked every 10 min to enhance virus distribution and adhesion. After 1 hr a further 8 mL of R-2 was added and the flasks were kept at 37˚C and 5% (v/v) CO_2. When strong cytopathic effect was apparent (usually after 2-3 d) the supernatant was centrifuged at 1500 x g for 5 min. Aliquots of 1000 µL were stored at -80˚C and thawed immediately prior to infection assays or determination of the viral titre via tissue culture infective dose assay.

2.2.3 Tissue Culture Infective Dose 50% assay ($TCID_{50}$)

The Tissue Culture Infective Dose 50% ($TCID_{50}$) assay was used to determine virus concentration and viral titre was calculated using a formula established by Reed/Munch (Mahy & Kangro, 1996; Reed & Muench, 1938).

To measure virus concentration, 96 well plates were seeded with $1x10^5$ Vero cells per well in 100 µL R-2 and kept at 37˚C in 5% (v/v) CO_2 for the cells to adhere. After 2 hr, 50 µL of a 10-fold serial dilution of virus stock in R-2 was added to each well with a minimum of 6 replicates for each dilution step. To an additional 6 wells, culture medium without virus was added as negative control. The plates were monitored for cytopathic effect (CPE) in the following days and all wells with visible CPE were marked. As confirmation, the supernatant was removed after 4 d and 100 µL of a 0.05% (w/v) solution of crystal violet (Sigma, Australia) in water was added to each well. After staining for 20 min the crystal violet solution was aspirated and the plates were washed twice with tap water. Wells without CPE were stained dark violet.

According to the number of wells with CPE at each dilution the concentration of active virus was calculated using the Reed-Muench method as described by Mahy and Kangro (Mahy & Kangro, 1996).

2.2.4 Virus heat inactivation

Heat inactivated virus was used in mock infections as a negative control. For inactivation, virus stocks were kept in a water bath at 65˚C for 1h and then frozen in aliquots. Inactivation efficiency was tested in preliminary experiments to assess a suitable time and temperature (Figure 2).

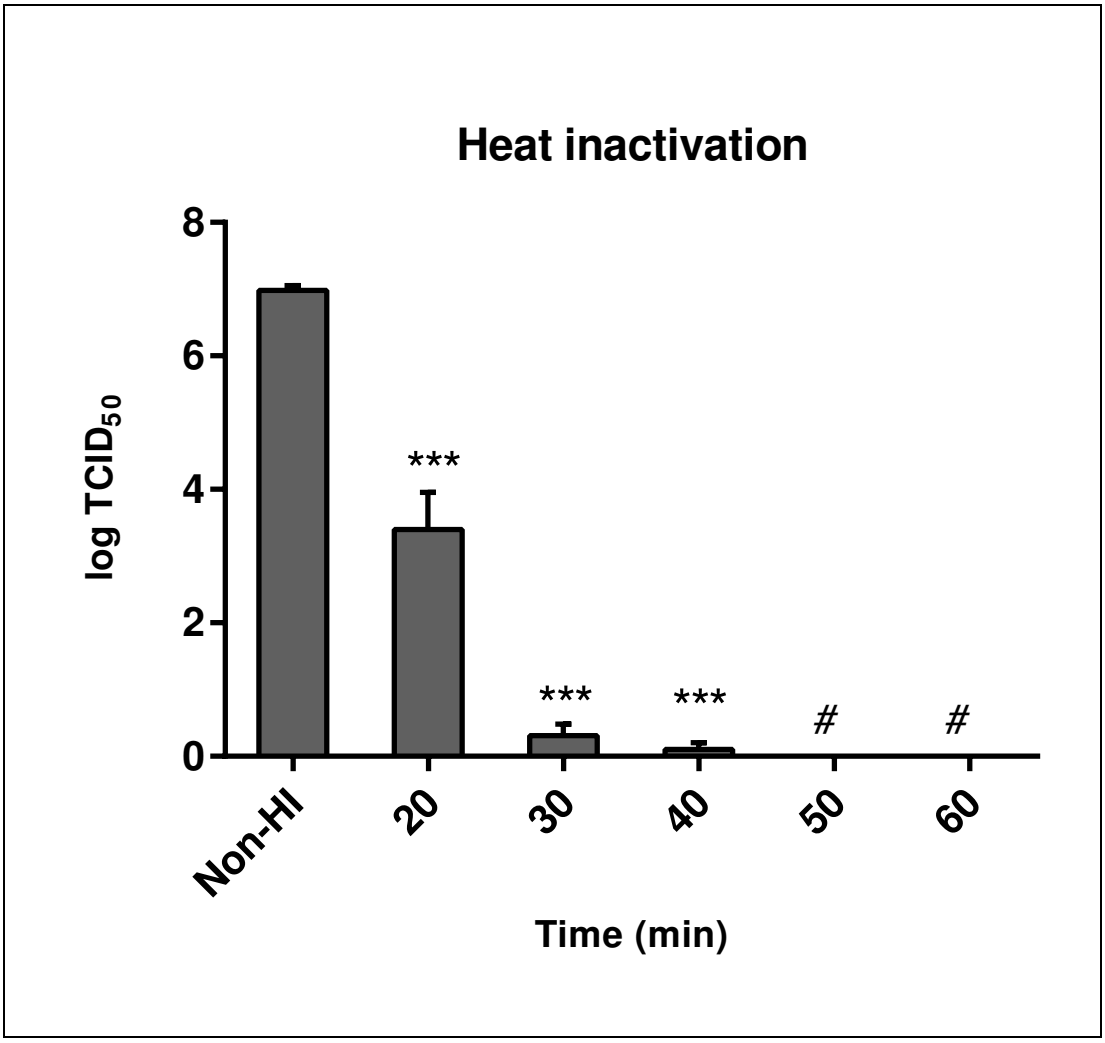

Figure 2: Heat inactivation of RRV DC7194 stock

RRV DC7194 stock was kept in a water bath at 65˚C and samples were taken at regular time intervals and a $TCID_{50}$ assay was performed on each sample. Non-HI = non-heat treated virus stock; # no CPE was detected; Viral load is expressed as log $TCID_{50}$ and data is shown in mean values ± SEM (n=4). ***($p \leq 0.001$) as determined by one-way ANOVA compared to non-heat treated virus.

2.3 Infection assays

Unless stated otherwise, cells were seeded at specified numbers as indicated in Table 5 for virus infection assays and kept at 37˚C and 5% CO_2 (v/v) in a humidified incubator. After 12 hr the media was aspirated and replaced with fresh culture medium. Appropriate dilutions of inhibitors and virus were added at the same time unless stated otherwise. Some wells only contained media or were challenged with heat inactivated RRV as negative controls. Positive control wells were treated with lipopolysaccharide (LPS) from *E.coli* (Sigma, Australia) where appropriate. Inhibitors were prepared as stock solution in ethanol (Thermo Fisher Scientific, Australia) or dimethyl sulphoxide (DMSO) (Sigma, Australia) and diluted in R-2 as required. A vehicle control with ethanol or DMSO only was included in each experiment.

Table 5: Tissue culture plates and cell numbers

Cell line	Culture media	Cell number / volume of supernatant		
		6 well plate	***12 well plate***	***24 well plate***
RAW264.7	R-2	$8x10^5$ / 2000 µL	$4x10^5$ / 1000 µL	$2x10^5$ / 500 µL
C2C12	R-2	$4x10^5$ / 2000 µL	$2x10^5$ / 1000 µL	$1x10^5$ / 500 µL
3T3-L1	D-10	confluent / 2000 µL	-	-

2.4 Cell viability assays

2.4.1 Trypan blue exclusion stain

Trypan blue exclusion stain was performed routinely for cell counting and establishing cell viability prior to experiments. Cells were used at viability rates of ≥ 90%.

Prior to seeding, 20 µL of cell suspension was added to 20 µL of 0.4% (w/v) trypan blue (Sigma, Australia) solution in sterile saline. Cells were either counted manually using a Neubauer haemocytometer under a light microscope or with an automated cell counter (Countess, Invitrogen, USA).

2.4.2 MTT viability assay

A stock solution of 5 mg/mL 3-(4,5-dimethylthiazol-2-yl)-2,5-diphenyl tetrazolium bromide (MTT) (Sigma-Aldrich, Australia) was prepared by dissolving 200 mg MTT in 40 mL of phosphate buffered saline (PBS). The solution was filter sterilised and stored at 4^{o}C for up to 1 month protected from light. For each assay, three 96 well plates were seeded with 100 µL of cell suspension in R-2 at a concentration of $1x10^4$ cells per well for RAW264.7 or $5x10^3$ cells per well for C2C12. The plates were kept at 37˚C and 5% (v/v) CO_2 for 24 hr after which 100 µL of test solution was added. Either 2- or 10-fold serial dilutions in R-2 were prepared for inhibitors or drug diluent and assayed in triplicates. Each plate included a negative control with only R-2.

At times 0, 24, and 48 hr the supernatant of one plate was aspirated and 100 µL of a 1/5 (v/v) dilution of MTT stock in R-2 was added to each well. After incubation for 1 hr at 37˚C, the supernatant was aspirated. Cells were then solubilised with 100 µL DMSO and the absorbance at 595 nm was determined. Cell viability was calculated for each dilution in relation to the untreated control wells.

2.4.3 Lactate dehydrogenase assay

To verify cell viability in each experiment a Lactate dehydrogenase (LDH) assay (Cayman Chemical Company, LDH Cytotoxicity Assay kit) was performed as per manufacturer's instructions.

Briefly, LDH reaction buffer was prepared freshly by mixing NAD^+, Lactic Acid, INT and reconstituted diaphorase in assay buffer. A volume of 100 µL of sample supernatant or freshly prepared LDH standard in serial dilution was transferred to a 96 well plate in duplicate and a further 100 µL of the reaction buffer was added to each well. The plate was incubated for 30 min at RT with gentle agitation. After incubation the absorbance at 490 nm was measured and LDH levels were calculated using the standard curve obtained.

2.5 Reverse Transcription PCR

2.5.1 mRNA extraction with TRI Reagent®

mRNA was extracted from cell monolayers using TRI Reagent® (Sigma-Aldrich, Australia) according to the manufacturer's instructions. In brief, appropriate amounts

of TRI Reagent® were added to tissue culture vessels and the cell lysate was homogenised via trituration. For mRNA extraction, a volume of 0.1 mL of 1-bromo-3-chloropropane (Sigma-Aldrich, Australia) per 1 mL of TRI Reagent® was added to the lysate and the mixture was shaken vigorously. After standing for 5 min at RT the samples were centrifuged at 12,000 x g for 15 min for complete phase separation. The upper aqueous phase was transferred to a new tube containing 0.5 mL isopropanol (Sigma, Australia) per 1 mL TRI Reagent® and mixed thoroughly. After 10 min resting on ice the samples were centrifuged at 12,000 x g for 10 min. The supernatant was carefully discarded and the RNA pellet was washed with 1 mL of ethanol per 1 mL of TRI reagent® used. After brief air drying at RT the RNA pellets were dissolved in water (UltraPure water, PCR grade, Fisher-Biotec, Australia) and the RNA concentration was determined with a BioSpec-nano (Shimadzu, Japan).

2.5.2 DNAse digestion

Prior to reverse transcription, mRNA was treated with RQ1 DNAse (Promega, USA) according to the manufacturer's instruction to remove contaminating DNA. In brief, 5 µg of sample RNA was mixed with 1 µL RQ1 DNAse 10x buffer (Promega, USA) and 2.5 µL RQ1-DNAse (Promega, USA) and adjusted to a volume of 10 µL with PCR grade water. The mixture was kept at 37˚C for 30 min, then 1 µL of RQ1 DNAse stop solution (Promega, USA) was added to each tube and the samples were incubated for a further 10 min at 65˚C.

2.5.3 Reverse transcription of mRNA

First strand cDNA synthesis was performed using a High Capacity cDNA Reverse Transcription kit (Applied Biosystems, USA) according to manufacturer's instructions. In brief, 2 µL of digested RNA mix was added to dNTP Mix (4 mM), RT buffer, random primers, MultiScribe^{TM} Reverse Transcriptase and PCR grade water (Fisher-Biotech, Australia). Reverse transcription was performed by heating the mixture for 10 min at 25°C, followed by 120 min at 37°C and 5 min at 85°C. cDNA was used immediately for PCR or stored at -20°C.

2.5.4 Polymerase chain reaction (PCR)

Polymerase chain reaction (PCR) was performed with 1 µL of cDNA in 12.5 µL reactions containing Taq-Ti DNA Polymerase buffer (Fisher Biotec, Australia), 2 mM $MgCl_2$ (Fisher Biotec, Australia), 200 µM dNTP (Promega, USA), 200 nM primer mix (see Table 7) and 0.5 units of Taq-Ti DNA-polymerase (Fisher Biotec, Australia) in

PCR grade water. For each set of reactions one tube without cDNA template was added as a non-template control. All newly transcribed cDNA samples were initially screened for G3PDH as a house-keeping gene to validate successful RNA extraction and transcription.

PCR amplifications were performed in a Veriti Thermocycler (Applied Biosystems, USA) using the conditions outlined in Table 6. The appropriate number of cycles was determined for each primer in initial experiments (data not shown). Final cycle numbers for each gene are shown in Table 7 (unless stated otherwise).

Table 6: Conditions for RT-PCR

Step		Time	Temperature
1) Initial denaturation		3 min	95˚C
2) Cycling #	Denaturation	20 sec	95˚C
	Annealing	20 sec	60˚C
	Extension	60 sec	72˚C
3) Final extension		5 min	72˚C

Cycle numbers for each gene are given in Table 7 (unless stated otherwise)

2.5.5 Primer design

Primers were constructed according to references listed in Table 7. Where no reference is given, primers were designed using Primer-BLAST (Basic logical Alignment Search Tool) provided by the National Centre for Biotechnology Information (NCBI) and Primer 3 software (Whitehead Institute and Howard Hughes Medical Institute). All self-designed primers were based on mouse mRNA sequences derived from the NCBI Genebank database. Primer pairs were chosen to give a PCR product with a length of 200-500 base pairs. All primers were commercially synthesized by Geneworks Australia, reconstituted in DNAse-free water (Fisher-Biotech, Australia) upon arrival and stored at -20˚C. Prior to use the primer sequence and product size for each primer pair was confirmed with Primer-BLAST.

2.5.6 Agarose gel electrophoresis

Amplified PCR products were visualised by agarose gel electrophoresis. 10 µL of PCR product was diluted with 2 µL of DNA loading buffer containing 0.25 % (w/v) bromophenol blue (Sigma, Australia), 0.25% (w/v) xylene cyanol (Sigma, Australia) and 15% Ficoll (type 400) polymer (Sigma, Australia) in ultra-pure water (Fisher Biotech, Australia) and pipetted into wells of a freshly prepared 2% (w/v) agarose gel (Agarose, Fisher-Biotec, Australia; in Tris-Acetate-EDTA buffer). A 100 base pair DNA ladder (Geneworks, Australia) was added to each gel to verify the size of each amplified gene product. Gels were run in an electrophoresis chamber (BioRad, USA) at 80 V for 55 min in Tris-acetate-EDTA buffer (40 mM tris(hydroxymethyl)aminomethane, Fisher Scientific, Australia; 20 mM Acetic acid, Fisher Scientific, Australia; 1 mM EDTA, Ajax Laboratories, Australia; adjusted to pH 8). After electrophoresis, the gel was stained for 30 min in the dark with 0.003% (v/v) GelRed® (Biotium, USA) in tris-acetate-EDTA buffer and then photographed with a KODAK EDAS DC120 (KODAK, USA) or Quantum ST4 Imaging system (Vilber Lourmat, France) under UV light. Unless stated otherwise, all representative photographs of agarose gels were derived from conventional RT-PCR. Semi-quantitative densiometrical analysis was performed using the program ImageJ developed by the National Institutes of Health, USA. A ratio of the density of the cytokine PCR product to the density of the respective G3PDH product was used to compare various samples for semi-quantification. As cycle numbers of cytokines often differed from cycle numbers for G3PDH, the densiometric ratio is not absolute and only gives an indication on up- or downregulation of cytokine mRNA expression.

Table 7: RT-PCR primer sequences and cycle numbers

Gene	Primer sequence		Product size	Number of PCR cycles	Reference / Genebank Accession number
	forward (5'-3')	reverse (3'-5')			
Mouse G3PDH	ACCACAGTCCATGCCATCAC	TCCACCACCCTGTTGCTGTA	452	35	(Paulukat et al., 2001)
Mycoplasma	ACACCATGGGAGYTGGTAAT	CTTCWTCGACTTYCAGACCCAAGGCAT	450	35	(Harasawa et al., 2005)
RRV-E2	GCGCGAATTCGTAGTGTAACAGAGCACTT	GCGCGAATTCCTGCGTTCGCCCTCGGTGCG	247	35	(Mahalingam & Lidbury, 2002)
Murine cytokines and chemokines					
HMGB1	ATGGGCAAAGGAGATCCTAA	CTCTGTAGGCAGCAATATCC	490	30	NM_031140
HMGB2	TACCCAGGTGTGGGGATTTA	TGCCCTCTCTCTACCTTCCA	228	30	NM_008252.3
HMGB3	GCGCTGTGATTGACACATCT	AATGCCTTGTCACACCAACA	248	30	NM_008253.3
IL-6	TGCTGGTGACAACCACGGCC	GTACTCCAGAAGACCAGAGG	308	30	(Wesselingh et al., 1994)
IL-10	CAGCCGGGAAGACAATAAC	TCATTTCCGATAAGGCTTGG	191	30	NM_010548.2
IL-18	GACAGCCTGTGTTCGAGGAT	TTTCAGGTGGATCCATTTCC	195	30	NM_008360.1
IL-28β	CTCTGTCCCCAAAAGAGCTG	GTGGTCAGGGCTGAGTCATT	214	40	NM_177396.1
IL-33	GCTGCGTCTGTTGACACATT	GACTTGCAGGACAGGGAGAC	202	35	NM_001164724.1
iNOS	CCTGTGTTCCACCAGGAGAT	GTCCCTGGCTAGTGCTTCAG	249	35	NM_0100927
MCP-1	CAGCACCAGCCAACTCTCACT	AAGGCATCACAGTTCGAGTCA	519	35	NM_011333
MIF	CACCATGCCTATGTTCATCGTGAACA	AGCGAAGGTGGAACCGTTCCA	349	40	NM_010798
TNFα	CCTGTAGCCCACGTCGTAGC	TTGACCTCAGCGCTGAGTTG	374	30	(Wesselingh et al., 1994)

2.6 Cytokine Real-time Polymerase chain reaction

A quantitative analysis of mRNA expression was performed by real time PCR analysis using SensiMix SYBR No-ROX Kit (Bioline, Australia) according to the manufacturer's instructions. In brief, 12.5 µL of SensiMix was mixed with 9.25 µL nuclease free water, 1.25 µL of 5 µM primer mix (see Table 7) and 2 µL of cDNA as prepared in 2.5.3. Two 10 µL aliquots of each reaction mix were analysed in duplicate in a Viia 7 (Life Technologies, Thermo Fisher, Australia) under given conditions (Table 8). A non-template control (NTC) and a 10-fold serial dilution of cDNA were included for each cytokine. G3PDH was used as 'housekeeping' gene and each cytokine sample was normalised against its corresponding G3PDH value. Analysis was performed with Viia 7 software and ratios of mRNA expression were calculated with Microsoft Excel 2010. Only normalised values were used to compare and calculate up- or down-regulation of cytokine mRNA expression.

Table 8: Real-time PCR conditions

Step		Time	Temperature
1)	**Initial denaturation**	3 min	95˚C
2)	**Cycling x 40**		
	Denaturation	20 sec	95˚C
	Annealing	20 sec	60˚C
	Extension	60 sec	72˚C
3)	**Final extension**	5 min	72˚C

2.7 ELISA

ELISA assays (Table 9) were performed according to manufacturer's instructions. Briefly, capture antibody was diluted to the working concentration in PBS, pipetted into a 96 well ELISA plate (Nunc Maxisorb, Nunc, Denmark) and kept at RT overnight. This step was not necessary for the HMGB1 ELISA since the kit includes a pre-coated plate. The ELISA plates were washed three times with 0.05% (w/v) Tween 20 (Sigma, Australia) in PBS (ELISA wash buffer) and 100 µl of sample or standard were added to the empty wells in duplicate or triplicate. Supplied standards were diluted in 1% (w/v) bovine serum albumin (BSA) (Serana, Australia) in PBS and at least 5 different concentrations were used to generate a standard curve. After

incubation for 2 hr at RT the plates were washed three times with ELISA wash buffer and 100 µL of capture antibody diluted to the working concentration in 1% (w/v) BSA in PBS was placed in the well. The plates were incubated for a further 2 hr at RT, washed twice with ELISA wash buffer and 100 µL of Horseradish-peroxidase-streptavidin diluted to the working concentration in 1% (w/v) BSA in PBS was added. The plates were kept at RT in the dark for 20 min, washed twice as previously and developed with 100 µL of substrate solution (TMB ready-to-use substrate, ELISA systems, Australia). After 20 min, 50 µL of 2 N sulphuric acid (Sigma Aldrich, Australia) was added to stop development and the plates were read at 450 nm on a multi plate reader.

Table 9: ELISA kits

Cytokine	ELISA kit	Cat number
TNFa	R&D Systems -Mouse TNFa ELISA Duo Set	DY 410
IL-6	R&D Systems -Mouse IL-6 ELISA Duo Set	DY406
IL-10	R&D Systems -Mouse IL-10 ELISA Duo Set	DY417
MIF	R&D Systems -Mouse MIF ELISA Duo Set	DY1978
HMGB1	Shino-Test HMGB1 ELISA kit	ST51011
PGE_2	Cayman Prostaglandin E_2 EIA kit – monoclonal	514010

2.8 Phagocytosis assay

For the phagocytosis assay, heat inactivated, fluorescein isothiocyanate (FITC) (Sigma, Australia) labelled *Escherichia coli* (ATCC 25922) or *Staphylococcus aureus* (ATCC 29213) bacteria were used. *E.coli* was chosen as a representative gram negative bacteria and *S.aureus* as a representative Gram positive bacteria.

2.8.1 Culture of bacteria

Mueller-Hinton (MH) broth (Oxoid, England) was prepared according to the manufacturer's instructions and autoclaved. Bacterial stock was kept at -80˚C in 20% (v/v) glycerol (Sigma, Australia) in Mueller-Hinton broth. *E.coli* or *S.aureus* stocks were thawed as needed and added to 10 mL MH broth and placed on an orbital shaker at 37˚C. Bacterial cultures were grown to an optical density (λ = 600nm) of approximately 0.8 for *E.coli* or 1.0 for *S.aureus*, which indicates an exponential growing phase for the bacteria. The culture was then centrifuged at

2500 x g for 15 min and the supernatant discarded. The bacterial pellet was resuspended in 5 mL PBS and the bacteria heat inactivated at 65˚C for 1 hr and mixed every 15 min. After heat inactivation the solution was cooled to RT and centrifuged. The pellet was washed with 5 mL PBS and resuspended in 1 mL PBS and stored at 4˚C. To verify heat inactivation, a 50 µL sample was streaked on Mueller-Hinton agar and the plate kept at 37˚C. If no growth was seen after 48 hr, the heat inactivated bacteria was labelled with FITC and used for phagocytosis assays.

2.8.2 FITC labelling of heat inactivated bacteria

Heat inactivated bacteria were incubated with 0.5 mL of 0.1% (w/v) FITC in 50 mM $NaHCO_3$ and 100 mM NaCl per 1 mL of bacterial suspension in the dark. After 20 min at RT, the suspension was centrifuged at 2500 x g for 15 min, the supernatant was discarded and the pellet washed twice with 10 mL of cold PBS and re-suspended in 5 mL of cold PBS. A 20 µL sample was observed under fluorescence (Fluorescence microscope Olympus DP71) to verify FITC labelling. Labelled bacteria suspension was kept in the dark at 4˚C for up to 1 week.

2.8.3 Phagocytosis assay – Fluorescent microscopy

RAW264.7 macrophages were resuspended in R-5 at $1x10^5$ cells/ml. 100 µL of this cell suspension was carefully pipetted onto sterile 13mm square glass cover slips in 6 well plates. Plates were kept in an incubator at 37˚C and 5% (v/v) CO_2 for cells to adhere and after 1 hr a further 1800 µL of R-5 was carefully added. Cells were incubated at 37˚C and 5% (v/v) CO_2 and exposed to culture medium or RRV suspension at an MOI of 1 for 48, 24 or 0 hr prior to the phagocytosis assay. At the beginning of the assay, the supernatant was removed and replaced with 1800 µL of fresh R-5. At appropriate times 200 µL of FITC labelled bacteria suspension was added to the cells and the plate incubated at 37˚C and 5% (v/v) CO_2. After 4 hr the supernatant was aspirated and the cells washed twice with 2 mL of cold PBS. Samples were fixed on ice with 800 µL/well of 4% (w/v) Paraformaldehyde (Electron Microscopy Services, USA) in PBS and the nuclei stained with 10 µL/well of propidium Iodide solution (1 mg/mL in water; Sigma, Australia). After 30 min the supernatant was discarded and the fixed cells were washed twice with ice cold PBS. Cover slips were examined under fluorescence (Olympus IX50) and photos taken with an attached Olympus DP71 digital camera. All steps involving FITC labelled

bacteria were carried out with minimum exposure of the samples to light to prevent bleaching.

2.8.4 Phagocytosis assay – Flow cytometry

RAW264.7 macrophages were resuspended at $1x10^6$ cells/mL in R-5 and 1000 µL of this cell suspension was seeded in 5 mL teflon pots to avoid adhesion. The plates were incubated at 37˚C and 5% (v/v) CO_2 and 100 µL of culture medium or RRV suspension was added 0, 24 or 48 hr prior to the phagocytosis assay. At appropriate time points, 200 µL of FITC labelled bacteria suspension was added to the wells and the plate was further incubated at 37˚C. After 4 hr the cells were resuspended in the supernatant and immediately transferred to 1.5 mL eppendorf tubes on ice. After centrifugation at 1000 x g for 10 min at 4˚C the supernatant was aspirated and the cells washed with 1 mL of cold PBS. After further centrifugation the supernatant was discarded and the cells fixed with 800 µL 4% (w/v) paraformaldehyde (Electron Microscopy Services, USA) in PBS. Nuclei were stained with additional 10 µL propidium Iodide (1 mg/mL in water). After 30 mins incubation on ice the cells were centrifuged and washed with 1 mL of cold PBS and resuspended in 1 mL of PBS. Samples were immediately analysed with a flow cytometer (Attune Flow cytometer, Applied Biosciences, USA). Analysis of raw data was performed with FlowJo (Version X, Tree Star Inc.) flow cytometric data analysis software.

2.9 L929 bioassay for TNFα

L929 bioassays were performed to determine bio-concentration and biological activity of TNFα (Evans, 2000; Hogan & Vogel, 1988, 2001). L929 fibroblasts were cultured to 90% confluence and trypsinised to dislodge. Cells were resuspended in R-5 at $5x10^5$ cells/mL and this suspension was seeded to a 96 well plate at 100 µL/well (i.e. $5x10^4$ cells per well). Plates were incubated at 37˚C and 5% (v/v) CO_2 for 16 hr and supernatant aspirated and replaced with 50 µL/well of fresh R-5. A 50 µL aliquot of sample supernatant or TNFα standard (recombinant rat TNFα, Sigma, Australia) in R-5 were added in triplicate. For samples with high TNFα levels, appropriate dilutions of supernatant were also assayed. An aliquot of 50 µL of 4 µg/mL Actinomycin D (Sigma, Australia) in RPMI was added to each well and the plate was incubated at 37˚C. After 24 hr, the supernatant was aspirated and cells stained with 100 µL of 0.1% (w/v) crystal violet (Sigma, Australia) in 1% (v/v) acetic acid (Sigma, Australia) for 30 min. The plates were washed three times with tap

water and allowed to air dry for 3-4 hr. The cells were solubilised with 100 µL of 1% (w/v) SDS in water and absorbance measured at 595 nm on a multi plate reader. Preliminary tests showed that RRV present in the sample supernatants did not interfere with L929 viability (Figure 3).

2.10 Measurement of nitrite

Measurement of nitric oxide (NO) is difficult due to its rapid oxidation in aqueous solutions to nitrite (NO_2^-) (Ignarro et al., 1993). Nitrite however is more stable and can be measured in the supernatant of NO releasing cells using the Griess assay (L. C. Green et al., 1982).

For each assay the Griess reagent (1% (w/v) sulphanilamide (Labchem, Australia) and 0.1% (w/v) N-1-naphthylethylenediamine dihydrochloride (ICN Biomedicals Inc, USA) in 2.5% (v/v) orthophosphoric acid (Ajax Finchem, Australia)) was prepared fresh. An aliquot of 50 µL of supernatant or standard was dispensed into a 96 well plate in triplicate and 50 µL of Griess reagent was added to each well. Plates were incubated at RT protected from light for 10 min and the absorbance was measured within 30 min at 595 nm. The standard curve was prepared using 2-fold serial dilutions of a 1 µM sodium nitrite (ChemSupply, Australia) in R-2.

2.11 Statistical analysis

Quantitative data is expressed as mean values ± standard error of mean (SEM) unless stated otherwise. Statistical analysis was performed with Graphpad Prism (Version 6) by one- or two-way analysis of variance (ANOVA). For cytokine assays without treatment the values were compared to mock infected samples (negative control). Treatment experiments compared values to non-treated infection. A p-value ≤ 0.05 was considered statistically significant and significance levels are consistently expressed as *($p \leq 0.05$), **($p \leq 0.01$), ***($p \leq 0.001$) throughout this thesis. Dr Richard Parsons (statistician, Curtin University) was consulted for statistical analysis.

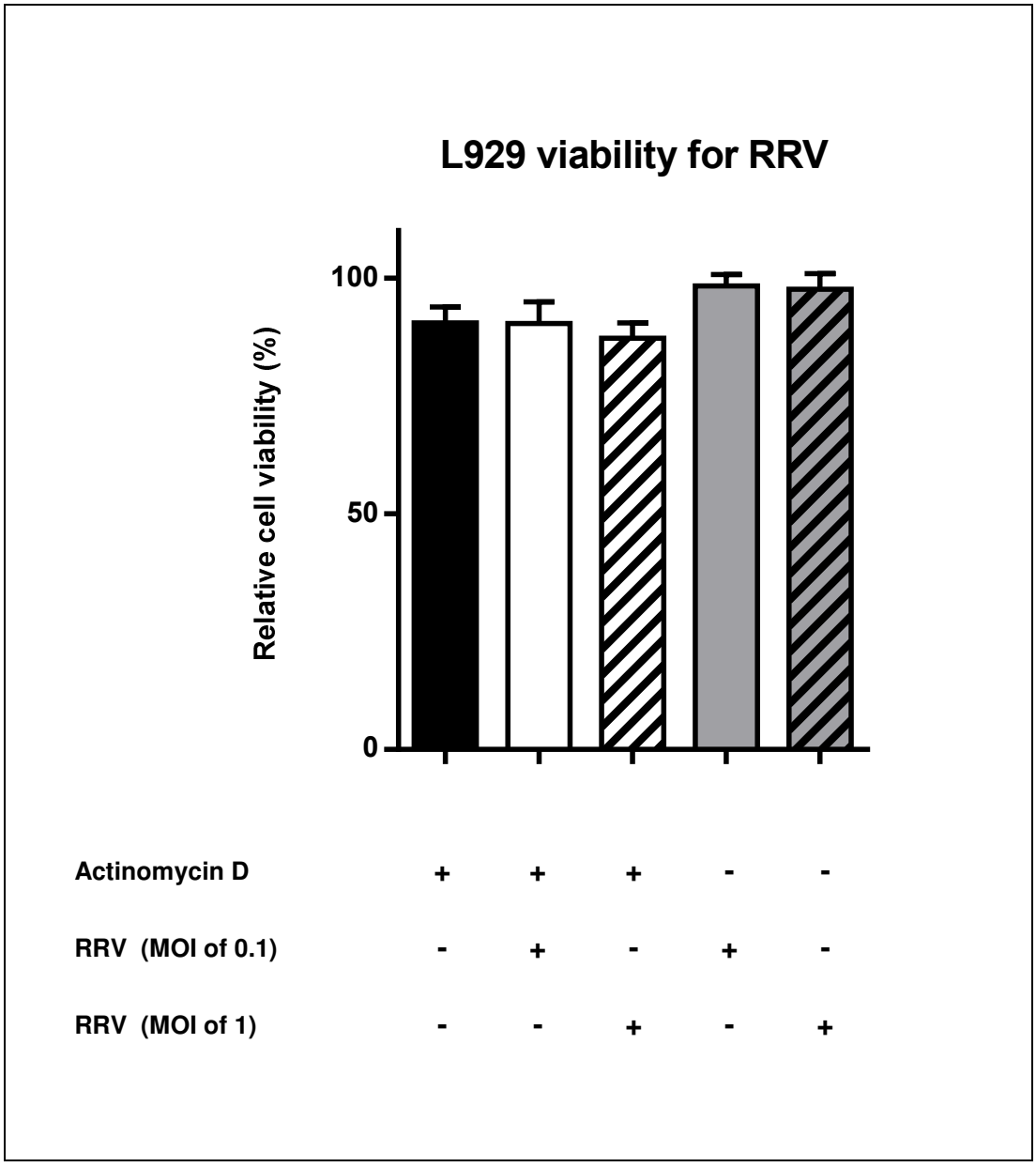

Figure 3: L929 cell viability after exposure to Ross River Virus

An L929 bioassay was performed with RRV DC7194 at an MOI of 0.1 and 1 with and without the presence of Actinomycin D. Non treated control cells were assigned a cell viability of 100%. Data shown is the relative cell viability compared to non-treated L929 cells and is expressed as mean value ± SEM (n=4). Statistical analysis by one-way ANOVA showed no significant change.

3. Results I: Differences in the pathology of various RRV strains

3.1 Introduction

Previous studies (Faragher et al., 1988) have compared the mouse-virulent RRV T48 strain and the mouse-avirulent NB5092 strain and showed that small genetic differences in the virus are responsible for the difference in virulence. The variation of genetic sequences in RRV strains was further investigated by Lindsay et al. (Lindsay et al., 1993) who reported that genomic differences were often linked to certain geographical regions. Sammels et al. (Sammels et al., 1995) confirmed and extended these findings by examining the nucleotide sequences of viral envelope 2 (E2) and envelope 3 (E3) genes in more detail. Numerous strains and their area of isolation were catalogued and it appeared that most genome groups are predominant in only small geographic regions. Some strains however could be isolated in various parts of the continent, indicating movement of the virus in either hosts or reservoirs. A connection between genome mutations and virulence could not yet be determined. Only more recently the genetic variations in the sequence of E2 and non-structural protein 1 (nsP1) genes were found to be responsible for the difference in virulence of RRV strains DC5692 and T48 (Jupille et al., 2013; Jupille et al., 2011; Stoermer Burrack et al., 2014). Apart from this work no other RRV strains have been investigated and compared in regards to virulence or pathology. As reviewed previously (Rulli et al., 2005), both duration and severity of Ross River Virus disease (RRVD) can vary considerably and it is possible that genetically different virus strains might contribute to this phenomenon.

In initial experiments we compared three RRV virus strains in order to investigate the influence of each strain on cellular pathology. RRV DC7194 and DC5692, kindly donated by the Arbovirus Surveillance group (Microbiology Department, University of Western Australia), were used with RRV T48 in preliminary investigations to determine which RRV strain would be the most appropriate for cytokine inhibitor experiments. Comparative tests for the three strains were carried out with regards to virus replication and cellular response to viral infection.

3.2 Cytopathic effect and viral replication of RRV strains T48, DC7194 and DC5692

RRV, like most other alphaviruses, has the ability to infect a variety of arthropod and vertebrate cells and cell lines and usually undergoes a cytolytic replication cycle in which virus titres increase repidly (Sharkey et al., 2001; Strauss & Strauss, 1994). This effect is utilised when growing virus stocks to high titre in Vero cells, resulting in cell lysis and virus release. To investigate if different RRV strains show variation in this cytopathic effect (CPE) and viral replication numbers, RRV T48, RRV DC7194 and RRV DC5692 were added to Vero cells at an MOI of 0.1 and cultures were observed daily for cytopathic effect. Supernatant was removed 3 d post-infection (p.i.) and examined for viral titres by tissue culture infective dose 50% assay ($TCID_{50}$). No visible difference in CPE was observed between the three virus strains however a difference was detected in viral titres in the supernatants as shown in Figure 4. Titres in the supernatants for T48 and DC7194 expressed in log $TCID_{50}$ were 6.72 ± 0.61 and 6.58 ± 0.51 respectively. The viral load in the supernatant for DC5692 was significantly ($p \leq 0.05$) lower with a log of 5.18 ± 0.55 as determined by one-way ANOVA. Both DC7192 and T48 consistently grew to higher titres in Vero cells as compared to DC5692.

3.3 Cytokine response by RAW264.7 macrophages in RRV infection

Infection of RAW264.7 macrophage cells with RRV results in the secretion of several cytokines, such as TNFα (Rulli et al., 2005) and MIF (Herrero et al., 2011). In order to examine whether the extent of cytokine release depends on the viral strain, RAW264.7 cells were exposed to RRV T48, DC7194 and DC5692 at an MOI of 4 and supernatant samples were taken 12 hr post-infection (p.i.) to determine the concentration of TNFα and IL-6 by ELISA. As shown in Figure 5, RRV T48 and RRV DC7194 induced high TNFα levels at 12 hr p.i. with concentrations reaching 2451 ± 103 pg/mL and 2140 ± 154 pg/mL respectively. RRV DC5692 induced significantly lower levels of TNFα with a concentration of 444 ± 69 pg/mL ($p \leq 0.001$) at 12 hr p.i. (Figure 5 A). As shown in Figure 5 B, IL-6 levels were analysed in parallel and showed that RRV T48 and RRV DC7194 increased IL-6 in the supernatant to 481 ± 32 pg/mL and 407 ± 18 pg/mL by 12 hr p.i., which was significantly higher than that induced by RRV DC5692, reaching 144 ± 18 pg/mL ($p \leq 0.001$). Exposure of RAW264.7 cells to RRV T48 or DC7194 induced a generally stronger cytokine response as compared to RRV DC5692.

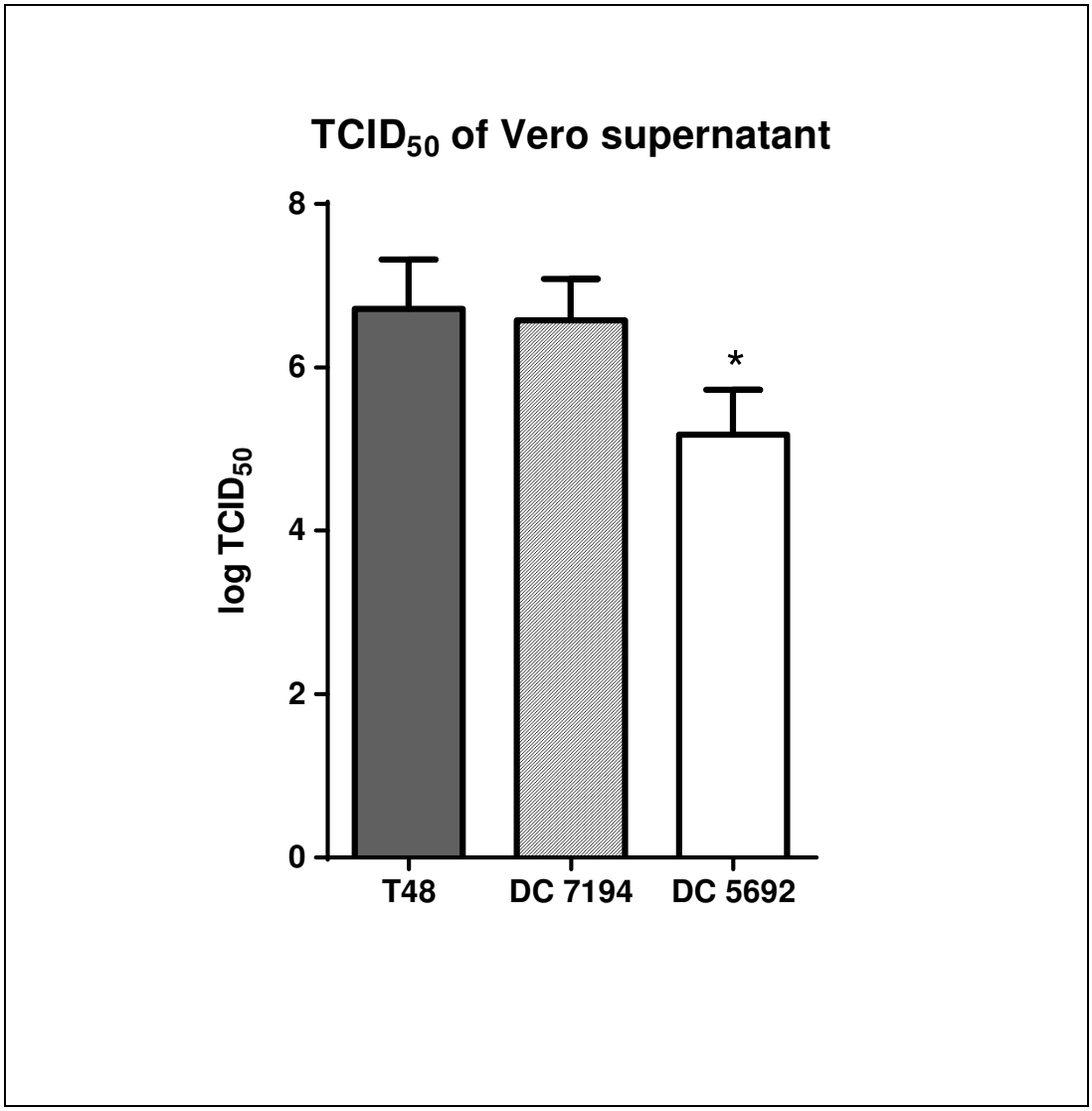

Figure 4: $TCID_{50}$ of the supernatant of Vero infected with various RRV strains

Vero cells were cultured to confluence, exposed to RRV strains T48, DC7194 and DC5692 at an MOI of 0.1 and observed daily for CPE. Supernatants were removed 3 d p.i. to determine viral titres via $TCID_{50}$ assay. Data shown are mean values ± SEM (n=4). *($p \leq 0.05$) as determined by one-way ANOVA compared to T48 or DC7194.

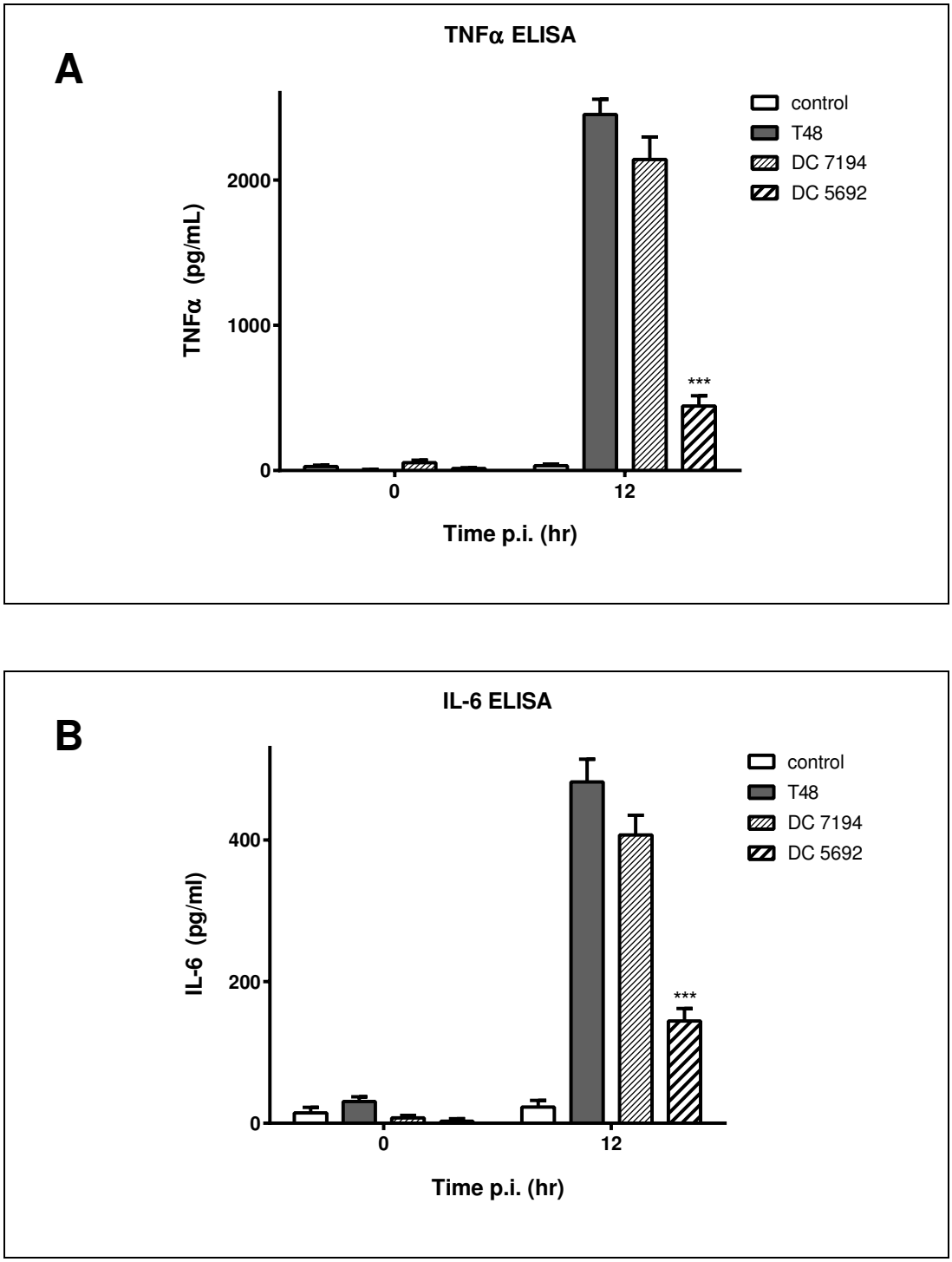

Figure 5: Cytokine release of RAW264.7 following infection with RRV strains

RAW264.7 macrophages were inoculated with RRV strains T48, DC7194 and DC5692 at an MOI of 4 and levels of TNFα (A) and IL-6 (B) were measured by ELISA at 0 hr and 12 hr post-infection. Data is expressed as mean values ± SEM (n=3). ***($p \leq 0.001$) as determined by one-way ANOVA compared to DC 7192 or T48. There was no significant difference between T48 and DC7194.

3.4 Influence of viral titres on cytokine response in infection of RAW264.7 macrophages with RRV

Viral titres in infection experiments are often expressed as multiplicity of infection (MOI), which is a numerical statement of the ratio of viruses to the number of target cells. The influence of different viral titre on the cellular response has been investigated for several viruses (Haas, 2004) and recent work by Chen et al. (W. Chen et al., 2014) has briefly investigated the response of osteoblasts exposed to RRV at varying MOIs. To examine the influence of virus titres on the magnitude of cytokine response from macrophages we infected RAW264.7 cells with RRV T48 at an MOI of 0.1, 1 or 10. Supernatant samples were taken at 12 and 24 hr p.i. and examined for TNFα concentration by ELISA (Figure 6 A) as well as bioassay (Figure 6 B). Measured cytokine levels did not show a significant difference between an MOI of 1 and an MOI of 10 at any time point for both assays. TNFα levels for an MOI of 10 and an MOI of 1 at 24 hr p.i. as measured by ELISA were not significantly different with 2255 ± 164 pg/mL and 2027 ± 117 pg/mL respectively. RRV at an MOI of 0.1 however resulted in significantly lower cytokine concentrations (1624 ± 120 pg/mL) compared to an MOI of 10 ($p \leq 0.01$). The TNFα concentration at 24 hr p.i. as determined by bioassay reached 1667 ± 121 pg/mL for an MOI of 10 and 1626 ± 230 pg/mL for an MOI of 1. An MOI of 0.1 gave a mean value of 1065 ± 132 pg/mL at 24 hr p.i., which was again significantly lower than the highest titre used ($p \leq 0.01$). Cell viability was determined for samples obtained 24 hr p.i. by LDH assay as outlined in Methods. Relative viability compared to non-treated cells in percent was 98.7 ± 1.2 for an MOI of 0.1, 94.7 ± 0.7 for an MOI of 1 and 90.7 ± 1.2 for an MOI of 10. A lower MOI of 0.1 gave less severe TNFα responses as compare to the higher MOI of 1 and 10. As expected, cell viability decreased with increasing MOI.

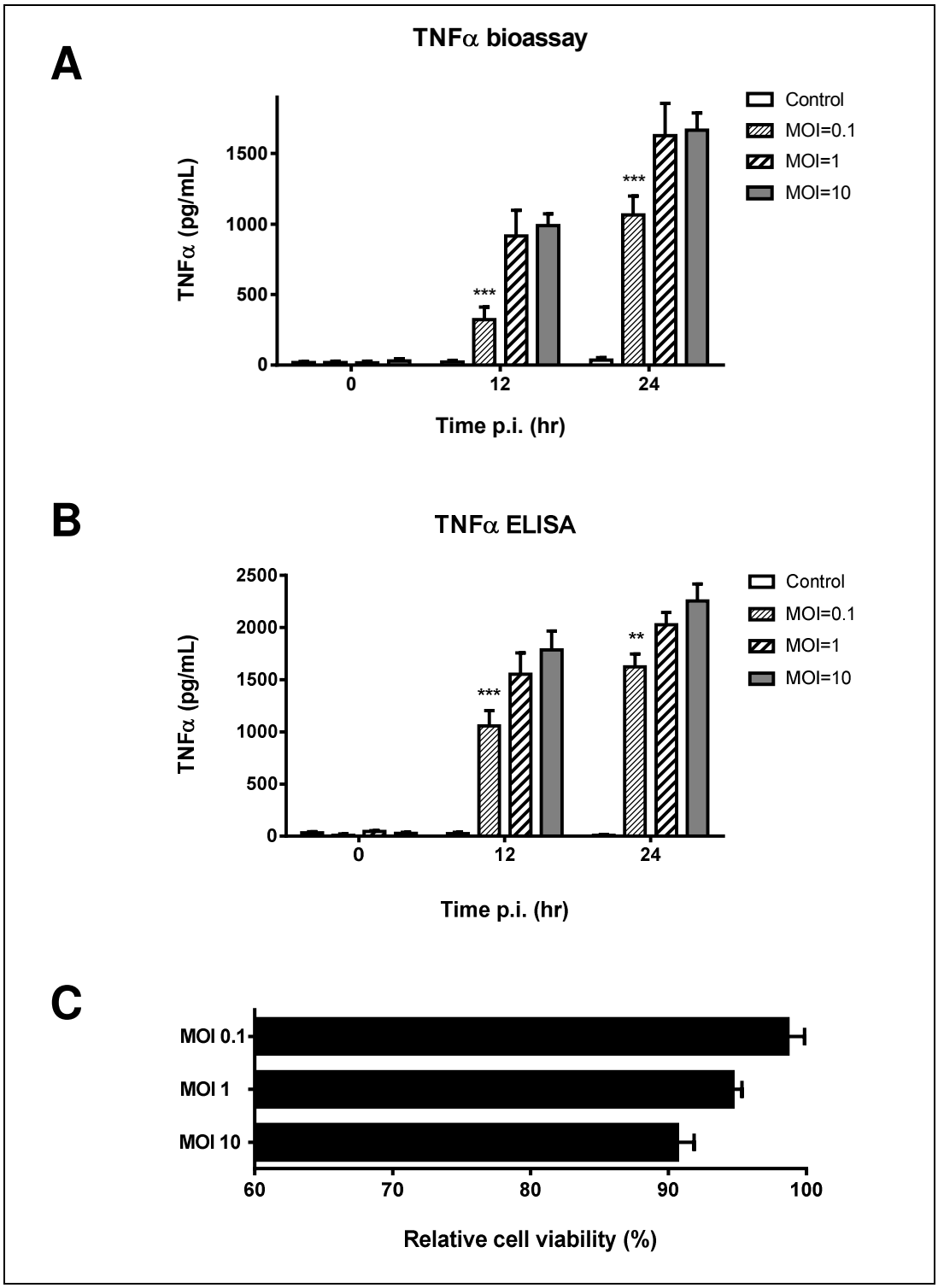

Figure 6: TNFα release from RAW264.7 infected with differing MOI of RRV T48

RAW264.7 macrophages were exposed to RRV T48 at an MOI of 0.1, 1 or 10. Supernatant samples taken at varying times were assayed for TNFα concentrations by ELISA (A) and TNFα bioassay (B). Cell viability at 24 hr p.i. was determined by LDH assay and expressed as relative viability compared to non-infected cells (C). Values are expressed in mean ± SEM (n=3). **(p≤0.01), ***(p≤0.001)

3.5 Discussion of preliminary results

RRV T48 and RRV DC5692 have previously been compared in a mouse model (Jupille et al., 2011) and DC5692 was reported to be mouse avirulent due to mutations in its genome sequence in the E2 and nsP1 region. We extended these findings *in vitro* with preliminary experiments showing that RRV DC5692 induces only weak cytokine responses in RAW264.7 macrophages as compared to RRV T48, as well as reduced characteristics in growth and cytolysis when incubated with Vero cells.

RRV DC7194 and RRV T48, which are both known to be mouse virulent, have shown very similar results in regards to viral titres when grown in Vero cells as well as TNFα and IL-6 release from infected RAW264.7 macrophages. Little is known about the genetic variation between these two strains but it may be assumed that their genetic variance in E2 and nsP1 is minimal. Research studies commonly utilise the T48 strain, which was one of the earliest RRV isolates, initially collected in North Queensland (R. Doherty et al., 1963; Lindsay et al., 1993) and considering the strong similarity of T48 and DC7194 in these initial experiments we continued to use RRV T48 only. An MOI of 1 was determined as optimal viral titre for infection assays with RAW264.7 macrophages since cellular responses were similar to an MOI of 10, however cell viability was consistently higher as determined by LDH assay. This needed consideration since some experiments were planned to run for up to 72 hr. RRV at an MOI of 0.1 produced a delayed response in TNFα release but seemed to reach similar cytokine levels as an MOI of 1 lagging approximately 12 hr behind. The delay is likely due to initial cytokine response being below the detection level and only after early cytolytic replication cycles the viral numbers increase enough to initiate a detectable response in the macrophages.

It was clearly noticeable that TNFα concentrations determined by bioassay showed a similar induction pattern although absolute concentrations seemed to be considerably lower compared to the results obtained by ELISA. The L929 bioassay uses recombinant rat TNFα as standard, which shares 97.4% homology with mouse TNFα protein (Kwon Ii et al., 1993). This difference in standard as well as possible loss of bioactivity of the samples or standards during storage likely causes that discrepancy between the two assays. ELISA assays can often still detect fragmented or denatured protein that lack bioactivity.

It should be noted that cell culture adaptive mutations have been reported for Sindbis virus, a member of the alphavirus genus (Klimstra et al., 1999), with significant differences in pathogenesis caused by those mutated viruses as compared to wild type isolates. To avoid these adaptive processes many researchers initially generate the T48 RRV strain by in vitro transcription of a cDNA plasmid initially constructed by Kuhn et al. (Kuhn et al., 1991) with further propagation in suitable cell lines. The T48 strain used in our experiments was kindly donated by Dr David Williams (Curtin University) and had low passage numbers in Vero cells after generation from the cDNA plasmid. To minimize the likelihood of mutations in the viral genome the initial virus stocks were prepared, aliquoted and kept in storage at -80˚C until use. Viral passages were kept to a minimum and did not exceed 8 passages in Vero cells. Despite the low divergence over time as reported by Sammels et al. (Sammels et al., 1995), adaptive mutations may be possible and can therefore not be excluded.

Another factor to consider is the cell line utilised for propagation of viral isolates. Commonly used cell lines for RRV are Vero cells or C6/36 mosquito cells (Jupille et al., 2013; Stoermer Burrack et al., 2014). Considering the natural transmission and reproduction of RRV in mosquito vectors, the use of C6/36 cells appears suitable, especially as it may mimic the naturally occurring step of replication in arthropods. Differences of mammalian and mosquito derived Sindbis viruses have been reported previously (Klimstra et al., 2003) and similarly Shabman et al. (Shabman et al., 2007) showed that mosquito-cell-derived RRV infected dendritic cells more efficiently as virus propagated in mammalian cells, however induced a less severe IFN response. This lack of IFN stimulation is attributed to the high mannose content of N-linked glycans on mosquito-derived viral E2 proteins as opposed to the complex glycans found on mammalian-derived virus.

To our knowledge it is not known whether RRV isolates differ in the induction of other cytokines which could therefore show variation in virus pathogenesis. Mosquito cell culture conditions greatly differ from conditions for most other cell lines and due to lack of suitable equipment we performed all virus propagation experiments using Vero cells.

4. Results II: Cellular response and cytokine production of RAW264.7 macrophages after RRV infection

4.1 Introduction:

As discussed previously, macrophages are known to play a pivotal role in inflammatory conditions found in arthritic and rheumatoid disorders and their ability to migrate and release pro-inflammatory cytokines is thought to contribute to progression of the local inflammation (Burmester et al., 1997; Kinne et al., 2000; Nathan, 1987). As an integral part of our innate immune system their general involvement in viral infections has been studied (Biron, 1998; Guidotti & Chisari, 2001) and Lidbury et al. (Lidbury et al., 2008) discussed their important role in the immune response to RRV infection. Macrophages can be found extensively in synovial linings of infected patients and mice and contribute to the characteristic joint inflammation in RRV infections. Considering these findings and the ability of macrophages to secrete an array of pro-inflammatory mediators, we decided to use RAW264.7 mouse macrophages to further investigate the cytokine network induced by RRV with the aim of identifying possible targets for pharmacotherapeutic intervention.

4.2 Infection of RAW cells with RRV

It has previously been demonstrated that RRV infect RAW264.7 macrophages despite the cells ability to produce antiviral cytokines (Lidbury & Mahalingam, 2000b; Lidbury et al., 2000). In order to evaluate successful infection under our conditions, RAW264.7 macrophages were incubated with RRV T48 at an MOI of 1 and samples of the supernatant were taken to be analysed for virus titres via $TCID_{50}$ assay. As shown in Figure 7 A, viral count decreased initially but started to increase again by day 2 post-exposure. To confirm that the virus had entered the cells, RNA was extracted at each time point and examined for expression of the RRV Envelope 2 (RRV-E2) gene (Figure 7 B). The primers used in the PCR were chosen to amplify the entire region of RRV-E2 (Mahalingam & Lidbury, 2002). A band on the electrophoresis gel can be seen in samples from 1 d p.i. onwards and confirmed, that RRV did infect and replicate in RAW264.7 macrophages.

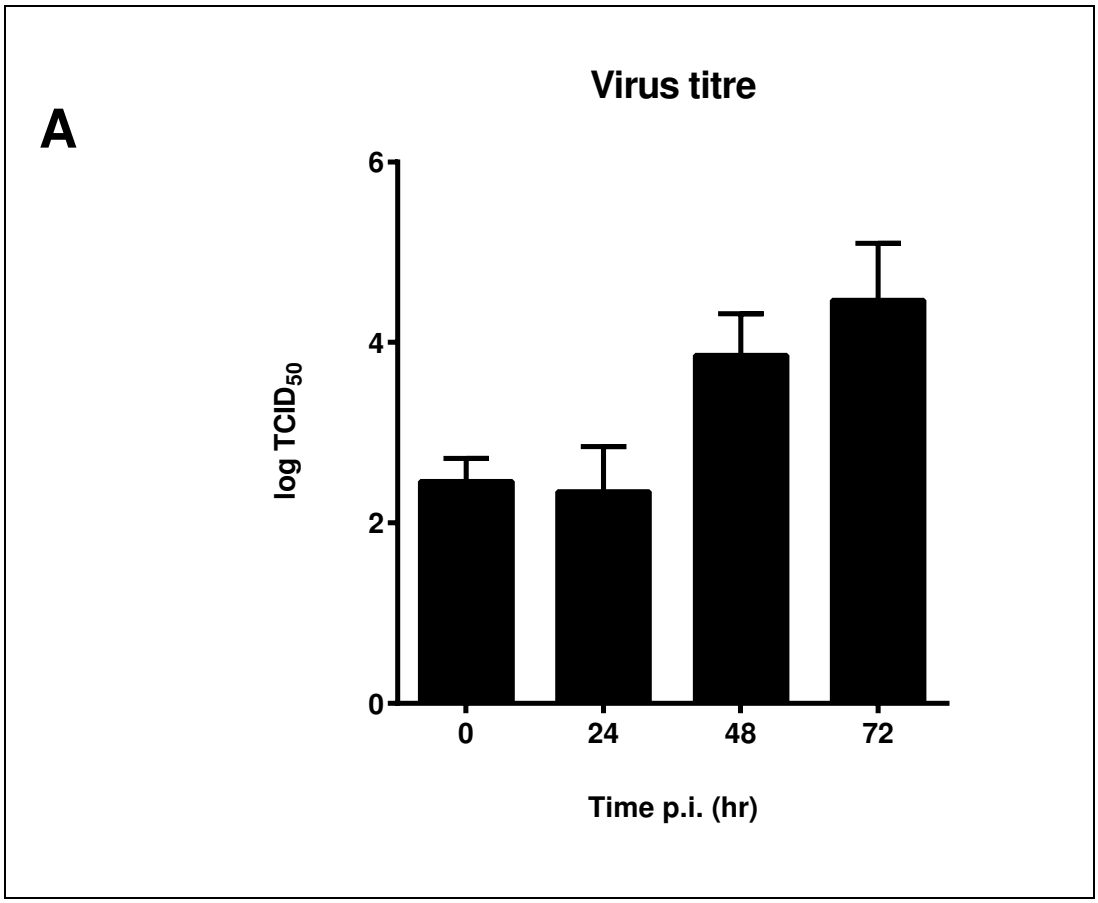

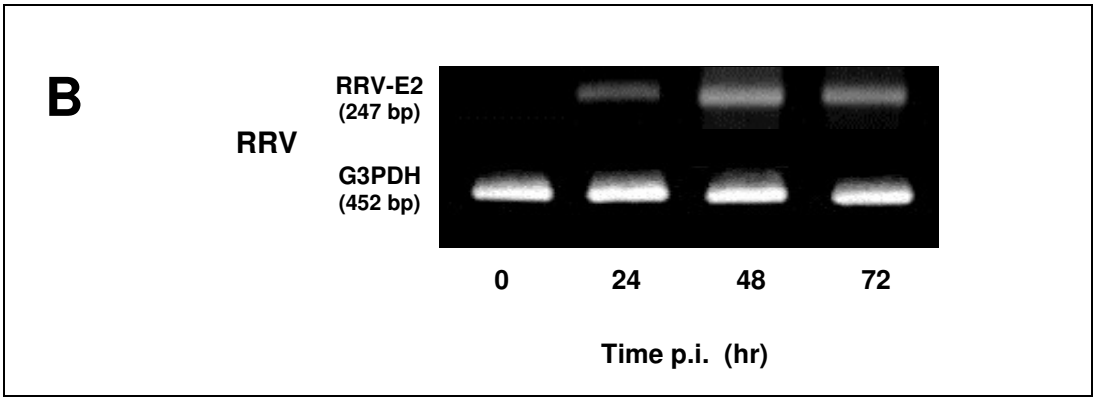

Figure 7: $TCID_{50}$ values of supernatant from RRV-infected RAW264.7 macrophages

RAW264.7 macrophages were infected with RRV T48 at an MOI of 1. Samples of the supernatant were taken at 0 hr, 24 hr, 48 hr and 72 hr post-infection and assayed for viral titres via $TCID_{50}$ assay (A). Values expressed are mean ± SEM (n=3). RNA was extracted at the same time points and expression of the viral E2 gene was determined by RT-PCR. (B) shows a representative photograph of the agarose gels (n=3).

4.3 Cytokine production of RAW264.7 following exposure to RRV

4.3.1 TNFα response to RRV infection

Lidbury et al (Lidbury et al., 2008) have shown that macrophages and the cytokines they release play an important role in RRV infection. Especially TNFα levels were found to be increased in plasma and synovial fluids of mice and humans with acute RRV infection (Iwamoto et al., 2008; Rulli et al., 2007).

In order to further investigate cytokine production of macrophages upon RRV infection, RAW264.7 cells were infected with RRV T48 at an MOI of 1 and supernatant samples were collected at suitable time intervals to determine TNFα concentration by ELISA and L929 bioassay. LPS (from *E.coli*) is known to induce TNFα secretion in RAW264.7 macrophages and was used as positive control (Beutler et al., 1985). As shown in Figure 8 A, a strong increase of TNFα concentration can be observed in the supernatant of RRV-infected cells in a time dependent manner to a level of 1673 ± 152 pg/mL by 12 hr p.i., with no significant change thereafter. To assess bioactivity of TNFα and to verify cytokine concentration, an L929 bioassay was performed (Figure 8 B). TNFα levels showed similar time dependent patterns of induction for the bioassay, however lower concentrations were detected with 1277 ± 120 pg/mL at 12 hr p.i. and 1640 ± 225 pg/mL at 24 hr p.i. As outlined in Methods, the significantly lower concentration of the bioassay as compared to the ELISA may result from a loss of bioactivity or the use of rat TNFα standard for the L929 assay. Both assays however confirmed an increase in TNFα secretion in RRV-infected RAW264.7 macrophages.

4.3.2 TNFα mRNA induction

To determine whether RRV infection induced TNFα mRNA expression, RAW264.7 cells were infected with RRV T48 at an MOI of 1 and mRNA was extracted at appropriate time points. Both quantitative real-time RT-PCR as well as conventional RT-PCR was performed to investigate expression of TNFα mRNA. Real time PCR data (Figure 9 A) shows up-regulation of TNFα mRNA expression in a time dependent manner with a maximum 3.24-fold increase at 24 hr p.i. This result was confirmed using conventional PCR as shown in Figure 9 B. Induction of TNFα mRNA could be detected as early as 4 hr p.i. for RRV and 2 hr post exposure for LPS. TNFα mRNA expression increased consistently up to 36 hr p.i. in RRV-infected RAW cells but peaked at 12 hr p.s. in LPS challenged macrophages.

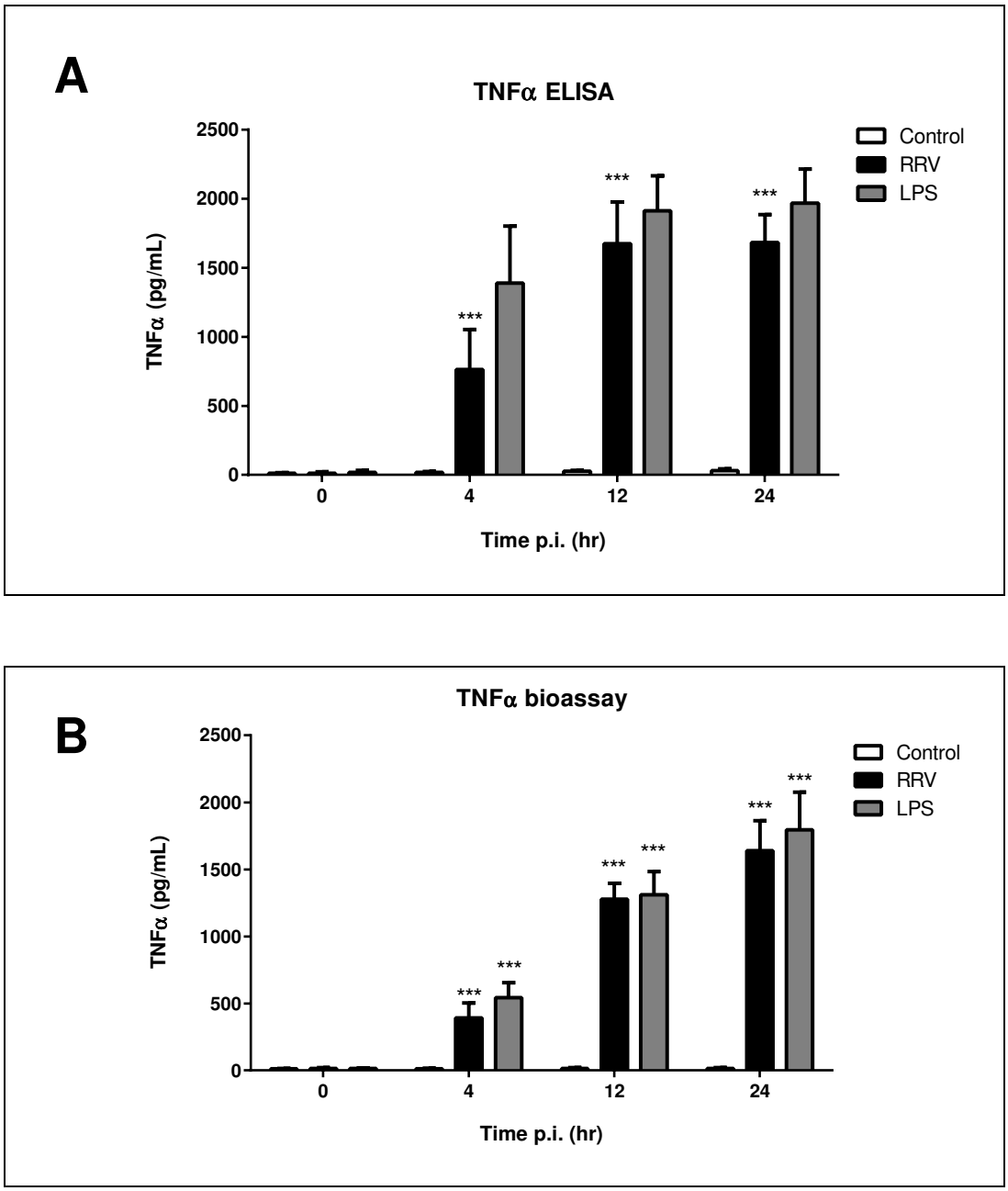

Figure 8: **Release of TNFα by RAW264.7 macrophages post RRV infection**

RAW264.7 macrophages were exposed to RRV DC7194 at an MOI of 1 or LPS (1 µg/mL) for varying periods of time and TNFα levels in the supernatant were determined via TNFα ELISA (A) and bioactivity of TNFα was tested in a L929-bioassay (B). Recombinant rat TNFα was used as standard for the bioassay. All values are expressed as mean ± SEM (n=4). ***($p \leq 0.001$) as determined by two-way ANOVA against controls (RAW264.7 mock infected with heat inactivated RRV).

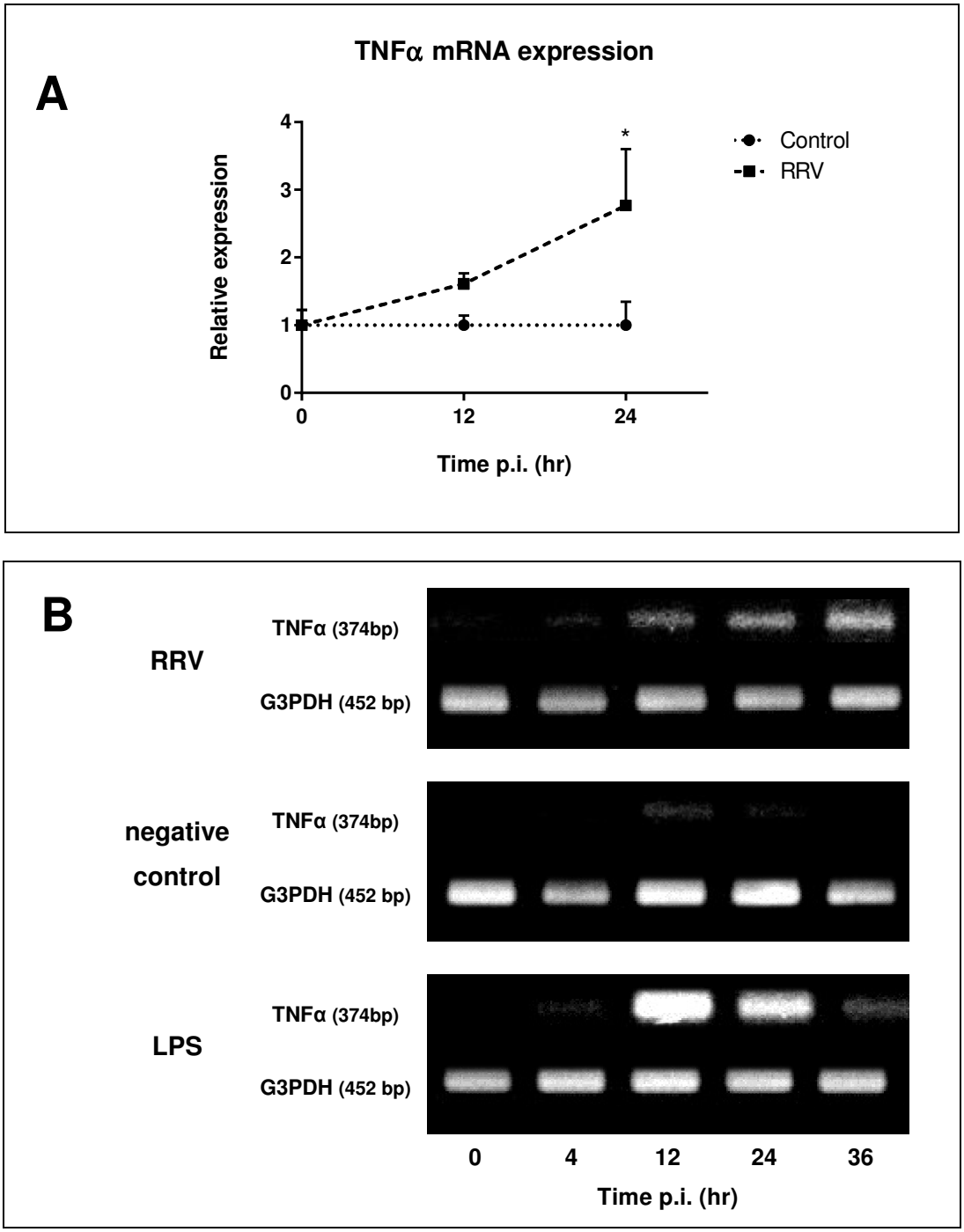

Figure 9: Increase in TNFα mRNA transcription post RRV infection

RAW264.7 macrophages were exposed to RRV T48 (MOI of 1) or LPS (1 µg/mL) for varying periods of time. Expression of TNFα mRNA was determined by quantitative real time PCR and the change of mRNA expression was graphed as the ratio of TNFα mRNA over TNFα mRNA in negative controls, which were exposed to HI-RRV. All data above is shown as mean + %CV (n=3), *(p≤0.05). (B) Shows representative photographs of agarose gels.

4.3.3 NO from RAW264.7 macrophages upon exposure to LPS or RRV

A Griess assay was performed on supernatant collected at appropriate time intervals from RRV T48-infected (MOI of 1) or LPS-stimulated (1 µg/mL) RAW264.7 cells (Figure 10). A significant increase of nitrite (NO_2^-) in the supernatant of LPS-treated macrophages could be detected as early as 12 hr p.i. At 36 hr p.i., NO_2^- levels were elevated to 30.93 ± 4.89 µM for cells treated with 1 µg/mL LPS (positive control). The supernatant of RRV-infected cells showed an slight increase of NO_2^- levels at 36 hr p.i., which was however not significant. It appears that RRV does not significantly induce the release of NO into the supernatant.

4.3.4 LPS induced NO secretion in RRV-infected RAW264.7 macrophages

Previous experiments showed that RRV did not induce significant NO secretion in RAW264.7 macrophages. In order to examine if RRV affects the ability of macrophages to secrete NO upon LPS stimulation, RAW264.7 cells were infected with RRV at an MOI of 1 for 0, 24 or 48 hr prior to stimulation with 1 µg/mL LPS. NO_2^- concentration in the supernatant was determined via Griess assay 24 hr post LPS stimulation (Figure 11). HI-RRV was used in mock infections with and without 24 hr LPS treatment as positive and negative control respectively. Macrophages infected with RRV at the start of the experiment (0 hr) and 24 hr prior showed no significant change in NO secretion upon LPS stimulation compared to mock infected macrophages, with concentrations reaching 40.91 ± 2.70 µM and 39.73 ± 1.92 µM respectively. Exposing RAW cells to RRV for 48 hr prior to LPS challenged significantly ($p \leq 0.001$) decreased NO secretion with levels of NO_2^- measured at 29.24 ± 2.52 µM. This indicates that infection with RRV reduces the NO response upon LPS stimulation in RAW264.7 macrophages.

4.3.5 Transcription of iNOS mRNA in RAW264.7 upon infection with RRV

To assess whether transcription of iNOS was induced, we performed both conventional RT-PCR as well as quantitative real time PCR on extracted mRNA using primers specific for iNOS mRNA. Expression levels for non-treated samples were below the detection limit of quantitative real-time PCR. Therefore a ratio of iNOS mRNA over the corresponding G3PDH mRNA was used in order to graph the change of cytokine mRNA transcription (Figure 12 A). Expression of iNOS mRNA could be detected as early as 4 hr p.i. with conventional RT-PCR and increased in a time dependent manner (Figure 12 B). Compared to NO_2^- in the supernatant, the onset of iNOS transcription was considerably early after exposure to RRV or LPS.

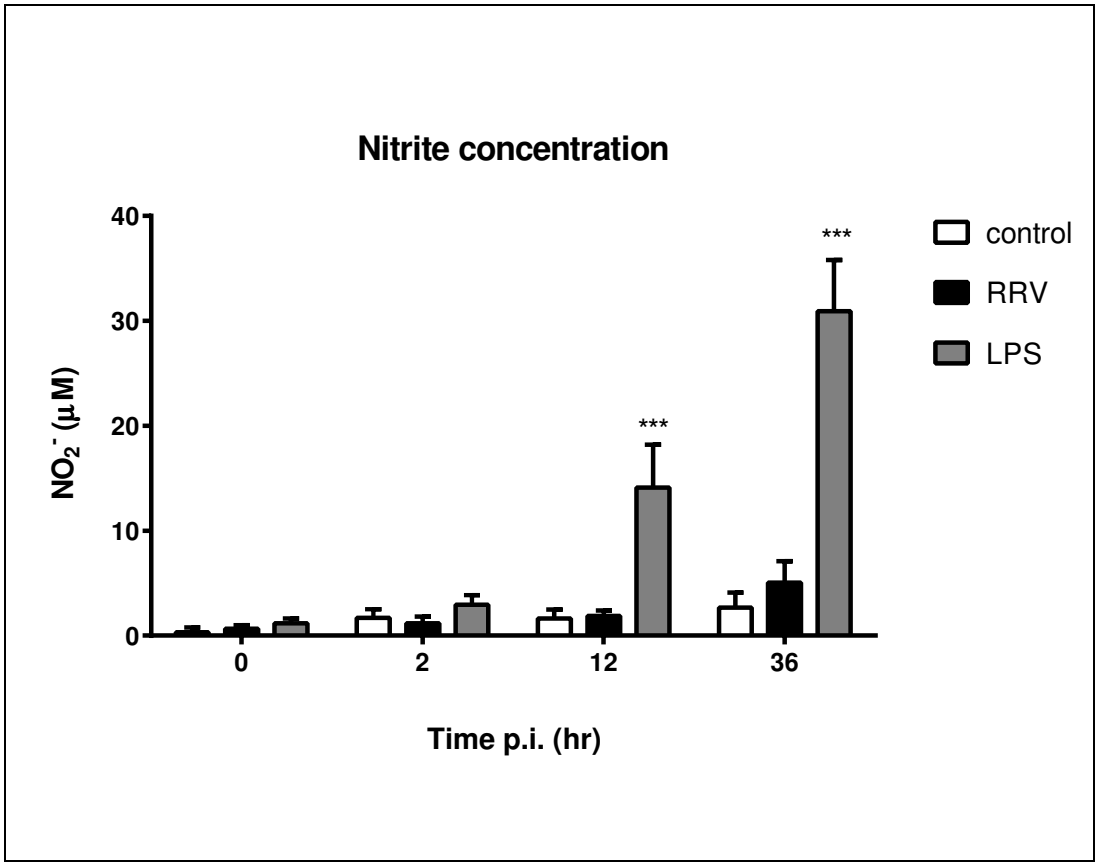

Figure 10: **Nitrite concentration in the supernatant of RAW264.7 cells post RRV infection**

RAW264.7 cells were exposed to RRV T48 at an MOI of 1 or LPS (1 µg/mL) and samples of the supernatant were assayed with Griess reagent for NO_2^- concentration at 0, 2, 12 and 36 hr post stimulation. Data shown are mean values ± SEM (n=4). ***(p≤0.001) for LPS stimulation compared to mock infected RAW264.7 cells (control).

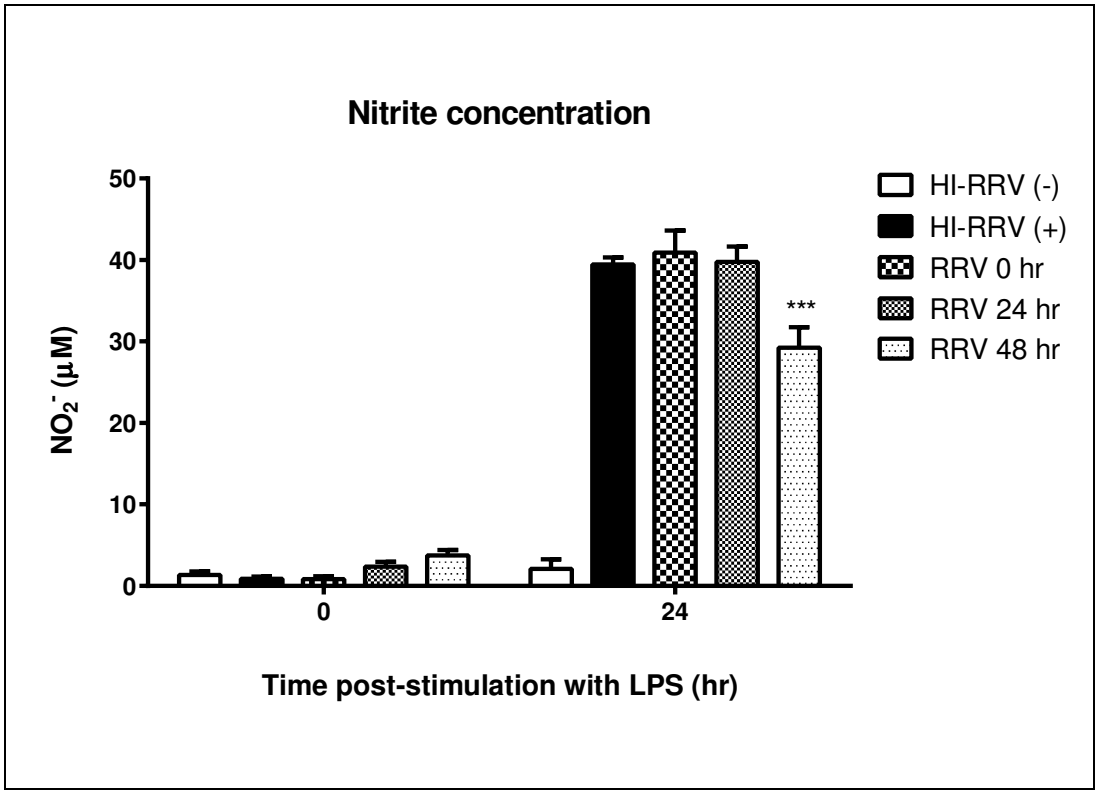

Figure 11: NO release from RAW264.7 macrophages infected with RRV prior to LPS stimulation

RAW264.7 macrophages were infected with RRV T48 at an MOI of 1 for 0, 24 and 48 hr prior to LPS (1 µg/mL) exposure. Controls were exposed to heat inactivated (HI) RRV 48 hr prior to experiment. Positive controls (HI-RRV(+)) were mock infected with HI-RRV and stimulated with LPS (1 µg/mL) whereas negative control wells (HI-RRV(-)) were mock infected with HI-RRV only. Supernatant samples were taken 24 hrs post stimulation with LPS and NO_2^- concentration was measured via Griess assay. Data is shown in mean values ± SEM (n=5 for RRV 48 hr, RRV 24 hr and RRV 0hr, n=4 for HI-RRV (+) and HI-RRV (-)). ***($p \leq 0.001$) Statistical analysis was performed by two-way ANOVA and compared to positive control (HI-RRV (+)).

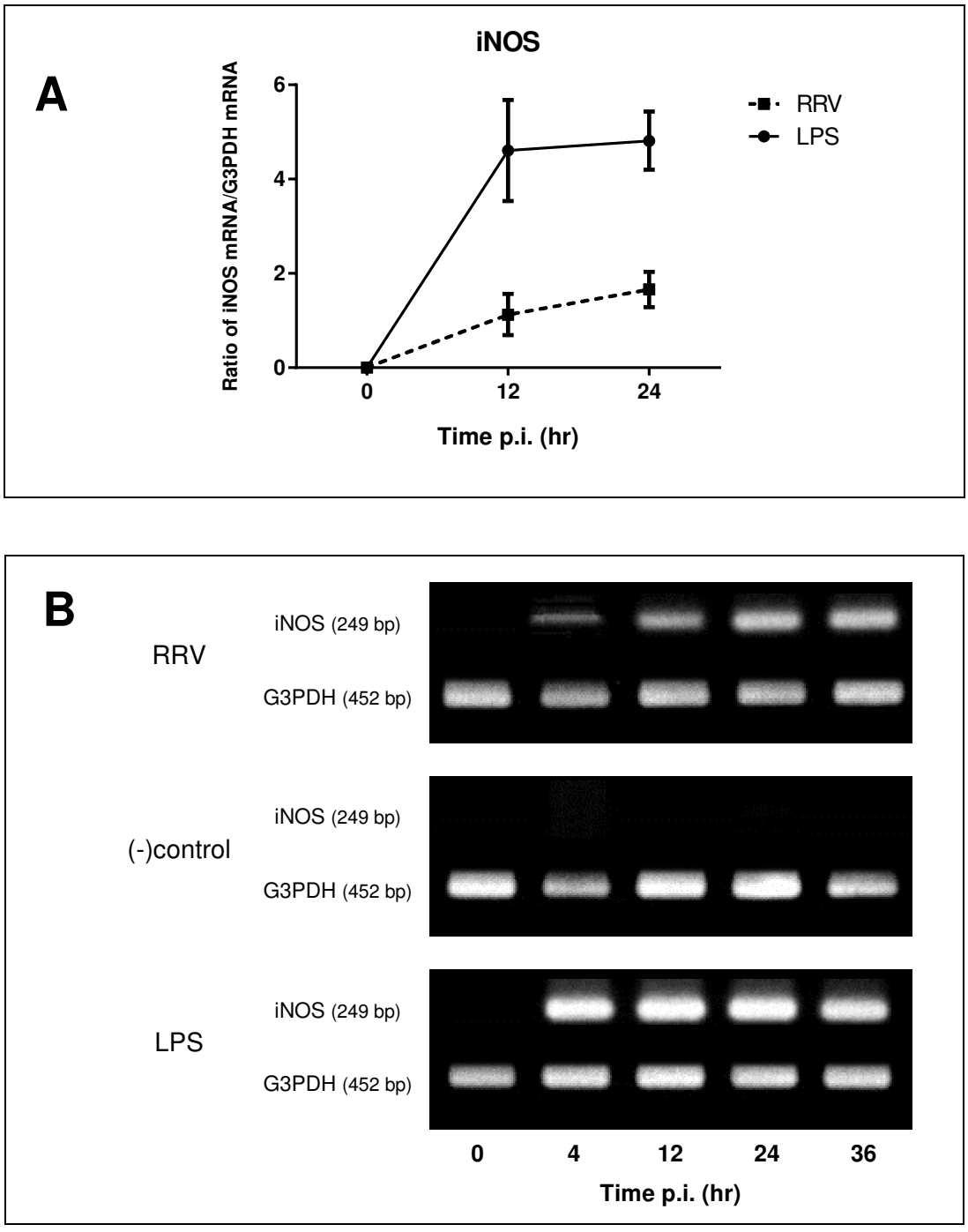

Figure 12: iNOS mRNA expression in RAW264.7 after exposure to RRV or LPS

RAW264.7 macrophages were exposed to RRV T48 (MOI of 1) or LPS (1 µg/mL) and mRNA was extracted at various times. (A) shows the ratio of iNOS mRNA over G3PDH mRNA expression as determined by real time PCR. Expression in control samples and treatment at 0 hr p.i. were below the detection level, thus the ratio of expression at 0 hr p.i. was allocated '0' by default. All data is expressed in mean values + %CV (n=3). (B) shows representative photographs of agarose gels (n=5).

4.3.6 IL-6 secretion from RRV-infected RAW264.7 macrophages

IL-6 has been previously reported to be induced in infections with various alphaviruses (Assuncao-Miranda et al., 2010; Chow et al., 2011). It appears however that it has so far not been investigated in RRV-infected cell lines (Assuncao-Miranda et al., 2013). To determine if RRV infection induces IL-6 secretion, RAW264.7 macrophages were exposed to RRV T48 at an MOI of 1 and supernatant samples were tested for IL-6 by ELISA (Figure 13). IL-6 could be detected in the supernatant from 2 hr p.i. onwards in RRV-infected cells and increased in a time dependent manner. By 36 hr p.i. the levels of IL-6 in RRV samples reached 567 ± 43pg/mL which was only marginally lower than levels in the supernatant of RAW cells stimulated with LPS at 1 µg/mL (644 ± 59 pg/mL). It is apparent that RRV significantly induces secretion of IL-6 in a time dependent manner.

4.3.7 Expression of IL-6 mRNA in RAW264.7 macrophages post RRV infection

In order to further investigate the increased production of IL-6, mRNA extracted from RRV-infected or LPS-stimulated RAW macrophages was screened for IL-6 mRNA. Interestingly, none of the RRV-infected macrophages showed increased IL-6 mRNA transcription. LPS stimulated RAW264.7 cells were used as positive control and showed significantly increased levels of IL-6 mRNA from 4 hr p.s. onwards peaking at 12 hr p.s. and decreasing thereafter (Figure 14), likely due to degradation of IL-6 mRNA.

4.3.8 MIF secretion in RAW264.7 macrophages upon RRV infection

A more recent study (Herrero et al., 2011) with mice highlighted the critical role of MIF in RRV induced arthritis *in vivo*. To investigate if MIF levels are elevated *in vitro* due to secretion of the cytokine by macrophages, we infected RAW264.7 cells with RRV and measured MIF concentration in the supernatant at various time points post-infection. LPS stimulated RAW cells were used as positive controls. As shown in Figure 15, an elevated concentration of MIF in the supernatant was detected by 4 hr p.i. increasing in a time dependent manner for both RRV- and LPS-treated samples with levels at 24 hr p.i. reaching 7765 ± 1657 pg/mL ($p \leq 0.001$) and 8230 ± 582 pg/mL ($p \leq 0.001$) respectively.

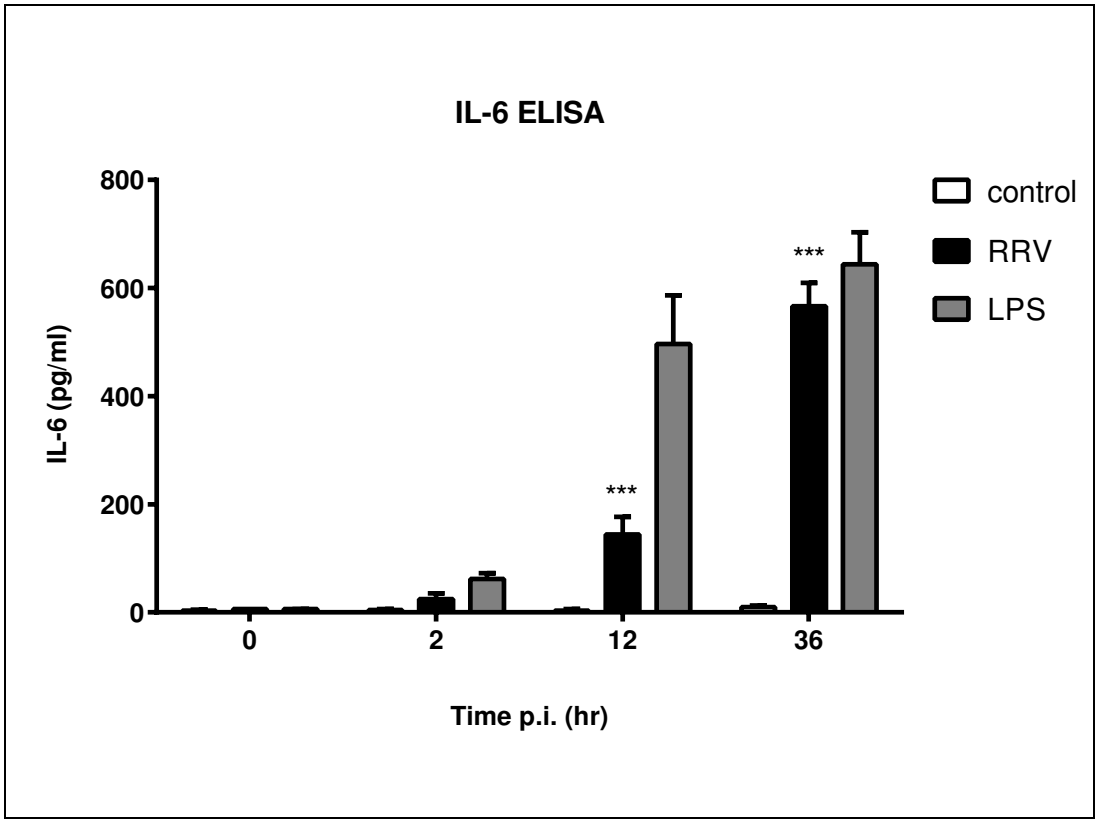

Figure 13: IL-6 secretion by RAW264.7 macrophages post RRV infection

RAW 264.7 macrophages were exposed to RRV T48 (MOI of 1) or LPS (1 µg/mL) for 0, 2, 12 or 36 hrs and supernatant was tested for IL-6 by ELISA. Heat inactivated RRV was used in mock infections as negative control. Data is expressed as mean values ± SEM (n=3). ***($p \leq 0.001$) compared to control as determined by two-way ANOVA.

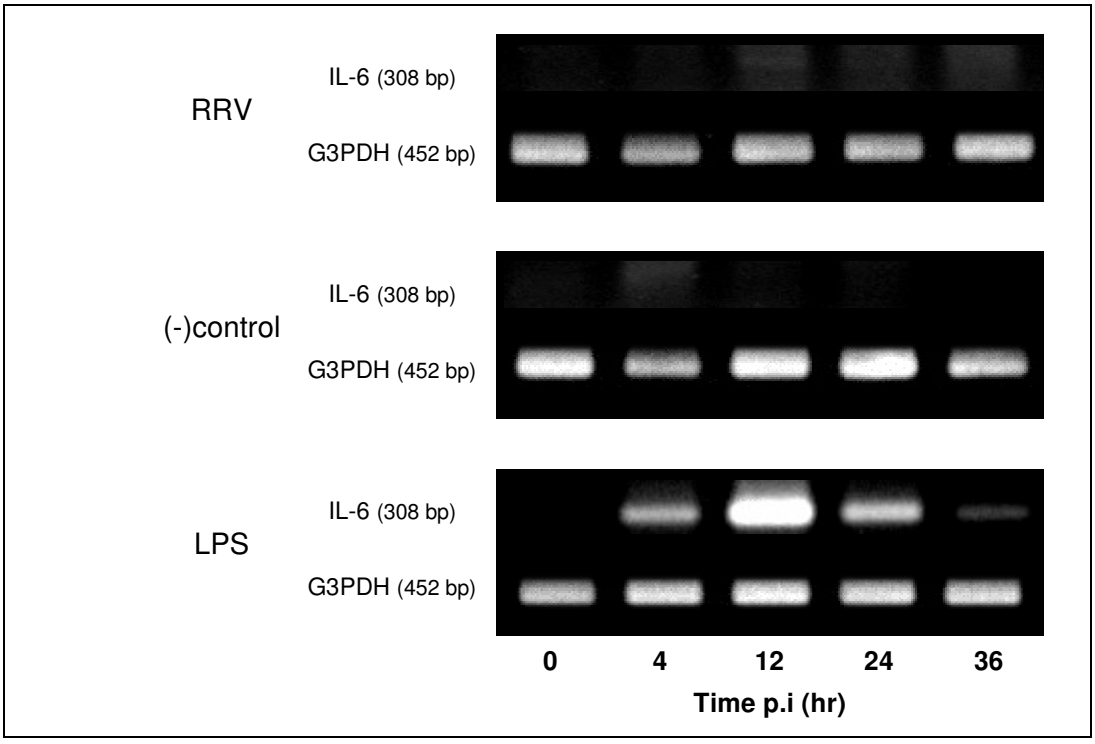

Figure 14: IL-6 mRNA expression in RAW264.7 macrophages after exposure to RRV and LPS

RAW264.7 cells were exposed to RRV T48 at an MOI of 1 or LPS (1 µg/mL) and mRNA was extracted at 0, 4, 12, 24 and 36 hrs post-infection. The expression of IL-6 mRNA was determined by RT-PCR. Figure shows representative photographs of agarose gels (n=5).

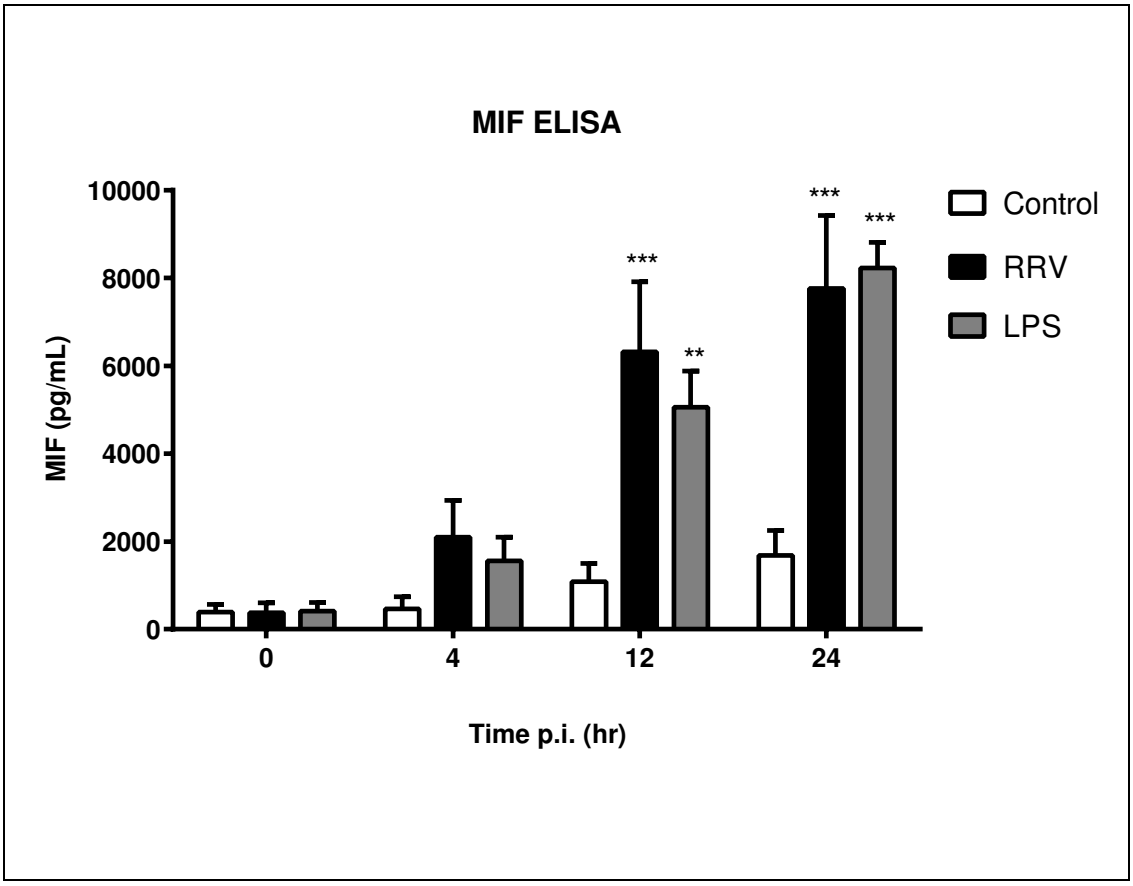

Figure 15: MIF concentration in RAW264.7 macrophages exposed to RRV or LPS

RAW264.7 macrophage cells were challenged with RRV T48 at an MOI of 1 or LPS (1 µg/mL) and supernatant samples were analysed by MIF ELISA at various time points post exposure. All data is shown in mean values ± SEM (n=3). **(p≤0.01), ***(p≤0.001) as determined by two-way ANOVA.

4.3.9 RRV infection alters transcription of MIF mRNA in RAW264.7

The mRNA of RAW macrophages infected with RRV T48 was extracted at appropriate times p.i. and examined for MIF mRNA expression. Macrophages stimulated with 1 µg/mL LPS were used as positive control. MIF mRNA was detectable from 12 hr onwards for both RRV-infected as well as LPS treated RAW cells as shown in Figure 16. Expression of MIF mRNA continued to at least 36 hr post-infection. The rate of expression in RRV induced macrophages however was considerably lower compared to the LPS control.

4.3.10 RRV infection induces secretion of HMGB1 in RAW264.7 macrophages

HMGB1 is universally expressed in most cells as architectural chromosomal protein, however it has also been discovered to function as a pro-inflammatory cytokine when released extracellularly (Muller et al., 2001; H. Wang et al., 1999). Stimulation with TNFα induces secretion of HMGB1 as a late mediator in inflammation (H. Wang et al., 1999). To investigate if RRV induces secretion of HMGB1 in macrophages, RAW264.7 cells were exposed to RRV T48 (MOI of 1) for variable amounts of time and the supernatant was tested for the presence and concentration of HMGB1 by ELISA (Figure 17). Macrophages infected with RRV showed slightly increased concentrations of HMGB1 in the supernatant samples by 24 hr p.i. as compared to mock infected controls, with levels reaching 6.5 ± 1.3 ng/mL and 12.1 ± 2.7 ng/mL at 36 hr post-infection. This increase was however not statistically significant. LPS treated RAW264.7 cells were used as positive control with HMGB1 concentrations significantly increasing to 25.8 ± 6.4 ng/mL ($p \leq 0.001$) and 38.6 ± 8.9 ng/mL ($p \leq 0.001$) by 24 and 36 hr p.i. respectively.

4.3.11 RRV infection decreases expression of HMGB1 mRNA in RAW264.7

To study the effect of RRV infection on HMGB1 mRNA expression, RAW264.7 macrophages were exposed to RRV at an MOI of 1 and mRNA was extracted at varying time periods post-infection and analysed by conventional as well as real time RT-PCR. As expected, HMGB1 mRNA could be detected at all analysed time points and in all samples. Interestingly the expression of HMGB1 mRNA seemed to decrease in RRV and LPS stimulated samples at 36 hr post treatment as indicated by agarose gel blots. The expression in the control however remained consistent (see Figure 18 B). Quantitative real-time data confirmed significant ($p \leq 0.05$) down-regulation of HMGB1 transcription in RRV-infected samples by almost 3.5 times as compared to non-treated controls (Figure 18 A).

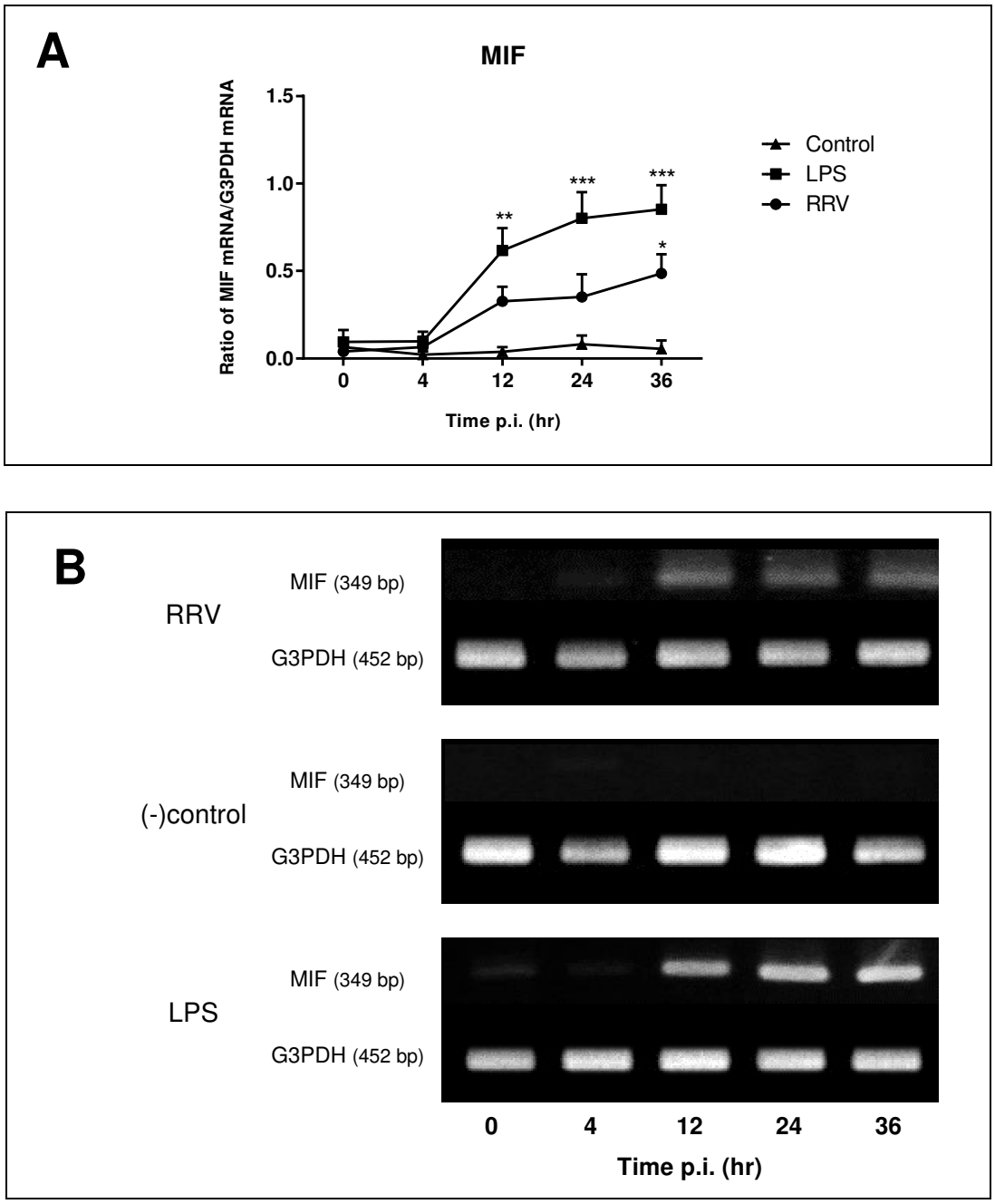

Figure 16: MIF mRNA expression in RAW264.7 after exposure to RRV and LPS

RAW264.7 macrophages were infected with RRV T48 at an MOI of 1 or stimulated with LPS (1 µg/mL) and mRNA was extracted at various time points. The expression of MIF mRNA was analysed via conventional PCR and densiometric analysis as samples for real time analysis were below the detection limit. The ratio of MIF mRNA over G3PDH mRNA is graphed in (A). Data shown are mean values ± SEM (n=3) *($p \leq 0.05$), **($p \leq 0.01$), ***($p \leq 0.001$). (B) shows representative photographs of agarose gels (n=3).

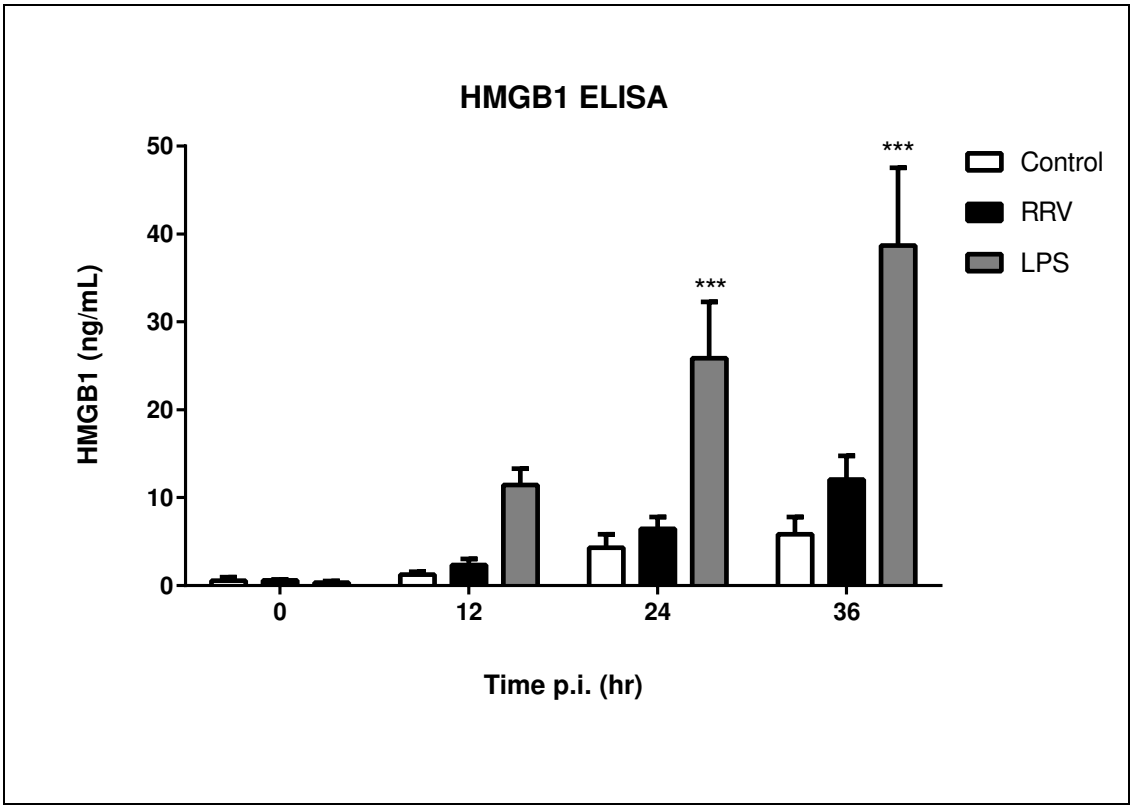

Figure 17: HMGB1 release of RAW264.7 macrophages upon stimulation with LPS or RRV T48

RAW264.7 macrophages were exposed to with RRV T48 at an MOI of 1 or LPS (1 µg/mL) and the supernatant was tested for HMGB1 concentration at varying time points post-infection by ELISA. Heat inactivated RRV was used in mock infections as negative control. Data is shown in mean values ± SEM (n=3). ***($p \leq 0.001$) as determined by two-way ANOVA compared to control.

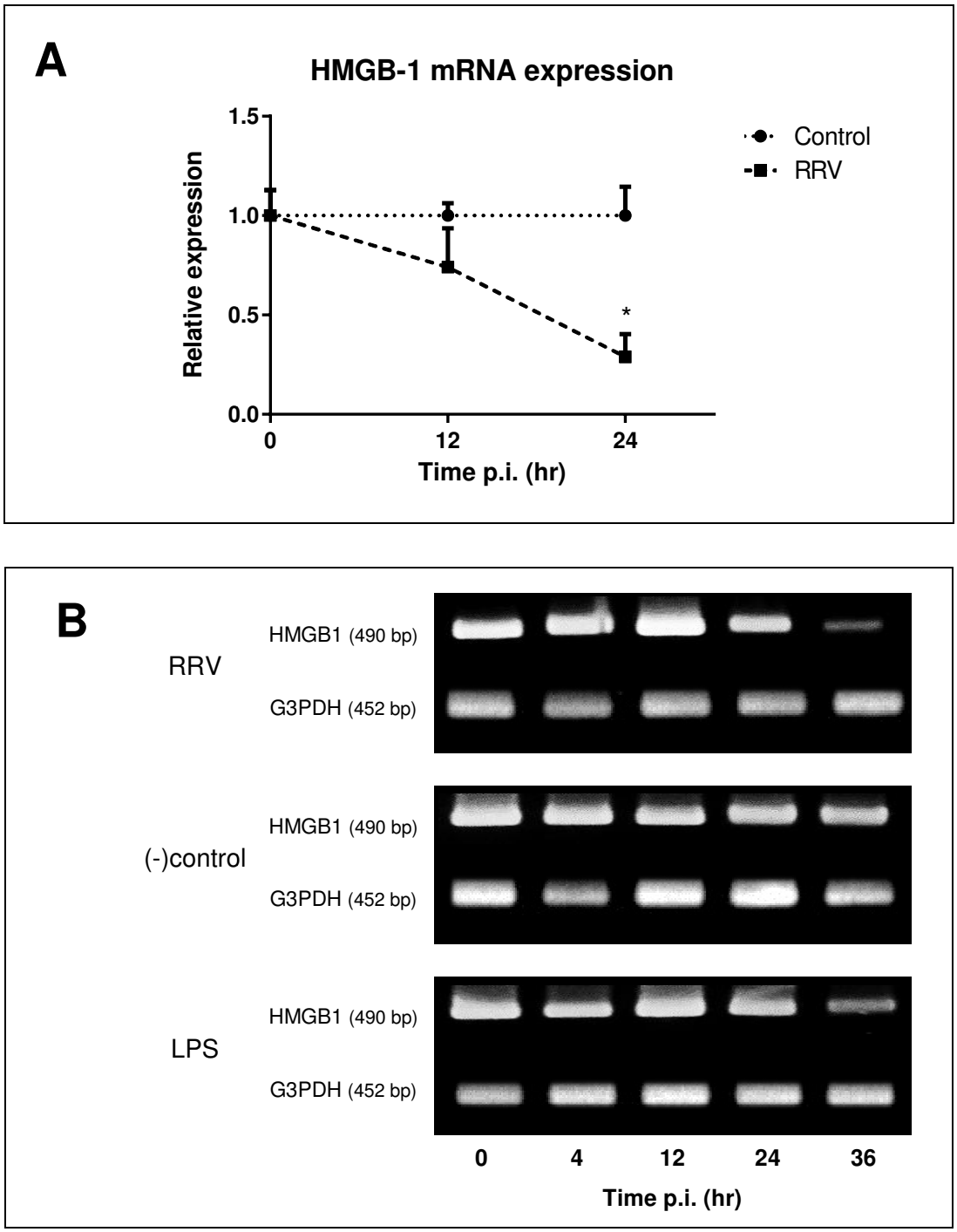

Figure 18: HMGB1 mRNA expression in RAW264.7 macrophages after exposure to RRV or LPS

RAW264.7 macrophages were inoculated with RRV DC 7194 at an MOI of 1 or stimulated with LPS (1 µg/mL) and mRNA was extracted at various times. mRNA was examined for HMGB1 transcription by quantitative real-time PCR (A) and by conventional RT-PCR with gel electrophoresis (B). All data is presented as mean values + %CV (n=3), *($p \leq 0.05$) as determined by two-way ANOVA compared to mock-infection. (B) shows representative photographs of PCR amplicons.

4.3.12 RRV increases the transcription of HMGB3 mRNA but does not affect HMGB2 mRNA expression in RAW264.7 cells

In order to determine the effect of RRV on the expression of HMGB2 and HMGB3 mRNA, RAW cells were infected with the virus at an MOI of 1 and mRNA extracted at various time points post-infection. HMGB3 mRNA could be detected in all samples and expression gradually increased p.i. in the RRV samples (Figure 19 B). LPS challenged samples in contrary showed a decrease in HMGB3 mRNA expression in a time dependent manner. Neither RRV nor LPS significantly changed the expression of HMGB2 mRNA (Figure 19 A, densiometric data not shown).

4.3.13 LPS and RRV induce IL-10 secretion in RAW264.7 macrophages

It has previously been shown that antibody dependent enhancement (ADE) of RRV infection can induce the secretion of the anti-inflammatory cytokine IL-10 in RAW 267.4 macrophages (Mahalingam & Lidbury, 2002) and it was later shown that this is also true for naive RRV infection (Morrison et al., 2008). To verify these findings for our conditions, RAW264.7 cells were infected with RRV T48 or exposed to LPS as a positive control and supernatant was tested for IL-10 by ELISA. As expected, LPS significantly ($p \leq 0.001$) induced the secretion of IL-10 into the supernatant by 4 hr post stimulation and peaked at 2244 ± 228 pg/mL by 12 hr post stimulation (Figure 20 A). A less pronounced increase of IL-10 levels in the supernatant of RRV-infected macrophages was noticeable by 12 hr p.i. and significantly ($p \leq 0.05$) increased by 24 hr p.i. reaching a concentration of 153 ± 25 pg/mL (Figure 20 B). For statistical calculation, IL-10 levels were compared to mock infection control.

4.3.14 RRV does not induce secretion of Prostaglandin E_2 in RAW264.7

The important functions of prostaglandin E_2 (PGE_2) in inflammatory and immune responses have long been established (Kalinski, 2012), however according to our literature research no data is available on the role of PGE_2 in alphavirus infections. To investigate if the regulation of this mediator is altered in RRV infection we analysed the supernatant of RAW264.7 macrophages exposed to LPS (1 µg/mL) or RRV T48 (MOI of 1). LPS stimulation has previously been shown to induce PGE_2 secretion in RAW264.7 macrophages and was therefore included as positive control (Salvemini et al., 1993). As Figure 21 shows, RRV T48 did not stimulate PGE_2 release from macrophages in contrast to LPS stimulation, which significantly ($p \leq 0.001$) increased PGE_2 concentration in the supernatant from 12 hr p.s. onwards.

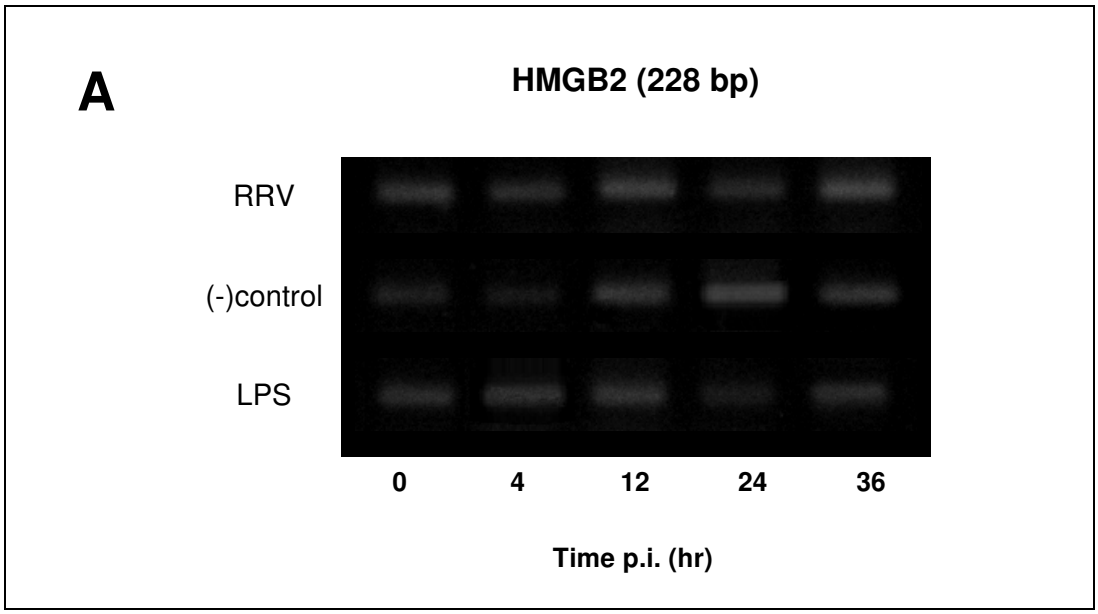

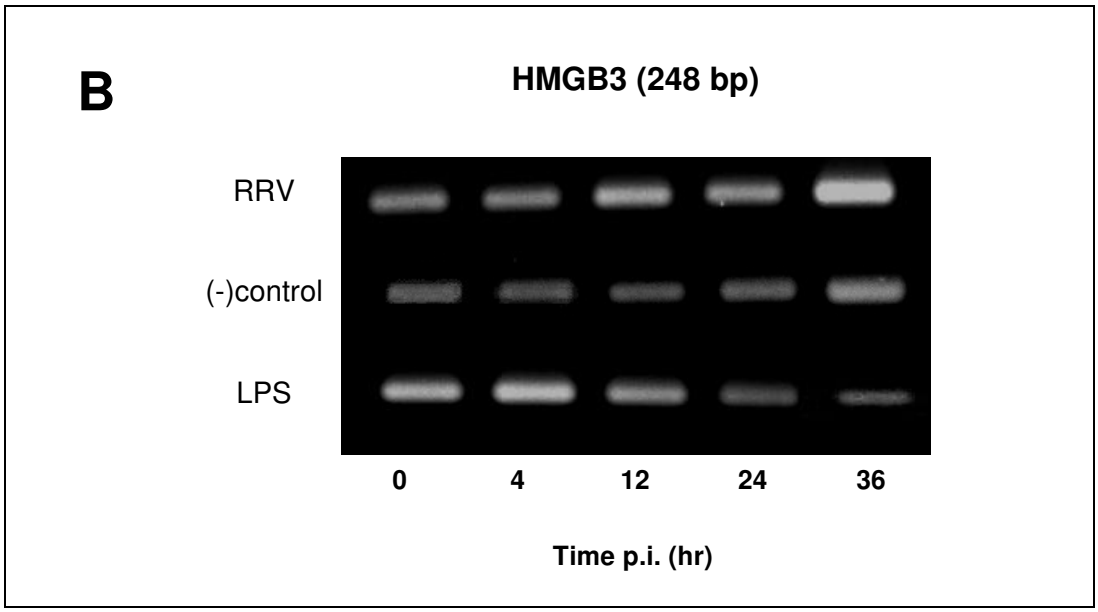

Figure 19: HMGB2 and HMGB3 mRNA expression in RAW264.7 macrophages after exposure to RRV or LPS

RAW264.7 macrophages were infected with RRV DC 7194 at an MOI of 1 or stimulated with LPS (1 µg/mL) and mRNA was extracted at various time points. A PCR with specific primers for HMGB2 (A) and HMGB3 (B) was performed. Pictured are representative photographs of agarose gels. G3PDH amplicons were used to ensure equal mRNA loading but are not shown. (n=3)

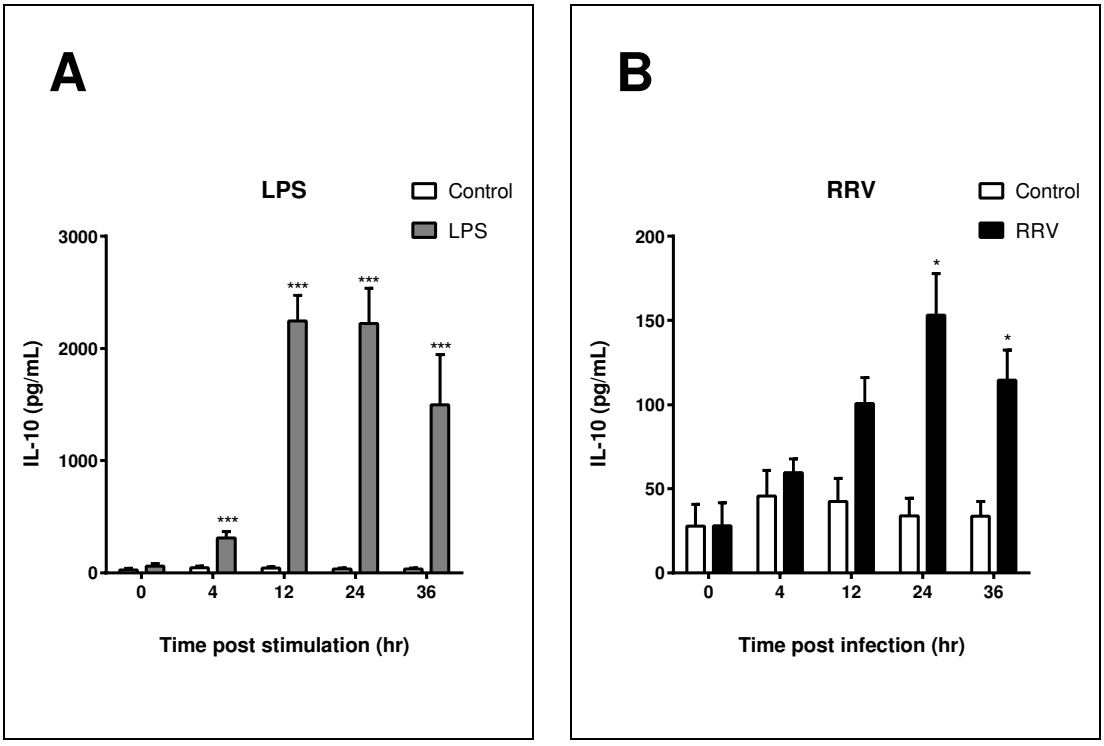

Figure 20: LPS and RRV induces IL-10 secretion in RAW264.7 macrophages

RAW264.7 macrophages were infected with RRV T48 at an MOI of 1 (B) or stimulated with 1 mg/uL LPS (A) for varying amounts of time. Control cells were mock-infected with heat inactivated RRV. IL-10 concentration of the supernatant samples was determined by ELISA as outlined in Methods. Data is expressed in mean values ± SEM (n=3). Induction of IL-10 secretion is significantly lower in RRV-infected cells compared to LPS treatment. *($p \leq 0.05$),***($p \leq 0.001$). Statistical analysis was performed by two-way ANOVA and compared to mock-infected samples. Note the difference in scale for both graphs.

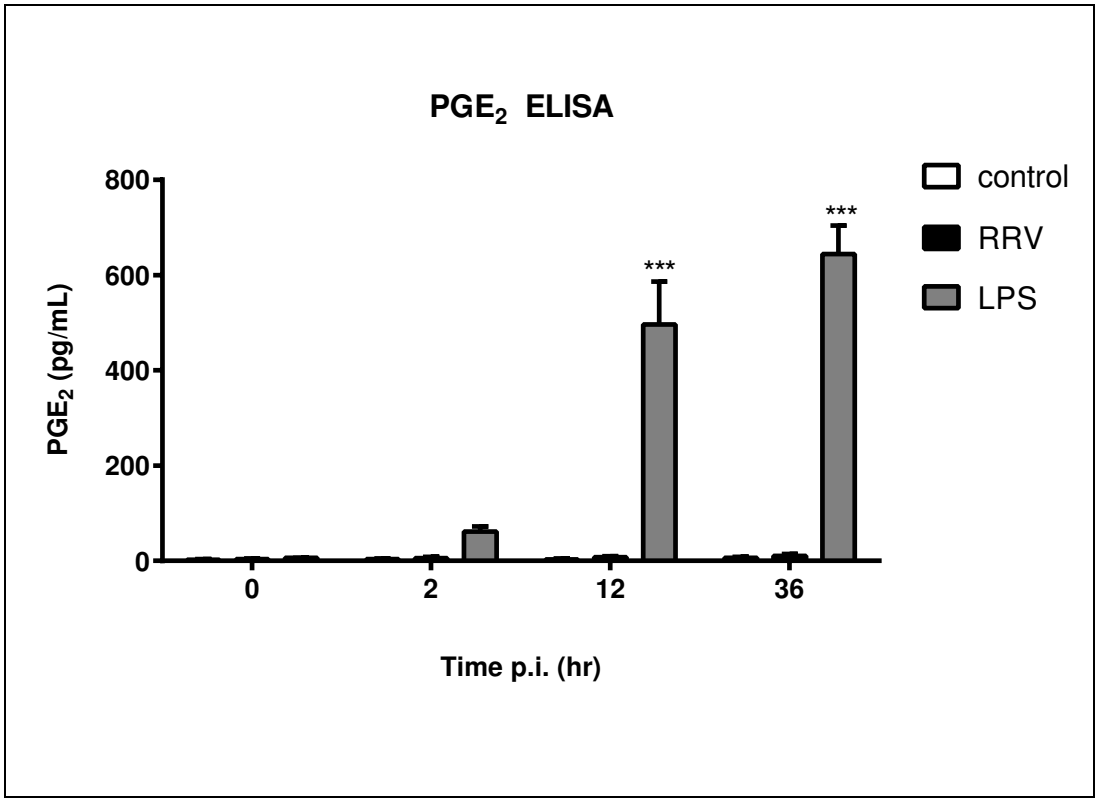

Figure 21: PGE_2 secretion of RAW264.7 macrophages exposed to RRV T48 or LPS

RAW264.7 macrophages were challenged with RRV T48 at an MOI of 1 or LPS (1 µg/mL) and supernatant samples were analysed by PGE_2 ELISA at various time points post exposure. All data is shown in mean values ± SEM (n=3), ***($p \leq 0.001$) as determined by two-way ANOVA compared to mock-infected control.

4.3.15 RRV infection induces IL-18 mRNA expression in RAW264.7 macrophages

Earlier research has shown that the secretion of the pro-inflammatory cytokine IL-18 by macrophages plays an important role in rheumatoid arthritis (Gracie et al., 1999), and more recently it was reported that plasma IL-18 levels are also increased in patients infected with CHIKV (Chirathaworn et al., 2010). To investigate if IL-18 possibly contributes to inflammatory processes in RRV infections, we exposed RAW264.7 macrophages to the T48 strain (MOI of 1) and extracted mRNA at various time points post-infection for conventional and real-time RT-PCR analysis. LPS was used as positive control (Tone et al., 1997). As shown in Figure 22 A, RRV-infected macrophages showed increased transcription of IL-18 mRNA from 12 hr p.i. onwards. This result was confirmed by real-time PCR analysis, as shown in Figure 22 B. The ratio of cytokine mRNA in RRV-infected samples was calculated against the mRNA of negative control samples. IL-18 mRNA expression was increased 3.1-fold by 12 hr p.i. ($p \leq 0.05$) and 4.8-fold by 24 hr p.i. ($p \leq 0.001$) as compared to mock infection. Exposure to LPS induced IL-18 mRNA in macrophages as expected and was detected from 4 hr p.s onwards with conventional RT-PCR. Amplicon density appeared to peak at 12 and 24 hr p.s. and decreased again by 36 hr p.s. (Figure 22 B).

4.3.16 The expression of IL-33 mRNA is induced in RRV-infected RAW264.7 macrophages

IL-33, a member of the IL-1 superfamily has previously been identified as an important cytokine in inflammatory conditions (Schmitz et al., 2005). It has been shown to contribute to the inflammatory development of rheumatoid arthritis by stimulating the release of pro-inflammatory cytokines (Moulin et al., 2007; D. Xu et al., 2008). In order to examine a possible role of IL-33 in RRV infections, RAW264.7 macrophages were exposed to RRV T48 at an MOI of 1 and mRNA was extracted at various time points post-infection. Extracted mRNA was analysed with conventional and real-time RT-PCR using primers specific for IL-33. LPS treated RAW cells showed strong induction of IL-33 mRNA transcription from 4 hr p.s. onwards as shown in Figure 23 B. Expression of IL-33 mRNA could be detected in RRV-infected cells from 12 hr p.i. onwards, with the density of the amplicons decreasing by 36 hr p.i. Due to insufficient expression in controls and 0 hr samples, real-time data could not be calculated as relative expression compared to mock infection. Instead the data was graphed as the ratio of IL-33 mRNA expression over

the corresponding G3PDH mRNA expression (Figure 23 A). This ratio was given the arbitrary value of '0' for 0 hr p.i. and is only used to visualise up- or down-regulation of mRNA expression. In both RRV as well as LPS treated samples the transcription of IL-33 mRNA is induced by 12 hr p.i., increasing in a time dependent manner for RRV samples. Expression levels for LPS challenged macrophages at 12 hr p.i. are slightly increased compared to RRV infection, however this increase is not significant. By 24 hr p.i. there appears to be no difference between the samples.

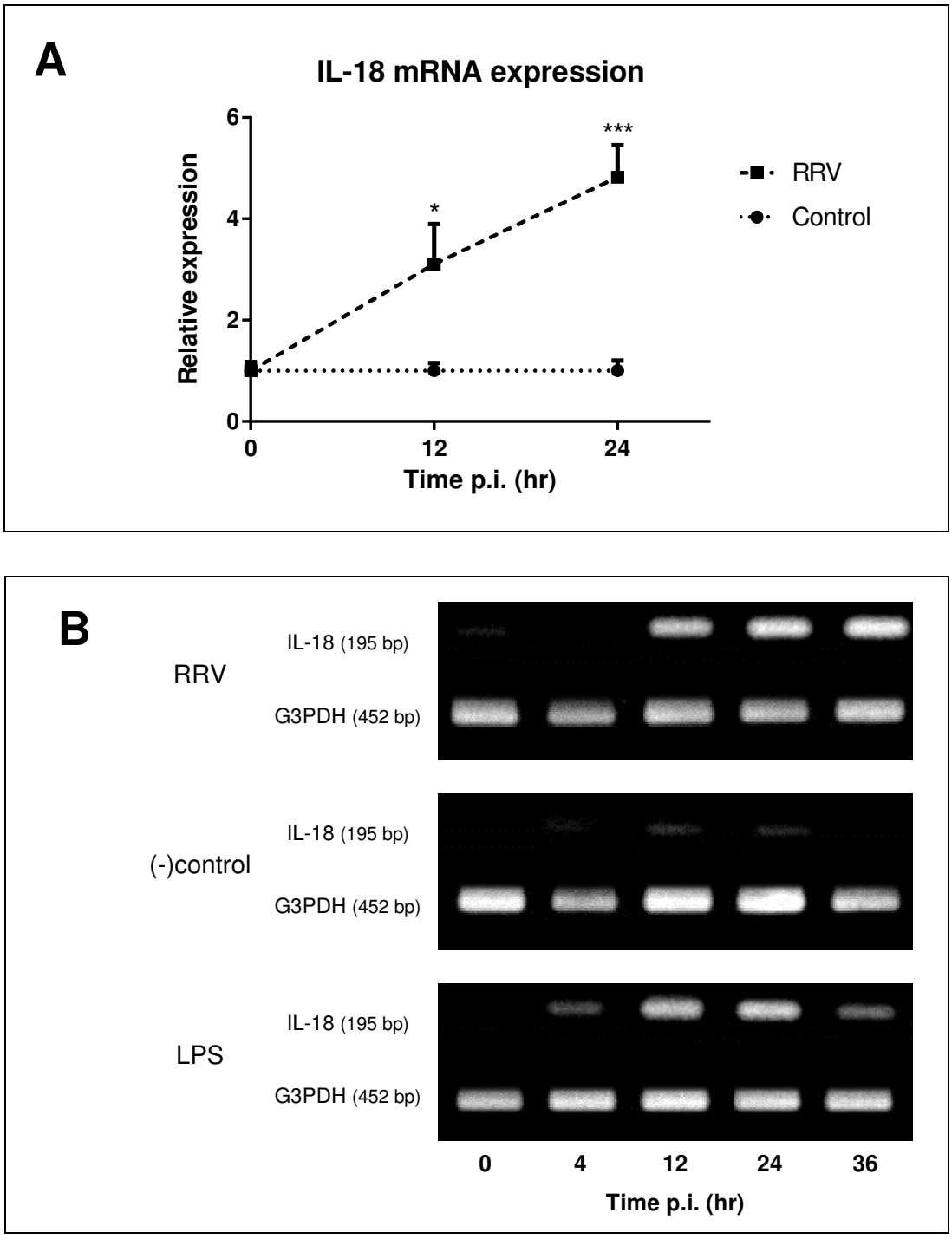

Figure 22: IL-18 mRNA expression in RAW264.7 after exposure to RRV or LPS

RAW264.7 macrophages were infected with RRV T 48 at an MOI of 1 or stimulated with LPS (1 µg/mL) and mRNA was extracted at various time points. mRNA expression of IL-18 and G3PDH were determined by quantitative RT-PCR and normalised ratios of the samples were compared to the respective negative control as graphed for each time point (A). Data shown are mean values + %CV (n=3). Statistical analysis was performed by two-way ANOVA, *($p \leq 0.05$), ***($p \leq 0.001$). (B) shows representative photographs of agarose gels.

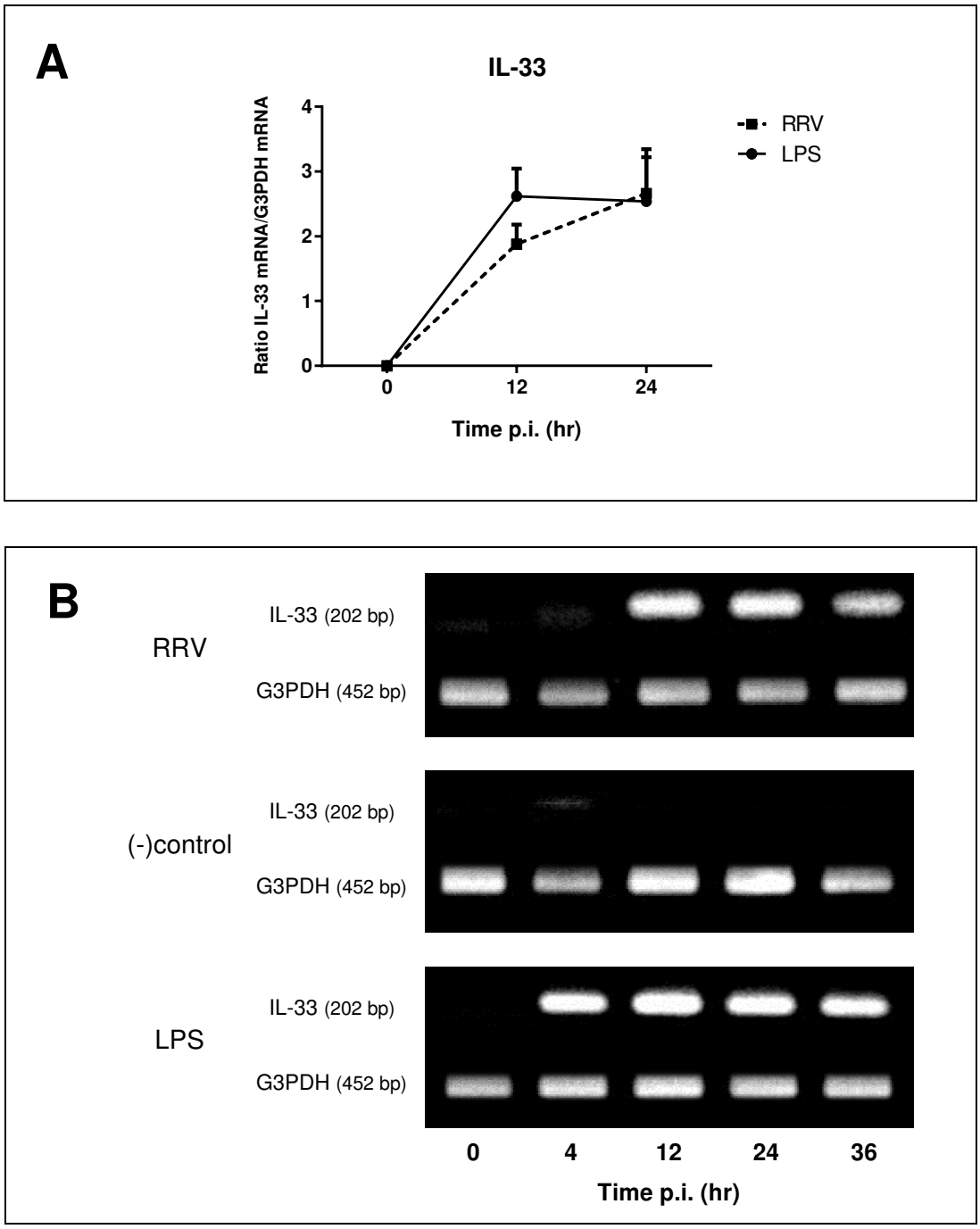

Figure 23: IL-33 mRNA expression in RAW264.7 after exposure to RRV or LPS

RAW264.7 macrophages were inoculated with RRV T 48 at an MOI of 1 or stimulated with LPS (1 µg/mL) and mRNA was extracted at different times. HI-RRV was used in infections as negative control. IL-33 mRNA expression levels for mock infection and time point 0 hr p.i. were below detection limits for real time PCR quantitation. Therefore the mRNA expression values as determined by quantitative RT-PCR were graphed as the ratio of cytokine mRNA over G3PDH mRNA (A). Expression at 0 hr p.i. was given the arbitrary value of '0'. Data is shown as mean values + %CV (n=3). (B) shows representative photographs of agarose gels.

4.4 Inhibitors and stimulants of cytokine release in RRV-infected RAW264.7 macrophages

4.4.1 Inhibition of TNFα in RAW cells post RRV infection

As mentioned in the Literature Review, many inhibitors for TNFα have been identified to this date. NSAIDs and corticosteroids like dexamethasone have been shown to inhibit TNFα release in macrophages and both have previously been used in the management of RRV induced arthritis (Suhrbier et al., 2012; Suhrbier & Mahalingam, 2009). Corticosteroids are however rarely used due to their possible immunosuppressive and gastro-intestinal side effects (Mylonas et al., 2004). Zaid et al. (Zaid et al., 2011) have trialled etanercept in the treatment of RRV-infected mice, but found that complete TNFα inhibition aggravated disease symptoms, likely due to impaired antiviral response. It may however be possible that moderate reduction in TNFα levels could suppress excessive inflammatory response without impairing immune responses to the infection. To our knowledge, apart from the aforementioned compounds, no other TNFα inhibitor has so far been examined in RRV infection.

4.4.1.1 Macrolide antibiotics

Apart from their antibiotic properties several macrolides have been investigated for their anti-inflammatory properties (Labro, 1998), however to this date no macrolide has been trialled to reduce inflammatory responses in RRV infection. To investigate the influence of three commonly used macrolides on cytokine production we infected RAW264.7 macrophages with RRV T48 in the presence of varying concentrations of macrolides and evaluated the cytokine response.

4.4.1.1.1 Erythromycin decreases TNFα secretion of RRV-infected macrophages

Early research suggested that Erythromycin (ERY) can reduce TNFα production in human monocytes (Iino et al., 1992). To investigate if ERY interferes with RRV induced TNFα secretion in macrophages, RAW264.7 cells were exposed to RRV T48 at an MOI of 1 with different concentrations of the macrolide present. Supernatant samples at various time points were examined for TNFα concentration by ELISA (Figure 24 A). Dose-dependent inhibition could be detected as early as 4 hr p.i. and was significant at 24 hr p.i. for both 10 µM and 100 µM ERY ($p \leq 0.001$). At 36hr p.i. the concentration of TNFα for 10 µM ERY was reduced by approximately 54.2 % from 1213 ± 138 pg/mL for non-treated cells to 555 ± 60 pg/mL for cells

treated with Erythromycin 10 µM. The decrease of TNFα in the supernatant for Erythromycin 100 µM treated cells at 36 hr p.i. was approximately 69.6 % to 369 ± 69 pg/mL. Lower concentrations (0.1, 1 and 10 µM) of Erythromycin were used in separate experiments and TNFα levels were determined by L929 bioassay (Figure 24 B). Again, inhibition could be detected from 4 hr p.i. onwards for all samples. Concentrations of 0.1 µM ERY showed decreased TNFα secretion, which was however not statistically significant. At concentrations of 1 µM and 10 µM ERY, a significant inhibition could be detected from 12 hr p.i. onwards ($p \leq 0.05$ and $p \leq 0.01$ respectively). In samples containing 1 µM ERY, TNFα levels decreased to 448 ± 126 pg/mL at 24 hr p.i. as compared to 974 ± 86 pg/mL for non-treated cells ($p \leq 0.001$). This reduction was even more pronounced in 10 µM ERY samples with levels dropping to 389 ± 119 pg/mL as determined by L929 bioassay ($p \leq 0.001$).

4.4.1.1.2 Clarithromycin inhibits secretion of TNFα in RRV-infected RAW264.7 macrophages

Similar to Erythromycin the macrolide clarithromycin (CLA) has been shown to reduce TNFα levels in the sera of LPS stimulated mice (Tkalcevic et al., 2008). In order to investigate a possible inhibition of TNFα secretion in RRV infections we exposed macrophages RRV T48 (MOI of 1) in the presence of 10 or 100 µM CLA. As shown in Figure 25 A, a reduction of TNFα in the supernatant could be detected by ELISA from 4 hr p.i. onwards. The maximum inhibitory effect was detected at 24 hrs p.i. with a reduction of TNFα levels from 1055 ± 90 pg/mL to 640 ± 97 pg/mL for 10 µM CLA and 380 ± 73 pg/mL for 100 µM CLA respectively. Up to 12 hr p.i. there was no significant difference in inhibition for both concentrations, however at 24 hr and 36 hr p.i. the increase in inhibition between 10 µM to 100 µM CLA was significant ($p \leq 0.05$). A TNFα bioassay on supernatant samples from a separate set of experiments showed significant reduction of TNFα compared to non-treatment at 24 hr p.i. for 0.1 µM CLA ($p \leq 0.01$), 1 µM CLA ($p \leq 0.001$) and 10 µM CLA ($p \leq 0.001$). The inhibitory effect on TNFα was both time- and dose-dependent as shown in Figure 25 B. Cytokine levels at 24 hr p.i. compared to non-treated macrophages dropped from 974 ± 86 pg/mL to 649 ± 100 pg/mL (0.1 µM CLA), 432 ± 81 pg/mL (1 µM CLA) and 360 ± 53 pg/mL (10 µM CLA) respectively.

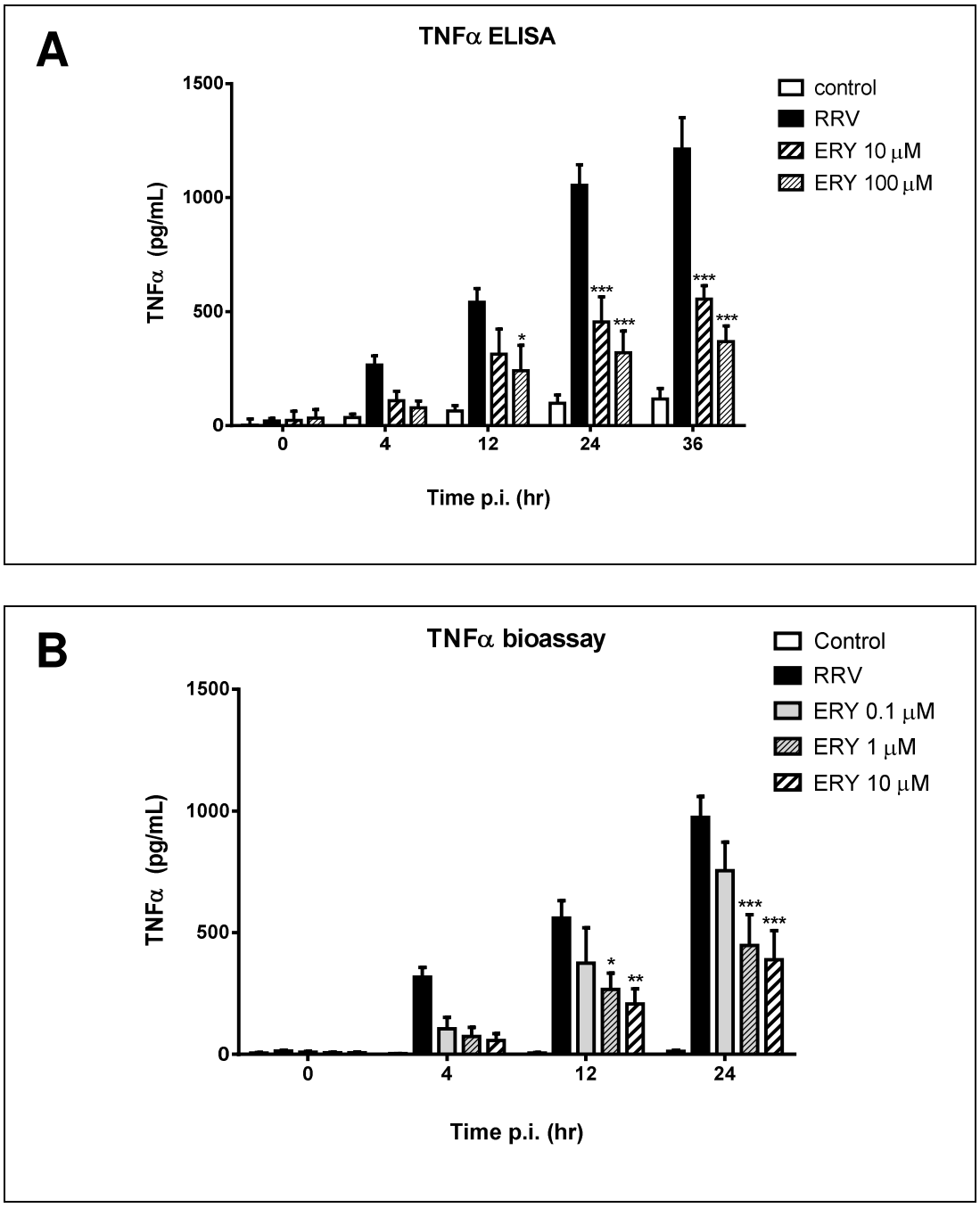

Figure 24: TNFα secretion of RAW264.7 macrophages after RRV infection and concurrent incubation with erythromycin

RAW264.7 macrophages were infected with RRV T48 at an MOI of 1 and concurrently treated with 0, 0.1, 1, 10 or 100 µM erythromycin. HI-RRV was used as negative control. An ELISA (A) and a TNFα bioassay (B) was performed on supernatant samples to determine TNFα concentration and bioactivity. All values are expressed as mean ± SEM (n=3). *(p≤0.05), **(p≤0.01), ***(p≤0.001) for treatment compared to non-treated samples.

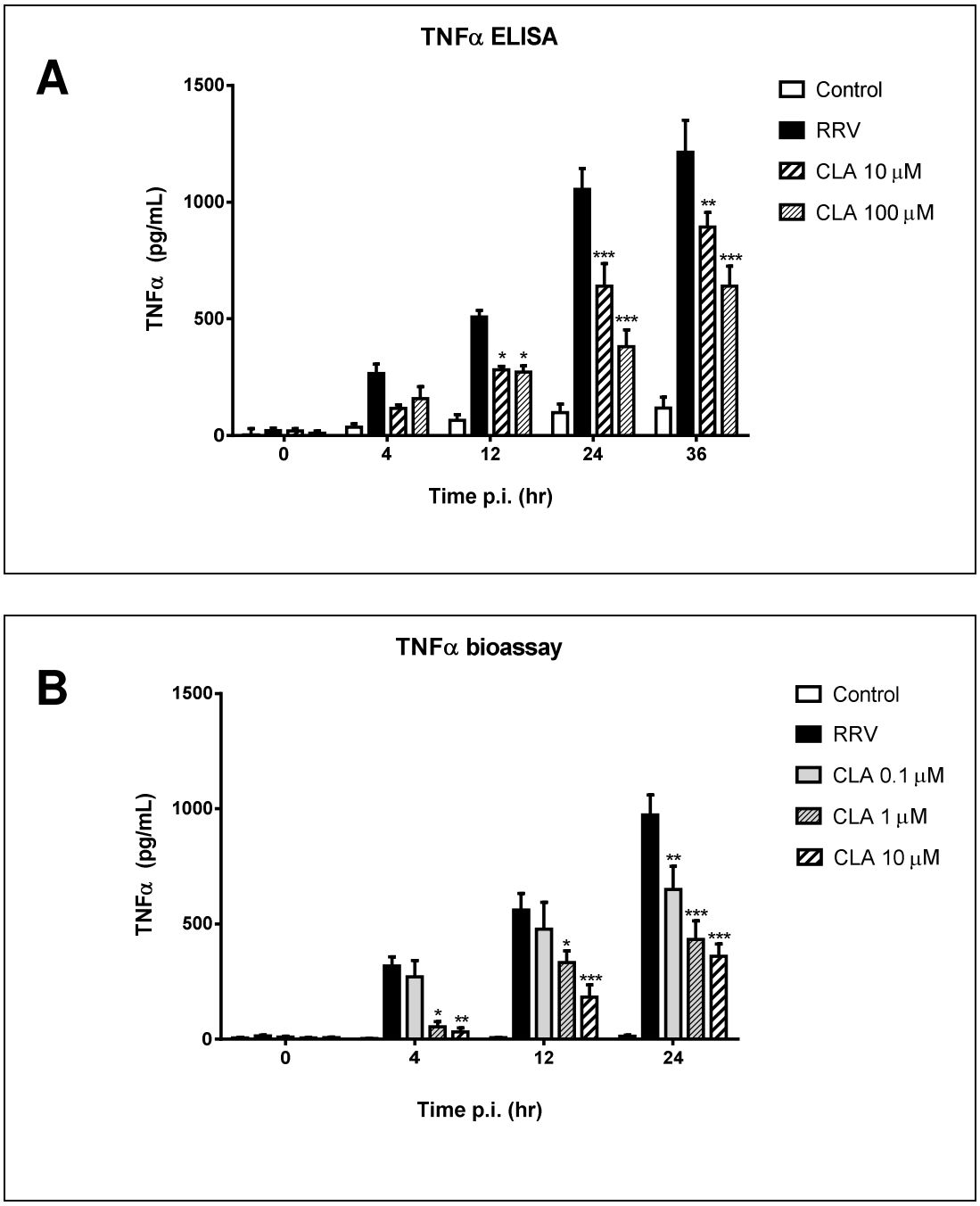

Figure 25: TNFα secretion of RAW264.7 macrophages after RRV infection and concurrent treatment with CLA

RAW264.7 macrophages were incubated with RRV T48 at an MOI of 1 and simultaneously treated with 0, 0.1, 1, 10 or 100 µM clarithromycin (CLA). HI-RRV was used as negative control. An ELISA (A) or a TNFα bioassay (B) was performed on supernatant samples to determine TNFα concentration. All values are expressed as mean ± SEM (n=3 for each set of experiments). *(p≤0.05), **(p≤0.01), ***(p≤0.001) as determined by two-way ANOVA compared to non-treated infection.

4.4.1.1.3 Roxithromycin alters TNFα secretion in RRV-infected macrophages

Iino et al. (Iino et al., 1992) reported that Erythromycin as well as Roxithromycin (RXM) were able to significantly inhibit TNFα secretion in human monocytes. This anti-inflammatory effect was further investigated in arthritic conditions and it was found that RXM specifically inhibits progression of collagen induced arthritis and suppresses cytokine release in macrophages (Urasaki et al., 2005).

To examine if this TNFα-suppressive effect can also be utilised in RRV infection we exposed RAW264.7 macrophages to RRV T48 (MOI of 1) and various concentrations of RXM. Supernatant samples were taken at various time points and examined for TNFα concentration by ELISA as shown in Figure 26 A. A reduction of TNFα levels was noticeable from 4 hr p.i. onwards for 10 µM RXM but only reached significance at 36 hr p.i. ($p \leq 0.05$) with TNFα concentrations of 956 ± 105 pg/mL as compared to 1213 ± 138 for infected macrophages without treatment. At a concentration of 100 µM RXM the reduction was more pronounced ($p \leq 0.001$) with levels reduced to 556 ± 90 pg/mL at 36 hr p.i. Lower concentrations of RXM were trialled in a separate set of experiments and TNFα levels were determined by bioassay (Figure 26 B). RXM at a concentration of 0.1 µM reduced TNFα as early as 4 hr p.i. reaching statistical significance by 12 hr p.i. ($p \leq 0.01$) with cytokine concentration measuring 286 ± 81 pg/mL as compared to 560 ± 72 pg/mL for non-treated infection. All samples significantly reduced TNFα secretion ($p \leq 0.001$) by 24 hr p.i. with TNFα concentrations of 648 ± 81 pg/mL (0.1 µM RXM), 576 ± 85 pg/mL (1 µM RXM) and 501 ± 67pg/mL (10 µM RXM) respectively as compared to 974 ± 86 pg/mL for non-treated infection.

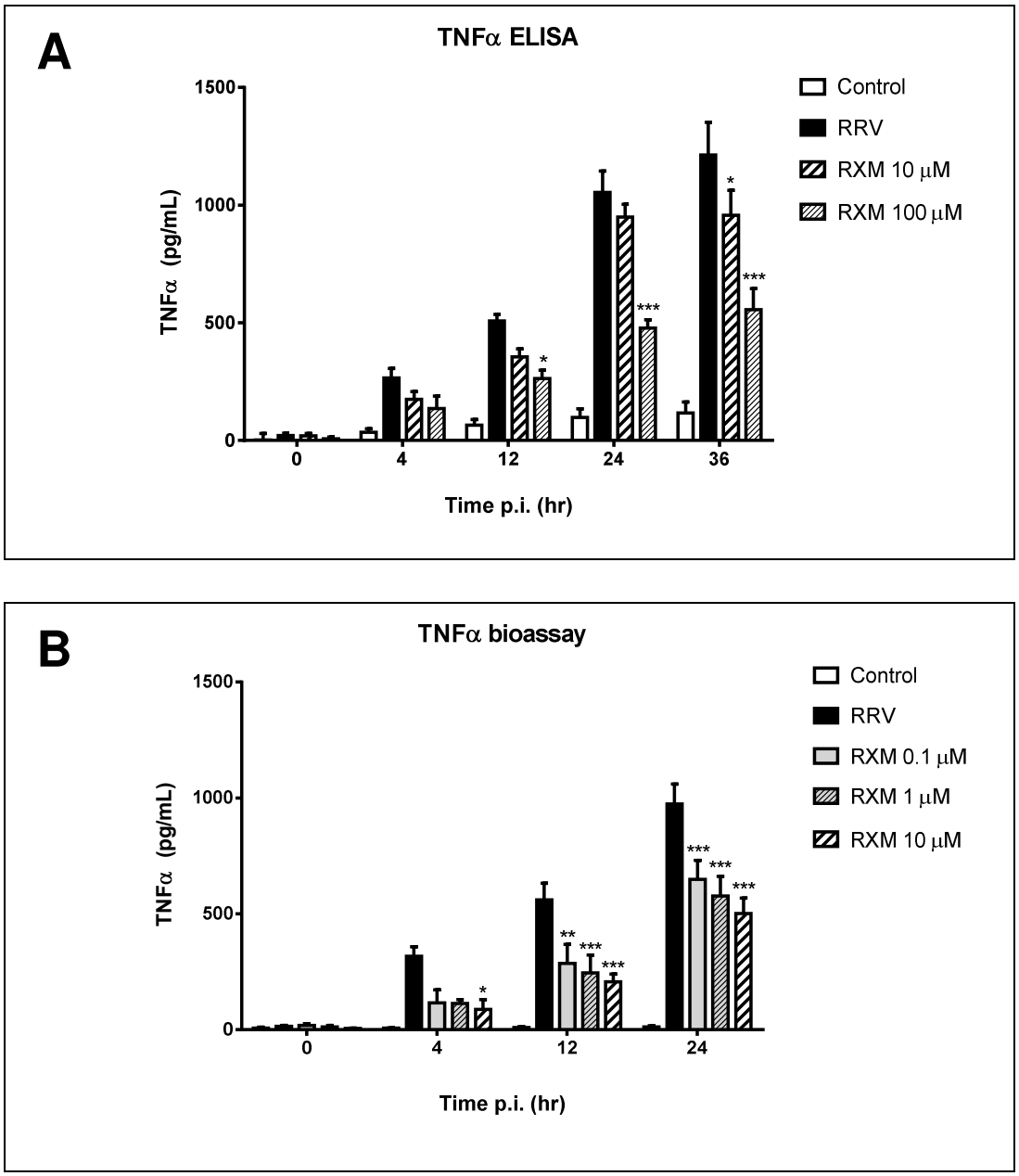

Figure 26: TNFα secretion of RAW264.7 macrophages after RRV infection and concurrent incubation with Roxithromycin

RAW264.7 macrophages were infected with RRV T48 at an MOI of 1 and concurrently treated with or without RXM (0, 0.1, 1, 10 or 100 µM). HI-RRV was used as negative control. An ELISA (A) or a L929 bioassay (B) was performed on supernatant samples to determine TNFα concentration. All values are expressed as mean ± SEM (n=3 for each set of experiments). *(p≤0.05), **(p≤0.01), ***(p≤0.001) as determined by two-way ANOVA compared to non-treated infection.

4.4.1.1.4 Influence of macrolides on transcription of TNFα mRNA in RRV-infected RAW264.7 macrophages

RAW264.7 macrophages were infected with RRV T48 at an MOI of 1 with or without concurrent treatment of 100 µM ERY, CLA or RXM. At appropriate time points the cells were lysed and quantitative RT-PCR was performed on extracted RNA using primers specific for TNFα. Each value obtained was normalised with the corresponding G3PDH value and the normalised values were then compared to their respective mock infection (control). RRV-infected samples concurrently treated with 100 µM ERY showed reduced TNFα mRNA expression at 12 hr and 24 hr p.i. as shown in Figure 27 A. Similar to ERY, CLA treatment resulted in reduced TNFα mRNA expression at 12 hr p.i. compared to non-treated infection (Figure 27 B). This inhibitory effect was still noticeable but less pronounced at 24 hr post-infection. Treatment with RXM showed strong inhibition on TNFα mRNA transcription at 12 hr p.i. and reached significance by 24 hr p.i. ($p \leq 0.05$) as determined by two-way ANOVA (Figure 27 C). Treatment with RXM but not ERY or CLA significantly reduced transcription of TNFα in RRV-infected RAW264.7 macrophages.

4.4.1.2 Ethyl pyruvate reduces TNFα secretion in RRV-infected RAW264.7

Previous research (Ulloa et al., 2002) showed that EP reduces the LPS stimulated release of the pro-inflammatory cytokines TNFα and HMGB1 by macrophages *in vivo* and *in vitro*. To examine if such a reduction in TNFα release is also achievable in RRV infection, we infected RAW264.7 macrophages with RRV T48 (MOI of 1) and added EP in various concentrations. As shown in Figure 28, both 100 µM and 1000 µM EP inhibited TNFα secretion significantly ($p \leq 0.05$) from 12 hr p.i. onwards as compared to non-treated infection. The cytokine levels at 36 hr p.i. were reduced by 3.2-fold from 1213 ± 138 pg/mL to 377 ± 98 pg/mL for non-treated cells and macrophages treated with 100 µM EP respectively. Interestingly, a 10-fold increase in concentration of EP to 1000 µM did not significantly increase inhibition at any given time point p.i. with the TNFα concentration in the supernatant reaching 387 ± 109 pg/mL by 36 hr p.i. for samples treated with 1000 µM EP.

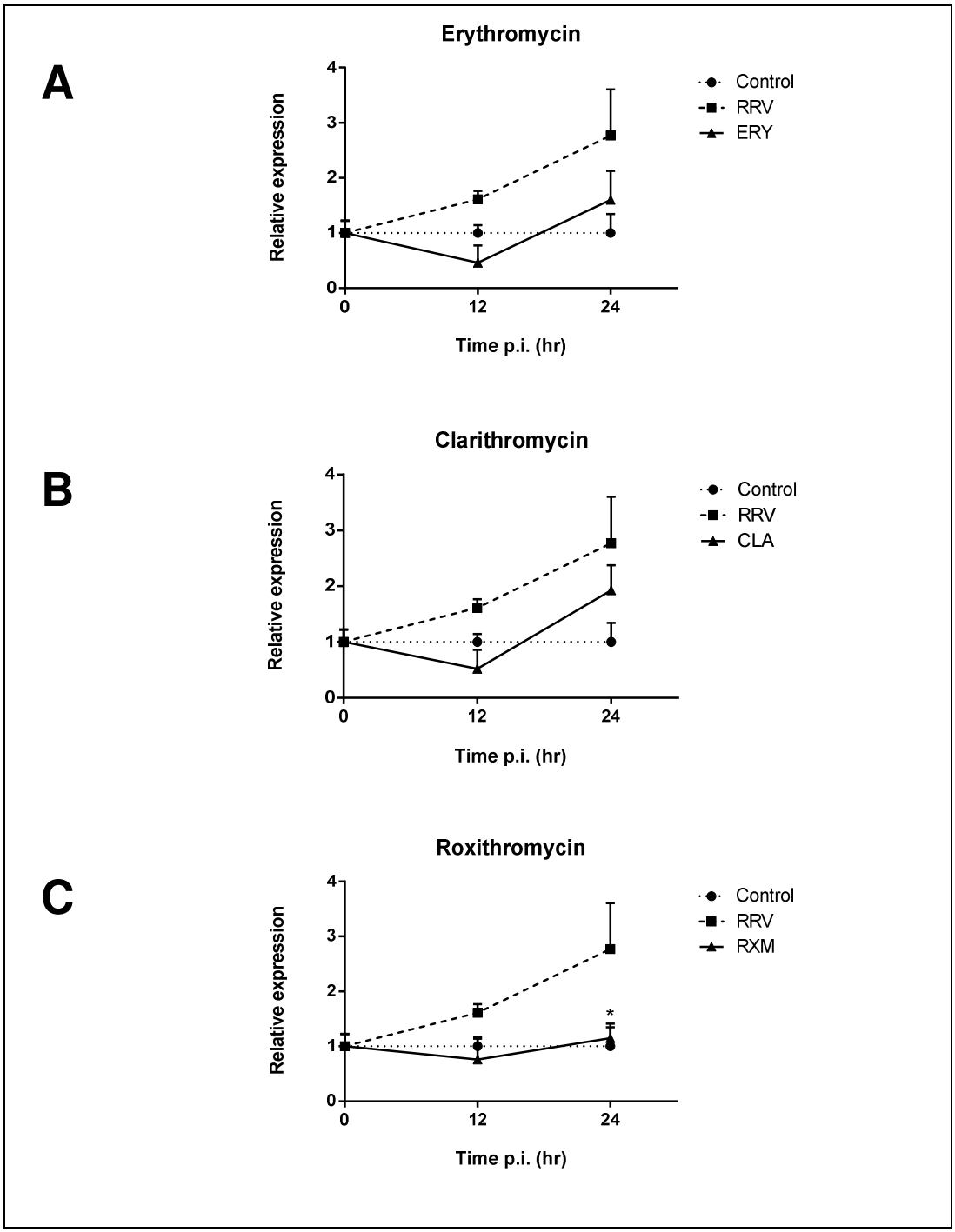

Figure 27: TNFα mRNA expression in RAW264.7 macrophages after infection with RRV and treatment with macrolide antibiotics

RAW264.7 macrophages were exposed to RRV T 48 at an MOI of 1 and concurrently treated with or without 100 µM ERY, CLA or RXM. RNA was extracted at different times and examined by quantitative real time PCR. HI-RRV was used as negative control. Relative expression was calculated as the normalised values of RRV-samples over the normalised values of the corresponding control. Data shown as mean values + %CV (n=3). *($p \leq 0.05$) as determined by two-way ANOVA.

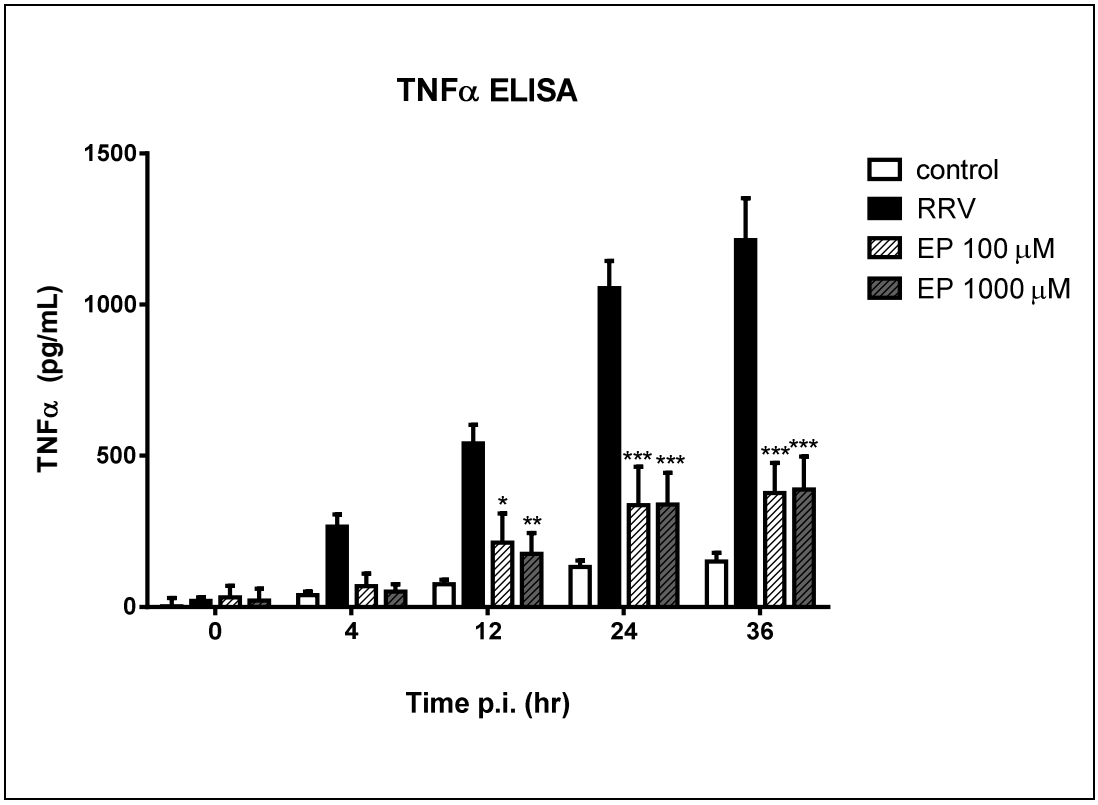

Figure 28: Secretion of TNFα in RRV-infected RAW264.7 macrophages co-treated with ethyl pyruvate

RAW264.7 macrophages were incubated with RRV T48 at an MOI of 1 with or without the presence of ethyl pyruvate (100 μM and 1000uM). HI-RRV was used in mock infections as negative control. A TNFα ELISA was performed on supernatant samples taken at various time points. All values are expressed as mean ± SEM (n=3). *(p≤0.05), **(p≤0.01), ***(p≤0.001) as determined by two-way ANOVA compared to non-treatment.

4.4.1.3 Pentoxifylline reduces TNFα release in RRV-infected RAW264.7

The ability of PXF to inhibit TNFα secretion in macrophages was reported earlier and has been investigated in various inflammatory conditions since (G. M. Doherty et al., 1991; Loftis et al., 1997; Marques et al., 1999). The beneficial effects of PXF in the treatment of refractory rheumatoid arthritis has been reported, the initial research however could not give conclusive results in regards to its TNFα inhibiting properties (Maksymowych et al., 1995). To investigate if PXF could reduce TNFα secretion by macrophages after RRV infection, RAW264.7 cells were exposed to RRV T48 (MOI of 1) with or without the presence of 100 µM or 1000 µM PXF. Supernatant samples at varying times were examined for TNFα levels by ELISA and graphed in Figure 29. Cells treated with 100 µM PXF showed significantly reduced levels of TNFα from 24 hr p.i. onwards ($p \leq 0.001$) with concentrations of TNFα in the supernatant at 36 hr p.i. decreasing to 434 ± 137 pg/mL as compared to 1213 ± 138 pg/mL in non-treated samples. Treatment of RRV infection with 1000 µM PXF reduced cytokine levels even further at 36 hr p.i. to 300 ± 91 pg/mL ($p \leq 0.001$), which equates to a 4-fold reduction in TNFα.

4.4.1.4 Resveratrol alters release of TNFα in RAW264.7 macrophages infected with RRV

Initial investigations on the effect of RVT on LPS challenged macrophages found both increased basal TNFα levels as well as TNFα secretion after stimulation, and PCR analysis confirmed up-regulation of TNFα mRNA in macrophages exposed to RVT (Wadsworth & Koop, 1999). Contrary to these findings a more recent study found a decrease in TNFα expression and secretion upon LPS stimulation in macrophages treated with RVT (Qureshi et al., 2012). To evaluate if resveratrol could have beneficial effects in RRV infection RAW264.7 macrophages were exposed to RRV T48 at an MOI of 1 and various concentrations of RVT ranging from 0 to 50 µM. Supernatant samples taken at several time points p.i. were analysed for TNFα levels by ELISA and the concentration was graphed as shown in Figure 30. RVT at concentrations of 5 and 50 µM significantly reduced the secretion of TNFα into the supernatant by 12 hr p.i. compared to non-treated infection ($p \leq 0.01$ and $p \leq 0.001$ respectively). TNFα concentration at 36 hr p.i. reached 358 ± 96 pg/mL for 5 µM RVT as compared to 1213 ± 138 pg/mL in the positive control. 50 µM RVT decreased TNFα levels even further to 221 ± 38 pg/mL by 36 hr p.i., which translates to a 5.5-fold reduction.

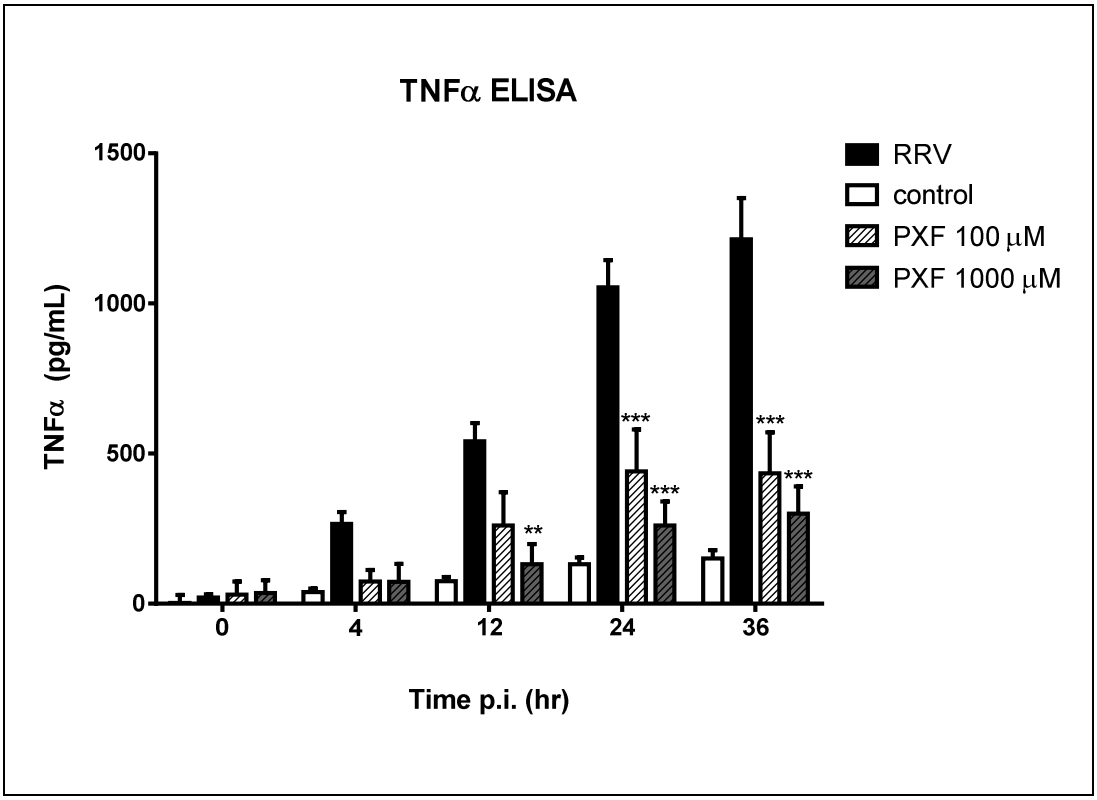

Figure 29: The effect of pentoxifylline on TNFα secretion in RRV-infected RAW264.7 macrophages

RAW264.7 macrophages were infected with RRV T48 at an MOI of 1 in the presence of PXF (100 μM and 1000 μM). Non-treated macrophages were infected with RRV in parallel and used as positive control. Supernatant samples were taken at various time points and examined for TNFα by ELISA. Data shown above is expressed in mean values ± SEM (n=3). **(p≤0.01), ***(p≤0.001) as determined by two-way ANOVA for PXF treated samples compared to non-treatment infection.

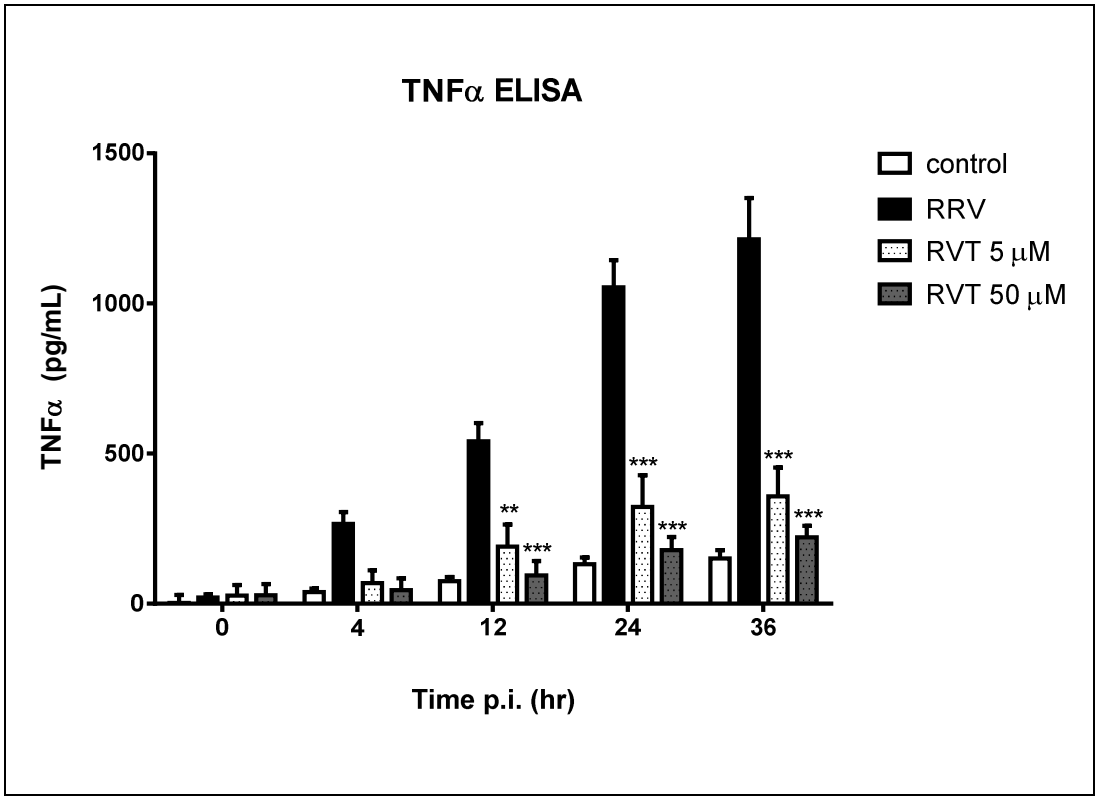

Figure 30: The effect of resveratrol on TNFα secretion in RRV-infected RAW264.7 macrophages

RAW264.7 macrophages were infected with RRV T48 at an MOI of 1 in the presence of resveratrol (RVT) (5 μM and 50 μM). Non-treated macrophages were infected with RRV in parallel and used as positive control. Supernatant samples were taken at various time points and examined for TNFα by ELISA. Data shown above is expressed in mean values ± SEM (n=3). **(p≤0.01), ***(p≤0.001) as determined by 2 way ANOVA for both concentrations of RVT compared to non-treatment.

4.4.1.5 Influence of resveratrol, ethyl pyruvate or pentoxifylline on TNFα mRNA expression in RRV-infected RAW264.7 macrophages

RNA extracted from RAW264.7 cells exposed to RRV T48 at an MOI of 1 and concurrent treatment with 1000 µM EP, 1000 µM PXF, 50 µM RVT or R-2 was examined for expression of TNFα mRNA by quantitative RT-PCR and normalised values were compared to respective controls. Concurrent treatment with EP did not show a reduction in TNFα transcription at 12 hr p.i. and only a slight down-regulation by 24 hr p.i., which was however not significant (Figure 31 A). Stronger inhibition of TNFα transcription was observed with PXF, which showed significant reduction at 12 hr p.i. ($p \leq 0.05$). The inhibitory effect however appeared to lessen by 24 hr p.i. as shown in Figure 31 B. Co-treatment of RRV infection with 50 µM RVT inhibited expression of TNFα in macrophages significantly by 24 hr p.i. ($p \leq 0.05$), with transcription levels below or similar to negative controls (Figure 31 C).

4.4.2 Inhibition of IL-6 release of RRV-infected RAW264.7 macrophages

4.4.2.1 Macrolide antibiotics

The influence of macrolides on IL-6 expression has been reported with greatly varying results in early research, depending on the conditions and cell lines used (Labro, 1998). An investigation into macrolide antibiotics as anti-inflammatory agents (Ianaro et al., 2000) has reported that several macrolides can reduce IL-6 expression amongst other cytokines in J774 murine macrophages. This IL-6 reducing effect was later confirmed for CLA and ERY in LPS stimulated RAW264.7 macrophages (Sato et al., 2007). To investigate a possible role for macrolide antibiotics in the treatment of alphavirus infections we exposed RAW264.7 macrophages to RRV T48 (MOI of 1) with or without the presence of varying concentrations of macrolide antibiotics and measured IL-6 production post-infection.

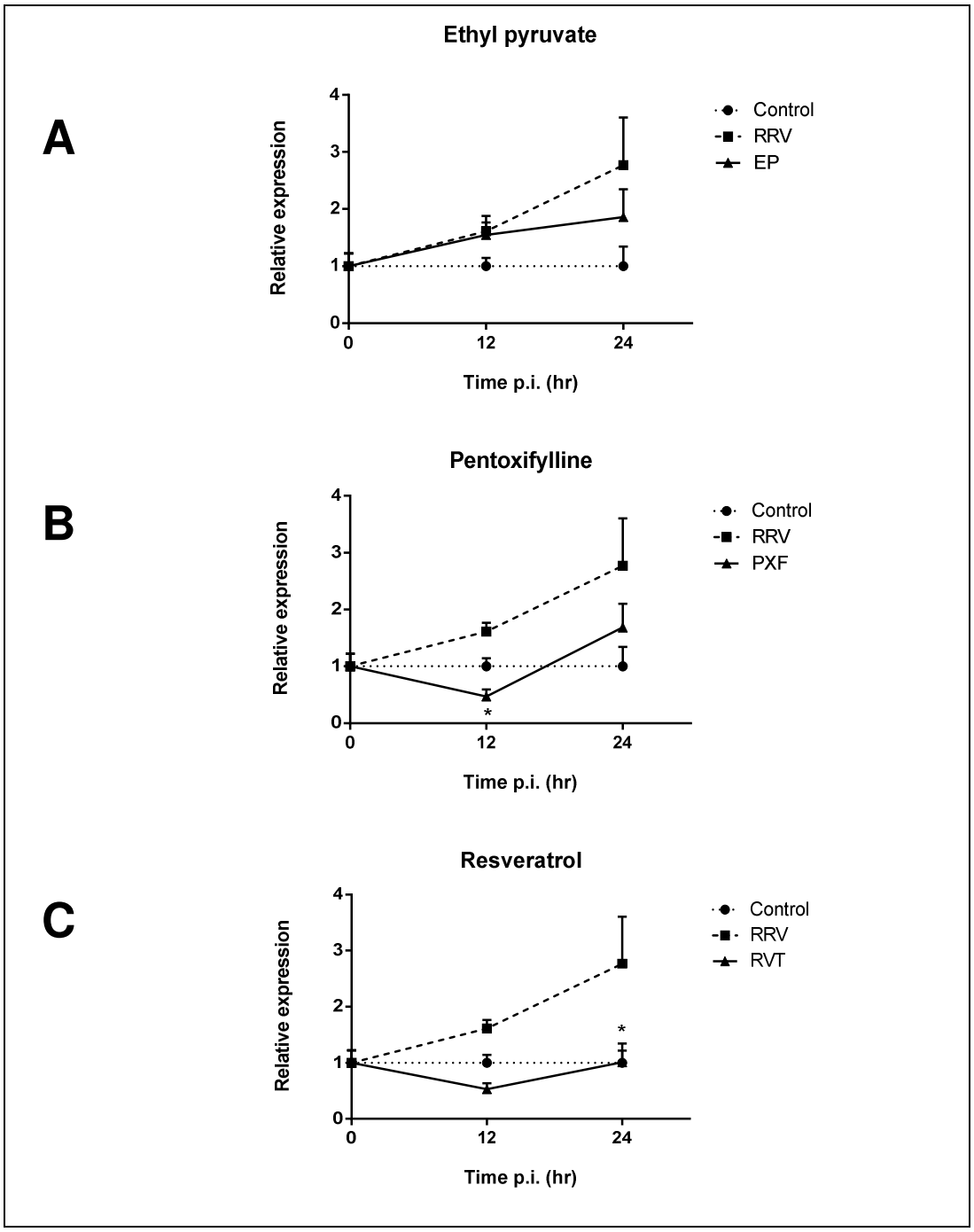

Figure 31: Expression of TNFα mRNA in RRV-infected RAW264.7 macrophages treated with ethyl pyruvate, pentoxifylline or resveratrol

RAW264.7 macrophages were infected with RRV T48 at an MOI of 1 and simultaneously treated with 100 µM EP, 1000 µM PXF or 50 µM RVT. RNA was extracted at different times and examined by quantitative real time PCR. HI-RRV was used as negative control. Relative expression was calculated as the normalised values of RRV-samples over the normalised values of the corresponding control. Data shown as mean values + %CV (n=3). *($p \leq 0.05$) as determined by two-way ANOVA.

4.4.2.1.1 Erythromycin inhibits secretion of IL-6 from RAW264.7 macrophages after RRV infection

RAW264.7 macrophages were infected with RRV T48 at an MOI of 1 in the presence of 10 µM or 100 µM ERY and supernatant at various time points p.i. was examined for IL-6 by ELISA (Figure 32). Supernatant levels of treated RAW264.7 cells were compared to macrophages exposed to RRV without macrolides. At 12 hr p.i. an inhibition of IL-6 from 276 ± 81 pg/mL to 165 ± 25 pg/mL was detected for 10 µM ERY, which was however not significant. The inhibitory effect appeared reduced over time with negligible inhibition at 36 hr post-infection for 10 µM ERY. Treatment with 100 µM ERY resulted in a stronger inhibition by 5.6-fold (to 49 ± 43 pg/mL) at 12 hr p.i. ($p \leq 0.01$) but decreased to 1.5-fold (360 ± 44 pg/mL) at 36 hr p.i. compared to 553 ± 71 pg/mL for non-treated samples ($p \leq 0.05$).

4.4.2.1.2 Clarithromycin inhibits IL-6 release from RRV-infected RAW264.7 macrophages

RAW264.7 macrophages were exposed to RRV T48 at an MOI of 1 and concurrently treated with 10 µM or 100 µM CLA as previously. Supernatant samples at various time points p.i. were screened for IL-6 concentrations by ELISA. Secretion of IL-6 into the supernatant was reduced from 12 hr p.i. onwards for both concentrations of CLA and inhibition was most prominent at 12 hr p.i. with a 1.8-fold and 6.4-fold reduction of IL-6 in 10 µM and 100 µM respectively (Figure 33). IL-6 levels were still significantly reduced at 36 hr p.i. in samples containing 100 µM CLA, however the inhibition was much less pronounced (1.5-fold). From 24 hr p.i. onwards the statistical difference between 10 µM and 100 µM was no longer significant.

4.4.2.1.3 Roxithromycin does not inhibit IL-6 secretion of RRV-infected RAW264.7 macrophages

To evaluate the ability of RXM to inhibit IL-6 in RRV infection we exposed RAW264.7 macrophages to RRV T48 at an MOI of 1 with or without the presence of 10 µM or 100 µM RXM and measured IL-6 concentration in the supernatant by ELISA (Figure 34). In contrast to the macrolides tested previously, 10 µM RXM did not significantly inhibit IL-6 secretion at any given time point post-infection. 100 µM RXM initially inhibited IL-6 release at 12 hr p.i. ($p \leq 0.01$) but this effect did not continue and no significant reduction in the cytokine concentration was detected at 24 or 36 hr p.i. It appears that RXM only delayed IL-6 release at 100 µM but did not result in a reduction at later stages.

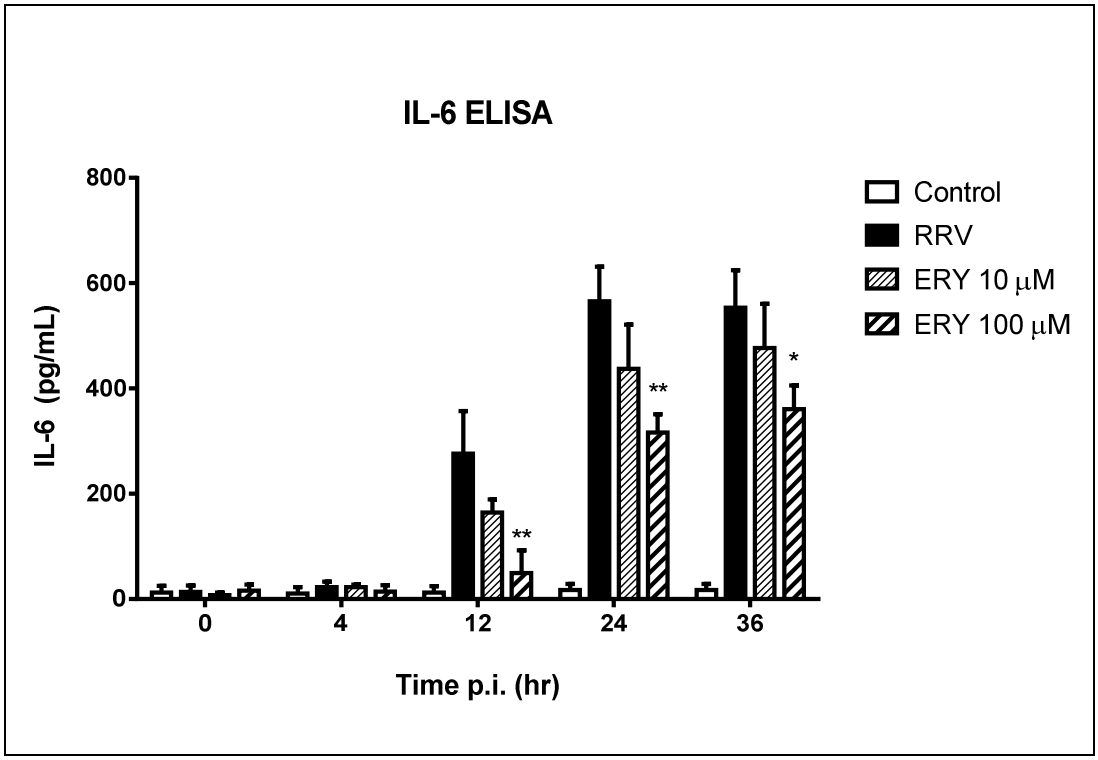

Figure 32: IL-6 secretion of RRV-infected RAW264.7 macrophages treated with erythromycin

RAW264.7 macrophages were exposed to RRV T48 at an MOI of 1 in the presence or absence of erythromycin (ERY) (10 and 100 μM). Supernatant samples were taken at various time points and examined for IL-6 by ELISA. Data shown above is expressed in mean values ± SEM (n=3). *(p≤0.05), **(p≤0.01) was determined by two-way ANOVA compared to non-treated infection.

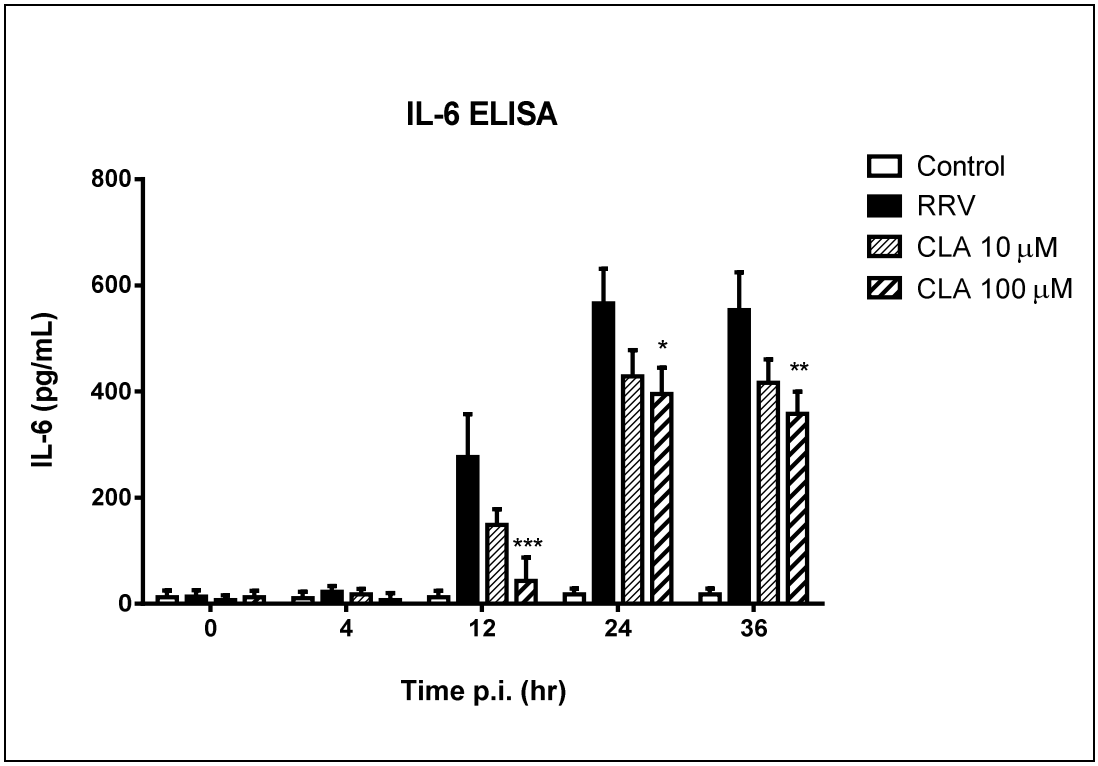

Figure 33: **IL-6 secretion of RRV-infected RAW264.7 macrophages treated with clarithromycin**

RAW264.7 macrophages were exposed to RRV T48 at an MOI of 1 in the presence or absence of clarithromycin (CLA) (10 and 100 μM). Supernatant samples were taken at various time points and examined for IL-6 by ELISA. Data shown above is expressed in mean values ± SEM (n=3). Statistical analysis was performed by two-way ANOVA and treatment was compared to non-treated infection. *($p \leq 0.05$), **($p \leq 0.01$), ***($p \leq 0.001$)

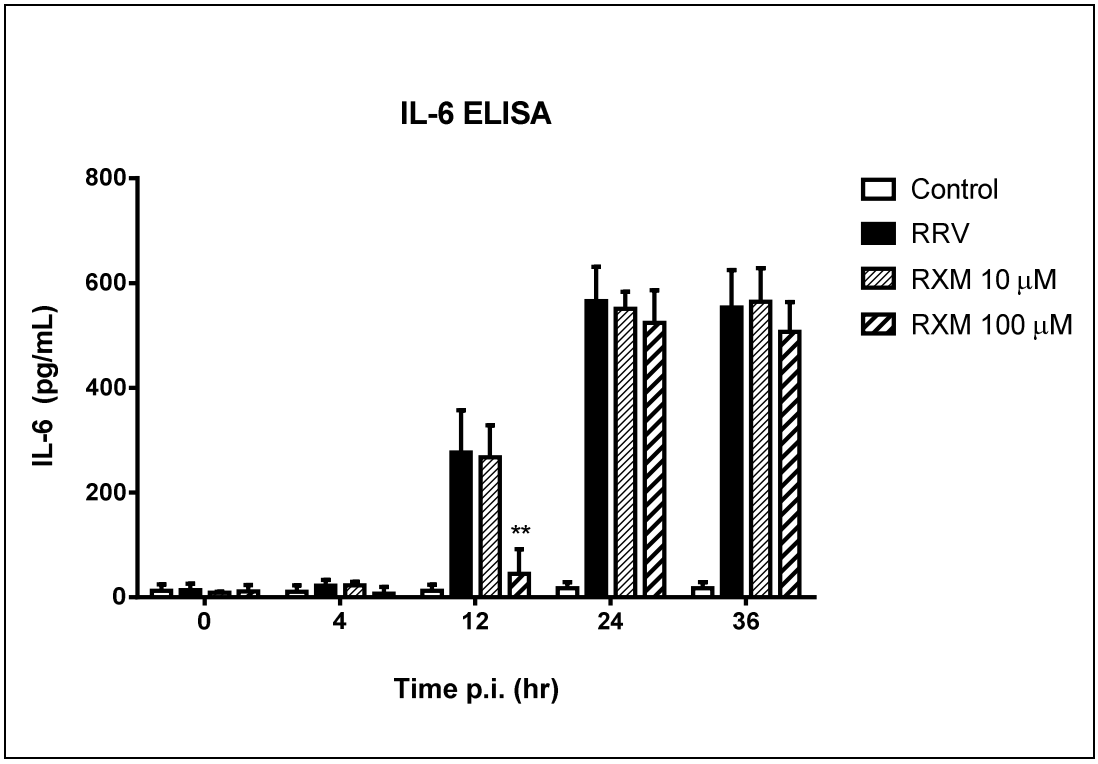

Figure 34: Effect on IL-6 secretion in RRV-infected RAW264.7 macrophages treated with roxithromycin

RAW264.7 macrophages were exposed to RRV T48 at an MOI of 1 in the presence or absence of roxithromycin (RXM) (10 and 100 μM). Supernatant samples were taken at various time points and examined for IL-6 by ELISA. Data shown above is expressed in mean values ± SEM (n=3). **(p≤0.01)

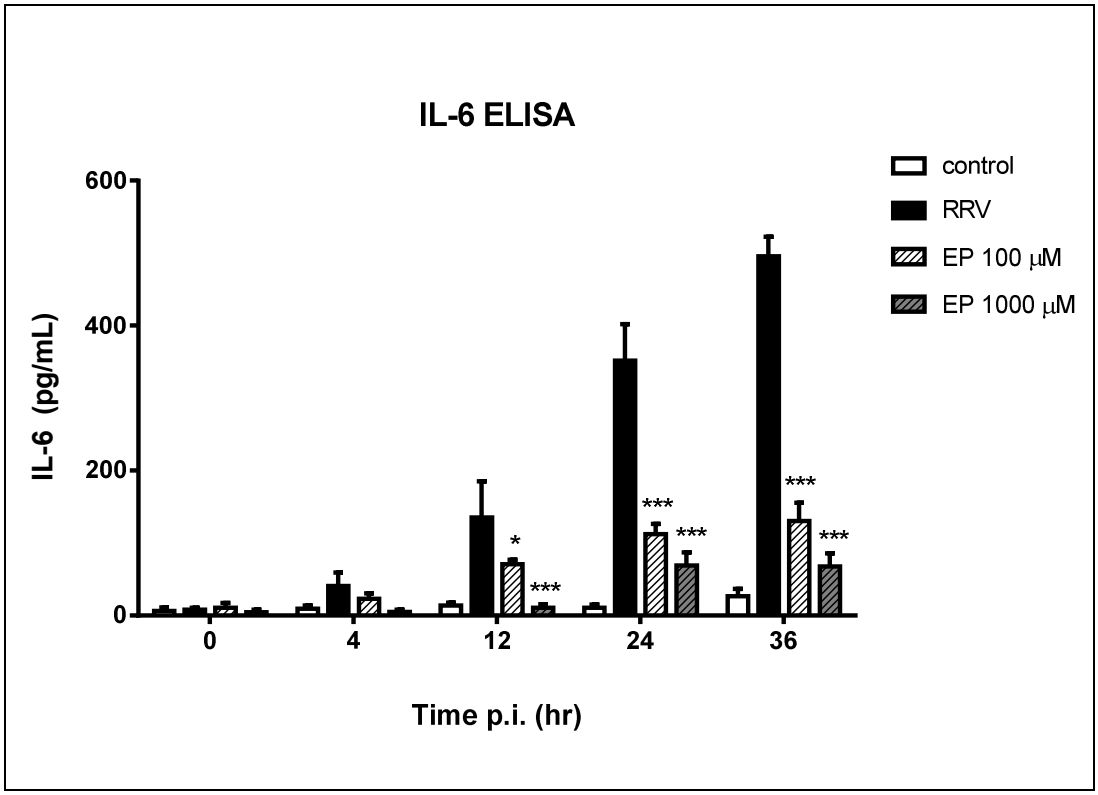

Figure 35: **IL-6 concentration in the supernatant of RRV-infected RAW264.7 macrophages co-treated with ethyl pyruvate**

RAW264.7 macrophages were exposed to RRV T48 at an MOI of 1 in the presence or absence of ethyl pyruvate (EP) (100 and 1000 μM). Supernatant samples were taken at various time points and examined for IL-6 by ELISA. Data shown above is expressed in mean values ± SEM (n=3). *(p≤0.05), ***(p≤0.001)

4.4.2.2 Ethyl pyruvate lowers IL-6 secretion in RRV-infected RAW264.7 macrophages

The anti-inflammatory effect of EP was previously described (Yang et al., 2002) and it was reported that expression of IL-6 mRNA, amongst other cytokines, is inhibited in mice subjected to haemorrhagic shock and treated with EP. Further investigations (Song et al., 2004) in LPS-stimulated RAW264.7 macrophages showed strong reduction of IL-6 secretion when treated with EP. To examine if release of IL-6 can also be reduced in RRV infection, the supernatant of RAW264.7 macrophages exposed to RRV and co-treated with varying concentrations of EP was analysed by IL-6 ELISA. As shown in Figure 35, the inhibitory effect of EP was both time- and dose-dependent. Significant reduction of IL-6 was detectable from 12 hr p.i. onwards for macrophages treated with 1000 µM EP ($p \leq 0.05$). At 36 hr p.i. inhibition was more pronounced with IL-6 concentration lowered from 496 ± 27 pg/mL (non-treated infection) to 130 ± 25 pg/mL and 68 ± 18 pg/mL for 100 µM EP and 1000 µM EP respectively ($p \leq 0.001$). This translates to a 3.8-fold (100 µM EP) and 7.2-fold (1000 µM EP) reduction of IL-6 secretion.

4.4.2.3 Influence of pentoxifylline on IL-6 release in RRV-infected RAW264.7

Early research with PXF has revealed its anti-inflammatory properties in endotoxin challenged volunteers by reducing serum TNFα levels without affecting IL-6 concentrations (Waage et al., 1990). Later reports (D'Hellencourt et al., 1996) confirmed these results, but highlighted that the effect of PXF on IL-6 secretion varies between whole blood culture and peripheral blood mononuclear cells (PBMCs). Further studies have shown the IL-6 inhibiting properties of PXF on alveolar macrophages in pulmonary sarcoidosis and in pig-serum-stimulated rats (Toda et al., 2009; Tong et al., 2003). Considering these variable findings we trialled PXF in our infection assay and examined its effect on IL-6 production. RAW264.7 macrophages were exposed to RRV T48 at an MOI of 1 with or without different concentrations of PXF and supernatant samples were analysed by IL-6 ELISA at various time points p.i. (Figure 36). Both 100 µM and 1000 µM PXF showed inhibition of IL-6 from 24 hr p.i. onwards, which was however not significant as compared to non-treatment.

PXF had shown a strong inhibitory effect on TNFα secretion earlier (4.4.1.3) but had no significant influence on IL-6 secretion. Comparable results were reported for endotoxin challenged PBMCs previously (Waage et al., 1990) and we were able to confirm these properties for PXF in RRV-infected RAW 264.7 macrophages.

4.4.2.4 Resveratrol

The inhibitory effect of RVT on IL-6 release from peritoneal mouse macrophages has been previously reported (Zhong et al., 1999) and was confirmed in LPS-stimulated RAW264.7 macrophages later (Capiralla et al., 2012). To investigate a possible IL-6 inhibiting effect in RRV infection we exposed RAW264.7 macrophages to RRV T48 at an MOI of 1 in the presence or absence of 5 µM and 50 µM RVT and analysed the supernatant by IL-6 ELISA (Figure 37). A time- and dose-dependent inhibition was detected immediately and reached significant levels for both concentrations by 12 hr p.i. ($p \leq 0.001$). Non-treated samples infected with RRV showed IL-6 levels of 496 ± 27 pg/mL by 36 hr p.i., whereas co-treatment with 5 µM RVT reduced the concentration 1.7-fold to 279 ± 32 pg/mL. Samples treated with 50 µM RVT showed a 3-fold decrease of IL-6 secretion (166 ± 26 pg/mL) at 36 hr p.i.

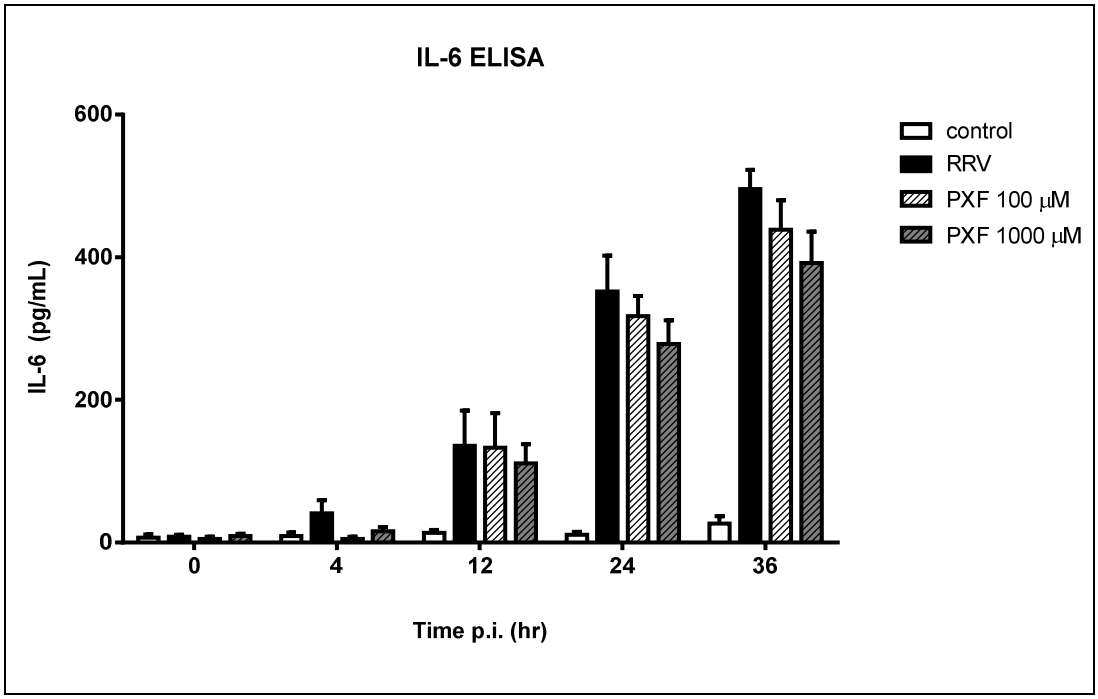

Figure 36: IL-6 release from RRV-infected RAW264.7 macrophages co-treated with PXF

RAW264.7 macrophages were exposed to RRV T48 at an MOI of 1 in the presence or absence of pentoxifylline (PXF) (100 and 1000 μM). Supernatant samples were taken at various time points and examined for IL-6 by ELISA. Data shown above is expressed in mean values ± SEM (n=3). No significant inhibition was detectable for both concentrations compared to non-treated infection (as determined by two-way ANOVA).

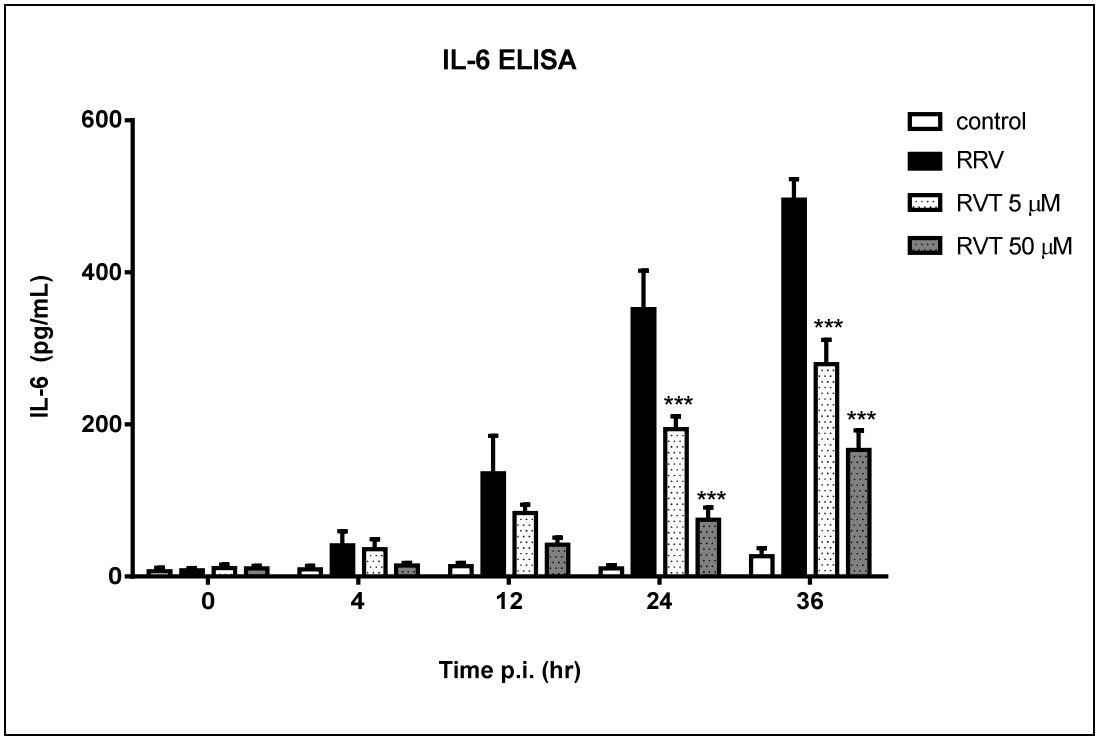

Figure 37: Effect of RVT on IL-6 release from RRV-infected RAW264.7 macrophages

RAW264.7 macrophages were exposed to RRV T48 at an MOI of 1 with or without resveratrol (RVT) (5 and 50 μM). Supernatant samples taken at various time points p.i. were analysed by IL-6 ELISA. Data shown is expressed in mean values ± SEM (n=3). ***($p \leq 0.001$) compared to non-treatment as determined by two-way ANOVA.

4.4.3 Macrolides increase in the secretion of the anti-inflammatory cytokine IL-10 in RAW264.7 macrophages

The therapeutic potential of macrolides as anti-inflammatories has previously been reviewed and the potential of some macrolides to increase levels of Interleukin 10 (IL-10) has been highlighted (Labro, 1998). These effects might be beneficial in the treatment of rheumatic diseases (Keystone et al., 1998), however are possibly not beneficial in RRV infection, as increased IL-10 levels are thought to result in reduced anti-viral responses (Rulli et al., 2005). As shown in earlier experiments (4.3.13), IL-10 is up-regulated in RRV infection and considering the potential of macrolide antibiotics to interfere with cytokine expression, we investigated the influence of macrolides on RRV-infected macrophages. RAW264.7 macrophages were infected with RRV T48 at an MOI of 1 and concurrently treated with 100 µM of ERY, CLA or RXM. Supernatant samples were taken at appropriate times and IL-10 levels determined by ELISA. All macrolide antibiotics tested resulted in elevated IL-10 levels by 4 hr p.i. compared to non-treated RRV-infected macrophages (Figure 38), however this increase was not significant for ERY. CLA treatment showed a significant 3.2-fold increase in IL-10 to 147 ± 22 pg/mL at 4 hr p.i. compared to 46 ± 15 pg/mL for non-treated samples ($p \leq 0.01$). This effect was even greater for RXM with IL-10 concentrations of 239 ± 42 pg/mL, which equates to a 5.2-fold increase ($p \leq 0.001$). At 12 hr p.i. and after there was no significant difference between RRV-infected non-treatment samples and ERY or CLA treated samples. The up-regulation of IL-10 secretion was significant for RXM at 4, 12 and 24 hr p.i., but dropped below significance levels at 36 hr p.i. For better comparison, IL-10 concentrations of the supernatant at 24 hr p.i. are shown in Table 10.

Table 10: Macrolide antibiotics alter IL-10 release in RAW264.7 macrophages

Macrolide antibiotic	IL-10 levels (pg/mL)	x-fold increase
no macrolide	153 ± 25	-
Erythromycin	126 ± 12	0.8
Clarithromycin	167 ± 22	1.1
Roxithromycin	252 ± 23	1.6

IL-10 levels were measured at 24 hr p.i. by ELISA. Data is expressed as mean value ± SEM (n=3 independent experiments).

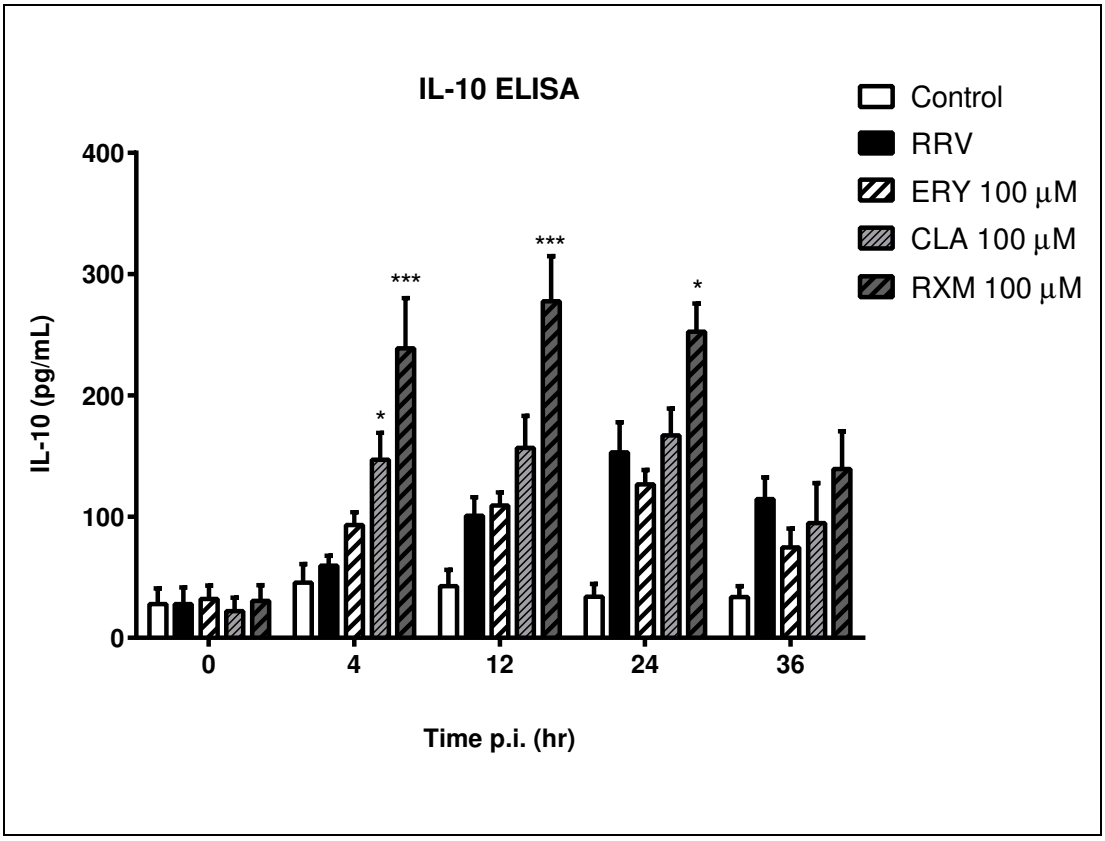

Figure 38: The effect of macrolide antibiotics on IL-10 secretion in RRV-infected RAW264.7 macrophages

RAW264.7 macrophages were infected with RRV T48 at an MOI of 1 in the presence of 100 µM erythromycin, clarithromycin or roxithromycin. Non-treated macrophages were infected with RRV in parallel and used as positive control. Supernatant samples were taken at various time points and examined for IL-10 by ELISA. Data shown above is expressed in mean values ± SEM (n=3). *($p \leq 0.05$), ***($p \leq 0.001$) as determined by two-way ANOVA for macrolide treatments compared to non-treatment infection.

4.4.4 Inhibition of MIF in RRV-infected RAW264.7 macrophages

A previous study (Herrero et al., 2011) has highlighted the important role of MIF in RRV infection and it was reported that treatment with the established MIF-inhibitor ISO-1 significantly reduced symptom manifestation in RRV-infected mice. More recently research has focused on MIF as a therapeutic target for inflammatory diseases and investigated several synthetic MIF inhibitors for possible therapeutic use (L. Xu et al., 2013). Our previous experiments with TNFα inhibitors have shown a strong effect on cytokine release from macrophages for several tested compounds. To assess if these agents also modulate MIF secretion in infected macrophages we exposed RAW264.7 cells to RRV T48 (MOI of 1) in the presence of various compounds and measured MIF concentration in the supernatant collected at different time points post-infection.

4.4.4.1 Macrolide antibiotics

RAW264.7 macrophages were exposed to RRV T48 at an MOI of 1 in the presence of 100 µM ERY, CLA or RXM and supernatant samples were collected at appropriate time points p.i. and analysed by MIF ELISA. None of the macrolide antibiotics tested showed significant reduction of MIF secretion at 12 or 24 hr p.i. (Figure 39). ERY treated samples showed a reduction of MIF concentration, which was however not significant (as determined by two-way ANOVA).

4.4.4.2 Ethyl pyruvate, pentoxifylline and resveratrol do not significantly reduce MIF secretion in RRV-infected macrophages

Similarly to previously tested macrolide antibiotics we analysed supernatants of RAW264.7 macrophages exposed to RRV and concurrent treatment with 1000 µM EP, 1000 µM PXF or 50 µM RVT. EP-treatment resulted in lower concentrations of MIF in the supernatant at 12 hr and 24 hr p.i., whereas RVT appeared to generally increase MIF secretion from macrophages (Figure 40). PXF had no influence on MIF concentration in the supernatant of treated cells. None of the effects was however statistically significant (as determined by two-way ANOVA).

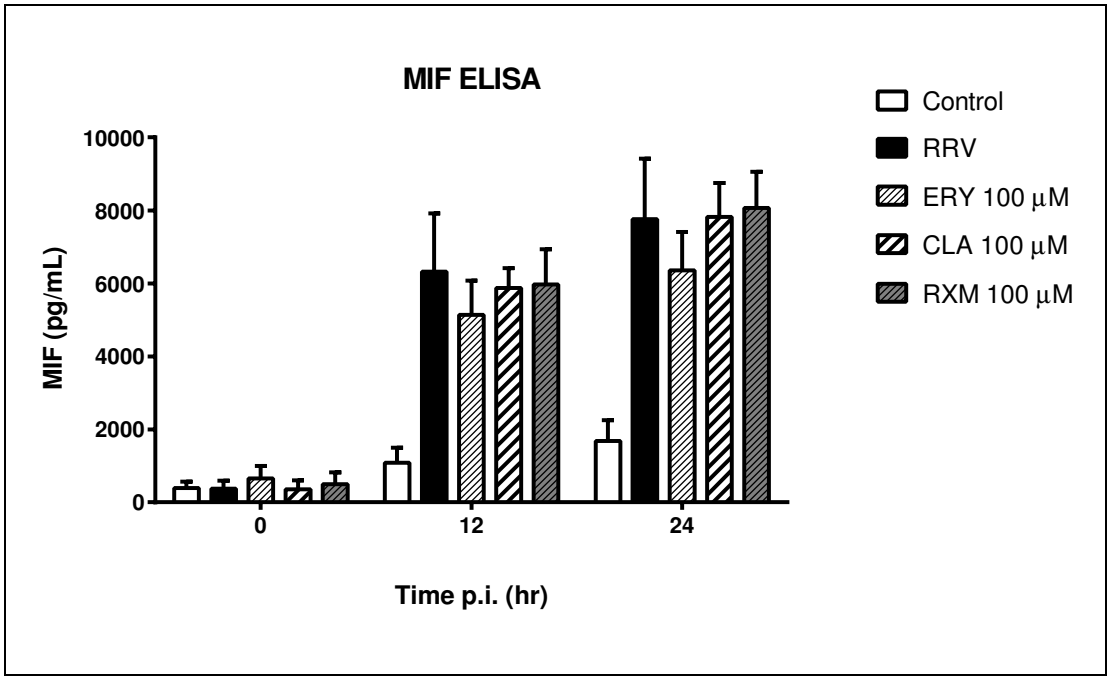

Figure 39: MIF concentration in the supernatant of RRV-infected macrophages with concurrent exposure to macrolide antibiotics

RAW264.7 macrophages were exposed to RRV T48 at an MOI of 1 with or without 100 µM erythromycin (ERY), clarithromycin (CLA) or roxithromycin (RXM). Samples collected at 0, 12 and 24 hr p.i. were analysed by MIF ELISA. Infection with HI-RRV was used as negative control (Control), non-treated RRV infection served as positive control (RRV). Data is expressed as mean value +- SEM (n=3). Statistical analysis was determined by two-way ANOVA.

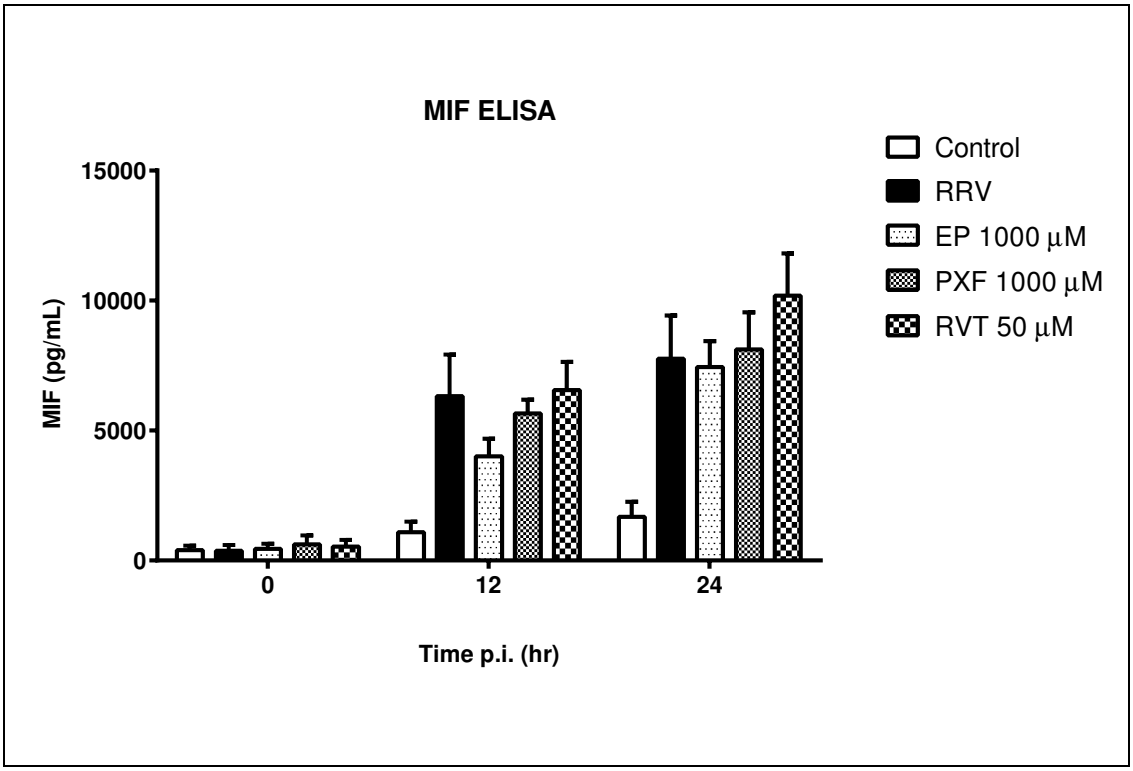

Figure 40: MIF concentration in the supernatant of RRV-infected macrophages treated with ethyl pyruvate, pentoxifylline or resveratrol

RAW264.7 macrophages were exposed to RRV T 48 at an MOI of 1 and concurrently treated with or without 1000 μM ethyl pyruvate (EP), pentoxifylline (PXF) or resveratrol (RVT). Samples collected at varying time points post-infection were analysed by MIF ELISA. HI-RRV was used as negative control in mock infection with (Control), non-treated RRV infection served as positive control (RRV). Data is expressed as mean value +- SEM (n=3). Statistical analysis was performed by two-way ANOVA.

4.4.5 Inhibition of IL-18 in RRV-infected macrophages

The important role of IL-18 in CHIKV infection has been highlighted previously (Chirathaworn et al., 2010) and inhibition of IL-18 was suggested as a possible target for the treatment of CHIKV disease. To our knowledge, no compounds have however so far been investigated for their influence on IL-18 production in alphavirus infections. In order to determine if any of the previously trialled compounds has a regulatory effect on IL-18 synthesis in macrophages we analysed extracted mRNA by quantitative real time PCR using primers specific for IL-18. Tested samples included treatment with 100 µM ERY, 100 µM CLA, 100 µM RXM, 1000 µM EP, 1000 µM PXF or 50 µM RVT. The normalised values were compared to the corresponding normalised control values and graphed as shown in Figure 41. From the tested compounds, EP and RVT exhibited a noticeable inhibitory effect on IL-18 mRNA transcription at 12 hr p.i. (Figure 41 D and F). At 24 hr p.i. significant inhibition as compared to non-treated infection was present in samples treated with ERY ($p \leq 0.01$), EP ($p \leq 0.01$) and RVT ($p \leq 0.05$). RXM and PXF showed some exhibitory effect, however not at a significant level. CLA appeared to have very little or no effect on IL-18 mRNA expression.

4.4.6 Inhibition of HMGB1 mRNA expression in RRV-infected RAW264.7 macrophages

Similar to previous experiments we investigated a possible inhibitory effect of various compounds on HMGB1 mRNA transcription in RRV infection. Again, mRNA extracted from RAW264.7 macrophages exposed to RRV T48 at an MOI of 1 was treated with either 100 µM ERY, 100 µM CLA, 100 µM RXM, 1000 µM EP, 1000 µM PXF or 50 µM RVT. Quantitative real time PCR analysis was performed with HMGB1-specific primers and the derived values were normalised with the corresponding G3PDH values as previously. Normalised values were graphed as a ratio to their corresponding negative control values. Only EP had a noticeable effect with HMGB1 mRNA expression similar to controls by 24 hr p.i. (Figure 42 D). None of the other compound showed significantly differing HMGB1 mRNA expression at 12 or 24 hr p.i. as compared to non-treatment.

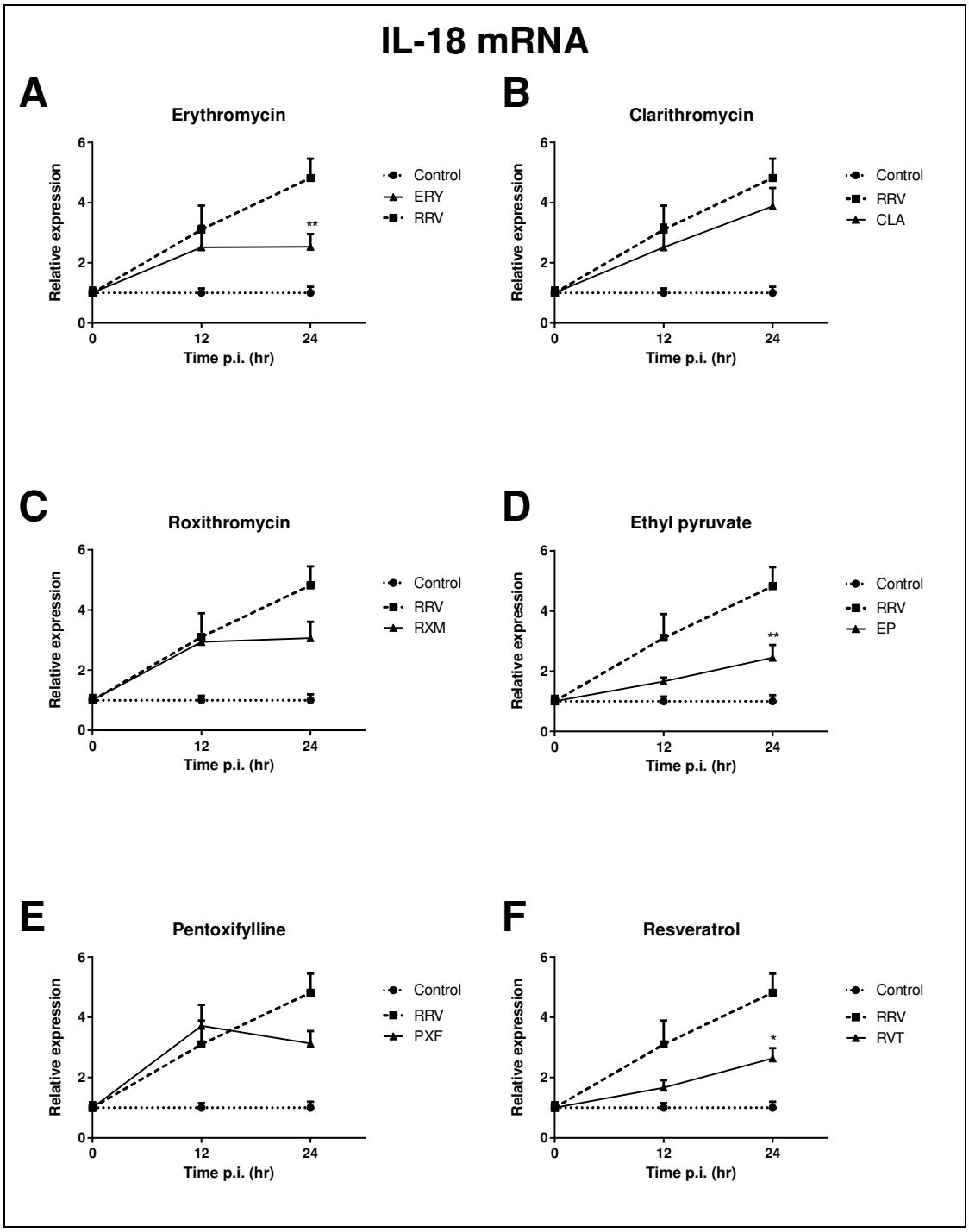

Figure 41: IL-18 mRNA expression in RRV-infected RAW264.7 with inhibitors

RAW264.7 macrophages infected with RRV T48 at an MOI of 1 were treated with 100 µM ERY, 100 µM CLA, 100 µM RXM, 1000 µM EP, 1000 µM PXF or 50 µM RVT. Non-treated infection served as positive control (RRV) whereas infection with HI-RRV was used as negative control (control). mRNA was analysed by quantitative RT-PCR and normalised values were graphed against their respective controls. Values are expressed as mean + %CV (n=3). *($p \leq 0.005$). **($p \leq 0.01$) as determined by two-way ANOVA.

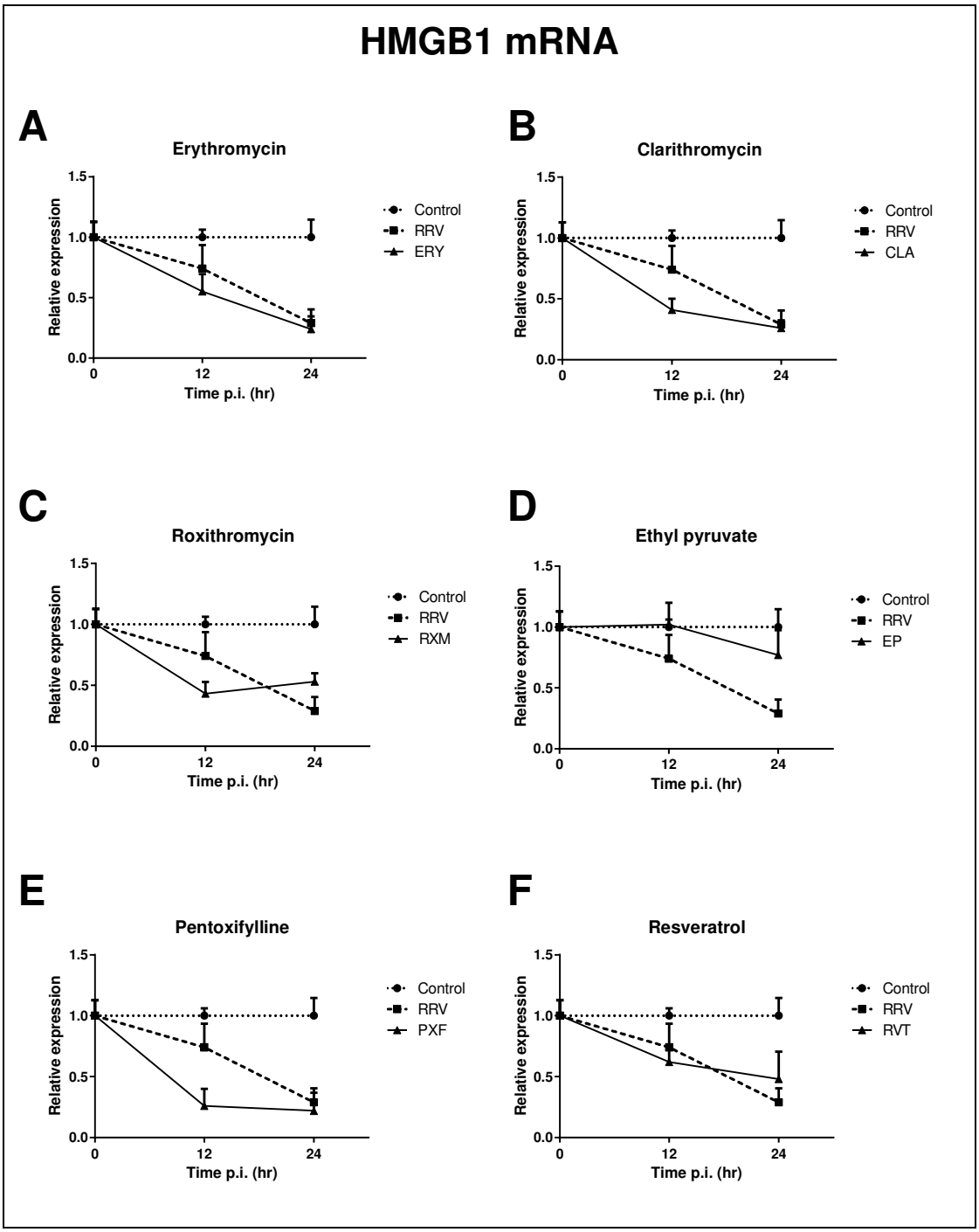

Figure 42: HMGB1 mRNA expression in RRV-infected RAW264.7 treated with inhibitors

RAW264.7 macrophages were exposed to RRV T48 at an MOI of 1 with or without the presence of 100 µM ERY, 100 µM CLA, 100 µM RXM, 1000 µM EP, 1000 µM PXF or 50 µM RVT. Non-treated infection was used as positive control (RRV), HI-RRV served as negative control (control). RNA was quantified by real time RT-PCR and normalised values were plotted against respective controls. Values are expressed as mean + %CV (n=3). Statistical analysis as per two-way ANOVA.

4.5 Phagocytic activity of RAW cells after RRV infection

Early studies have shown a link between phagocytic activity of macrophages and the severity of symptoms in rheumatoid arthritis (Burmester et al., 1997) and it was later reported that persistent RRV infection causes an increase in phagocytic activity in murine macrophages (Way et al., 2002). No studies have been conducted on acute RRV infection in macrophages and the influence on phagocytosis. To investigate if phagocytic activity is altered in acute RRV infection, RAW264.7 macrophages were exposed to RRV for varying times prior to a phagocytosis assay. Heat inactivated and FITC labelled bacteria were utilised to visualise and quantitate phagocytosis. Both Gram positive (*Staphylococcus aureus*) as well as gram negative bacteria (*Escherichia coli*) were used in the assay.

4.5.1 Analysis of phagocytic activity in RRV-infected RAW264.7 by fluorescence microscopy

To investigate the influence of acute RRV infection on macrophages we exposed RAW264.7 cells to RRV T48 (MOI of 1) for 24 and 48 hr prior to the phagocytosis assay. HI-RRV was used in a mock infection 48 hr prior to the assay and used as control. FITC-staining of the bacteria was confirmed by fluorescence microscopy prior to addition (Figure 43). To ensure that phagocytosis was evaluated independently, both a Gram positive (*S.aureus*) as well as a gram negative (*E.coli*) bacterial strain was used in separate experiments. As pictured in Figure 44 (A and C), no difference in phagocytosis was visible for any of the samples at 1 hr post exposure to labelled *E.coli*. At 4 hr post exposure the RAW264.7 cells infected with RRV 24 hr prior to the assay consistently showed increased phagocytic activity (Figure 44 B and D). The macrophages had taken up more labelled bacteria compared to non-treated samples and it also appeared that more cells were showing phagocytosis. The effect was even more pronounced in RAW264.7 macrophages that were infected with RRV 48 hr prior to the assay (Figure 44 E and F). A similar result was obtained with *S. aureus*, with an increased phagocytic activity already apparent at 1 hr post exposure to labelled bacteria for RAW264.7 cells infected with RRV (Figure 45 A, C and E). Again, at 4 hr post exposure an increase in phagocytic activity was observed for RRV-infected macrophages compared to mock infected controls. There was no clear visual difference between 24 hr and 48 hr pre-treatment with RRV.

A

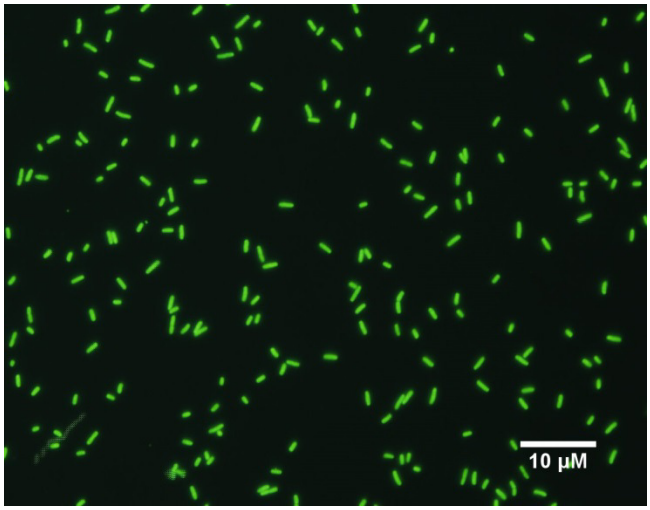

FITC labelled *E.coli*

B

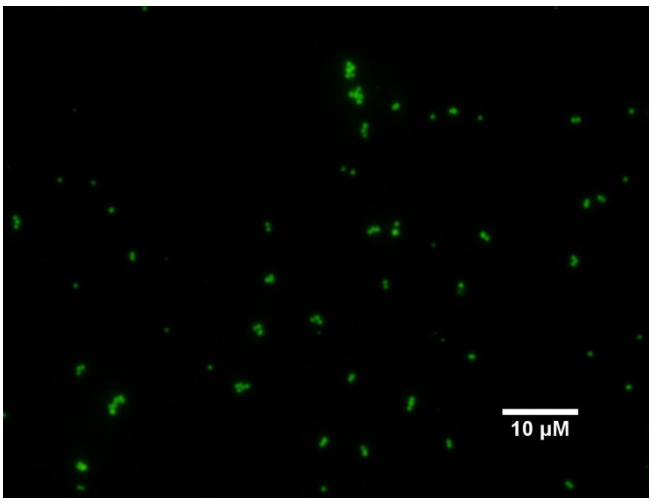

FITC labelled *S.aureus*

Figure 43: FITC labelled *E.coli* and *S.aureus*

Heat inactivated *E.coli* or *S.aureus* were incubated with FITC as described in Methods. Prior to the phagocytosis assay fluorescent labelling was confirmed by microscopy under UV light. Above are representative pictures of FITC labelled *E.coli* (A) and FITC labelled *S.aureus* (B) under 40x magnification.

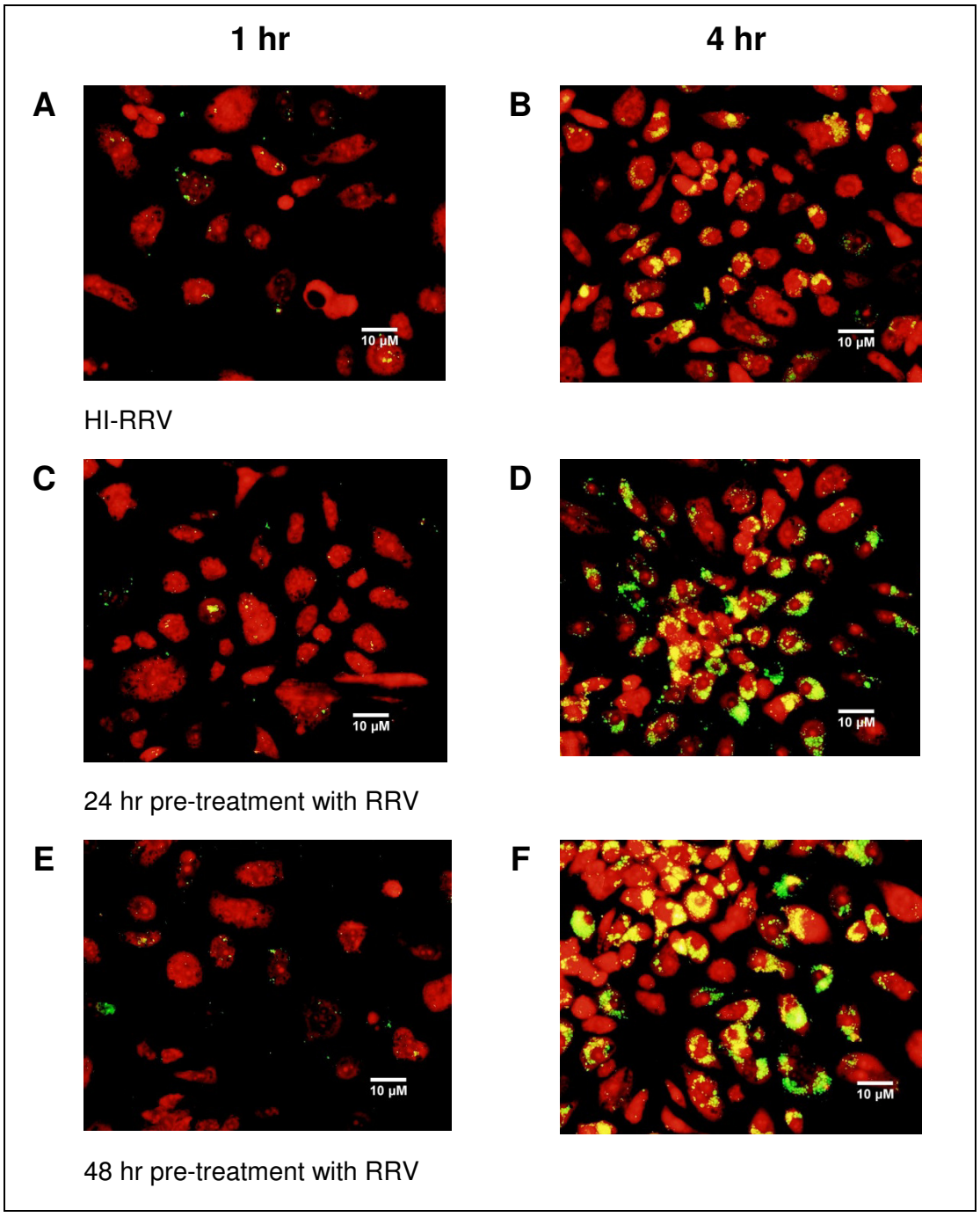

Figure 44: Phagocytosis of FITC-labelled *E.coli* by RAW264.7 macrophages after RRV infection

RAW264.7 macrophages were exposed to RRV T48 for 24 or 48 hr prior to addition of FITC labelled *E.coli*. HI-RRV was added to control wells 48 hr prior to the phagocytosis assay. Cells were fixed and stained with PI as described in Methods. Photographs were taken under fluorescence after 1 hr (A, C and E) and 4 hr (B, D and F) of exposure to FITC labelled bacteria. Shown are representative photomicrographs at 40x magnification.

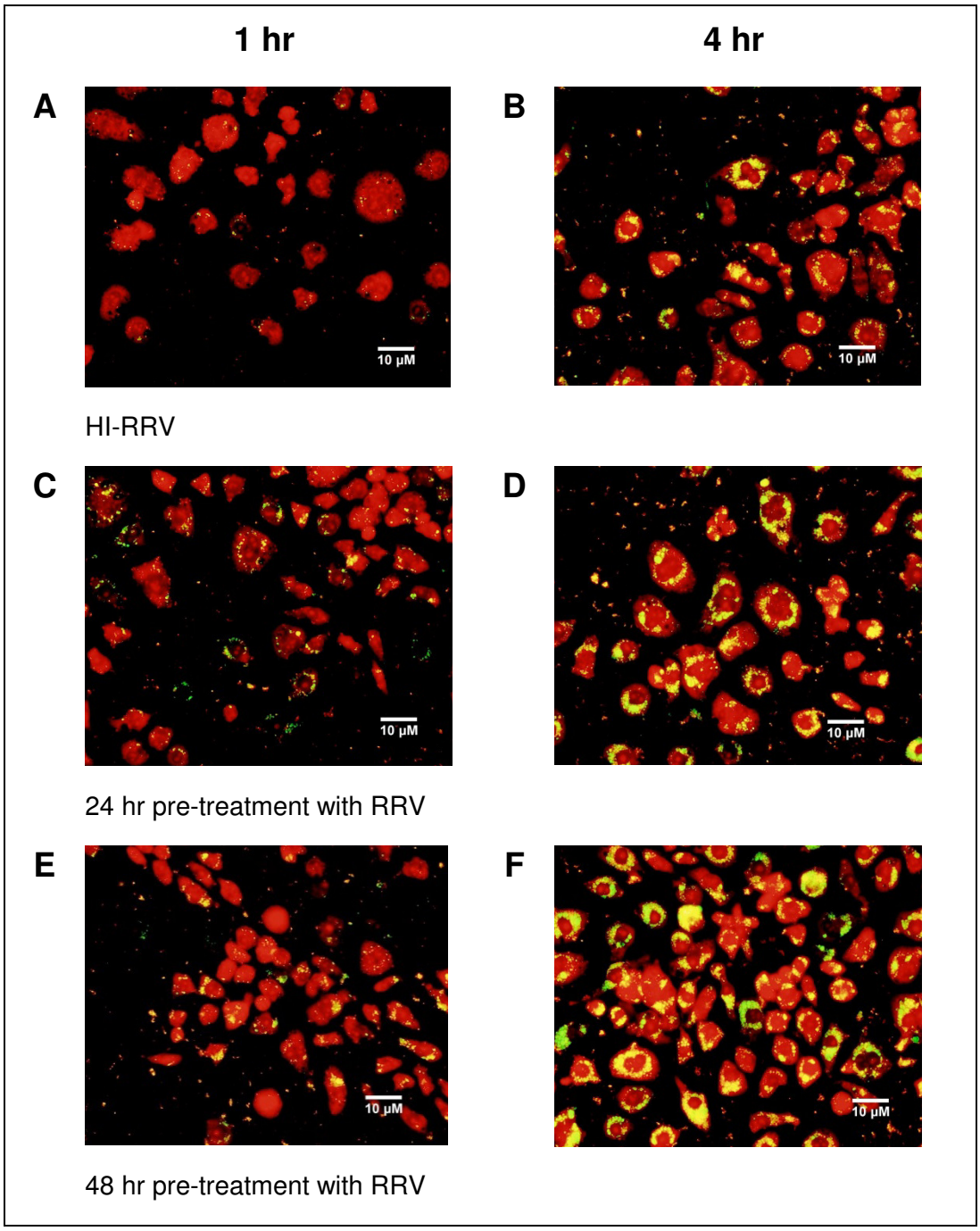

Figure 45: Phagocytosis of FITC-labelled *S.aureus* by RAW264.7 cells after RRV infection

RAW264.7 macrophages were exposed to RRV T48 for 24 or 48 hr prior to addition of FITC labelled *S.aureus*. HI-RRV was added to control wells 48 hr prior to the phagocytosis assay as control. Cells were fixed and stained with PI as described in Methods. Photographs were taken under fluorescence after 1 hr (A, C and E) and 4 hr (B, D and F) of exposure to FITC labelled bacteria. Above are representative photomicrographs at 40x magnification.

4.5.2 Flow cytometric analysis of phagocytic activity in RRV-infected RAW264.7 macrophages

Due to the limitations of fluorescence microscopy in regards to quantitation, the phagocytosis experiments were repeated and the RAW264.7 macrophages were examined in an Attune flow cytometer using a 488 nm excitation laser to quantify phagocytic activity. To avoid adherence of the macrophages to tissue culture vessels, all cells were grown in teflon culture vessels and further processed as outlined in Methods. Both *E.coli* and *S.aureus* were used to confirm the previously observed increase in phagocytic activity.

In brief, similar to the previous assay, RAW264.7 macrophages were exposed to RRV T48 at an MOI of 1 for 24 or 48 hr prior to the start of the assay. Mock infection with heat–inactivated RRV was performed on additional samples 48 hr prior to the experiment and used as negative control. Macrophages were exposed to FITC-labelled *E.coli* or *S.aureus* for 0, 1 or 4 hrs and washed, fixed and stained before being analysed on an Attune flow cytometer.

4.5.2.1 Compensation

Initial experiments determined emission levels at the appropriate wave lengths for both flouorophores in the assay. Propidium iodide (PI) was used to stain the nuclei of the macrophages and its emission was measured through a 574/26 nm filter, whereas bacteria was labelled with fluorescein isothiocyanate (FITC) and detected with a 530/30 nm emission filter. To ensure that any 'spillover' fluorescence could be compensated, initial samples were run for FITC positive samples without PI stain (macrophages at 4 hr post exposure to FITC labelled *E.coli* or *S.aureus* without further stain) as well as PI labelled macrophages that were not exposed to labelled bacteria (Figure 46 A and C). Since FITC only samples showed spillover signals at higher emission and *vice versa*, an automated compensation was run on the Flojo analysis software to accommodate for this shift in emission (Figure 46 B and D). Automatic compensation was always manually confirmed for FITC- and PI-only samples and adjusted if required. Compensation was performed for each separate experiment and further samples were analysed under compensated settings.

4.5.2.2 Gating strategy

To select only RAW264.7 macrophages but exclude debris or unbound bacteria, an initial gate was set for the desired population ('cells') and applied to all samples (Figure 47 A). Gate settings were confirmed for each specimen population separately and the gat was adjusted if required. The gated population ('cells') was

graphed in a histogram of forward scatter (height) (FSC-H) over forward scatter (area) (FSC-A) as shown in Figure 47 B. Single cells show a linear relationship between FSC-H and FSC-A and were separately gated to avoid detection of doublets or larger cell clumps, which appeared mostly at the top edge of the histogram. The unstained 'single cells' sample was further graphed as PI- and FITC-detection plot (Figure 47 C) and separate gates were drawn for PI-only, FITC-only and PI+FITC containing populations and again applied to all samples.

4.5.2.3 RRV infection increases the number of macrophages showing phagocytic activity

Analysis with Flowjo software showed a time dependent rise in the numbers of FITC+PI positive cells out of all detected cells, which indicates an increased number of cells with phagocytic activity. This was observed for both *E.coli* and *S.aureus* and in all samples, however RAW264.7 cells that had been exposed to RRV prior to the assay generally showed higher percentages of cell numbers with phagocytic activity (see Figure 48). This increase was significant for *S.aureus* samples at 1 hr post exposure to bacteria for macrophages infected with RRV for 24 hrs ($p \leq 0.01$) and 48 hrs ($p \leq 0.05$) prior to the assay (Figure 48B). There was no significant difference in cell numbers between 24 hr and 48 hr pre-exposure to RRV.

4.5.2.4 RRV infection increases the mean phagocytic activity in RAW264.7 macrophages

For further analysis, the mean fluorescent intensity (MFI) for FITC+PI positive cell populations was compared in order to determine whether an increase in phagocytic activity was detectable. As expected, the MFI increased in a time dependent manner in all samples, meaning each detected cell had adsorbed an increasing number of bacteria over time (Figure 49). Samples exposed to RRV prior to the experiment showed generally higher MFI for both bacteria strains at 1 hr post exposure and reached significantly higher levels at 4 hr post exposure. Again, no significant difference was detectable between the 24 hr and 48 hr RRV samples, although it appeared that samples with 48 hr pre-infection showed slightly increased phagocytic activity (Figure 50).

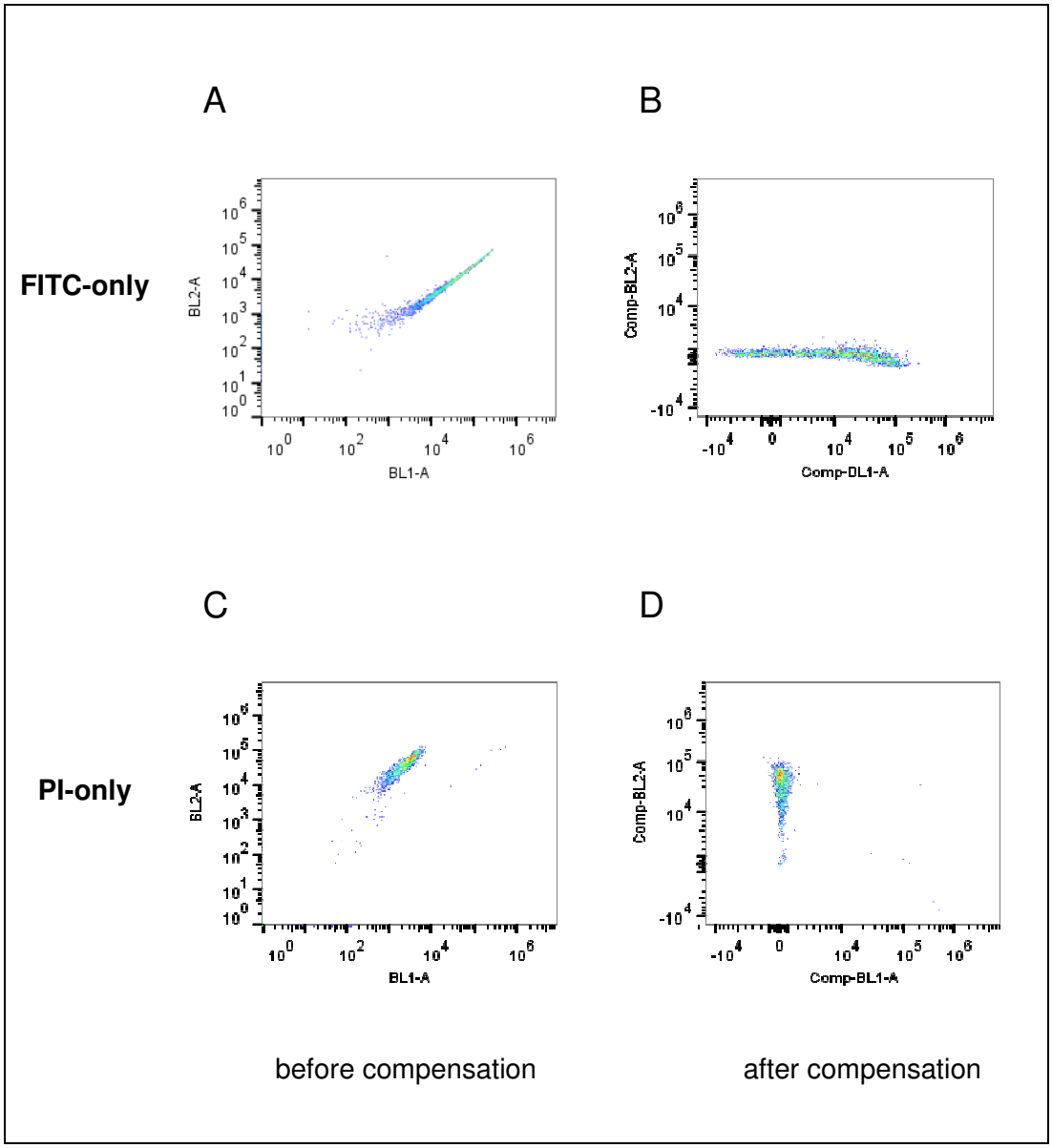

Figure 46: Compensation strategy for FACS analysis

Samples containing macrophages with FITC-labelled bacteria but without PI (FITC-only) and macrophages stained with PI only (PI-only) were analysed to allow compensation of 'spillover' emission. Shown above are representative emission plots of non-compensated FITC-only (A) and PI-only samples (B). Automated compensation was performed for each experiment with FloJo X software and manually adjusted as required. Emission plots of the same data under compensation settings show cancellation of spillover (B and D). BL-1 = Detection filter used for FITC, BL-2 = Detection filter used for PI

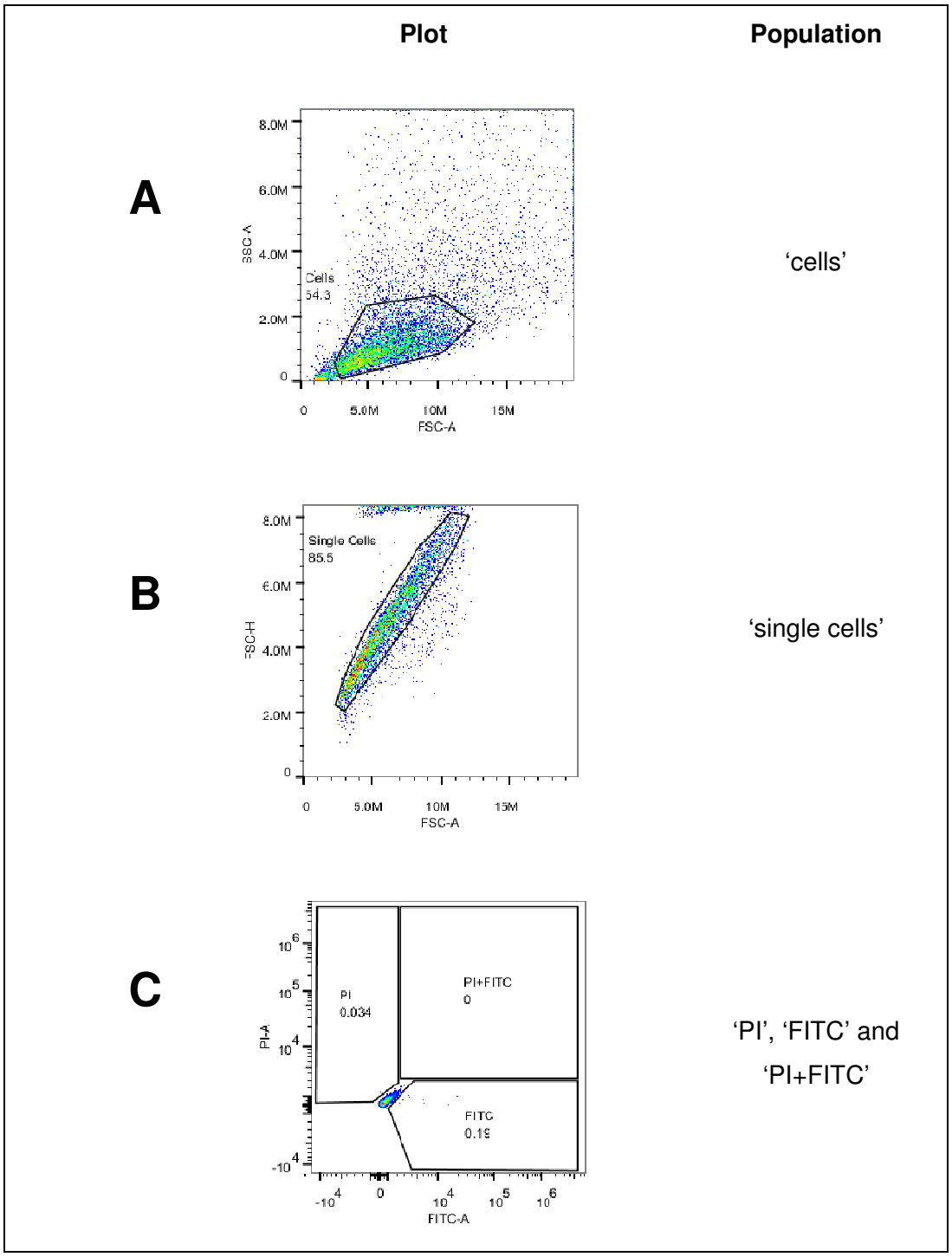

Figure 47: Gating strategy for flowcytometry analysis

A side scatter (SSC) over forward scatter (FSC) plot of unstained macrophages was graphed and cell population ('cells') was gated to exclude debris as shown in (A). This population was graphed in a forward scatter (FSC) height over area plot and gated for a 'single cells' subpopulation (B). 'Single cells' were plotted as PI- over FITC-detection and gates were drawn for PI-, FITC- and PI+FITC-containing cells (C). Shown above are representative plots as graphed with Flojo X software. Gating was performed separately for each individual experiment.

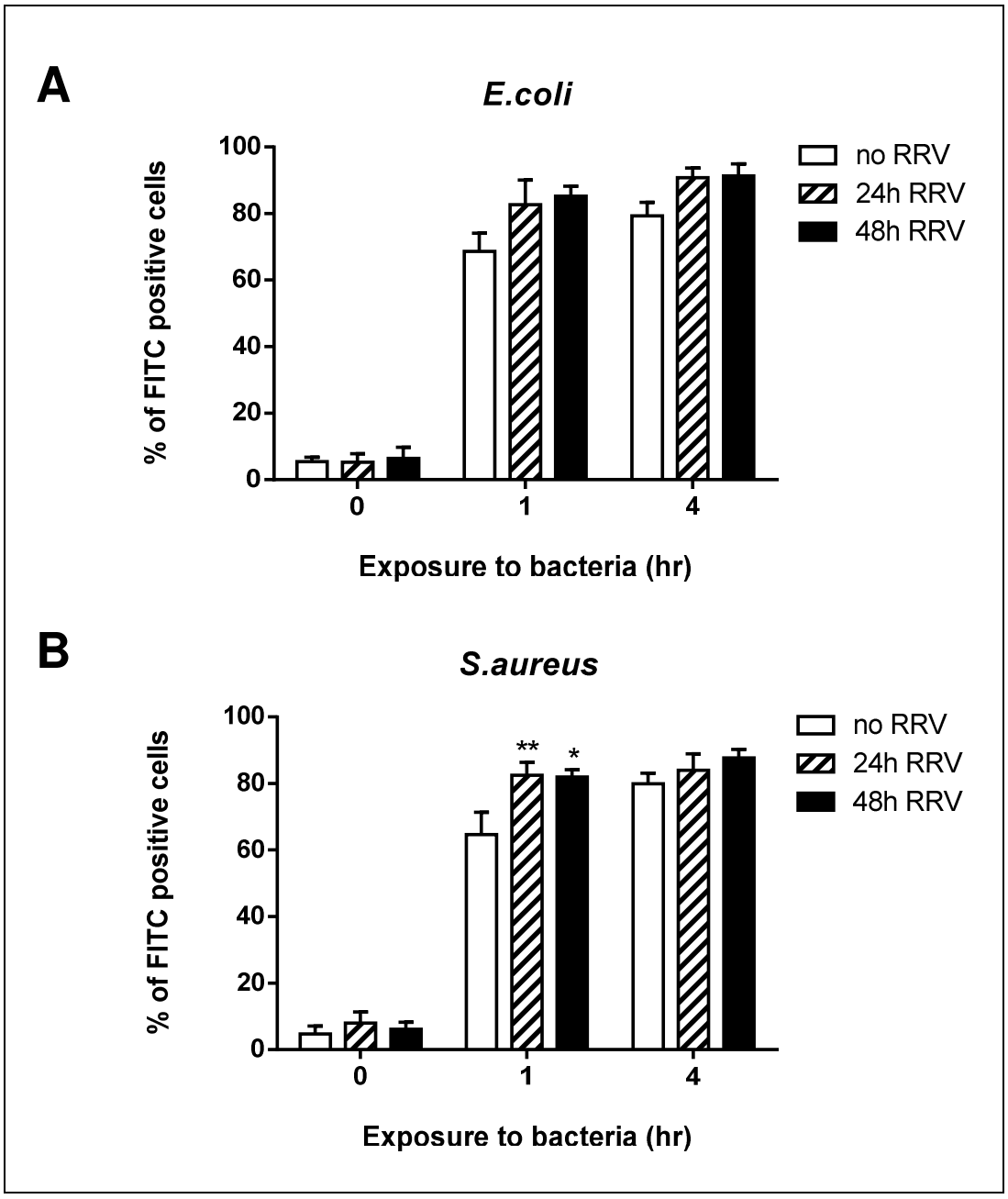

Figure 48: Percentage of cells showing phagocytic activity in RAW264.7 macrophages with and without pre-exposure to RRV T48

RAW264.7 macrophages were infected with RRV T48 at an MOI of 1 for 24 or 48 hr prior to the phagocytosis assay and exposed to FITC-labelled *E.coli* (A) or *S.aureus* (B) for varying time points. Macrophages were washed, fixed and stained as outlined in Methods and analysed by flow cytometry. Graphed above is the percentage of the FITC+PI-positive population out of all PI-positive cells. Data is expressed in mean values ± SEM (n=3 independent experiments). *($p \leq 0.05$), **($p \leq 0.001$) as determined by two-way ANOVA. Note the non-linear scale for time exposure to bacteria.

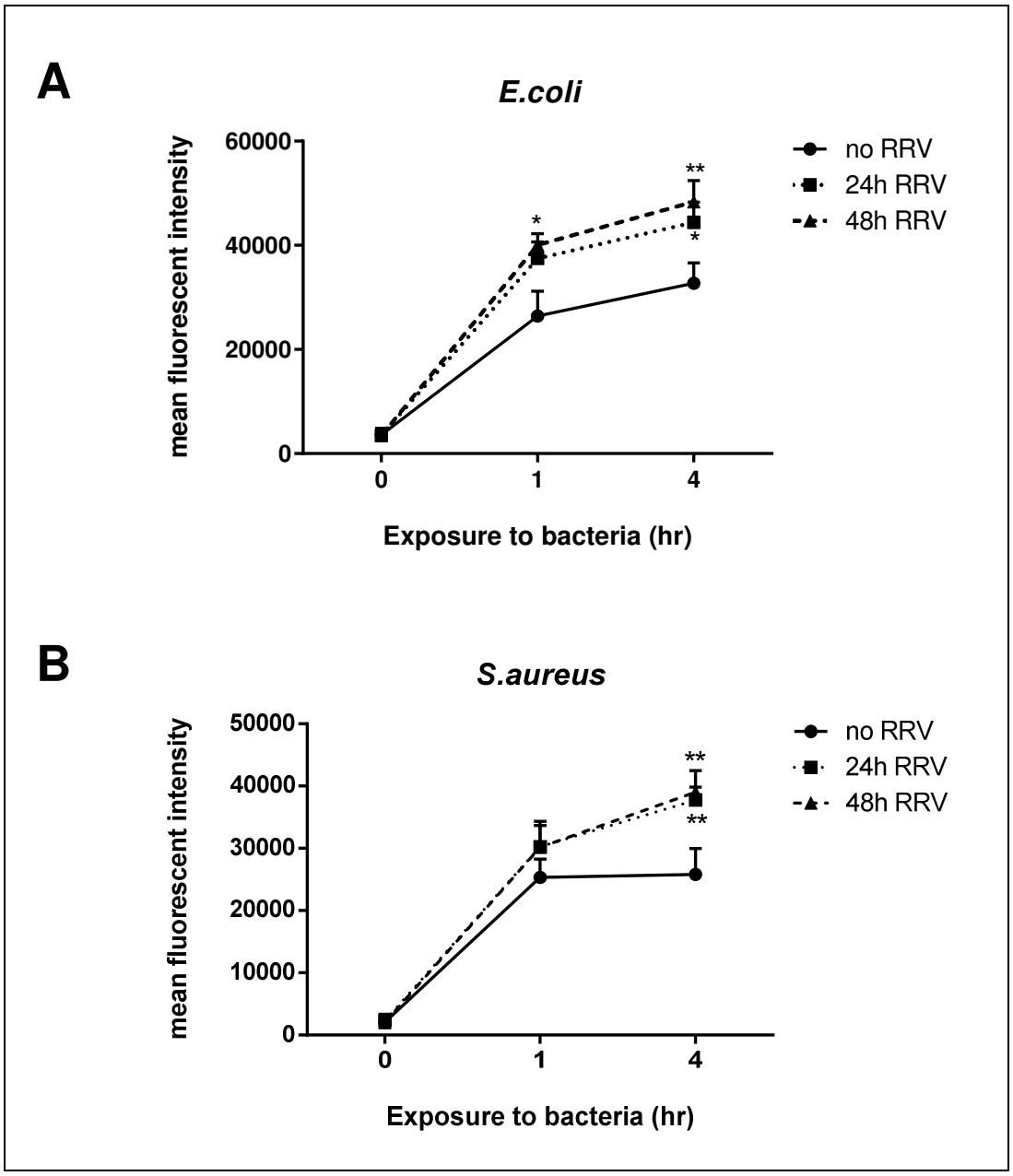

Figure 49: Phagocytic activity of RAW264.7 macrophages with or without pre-exposure to RRV

RAW264.7 macrophages were infected with RRV T48 at an MOI of 1 for 24 or 48 hr prior to the phagocytosis assay and exposed to FITC-labelled *E.coli* (A) or *S.aureus* (B) for varying time points. Macrophages were washed, fixed and stained as outlined in Methods and analysed by flow cytometry. The graphs above show the mean fluorescent intensity (MFI) of the FITC+PI positive population, i.e. only cells that have shown some degree of phagocytosis. MFI is expressed in arbitrary values as mean ± SEM (n=3 independent experiments). *($p \leq 0.05$), **($p \leq 0.001$) as determined by two-way ANOVA. Note the non-linear scale for time exposure to bacteria.

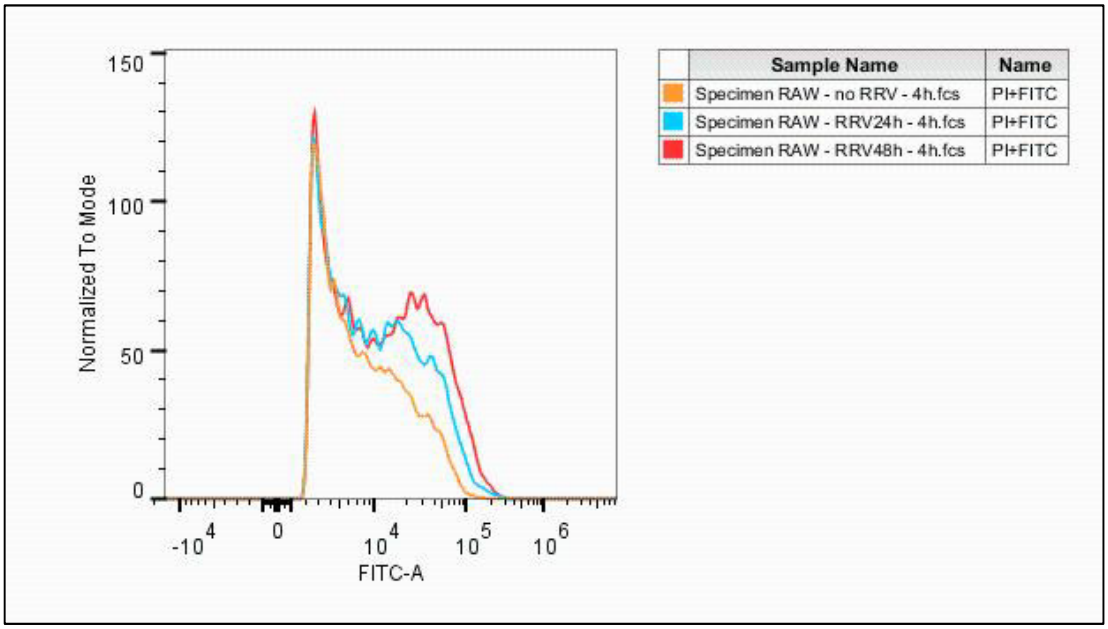

Figure 50: Phagocytic activity of RAW264.7 macrophages with our without pre-exposure to RRV

Data derived from the phagocytosis experiments with *S.aureus* was graphed as a histogram over FITC detection to visualise the change in phagocytic activity with pre-exposure to RRV T48 at an MOI of 1. Above diagram shows a representative overlay of samples exposed to *S.aureus* at 4 hr post exposure to the bacteria. Specimen RAW – no RRV – 4h.fcs = RAW264.7 macrophages without exposure to RRV T48, Specimen RAW – RRV24h – 4h.fcs = RAW264.7 macrophages with 24 hr pre-exposure to RRV T48, Specimen RAW – RRV48h – 4h.fcs = RAW264.7 macrophages with 48 hr pre-exposure to RRV T48.

4.6 Discussion of RAW264.7 results

A recent study (Taylor et al., 2013) has once more confirmed the important role of macrophages in RRVD progression and the release of macrophage-derived mediators is now considered to be a major contributing factor to the development of inflammatory joint conditions during infection (Assuncao-Miranda et al., 2013). With our experiments, we could confirm and further investigate the increased expression and secretion of several of those cytokines from macrophages during RRV infection *in vitro*, including TNFα (Lidbury et al., 2008) and MIF (Herrero et al., 2011). Although elevated IL-6 levels have been reported in CHIKV infections (Ng et al., 2009), its role in RRVD has so far not been investigated. We could show that the release of IL-6 but not the expression of IL-6 mRNA is increased in RAW264.7 macrophages upon RRV infection *in vitro*. It has previously been suggested that altered IL-6 mRNA degradation may occur during viral infection of airway epithelial cells (Lutter et al., 2000) and it remains to be determined whether RRV interferes with the decay of IL-6 mRNA during infection. Furthermore, increased expression of IL-18 mRNA has previously been recognized for CHIKV infections (Chirathaworn et al., 2010) and we established a comparable stimulation pattern for the expression of IL-18 mRNA in RRV infections. We were able to show an increase of IL-33 and IL-10 mRNA expression during infection and established the non-involvement of PGE_2 in macrophage regulated processes during RRV infection.

The role of HMGB1 in RRV-infected macrophages remains unclear and further investigations are necessary. Release of HMGB1 was increased in infected RAW264.7 macrophages but did not reach significant levels. Considering the function of HMGB1 as a 'late response mediator' (Harris et al., 2012) more long term experiments are necessary to investigate whether delayed HMGB1 release is significantly altered in RRV infection. Apart from its function as an inflammatory cytokine HMGB1 may also be involved in the elimination of viral particles, as a recent study (W. Wang et al., 2014) suggested. Knock-out mice with HMGB1-depleted dendritic cells showed increased and more effective clearance of vaccinia virus. Due to the cost of HMGB1 ELISA kits however we decided to focus on other cytokines.

Contrary to previous reports we found only low levels of NO in the supernatant of RRV infected cells despite transcription of iNOS mRNA (K. Burrack et al., 2014). Production of iNOS upon infection is likely an antiviral response and it has been reported previously (Lidbury & Mahalingam, 2000b) that RRV exerts an inhibitory

effect on iNOS transcription in LPS-stimulated macrophages during antibody dependent enhanced infection. We could show that RRV was able to inhibit the NO response from LPS challenged macrophages independent of the infection pathway. Exposure of RAW264.7 cells to RRV for 48 hr prior to stimulation resulted in a significant reduction of NO release, which indicates that RRV interferes with the cellular antiviral response. It remains to be clarified how RRV induces iNOS expression without increasing nitrite levels. Stimulation with LPS gave positive NO results and served as assay control.

With this more comprehensive understanding of cytokine regulation during RRV infection we investigated possible inhibitors to target these inflammatory mediators. The anti-inflammatory properties of macrolides have been reported numerous times and more recent data attributes this effect to the inhibition of cytokines (Zarogoulidis et al., 2012). We could show that erythromycin strongly inhibits TNFα and IL-6 but not IL-10 release from RRV-infected macrophages. A reduction of IL-18 and MIF mRNA transcription was detected, although MIF inhibition did not reach significant levels. Clarithromycin similarly reduced TNFα and IL-6 secretion and slightly increased the concentration of IL-10 in the supernatant of infected RAW264.7 macrophages. No significant effect was detected for IL-18 or MIF mRNA expression. Roxithromycin exhibited a slight inhibitory effect on TNFα but did not reduce secretion of IL-6 or mRNA expression of MIF. A significant increase in IL-10 was however detected for RXM, while expression of IL-18 mRNA was reduced.

We could show for the first time that macrolide treatment on RRV-infected macrophages has varying inhibitory effects on the regulation of pro-inflammatory cytokines, such as TNFα, MIF, IL-6 and IL-18 as well as the anti-inflammatory cytokine IL-10. Interleukin 10 is an important mediator in the host's antiviral response and also possesses anti-inflammatory properties, however it has been suggested that a decrease in IL-10 secretion might be desirable in RRV infection (Rulli et al., 2005). It remains to be determined whether this decrease is in fact beneficial *in vivo* or if the anti-inflammatory effect of IL-10 outweighs it. From the tested macrolides RXM appears to induce IL-10 secretion in RRV infected macrophages. Future research projects are needed to determine if RXM-induced increase of IL-10 interferes with the replication cycle of RRV in macrophages or other cell types such as Vero or C2C12 cells.

ERY has shown very promising results in these *in vitro* experiments and future research projects should extend to macrophages derived from human PBMCs. If

these experiments confirm the anti-inflammatory effect of ERY it may be considered as a treatment option in an established mouse model of RRV (Taylor et al., 2014). The concentration levels of ERY in the inhibitor experiments were similar to the peak plasma concentration levels in standard antibiotic therapy with 500 mg ERY four times daily (Krasniqi et al., 2012).

Ethyl pyruvate has previously been recognised as an anti-inflammatory agent (Fink, 2007) and our experiments indicated an anti-inflammatory effect of EP on RRV-infected macrophages. TNFα secretion into the supernatant was reduced in a dose-independent manner, consistent with previous findings (Nativel et al., 2013) that reported of a dose-independent reduction of IL-6 secretion in an LPS-challenged human liposarcoma cell line when treated with similar concentrations of EP. Further investigations are necessary to expose the molecular processes and pathways involved in this inhibitory effect. We could also show that EP significantly reduces IL-6 secretion and expression of both MIF and IL-18 mRNA in RRV infected RAW264.7 macrophages. These results and the well documented inhibitory effect on HMGB1 secretion indicate a possible role of EP in the treatment of RRV infections. Future research projects need to establish if the aforementioned cytokines are inhibited in human macrophages and whether EP should be tested as treatment option in a mouse model.

Anti-TNFα therapy with pentoxifylline has previously been reported to reduce inflammatory symptoms in a mouse model of antigen-induced arthritis (Queiroz-Junior et al., 2013). We could show that PXF similarly reduces TNFα release from macrophages in RRV infection but has no or little effect on IL-6 secretion. No significant effect on MIF or IL-18 mRNA was detected. Similarly to the previously tested inhibitors, resveratrol reduced levels of TNFα and IL-6 in the supernatant of infected RAW264.7 macrophages, and did inhibit IL-18 mRNA but not MIF mRNA expression. A rat model recently confirmed the anti-inflammatory effect of RVT in arthritic conditions (Riveiro-Naveira et al., 2014).

An increase in the phagocytic activity of macrophages persistently infected with RRV was previously reported (Way et al., 2002). Our experiments could show that this increase in phagocytic activity is also occurring in acutely infected RAW264.7 macrophages and it appears to be independent of the phagocytic stimuli. A Gram positive, as well as a gram negative bacterial strain were used in the assay with both situations confirming increased phagocytic activity of RRV infected macrophages. There was no significant difference between 24 hr and 48 hr pre-exposure to RRV.

The increased phagocytic activity indicates activation of the macrophages upon infection.

Other assay setups that were considered and may be included in future studies are plate based fluorescence assays. This would reduce the steps involved in the sample preparation, however likely give less sensitive results as compared to flow cytometric analysis.

5. Results III: C2C12 cells after RRV infection

5.1 Introduction

Early investigations into the pathogenesis of Ross River Virus infection in mice have revealed rapid viral growth in muscle tissue, with viral titres peaking at 4 d post-infection (p.i.), as well as severe muscle fibre damage from 7 d p.i. onwards (Murphy et al., 1973). Further studies (Eaton & Hapel, 1976) however gave contrary results and found that RRV could persistently infect primary mouse muscle cells in a non-cytolytic way. Lidbury et al. (Lidbury et al., 2000) concluded from these two opposing findings that the cytopathic effect RRV exerts on mouse muscles *in vivo* must be caused by host response mechanisms which had not been recognized yet. In their studies a strong infiltration of macrophages into infected mouse muscle tissue was identified and it was proposed that macrophages likely are the major contributor to the pathological symptoms observed in RRV infection. These findings were summarised in a review (Rulli et al., 2005), and it was suggested that specifically macrophage derived chemokines may be responsible for the observed muscle pathology. Later investigations (Morrison et al., 2007) confirmed the infiltration of inflammatory cells and found the involvement of complement as a host-specific response to contribute to tissue destruction *in vivo* as compared to *in vitro* infections. Most research in the pathology of RRV disease focused on macrophages and macrophage-derived cytokines since (Lidbury et al., 2008). However, with reports of myocytes secreting an array of pro-inflammatory cytokines (Pedersen et al., 2007) we considered re-investigating the possible role of muscle cells in RRV infection.

5.2 RRV propagates in a cytolytic replication cycle in C2C12 myoblast cells

To investigate the effect of RRV on muscle cells we decided to use C2C12 myoblast cells, as they have previously been shown to be susceptible to infection in studies with alphavirus vectors (Wahlfors et al., 2000). Initial experiments were conducted to establish if RRV does infect the cell line under our conditions. C2C12 cells were exposed to RRV T48 at an MOI of 1 and observed for cytopathic effects under a light microscope. Morphological changes were visible in infected cells from 12 hr p.i. onwards and lysis of numerous cells was obvious by 24 hr p.i. (Figure 51). By 36 hr

p.i. most cells had lysed and detached from the tissue culture plate with only very few cells appearing viable.

RNA extracted at various time points post-infection was analysed by conventional PCR using primers specific for the RRV-E2 RNA sequence. As shown in Figure 52, virus RNA was detectable from 4 hr p.i. onwards showing a very faint band which increased in intensity by 12 and 24 hr post-infection. This indicates that viral RNA is synthesized in C2C12 cells upon infection with RRV. Supernatant samples taken at the same time points were examined by LDH assay as described in Methods to determine cell viability (Figure 53). As expected, reduced viability, expressed in increased LDH levels, was observed from 12 hr p.i. ($p \leq 0.01$) onwards and most pronounced by 36 hr p.i. ($p \leq 0.001$) compared to non-infected cells. Exposure to LPS did not affect cell viability. These results were confirmed with an MTT assay as shown in Figure 54. C2C12 cells were infected 36, 24, 12 and 0 hr before performing a MTT assay as outlined in Methods. Cell viability was calculated as relative viability to non-infected cells which was given the arbitrary value of 100% viability. Cells that had been infected 0 hr and 12 hr before the MTT assay did not show any significant change in viability (Figure 54). C2C12 cells that had been exposed to RRV 24 hr prior to the assay showed significant reduction in viability to 79.6 ± 9.1 % ($p \leq 0.001$). Exposure to RRV for 36 hr reduced relative cell viability to 26.0 ± 10.8 % ($p \leq 0.001$). This data confirmed the viability results obtained by LDH assay previously.

It appeared that cell death was due to a cytolytic replication cycle of the virus in C2C12 myoblasts. To investigate if this was true, we exposed C2C12 cells to RRV T48 in culture medium adjusted to a TCID50 of $1x10^4$ and took supernatant samples daily to determine viral titres. Some wells contained no cells but culture medium and virus only and were used as control samples. As expected, viral titres in controls decreased over time and by day 4 no active virus was detectable by standard TCID50 assay (Figure 55). RRV appears to slowly degrade over time at 37˚C. Interestingly, viral titres significantly increased within 1 d p.i. ($p \leq 0.05$) and reached peak levels at 2 d p.i. ($p \leq 0.001$) in samples that contained C2C12 myoblasts. Viral titres thereafter slowly decreased but still showed significantly higher levels compared to controls ($p \leq 0.001$). Observations under the light microscope confirmed increasing cell damage and lysis of C2C12 myoblasts over time and by 2 d p.i. only few cells appeared to still be viable (see Figure 51).

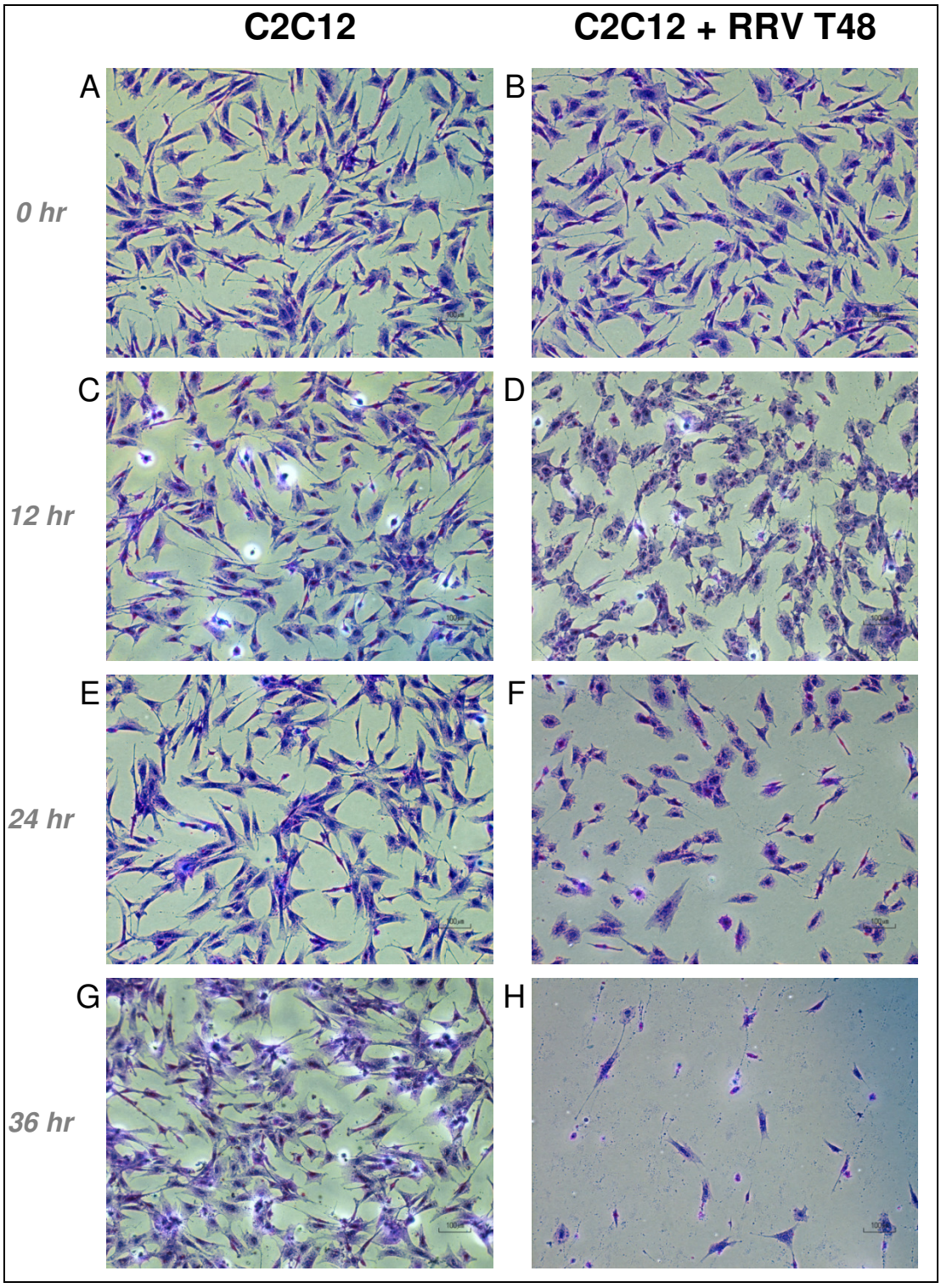

Figure 51: C2C12 cells exposed to RRV T48

C2C12 cells were exposed to RRV T48 or HI-RRV at an MOI of 1 for various times and then stained with 0.1 % (w/v) crystal violet to visualise viable cells. Representative photographs taken under 40x magnification are shown above for control cells (A,C,E,G) and RRV-infected cells (B,D,F,H). (n=4)

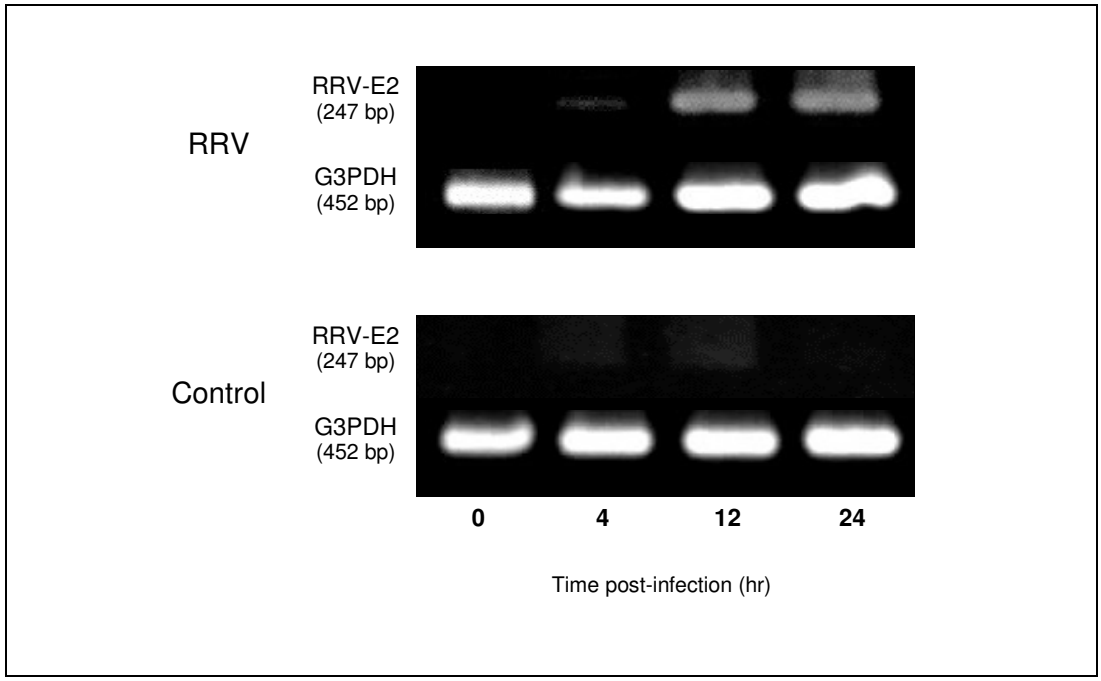

Figure 52: Expression of RRV-E2 mRNA in C2C12 cells post-infection

C2C12 myoblasts were exposed to RRV T48 at an MOI of 1 and RNA was extracted at various time points post-infection. After transcription in to first strand cDNA the samples were analysed by RT-PCR with primers specific for the RRV-E2 sequence. Shown above are representative photograph of the agarose gels under UV light stained with GelRed®.

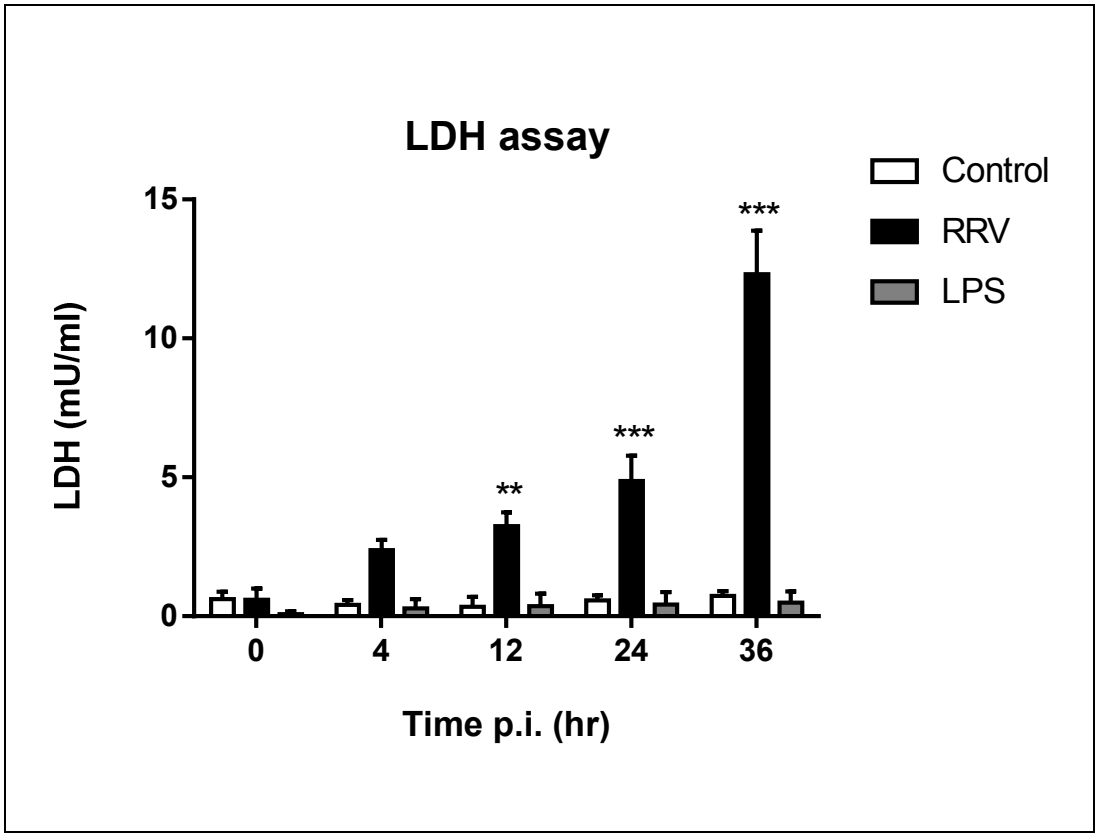

Figure 53: Cell viability of C2C12 myoblasts post RRV exposure

Supernatant of C2C12 myoblasts exposed to RRV was examined by LDH assay for cell viability. As outlined in Methods, increased LDH levels indicate cell lysis and therefore correlate to cell death. C2C12 cells were exposed to HI-RRV and used as control. LPS was tested as a stimulant for further experiments. All data is expressed in mean values ± SEM (n=6). **($p \leq 0.01$), ***($p \leq 0.001$) as determined by two-way ANOVA against control.

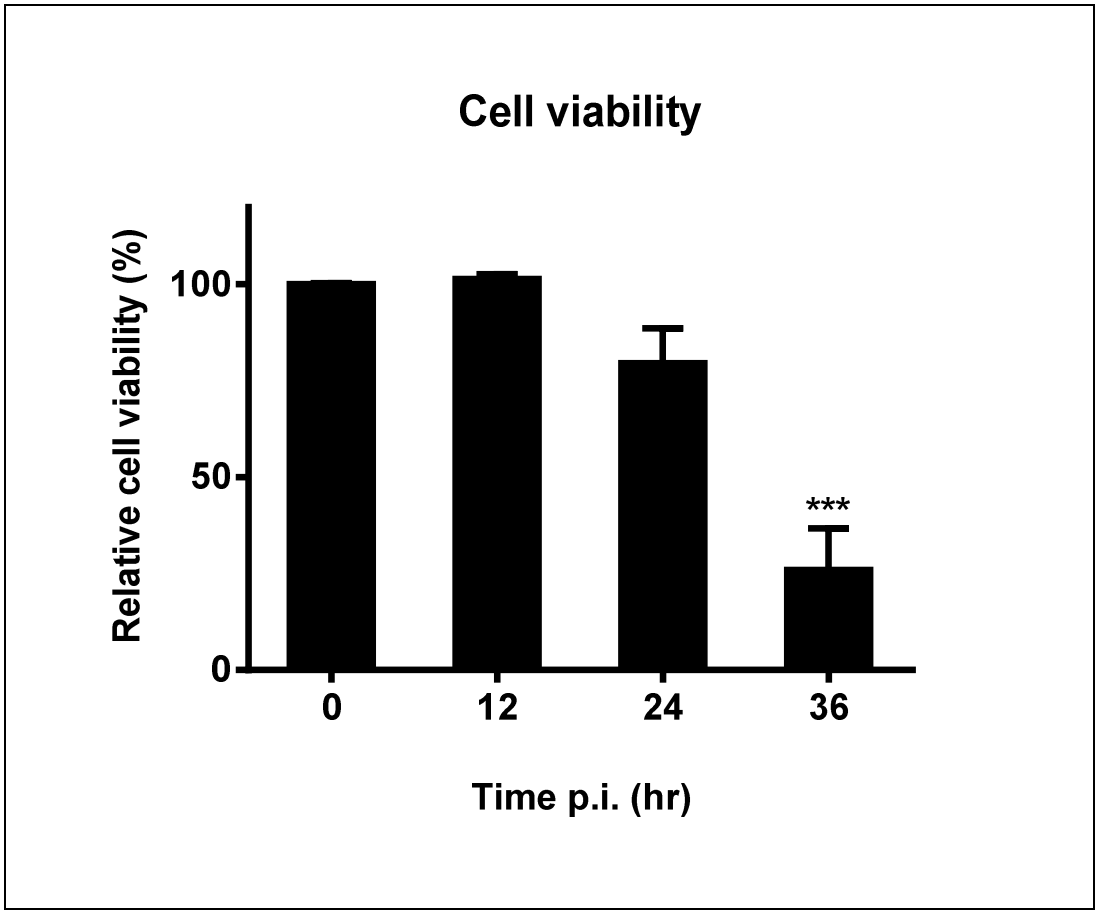

Figure 54: MTT assay on C2C12 after RRV infection for varying time periods

C2C12 cells were pre-treated with media containing RRV T48 at an MOI of 2 for 0, 12, 24 or 36 hr and a MTT assay was performed to determine cell viability. Non-infected cells were used as controls and given the arbitrary value of 100%. Viability of the samples was calculated as relative viability compared to controls. Data shown above are mean values ± SEM (n=3). ***($p \leq 0.001$) as determined by one-way ANOVA compared to controls.

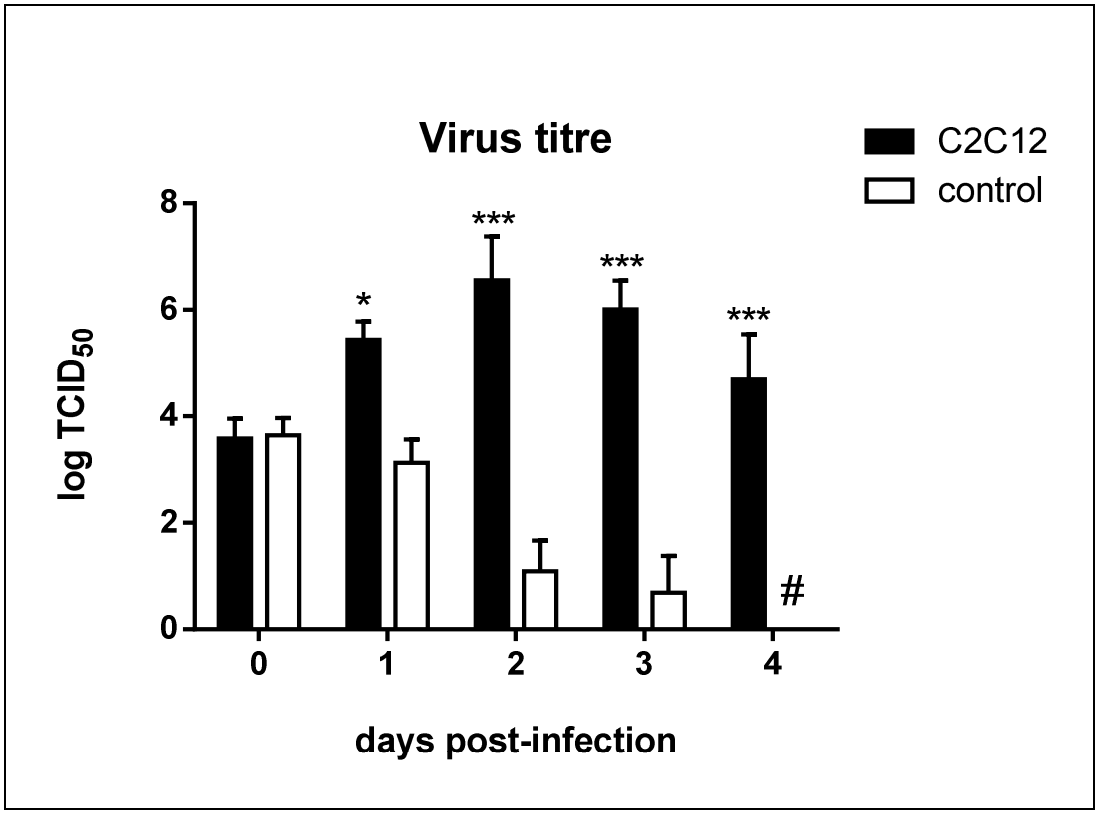

Figure 55: Virus titres after infection of C2C12 cells with RRV T48

C2C12 cells were exposed to RRV T48 (in culture medium with virus at a TCID50 of $1x10^4$) and supernatant samples taken daily were examined for viral titres by standard TCID50 assay. RRV T48 at the same concentration was used in control wells without any cells and kept under the same conditions at 37˚C and 5% (v/v) CO2 in a humidified incubator. Data shown is expressed in log $TCID_{50}$ as mean values ± SEM (n=3 independent infection experiments). *(p≤0.05), ***(p≤0.001) # virus titre below detection limit

5.3 Cytokine production

As reviewed earlier, muscle cells have previously been shown to release an array of cytokines (often labelled 'myokines') that can contribute to inflammatory processes. To investigate if the release of these myokines could potentially play a role in RRV infection, we exposed C2C12 myoblasts to RRV T48 at an MOI of 1 and examined supernatant samples for cytokine levels. Considering our findings of a cytolytic replication cycle in C2C12 cells we investigated cytokine release for up to 24 hr p.i. only, since cell viability seemed to significantly decrease thereafter and mediators might be released due to cell lysis rather than active secretion as cytokines.

5.3.1 RRV induces TNFα secretion in infected C2C12 myoblasts

Supernatant samples of RRV-infected C2C12 cells were taken at appropriate times p.i. and assayed for TNFα concentrations by ELISA. C2C12 cells mock infected with heat inactivated RRV (HI-RRV) were used as control. LPS exposure does stimulate expression of both TNFα and IL-6 in C2C12 cells and was therefore included as positive control (Frost et al., 2002). As expected, TNFα concentrations for LPS samples increased in a time dependent manner and reached 317 ± 82 pg/mL by 24 hr post stimulation ($p \leq 0.001$) (Figure 56). Supernatant of RRV-infected C2C12 cells did show a time dependent increase in TNFα concentrations detectable from 4 hr p.i. onwards to 340 ± 89 pg/mL by 24 hr p.i. ($p \leq 0.001$).

5.3.2 RRV induces expression of TNFα mRNA in C2C12 myoblasts

To examine expression of cytokine mRNA in RRV-infected C2C12 myoblasts, RNA was extracted at varying times p.i. and PCR analysis was performed using primers specific for TNFα. Gel electrophoresis of the PCR amplicons confirmed that expression of TNFα mRNA is induced by RRV, increasing in a time-dependent manner (Figure 57). LPS challenged C2C12 cells were used as positive control and showed a similar pattern of mRNA expression, with induction of TNFα mRNA detectable by 4 hr p.i. increasing in a time-dependent manner. Very weak bands were detected in C2C12 cells mock infected with heat-inactivated RRV.

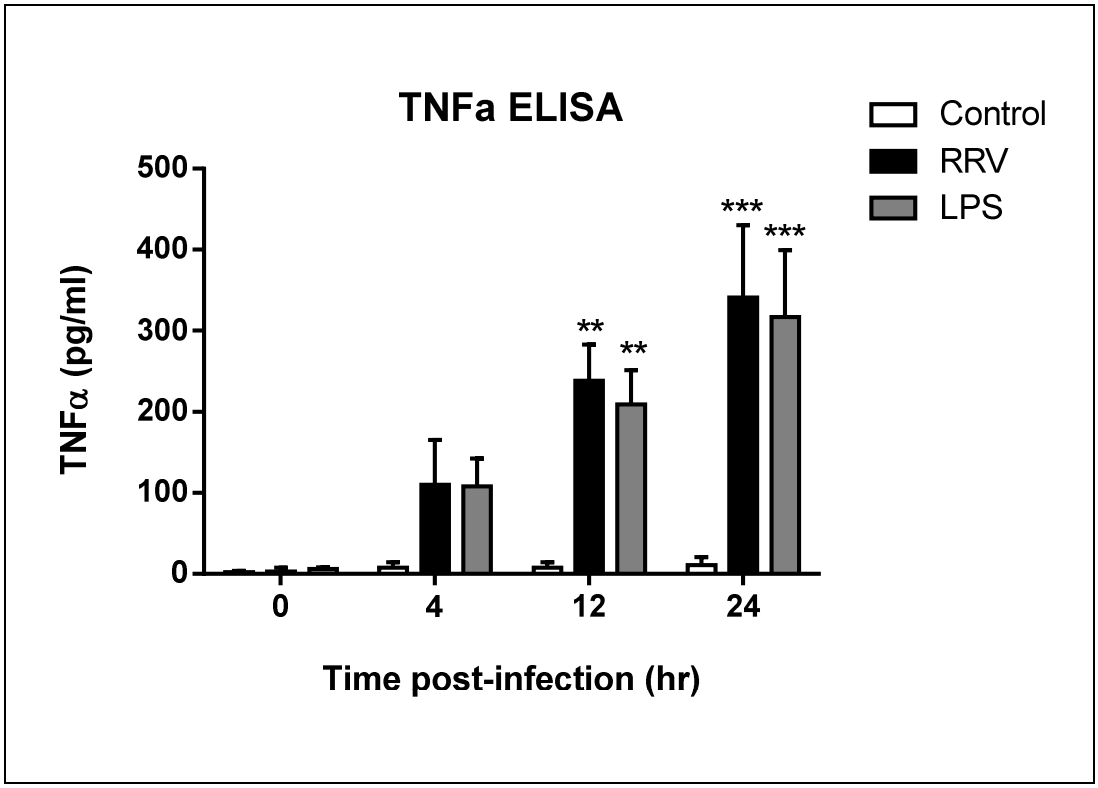

Figure 56: TNFα secretion of C2C12 exposed to RRV or LPS

C2C12 myoblasts were treated with RRV T48 at an MOI of 1 or LPS (1µg/mL) and supernatant samples taken at varying time points were analysed by TNFα ELISA. HI-RRV was used as negative control sample (Control). All data is expressed in mean values ± SEM (n=4). **(p≤0.01), ***(p≤0.001) as determined by two way ANOVA compared to mock infected C2C12 controls.

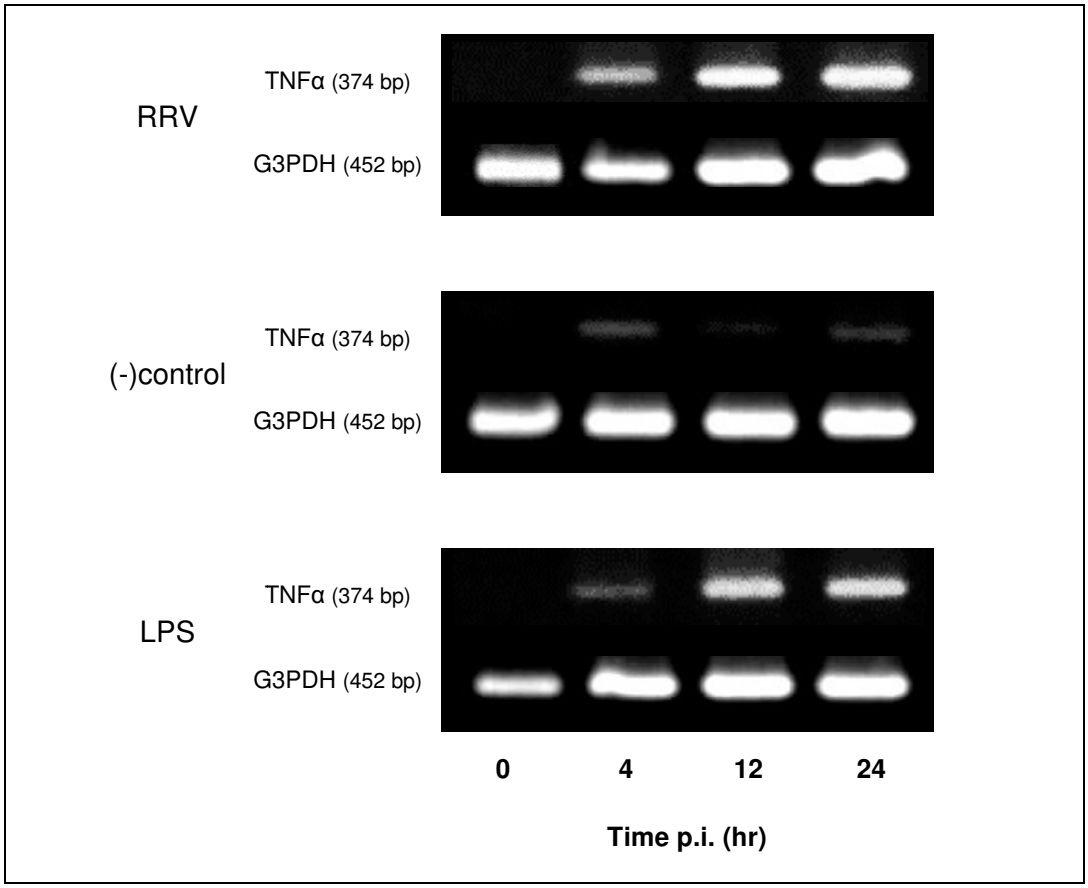

Figure 57: TNFα mRNA in RRV and LPS treated C2C12 myoblast cells

C2C12 myocytes were exposed to RRV T48 at an MOI of 1, LPS (1 µg/mL) or HI-RRV for varying amounts of time and extracted RNA was analysed by RT-PCR using primers specific for TNFα. Figure shows representative photographs of agarose gels taken under UV light exposure with GelRed® stain (n=4).

5.3.3 RRV does not induce NO-secretion in infected C2C12 myoblasts

To examine if RRV induces the release of nitric oxide (NO), we assayed the supernatant of infected C2C12 cells with Griess reagent for nitrite, a stable oxidation product of nitric oxide. Our experimental setup mostly used LPS as a positive control to stimulate cytokines in C2C12 cells, however it has previously been shown that LPS alone does not induce the secretion of NO in C2C12 myoblasts (G. Williams et al., 1994). Supernatant derived from LPS stimulated RAW264.7 macrophages were included as assay control. As Figure 58 shows, neither LPS, nor RRV altered the concentration of nitrite in the supernatant of exposed C2C12 myoblasts. 24 hr pre-exposure to RRV T48 at an MOI of 1 followed by LPS stimulation (1 µg/mL) was trialled as well but failed to induce NO by 24 hr post exposure.

5.3.4 iNOS mRNA is induced in RRV-infected C2C12 myoblasts

RNA was extracted at certain time points post stimulation from C2C12 cells exposed to RRV or LPS and screened for inducible nitric oxide synthase (iNOS) mRNA by RT-PCR. Despite the lack of significant NO release into the supernatant, iNOS mRNA is induced in C2C12 exposed to RRV (Figure 59). The PCR amplicons were visible by 4 hr p.i. and density increased in a time-dependent manner. LPS challenged samples showed similar patterns. As expected, no iNOS mRNA was detectable in control samples.

As samples for various cytokine assays were often obtained from the same experiments, we did not have a positive control for this particular assay. NO stimulation assays however showed similar results in other cell lines with iNOS mRNA being increasingly expressed but no NO detectable in the supernatant of RRV-infected cells. Supernatant from LPS-challenged RAW264.7 macrophages were included as assay control.

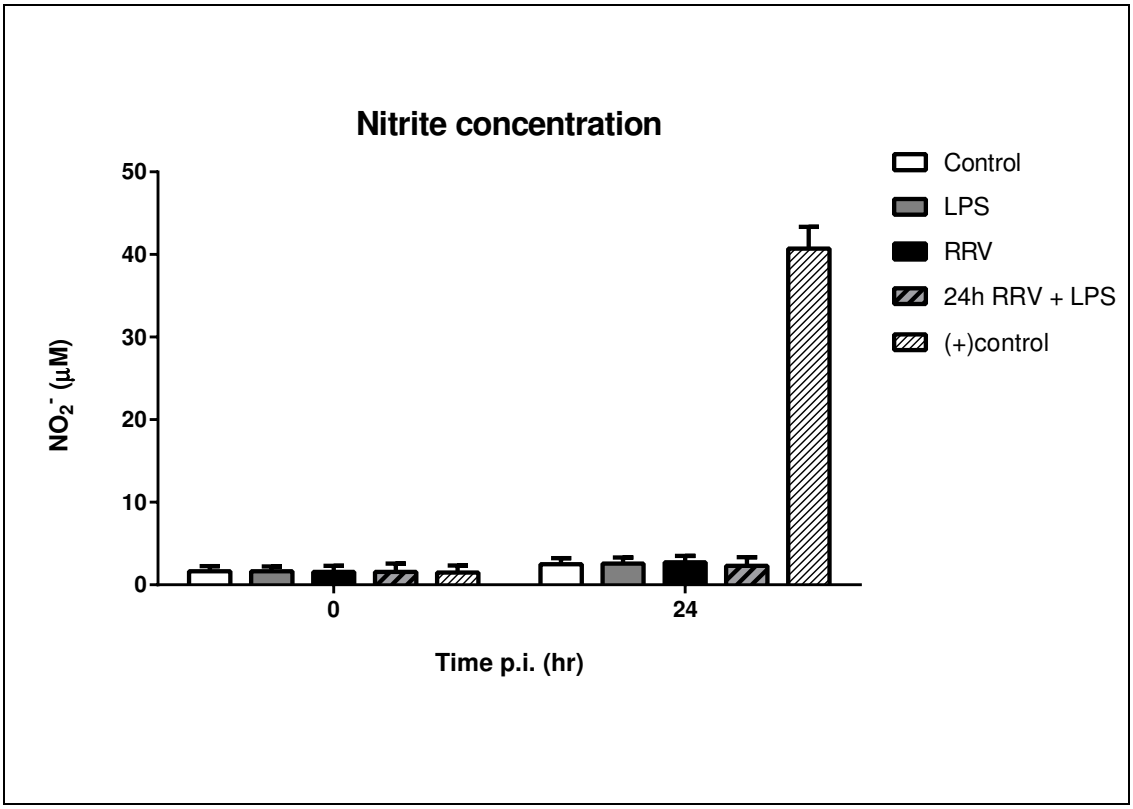

Figure 58: Nitrite concentration in supernatant of C2C12 exposed to RRV and/or LPS

C2C12 myoblasts were exposed to RRV T48 at an MOI of 1, LPS (1 μg/mL) or HI-RRV and supernatant samples were taken at varying time points and analysed for nitrite concentrations by Griess assay. Other samples were exposed to RRV T48 at an MOI of 1 for 24 hr prior to stimulation with 1 μg/mL LPS (24h RRV + LPS). All data is expressed in mean values ± SEM (n=6 for control, RRV and LPS, n=4 for 24h RRV + LPS). Supernatant taken from RAW264.7 macrophages challenged with LPS (1ug/mL) for 24 hr was used as positive assay control ((+)control). Statistical analysis was performed by two-way ANOVA.

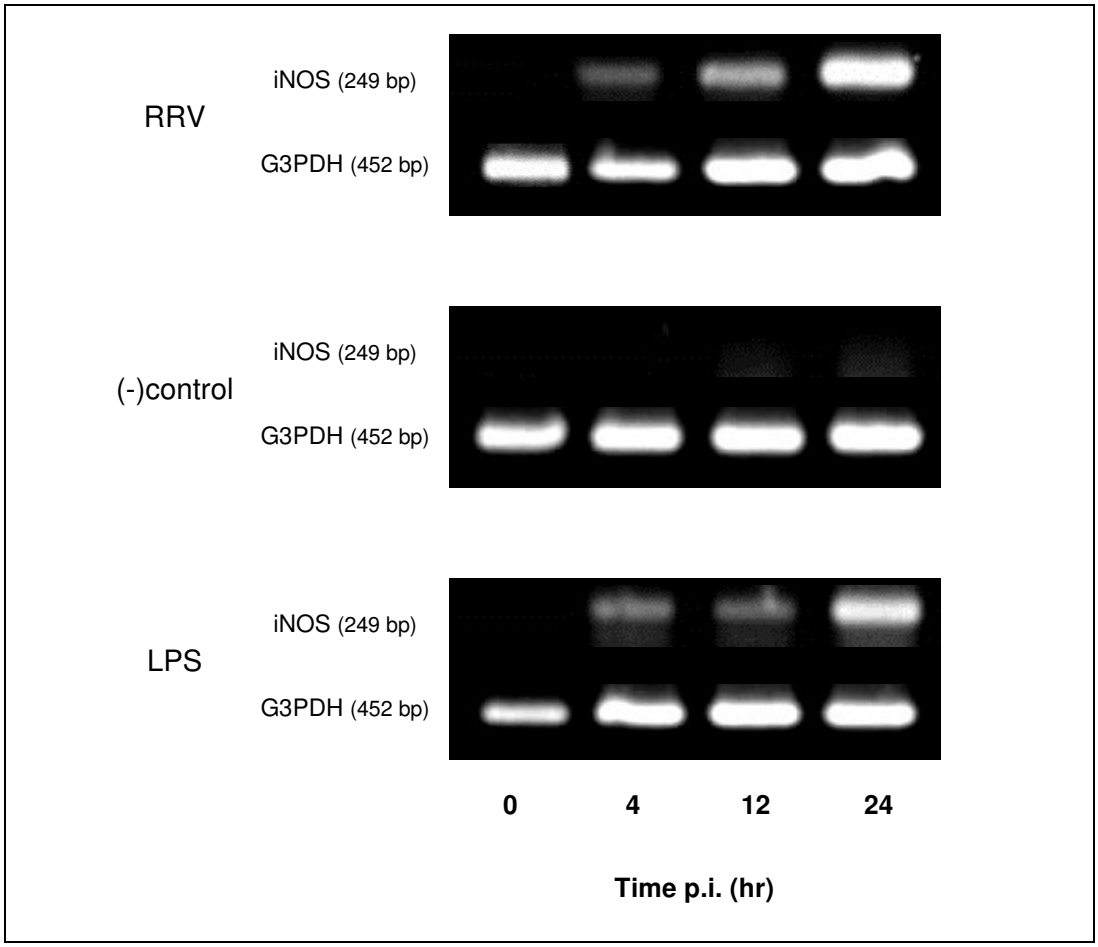

Figure 59: iNOS mRNA expression in C2C12 myoblasts exposed to RRV or LPS

C2C12 myocytes were exposed to RRV T48 at an MOI of 1, LPS (1 µg/mL) or HI-RRV at an MOI of 1 for varying amounts of time and extracted RNA was analysed by RT-PCR using primers specific for iNOS. The figure above shows representative photographs of agarose gels taken under UV light exposure with GelRed® stain.

5.3.5 RRV induces IL-6 secretion in infected C2C12 cells

It has previously been reported that LPS and various cytokines stimulate the release of IL-6 from C2C12 myoblasts (Frost et al., 2003). To investigate if RRV also induces secretion of IL-6 we analysed the supernatant of infected C2C12 at various times p.i. by ELISA. Stimulation with LPS (1 µg/mL) was used in positive control samples. As Figure 60 shows, exposure to RRV sharply increased IL-6 levels in the supernatant by 4 hr p.i. to 316 ± 91 pg/mL and reached 341 ± 83 pg/mL by 24 hr p.i. ($p \leq 0.001$). LPS induced IL-6 release at a lower rate but reached similar levels by 24 hr p.i., with concentrations of 356 ±70 pg/mL ($p \leq 0.001$). Mock infection with heat inactivated RRV did not significantly increase IL-6 concentration in the supernatant at any time.

5.3.6 IL-6 mRNA expression is induced in C2C12 after exposure to LPS or RRV T48

RNA was extracted at the same time points the supernatant samples were taken and analysed by RT-PCR using primers specific for IL-6. Expression of IL-6 mRNA was detectable from 12 hr post exposure onwards for RRV samples, with transcription increasing in a time-dependent manner (Figure 61). LPS samples generally showed earlier induction of IL-6 mRNA with faint bands detectable by 4 hr post stimulation. The intensity of the bands also increased in a time-dependent manner indicating up-regulation of IL-6 mRNA expression. No IL-6 mRNA was detected in control samples.

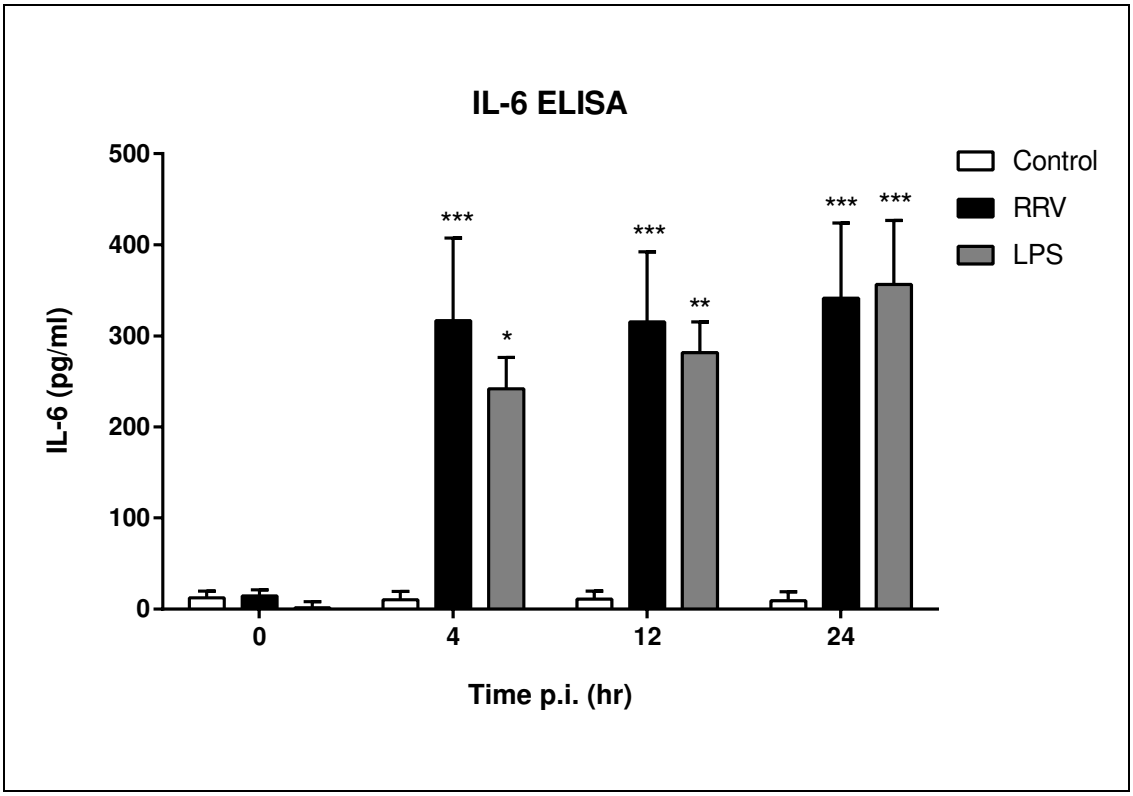

Figure 60: IL-6 concentration in the supernatant of C2C12 exposed to RRV or LPS

C2C12 myoblasts were exposed to RRV T48 at an MOI of 1 or LPS (1 μg/mL) and supernatant was analysed by IL-6 ELISA. Mock infection with heat inactivated RRV was used as negative control. Data is expressed in mean values ± SEM (n=6). *(p≤0.05), **(p≤0.01), ***(p≤0.001) as determined by two-way ANOVA compared to control.

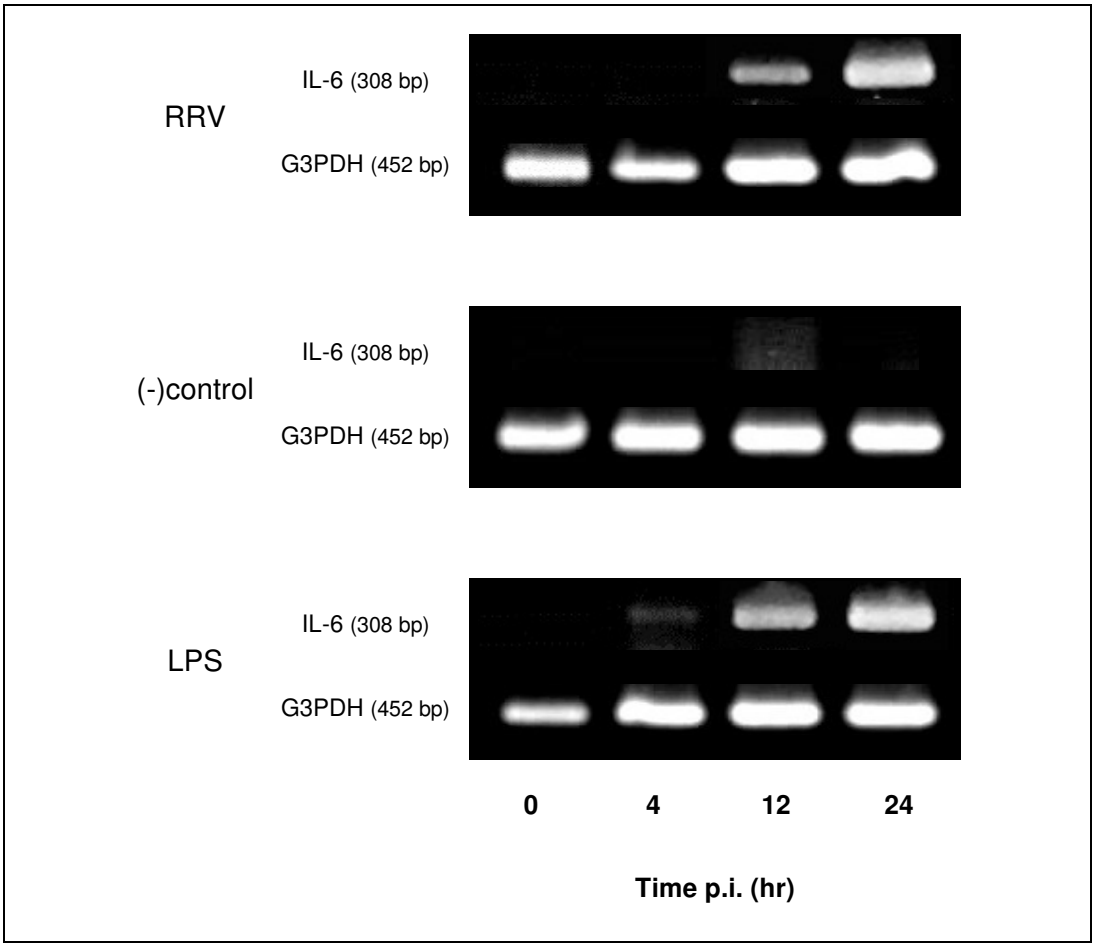

Figure 61: IL-6 mRNA expression in C2C12 muscle cells exposed to RRV or LPS

C2C12 myocytes were exposed to RRV T48 (MOI of 1), LPS (1 µg/mL) or HI-RRV (MOI of 1) for varying amounts of time and extracted RNA was analysed by RT-PCR using primers specific for IL-6 or G3PDH. The figure above shows representative photographs of agarose gels.

5.3.7 RRV and LPS stimulate MIF secretion in C2C12 myoblasts but do not induce MIF mRNA transcription

Challenge of L6 rat myoblasts with TNFα stimulates secretion of macrophage migration inhibitory factor (MIF) (Benigni et al., 2000) and more recently a mouse model has revealed the crucial role of MIF in the pathogenesis of RRV infection (Herrero et al., 2011). Considering these reports together with previous findings (Lidbury et al., 2000) of macrophage migration into the muscle of RRV-infected mice, we decided to investigate if MIF is secreted from muscle cells during RRV infection. C2C12 myoblasts were exposed to LPS (1 µg/mL) or RRV T48 (MOI of 1) and supernatant samples were taken and analysed for MIF concentrations by ELISA (Figure 62). It appears that C2C12 show some basal secretion of MIF since levels in control wells varied between 257 ± 28 pg/mL and 414 ± 47 pg/mL at 4 h and 24 hr p.i. respectively. Exposure to LPS increased MIF concentrations in the supernatant in a time dependent manner to 2736 ± 787 pg/mL by 24 hr p.s. ($p \leq 0.01$). MIF release was detectable from 4 hr p.i. onwards for samples exposed to RRV and reached concentrations of 2871 ± 730 pg/mL by 12 hr p.i. ($p \leq 0.001$) and 4332 ± 864 pg/mL by 24 hr p.i. ($p \leq 0.001$). RNA extracted from the samples at the same time points was analysed by RT-PCR for expression of MIF mRNA (Figure 63). MIF mRNA expression was below the detection limit for control and RRV samples, but showed the respective amplicon for LPS challenged myoblasts at 24 hr p.i. MIF positive cDNA samples were run in parallel as RT-PCR control.

5.3.8 Neither RRV nor LPS induce secretion of IL-10 in C2C12 myoblasts

Increased interleukin-10 (IL-10) levels have previously been reported for macrophages in antibody-dependent enhanced infection of Ross River virus (ADE-RRV) (Mahalingam & Lidbury, 2002). To investigate if IL-10 is also released by infected muscle cells we exposed C2C12 myoblasts to RRV T48 at an MOI of 1 and analysed the supernatant at various time points post-infection by IL-10 ELISA. Exposure to 1 µg/mL LPS was used in previous experiments as stimulant control and the same supernatant samples were analysed for IL-10. Neither RRV nor LPS increased inteleukin-10 levels at any time point post stimulation in C2C12 (Figure 64). RNA extracted at the same time points was analysed by RT-PCR and confirmed the lack of expression of IL-10 mRNA (data not shown).

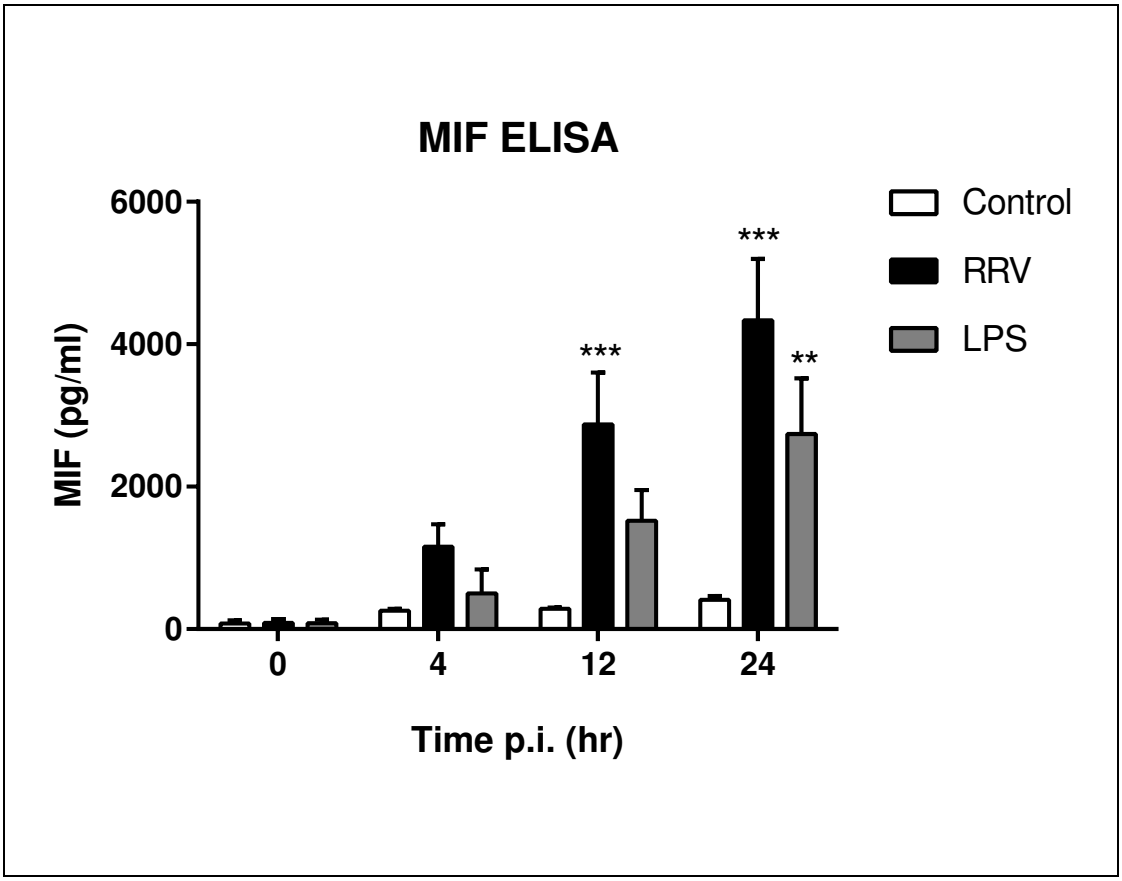

Figure 62: MIF concentration in the supernatant of C2C12 myoblasts exposed to RRV or LPS

MIF levels in the supernatant of C2C12 exposed to RRV T48 at an MOI of 1 or LPS (1 µg/mL) were determined by ELISA at appropriate time points post stimulation. Exposure to HI-RRV was used as negative control (Control). All data is expressed in median values ± SEM (n=5). **(p≤0.01), ***(p≤0.001) determined by two-way ANOVA compared to control.

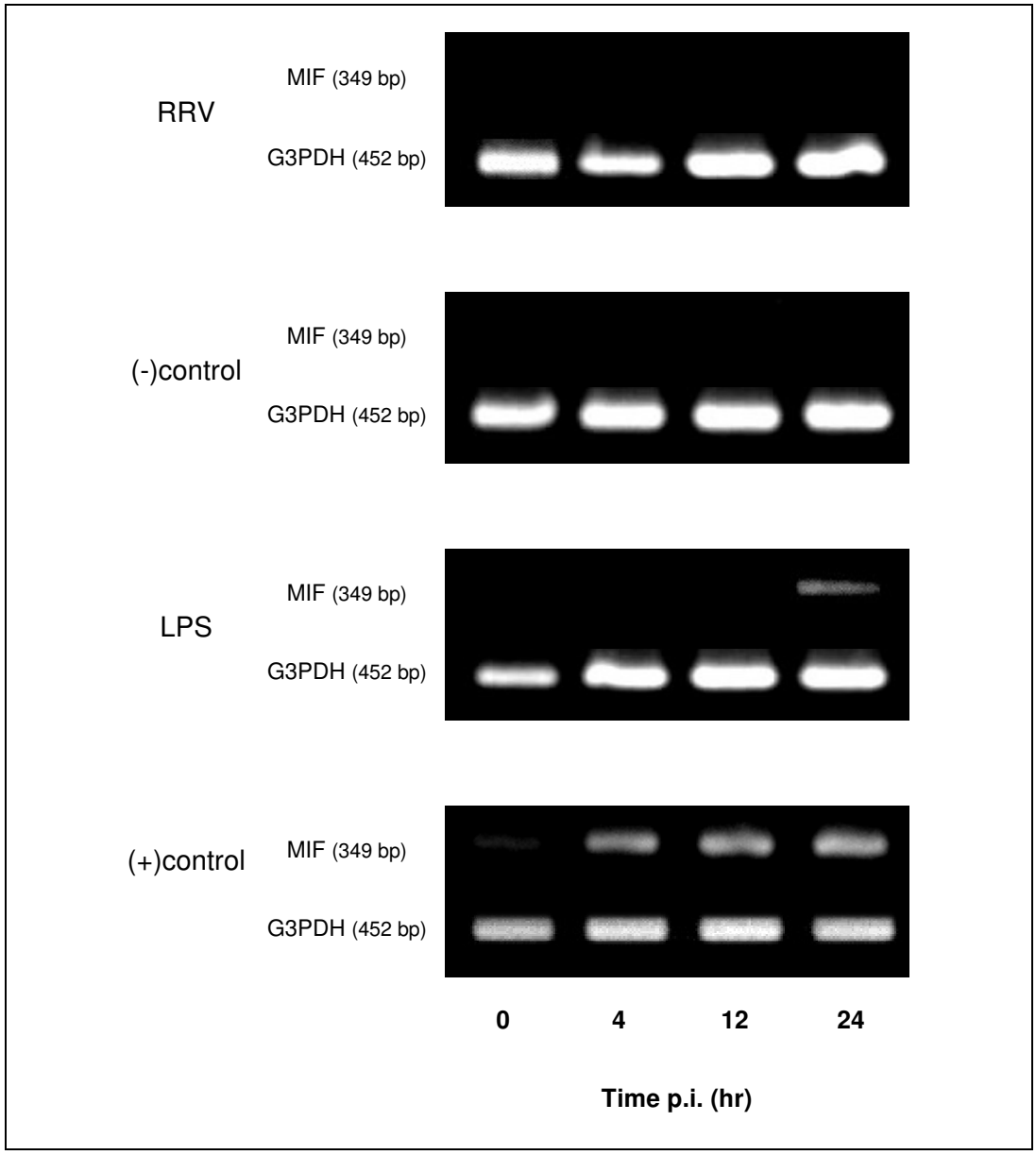

Figure 63: MIF mRNA expression in C2C12 myoblast cells upon exposure to RRV or LPS

C2C12 myocytes were exposed to RRV T48 at an MOI of 1, LPS (1 µg/mL) or HI-RRV for varying amounts of time and extracted RNA was analysed by RT-PCR using primers specific for MIF or G3PDH. Previously extracted mRNA from RAW264.7 stimulated with 1 µg/mL LPS was used as positive RT-PCR assay control. Shown above are representative photographs of agarose gels (n=3).

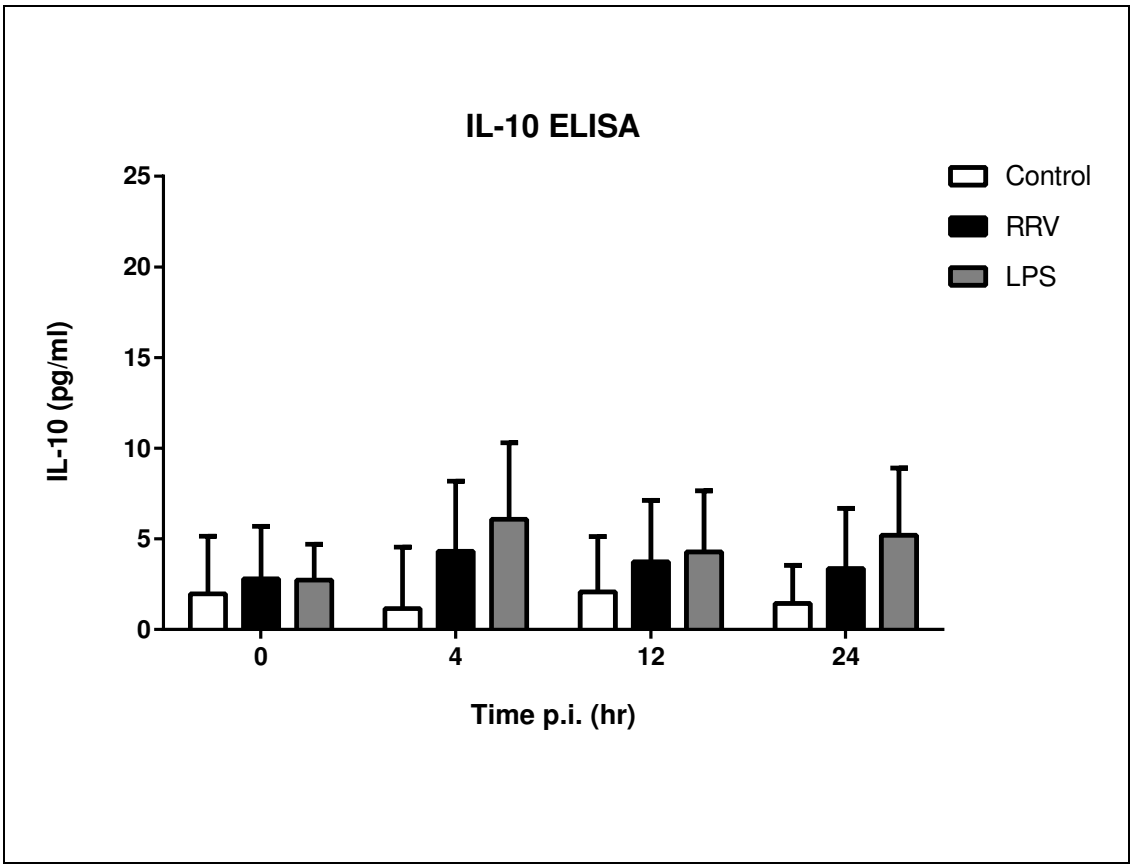

Figure 64: IL-10 concentration in the supernatant of RRV- or LPS-stimulated C2C12

C2C12 cells were exposed to RRV T48 at an MOI of 1, LPS (1µg/mL) or HI-RRV and supernatant samples were examined for IL-10 concentration by ELISA. All data is expressed as mean values ± SEM (n=4). Statistical analysis was performed with two-way ANOVA.

5.3.9 Transcription of HMGB-protein mRNAs is down-regulated by RRV and up-regulated by LPS in C2C12 myoblast cells

As mentioned earlier, HMGB1 protein has been investigated as a pro-inflammatory cytokine and recent research identified it as a possible target for inflammation control (Nogueira-Machado & de Oliveira Volpe, 2012). The other members of the HMGB-family, HMGB2 and HMGB3, have previously also been identified as regulatory elements in inflammation and immunity (Yanai et al., 2012). To determine if expression of these modulators is altered in RRV infection, we extracted RNA from C2C12 myoblasts after exposure to RRV T48 (MOI of 1) or LPS (1 µg/mL) and analysed it by RT-PCR using specific primers for the members of the HMGB-protein family (Figure 65). Considering the ubiquitous function of HMGB1 as an architectural DNA-stabilising protein as well as a cytokine it was not surprising to see basal expression of mRNA in all samples and increased transcription of mRNA at 24 hr post exposure in LPS stimulated samples (Andersson et al., 2002). Exposure to RRV T48 however decreased transcription of HMGB1 by 4 hr p.i. and expression stayed reduced thereafter. Similar patterns were detected for HMGB2 and HMGB3 (Figure 65 B and C). Exposure to RRV T48 down-regulated transcription of the specific mRNA whereas stimulation with LPS up-regulated its expression.

5.3.10 Expression of IL-18 mRNA in C2C12 myoblasts is induced by RRV T48 or LPS

Previous studies (Frost et al., 2002) have identified numerous cytokines released by LPS stimulated C2C12 myoblasts and reported of an initial increase followed by a decrease of IL-18 mRNA transcription post stimulation. We have analysed RNA samples extracted from RRV-exposed (MOI of 1) or LPS stimulated (1 µg/mL) C2C12 myoblasts by RT-PCR for expression of IL-18 mRNA. Contrary to previous findings we could see a strong increase in IL-18 mRNA transcription post exposure to LPS (Figure 66). Infection with RRV T48 also resulted in up-regulation of IL-18 mRNA from 4 hr p.i. onwards, increasing in a timely manner. Cells exposed to HI-RRV showed little induction of IL-18 mRNA by 12 hr and 24 hr p.i

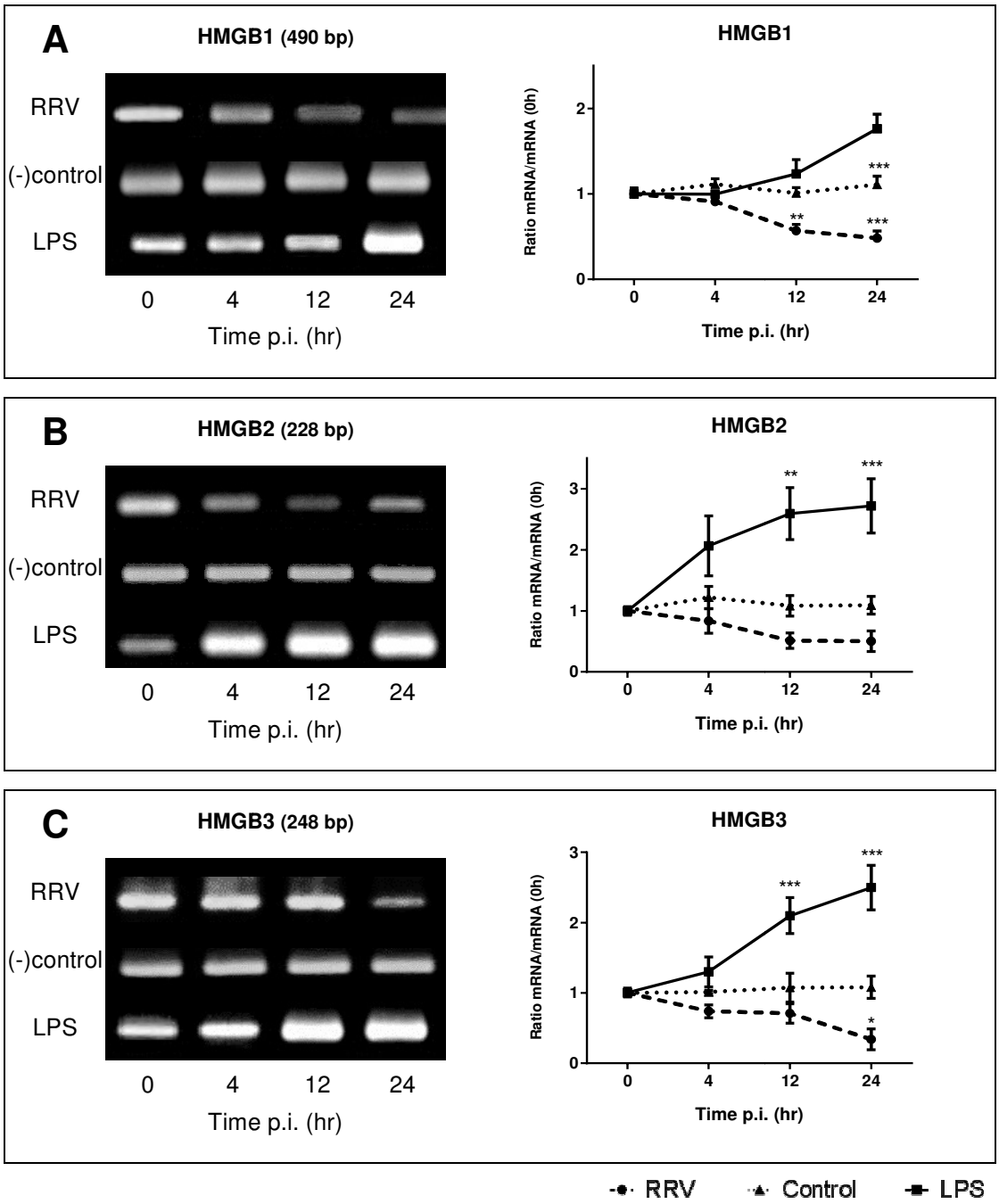

Figure 65: HMGB mRNA expression in RRV- or LPS treated C2C12 cells

C2C12 were exposed to RRV T48 at an MOI of 1, LPS (1 µg/mL) or HI-RRV for various times and extracted RNA was analysed by RT-PCR with primers specific for HMGB1 (A), HMGB2 (B) or HMGB3 (C). Equal RNA loading was validated with G3PDH RT-PCR as shown in previous figures (Figure 63). Densiometric analysis of the PCR amplicons was performed with ImageJ and graphed as the ratio expression at each time point over the respective expression at 0 hr. Data is expressed as mean values ± SEM (n=3). *(p≤0.05), **(p≤0.01), ***(p≤0.001) as determined by two-way ANOVA compared to negative controls. Shown above are representative photographs of agarose gels.

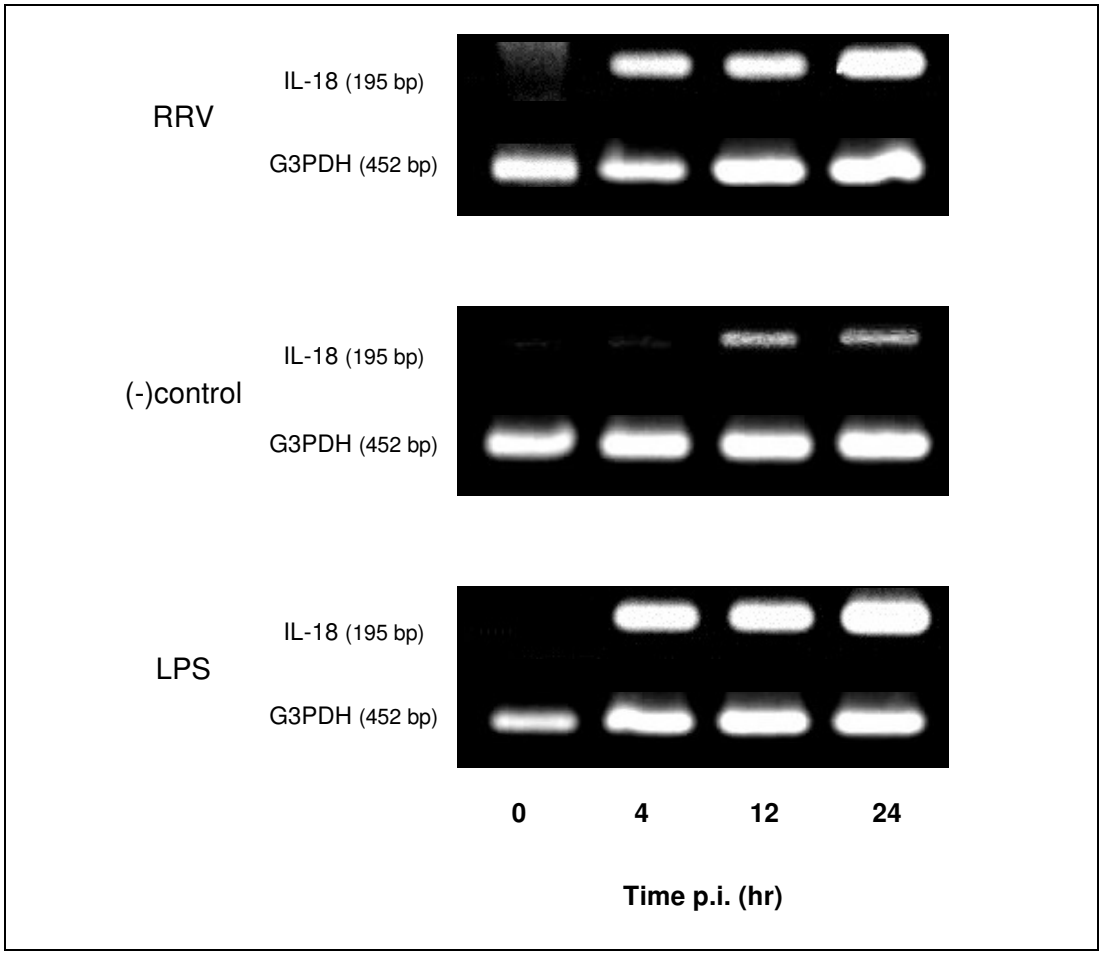

Figure 66: IL-18 mRNA expression in C2C12 macrophages stimulated with RRV or LPS

C2C12 myocytes were exposed to RRV T48 at an MOI of 1, LPS (1 µg/mL) or HI-RRV for varying amounts of time and extracted RNA was analysed by RT-PCR using primers specific for IL-18. Pictured above are representative photographs of agarose gels taken under UV light exposure with GelRed® stain.

5.3.11 RRV and LPS induce expression of IL-33 mRNA in C2C12 myoblasts

IL-33, a rather novel cytokine of the IL-1 family has been identified as a pro-inflammatory mediator in rheumatoid arthritis (D. Xu et al., 2008). The expression of IL-33 in skeletal muscle of canines had been reported long before its role as cytokine was reported (Onda et al., 1999). To investigate if RRV possibly affects IL-33 expression in muscle cells we exposed C2C12 myoblasts to RRV T48 (MOI of 1) or LPS (1 µg/mL) and extracted RNA at varying times post stimulation. Conventional RT-PCR was performed with primers specific for IL-33. Interestingly, exposure to LPS induced IL-33 mRNA expression in a time-dependent manner from 4 hr p.s. onwards (Figure 67). A similar, but even stronger inducing effect was apparent for RRV-infected C2C12 myoblasts, with mRNA expression detected by 4 hr p.i. with transcription increasing over time.

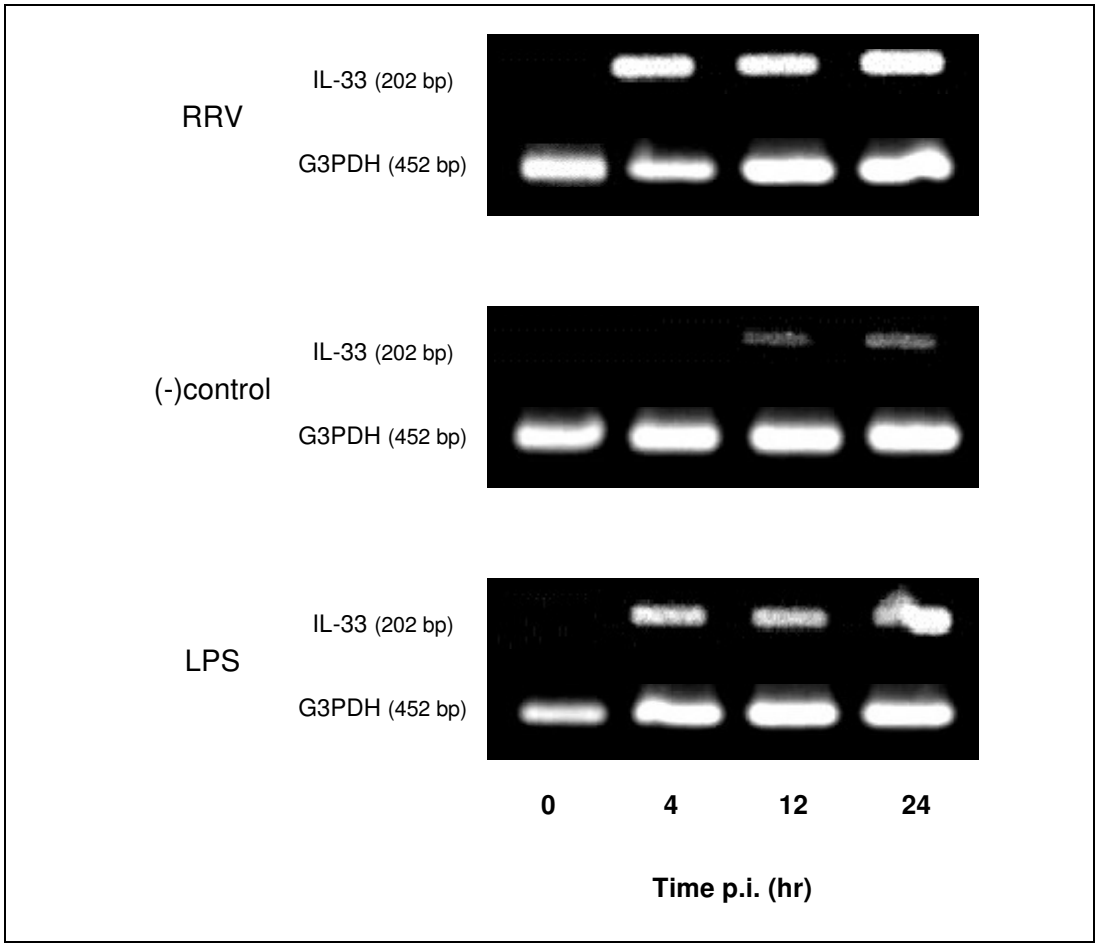

Figure 67: IL-33 mRNA expression in C2C12 myoblasts post exposure to LPS or RRV

C2C12 myoblast cells were infected with RRV T48 at an MOI of 1 or stimulated with LPS (1 μg/mL) and RNA was extracted at varying time points post exposure. HI-RRV was used in mock infections as negative control. Shown above are representative photographs of the PCR amplicons. (n=3 independent experiments).

5.4 Inhibition of cytokine production in C2C12 cells

5.4.1 Introduction

Febbraio et al. (M. A. Febbraio et al., 2010) reviewed the role of muscle derived IL-6 in inflammatory diseases like rheumatoid arthritis and evaluated the therapeutic potential of IL-6 receptor blockers as anti-inflammatory agents. Considering this proposed anti-inflammatory effect of IL-6 receptor blocking antibodies, we suggest that inhibition of IL-6 release may potentially decrease the inflammatory response commonly observed in RRV infection. As shown in previous experiments, several compounds decreased IL-6 release in RRV-infected RAW264.7 macrophages.

In order to see if a similar reduction of IL-6 secretion can also be observed in mouse myoblasts we infected C2C12 cells in the presence of these agents and measured IL-6 concentration in the supernatant at appropriate times post-infection. Initial MTT viability assays with C2C12 cells showed no cytotoxicity at the previously used maximum concentration except for pentoxifylline (PXF) (data not shown). PXF was therefore excluded in further experiments with C2C12 myoblasts.

5.4.2 Macrolide antibiotics do not significantly reduce IL-6 release in RRV-infected C2C12 myoblasts

Erythromycin (ERY) and Clarithromycin (CLA) but not Roxithromycin (RXM) have previously shown an inhibitory effect on IL-6 release in RRV-infected RAW264.7 macrophages. To investigate the influence of these macrolide antibiotics on the IL-6 release of muscle cells in RRV infection, we exposed C2C12 myoblast cells to RRV T48 at an MOI of 1 with or without the presence of 100 uM ERY, CLA or RXM and analysed the supernatant at appropriate times p.i. by IL-6 ELISA. As Figure 68 shows, IL-6 levels in the supernatant of RRV-infected C2C12 were generally lower for all three macrolides in comparison to non-treated RRV infection, however this reduction was not significant as determined by two-way ANOVA (see also Table 11).

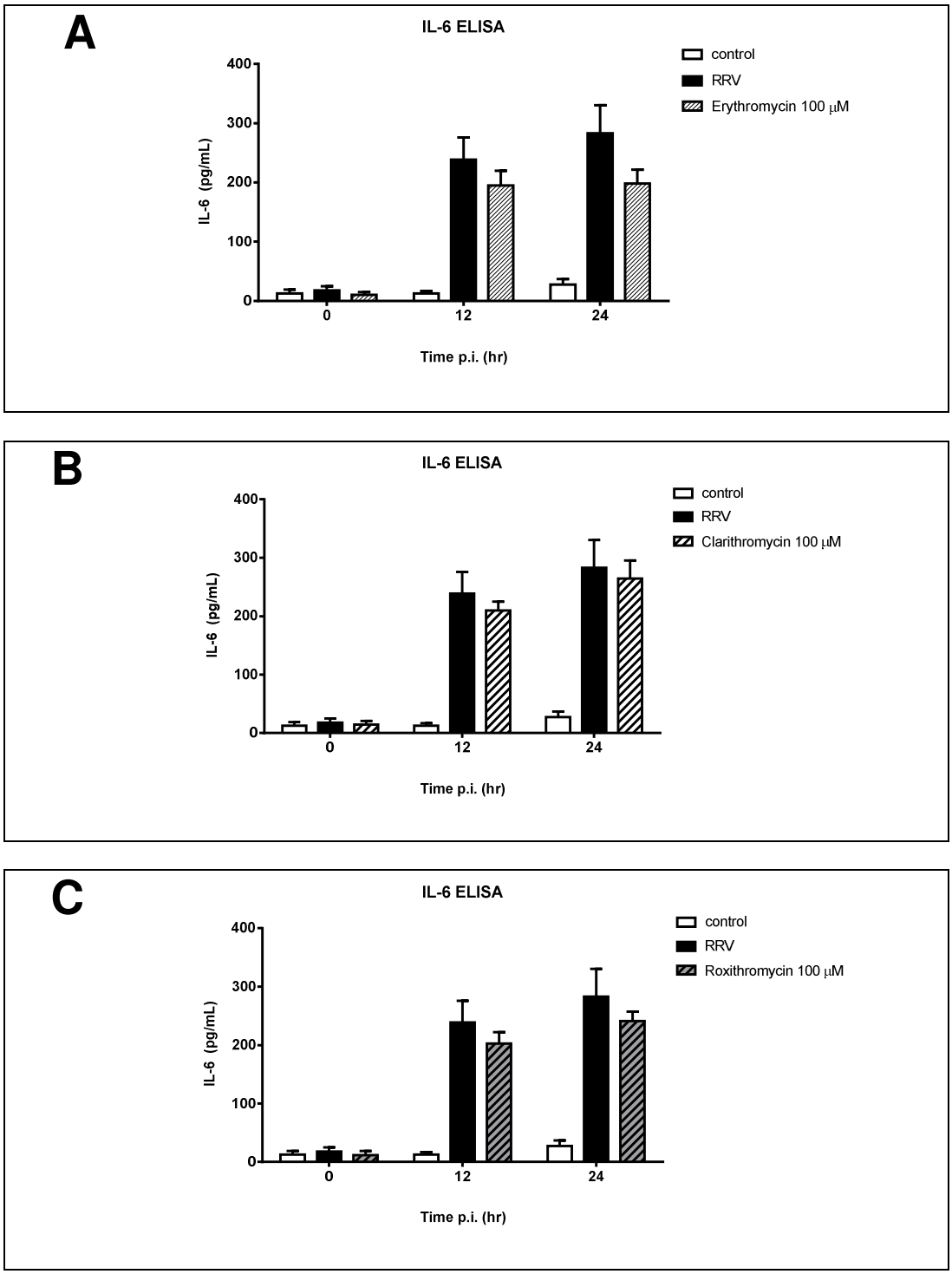

Figure 68: IL-6 secretion of RRV-infected C2C12 in the presence of macrolides

C2C12 myoblasts were exposed to RRV T48 at an MOI of 1 in the presence or absence of 100 µM ERY (A), CLA (B) or RXM (C) and the supernatant was analysed at various times p.i. by IL-6 ELISA. Infection with HI-RRV was used as negative control, non-treated infection was used as positive control (RRV). Data is expressed in mean values ± SEM (n=3). Statistical analysis was performed by two-way ANOVA compared to non-treated RRV infection.

5.4.3 Ethyl pyruvate does not reduce IL-6 secretion in RRV-infected C2C12 mouse myoblasts

Previous experiments with RRV-infected RAW264.7 macrophages have shown significant reductions of IL-6 release in the presence of ethyl pyruvate (EP). To see if EP also reduces IL-6 secretion in RRV-infected myoblasts we infected C2C12 cells with RRV T48 at an MOI of 1 in the presence of 1000 uM EP and analysed the supernatant at 12 and 24 hr p.i. by IL-6 ELISA. Non treated infection was used as positive control and compared to treatment. EP did not significantly reduce IL-6 release from C2C12 myoblasts into the supernatant during RRV infection (Figure 69).

5.4.4 Resveratrol does not significantly alter IL-6 release in C2C12 myoblasts during RRV infection

Similarly to the previous compounds, resveratrol (RVT) showed strong inhibitory effects on the IL-6 release of RAW264.7 macrophages during RRV infection. To investigate a possible effect on C2C12 we infected mouse myoblasts with RRV with or without the presence of 50 µM RVT and analysed the supernatant at various times post exposure to the virus (Figure 70). RVT did not significantly alter IL-6 release of RRV-infected C2C12 myoblasts at any time point p.i. (Table 11).

Table 11: IL-6 concentration of RRV-infected C2C12

Inhibitor	IL-6 (pg/mL) at 24 hr p.i.	Significance
No inhibitor	283±48	
ERY (100 µM)	198±24	ns
CLA (100 µM)	264±31	ns
RXM (100 µM)	241±16	ns
EP (1000 µM)	261±27	ns
RVT (50 µM)	266±33	ns

IL-6 levels in C2C12 supernatant were measured at 24 hr p.i. with RRV T48 (MOI of 1) with or without the presence of ERY, CLA, RXM, EP or RVT. Data is expressed as mean values ± SEM (n=3); ns = not significant (as determined by two-way ANOVA and compared to non-treated infection).

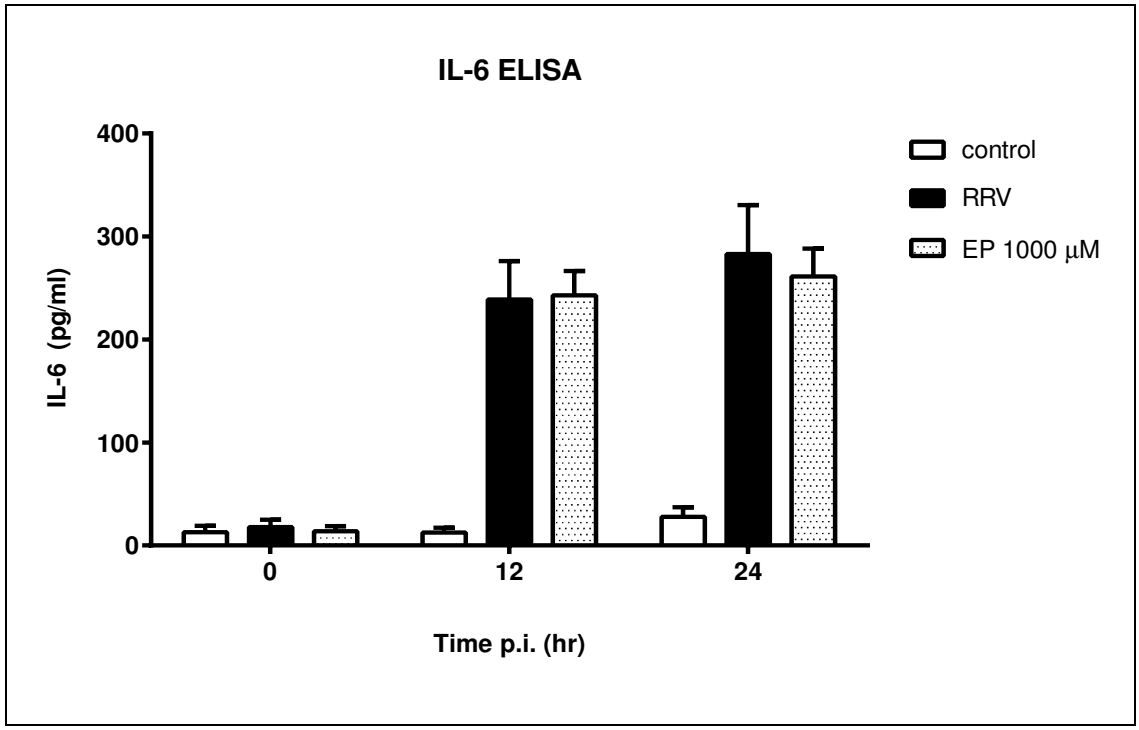

Figure 69: IL-6 concentration of RRV-infected C2C12 in the presence of ethyl pyruvate

C2C12 myoblasts were exposed to RRV T48 at an MOI of 1 in the presence or absence of 1000 uM EP and supernatant samples were taken at 12 and 24 hr p.i. and analysed by IL-6 ELISA. Mock infection with HI-RRV was used as negative control, non-treated infection (RRV) was used as positive control. Data is expressed in mean values ± SEM (n=3). Statistical analysis was performed by two-way ANOVA compared to positive control.

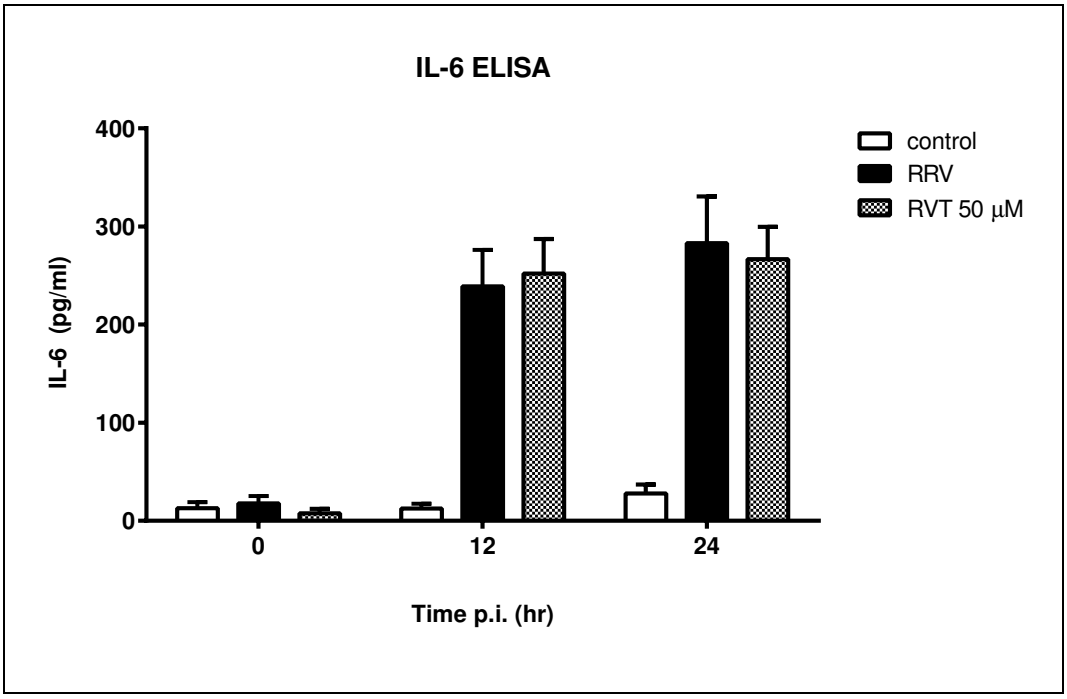

Figure 70: IL-6 concentration in the supernatant of RRV-infected C2C12 myoblasts co-treated with resveratrol (RVT)

C2C12 myoblasts were infected with RRV T48 at an MOI of 1 in the presence or absence of 50 uM RVT and supernatant samples taken at 12 and 24 hr p.i. were analysed by IL-6 ELISA. Non-treated infection was used as positive control (RRV) whereas mock infection with HI-RRV served as negative control. All data is graphed in mean values ± SEM (n=3). Statistical analysis was performed by two-way ANOVA and compared to positive control.

5.5 Inhibition of virus reproducibility with kinos extract

5.5.1 Introduction

Locher and Currie (Locher & Currie, 2010) previously published a review on the chemistry and pharmacological properties of kinos, a characteristical plant exudate often derived from trees of Australian *Eucalyptus* species. Kinos are strong astringents with a high content of polyphenolic tannins and aqueous kino extracts (KE) have traditionally been used as antiviral and antibacterial preparations, mainly in gastro-intestinal infections. Martha Y. Mungkaje (School of Pharmacy, Curtin University, Australia) has investigated kinos extract for its anti-inflammatory properties and found that aqueous KE derived from *Eucalyptus calophylla* reduced TNFα and NO release in LPS stimulated macrophages (personal communication).

Considering these findings we decided to investigate kino for its possible antiviral and anti-inflammatory properties in RRV infection. Aqueous kino extract was obtained by cold maceration of raw kino in water followed by sterile filtration and adjustment to a stock solution containing 33 mg/mL of raw kino. The extracts were prepared and kindly donated by Martha Y. Mungkaje (Curtin University, Western Australia). Initial viability studies were conducted to examine cytotoxicity of the extract on C2C12 myoblast cells. An MTT assay was performed with aqueous KE at a maximum concentration of 0.5 mg/mL and two-fold serial dilutions thereof (Figure 71). Relative viability was calculated against the respective controls of untreated C2C12 cells. Viability was not compromised for kino concentrations of up to 0.125 mg/mL. At concentrations of 0.25 mg/mL and higher cell viability was significantly compromised by 48 hr post exposure ($p \leq 0.01$).

5.5.2 RRV infection in C2C12 myoblasts and Vero cells with concurrent incubation with kino extract

The next step after determining cytotoxicity was to investigate if RRV does infect C2C12 cells as previously established in the presence of KE. C2C12 muscle cells were incubated with 0.1 mg/mL KE and concurrently infected with RRV T48 at an MOI of 1. Supernatant samples were taken at regular time intervals and examined for the presence of active viral particles. The supernatant of C2C12 cells treated with 0.1 mg/mL KE showed significantly reduced viral load at 1 d ($p \leq 0.001$) and 3 d ($p \leq 0.01$) post-infection (Figure 72).

Photographs of the cells were taken daily p.i. and a progressive cytopathic effect was observed in RRV-infected C2C12 myoblasts (Figure 73 B and D) as compared to non-infected controls (Figure 73 A and C). Samples exposed to RRV and concurrently treated with 0.1 mg/mL KE showed no CPE by 1 d post exposure (Figure 73 F) and reduced CPE by 3 d post exposure (Figure 73 H) when compared to non-treatment. C2C12 mock infected with HI-RRV (MOI of 1) showed increasing morphological changes by 3 d post exposure to kino, with cells presenting more rounded and formation of vacuoles within the cytosol (Figure 73 G).

To examine if the reduction in viral titres upon kino exposure is specific to C2C12 myoblasts or if it also occurs in other cell lines we exposed Vero cells to 0.1 mg/mL KE and determined viral load in the supernatant at appropriate time points post-infection (Figure 74). Viral titres showed a similar pattern with significantly lower viral titres at 1 and 3 d p.i. compared to non-treated infection ($p \leq 0.001$). Observation under the light microscope confirmed the reduced cytopathic effect in KE-treated Vero cells (Figure 75). Exposure to 0.1 mg/mL of kino extract resulted in increased vacuolisation within the cytoplasm of the cells for both infected and non-infected samples (Figure 75 E-H). Cell lysis in RRV-infected samples appeared however reduced with concurrent kino treatment as compared to samples without KE, which was most evident by 3 d p.i. (Figure 75 D and H). Cell viability of Vero cells was not reduced with 0.1 mg/mL KE as determined by MTT assay (data not shown).

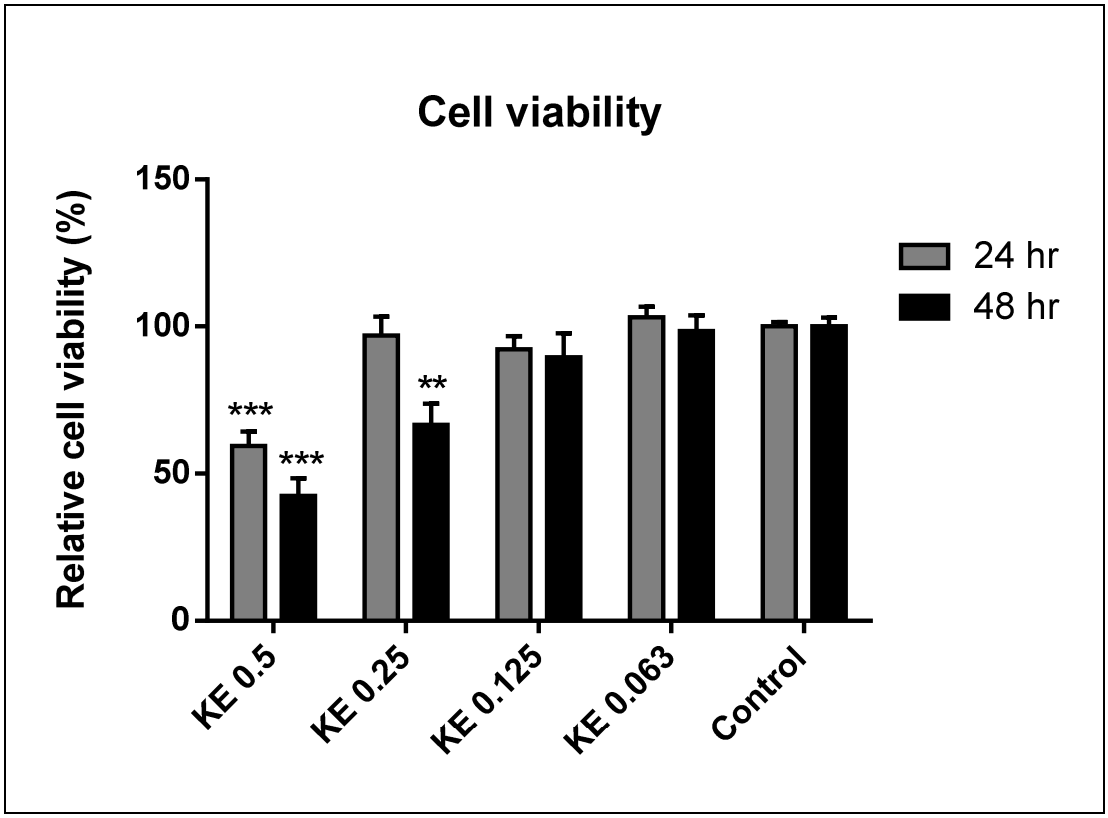

Figure 71: Cell viability of C2C12 myoblasts after exposure to different concentrations of KE

A MTT viability assay was performed on C2C12 myoblasts using aqueous kino extract (KE) at concentrations of 0.5 mg/mL (KE 0.5) and two-fold serial dilutions thereof (KE 0.25, KE 0.125 and KE 0.063) for 24 and 48 hr. Relative viability was calculated against non-treated control wells, which were given the arbitrary value of 100% viability. All data shown are mean values ± SEM (n=3). Statistical analysis was performed by two-way ANOVA and compared to the respective control for 24 and 48 hr samples. **($p \leq 0.01$), ***($p \leq 0.001$)

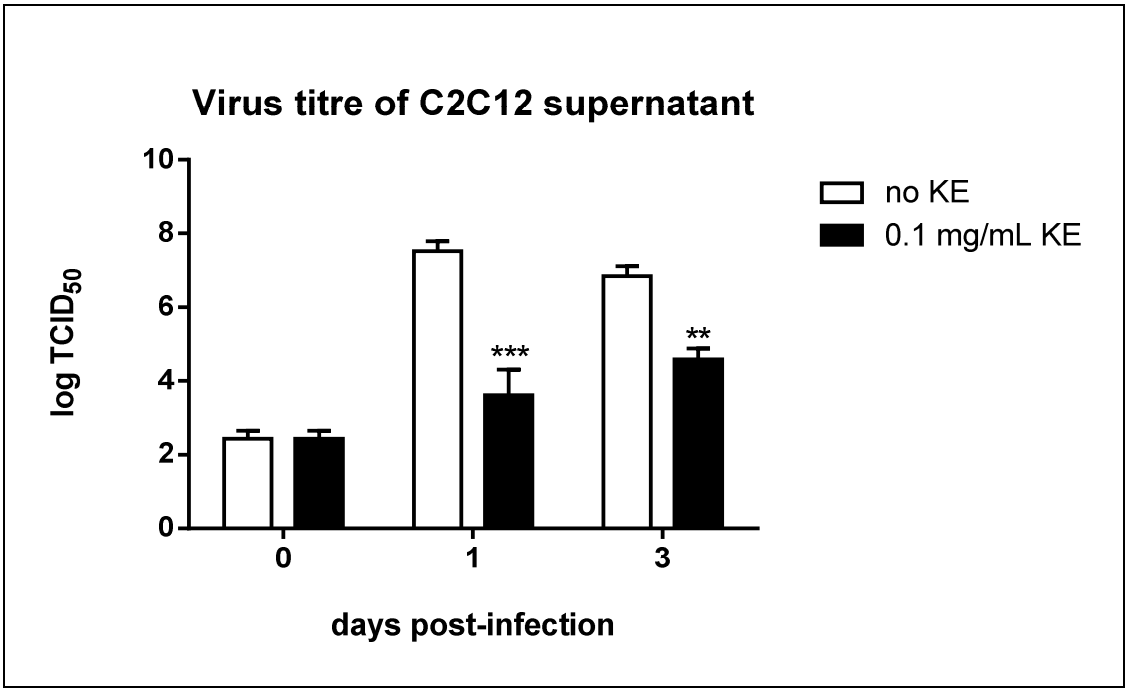

Figure 72: Virus titre of C2C12 supernatant post RRV infection with and without concurrent treatment with kino extract

C2C12 myoblasts were infected with RRV at an MOI of 1 with or without the presence of 0.1 mg/mL kino extract. Supernatant samples were taken at various days post-infection and viral titres were determined by $TCID_{50}$ assay. All data is graphed as mean values ± SEM (n=3). Statistical analysis was performed by two-way ANOVA compared to respective non-treated infection. **(p≤0.01), ***(p≤0.001)

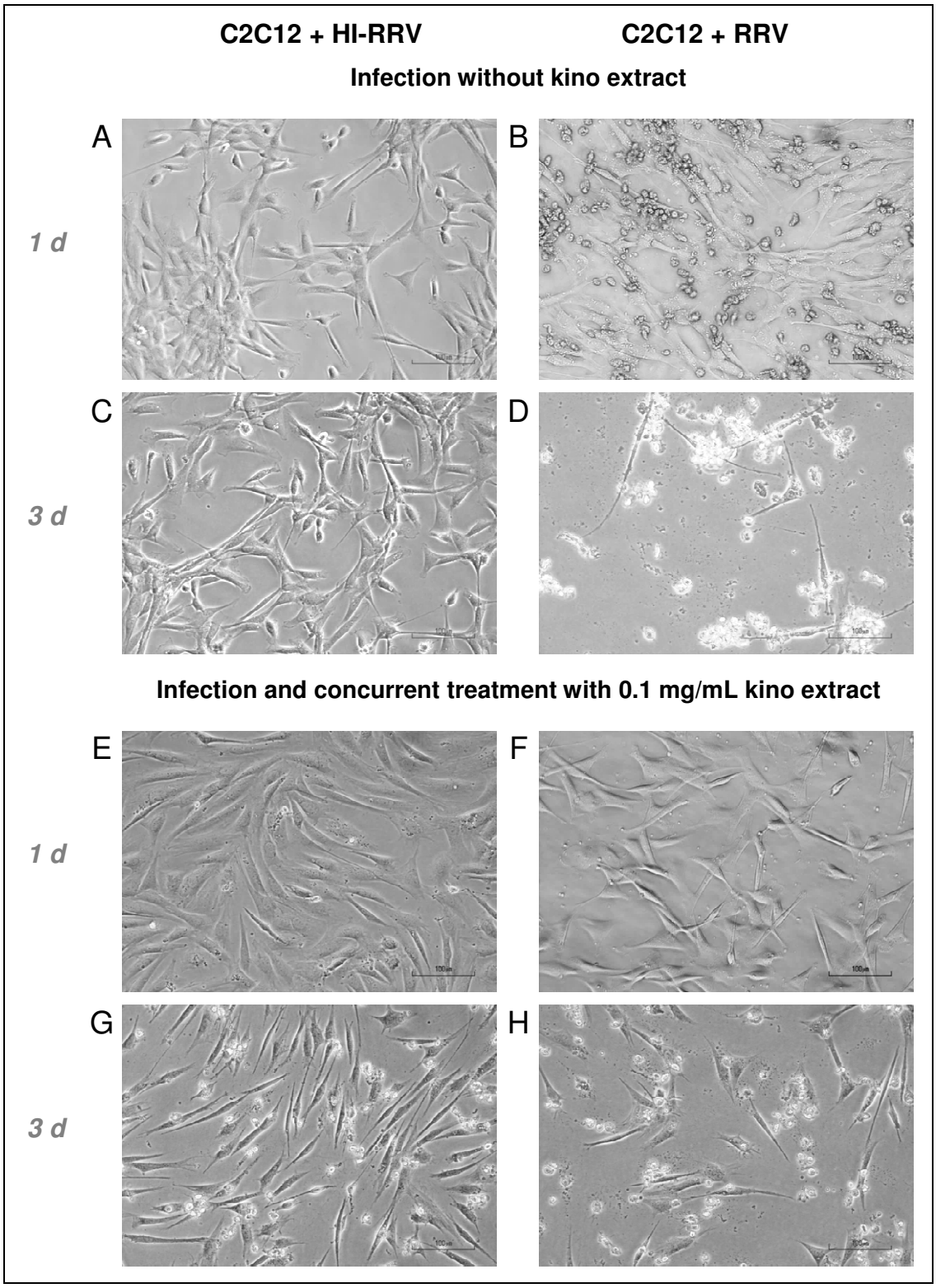

Figure 73: C2C12 cells infected with RRV and concurrent treatment with kino

C2C12 cells were inoculated with RRV (MOI of 1) in the presence (F,H) or absence (B,D) of 0.1 mg/mL kino extract. Infection with HI-RRV was used as negative control (A,C,E,G). Shown are representative photographs at 1 d (A,B,E,F) and 3 d (C,D,G,H) post-infection. The colour has been adjusted to grayscale.

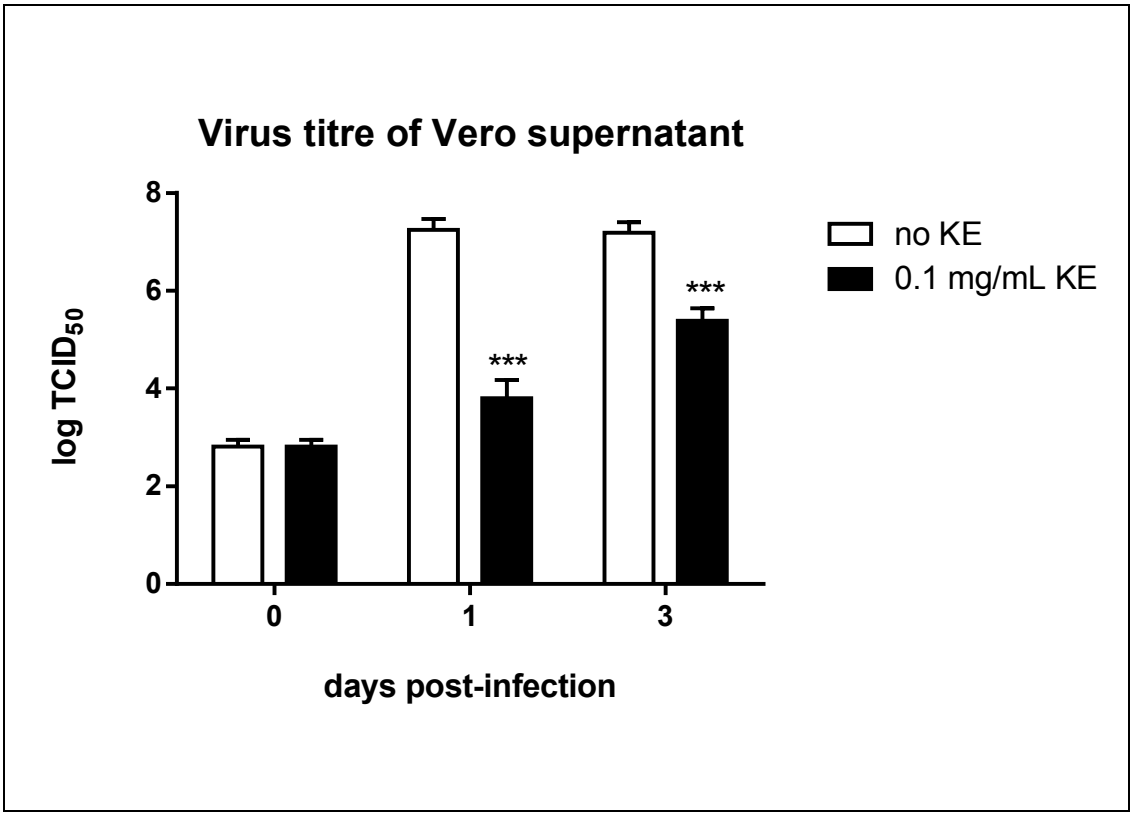

Figure 74: Virus titre of Vero supernatant post RRV infection with and without concurrent treatment with kino extract

Vero cells were infected with RRV at an MOI of 1 with or without the presence of 0.1 mg/mL kino extract. Supernatant samples were taken at various days post-infection and viral titres were determined by TCID50 assay. All data is graphed as mean values ± SEM (n=3). Statistical analysis was performed by two-way ANOVA compared to respective non-treated infection. ***($p \leq 0.001$)

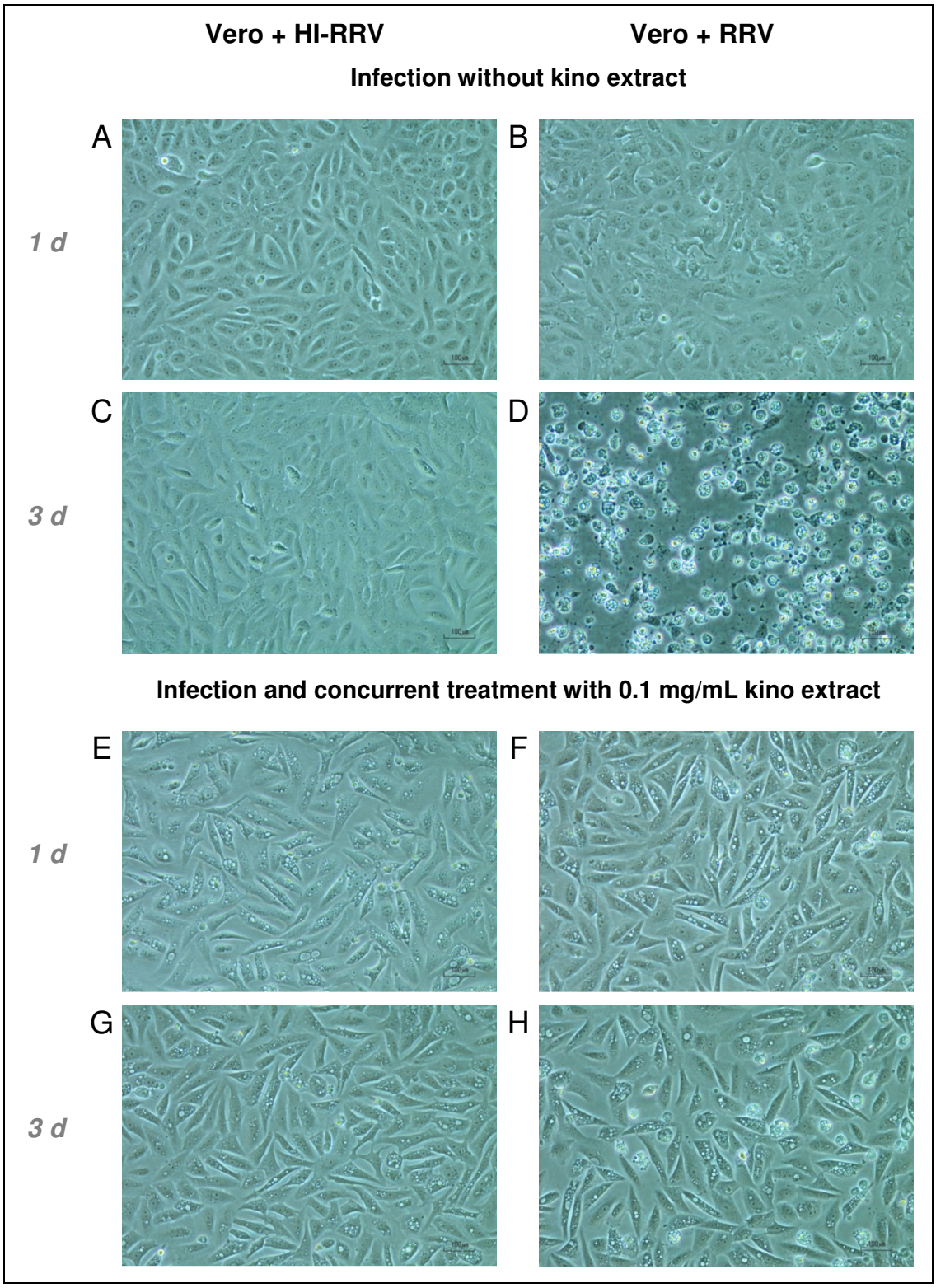

Figure 75: Vero cells infected with RRV and concurrent treatment with kino

Vero cells were infected with RRV T48 at an MOI of 1 in the presence (F,H) or absence (B,D) of 0.1 mg/mL KE. HI-RRV was used as control (A,C,E,G). Shown above are representative photographs of the cells taken at 40x magnification by 1 d (A,B,E,F) and 3 d (C,D,G,H) post-infection.

5.5.3 Kino extract does not have direct antiviral properties

In order to investigate if the decrease in viral titres is due to reduced viral replication or due to direct antiviral activity of KE we incubated RRV T48 stock with kino extract and determined viral titres as previously. RRV T48 stock solution with a $TCID_{50}$ adjusted to $10^{6.5}$ was incubated at 4˚C with or without 0.1 and 1 mg/mL KE for 24 or 48 hr and the number of active virus particles was determined by $TCID_{50}$ assay. As shown in Figure 76, virus titres were not significantly reduced upon incubation with 0.1 or 1 mg/mL KE as compared to the appropriate control, thus ruling out a direct antiviral effect. As expected, the number of active viruses in 48 hr samples show lower titres as compared to 24 hr samples due to progressive virus degradation over time.

5.5.4 Virus replication in C2C12 and Vero cells after 24hr pre-treatment with aqueous kino extract

Considering the effect of kino extract on viral replication in both C2C12 and Vero cells, we decided to investigate whether prophylactic treatment with KE can successfully inhibit viral replication.

C2C12 or Vero cells were incubated with 0.1 mg/mL aqueous kino extract for 24 hr, washed twice with PBS and then exposed to RRV at an MOI of 1 in the absence of KE. Supernatant samples were taken daily and virus titres were determined by TCID50 assay as previously. As shown in Figure 77, pre-exposure to 0.1 mg/mL KE significantly reduced viral titres in the supernatant of infected C2C12 myoblasts in the days post exposure ($p \leq 0.001$). Low titres were still detectable at 1 d p.i. but by 3 d p.i. no active virus could be detected by TCID50 assay. Initial experiments included 0.5 mg/mL KE samples but were omitted due to the cytotoxicity as shown previously (see 5.5.1). In samples pre-treated with 0.5 mg/mL KE no virus was detected at 1 or 3 d p.i. (data not shown).

Photographs taken at the time of sample collection show increasing cytopathic effect (CPE) in non-treated infection, with characteristic CPE foci visible from 1 d p.i. (Figure 78 B and D). Extensive CPE and cell lysis was observed at 3 d post-infection. Samples treated with 0.1 mg/mL KE showed reduced growth compared to non-treated cells at day 1 and 3 of the experiment with increasing morphological changes and rounded cells in both infected as well as mock infected samples. Otherwise no obvious difference could be observed between infected and mock infected samples at 1 d p.i. (Figure 78 E and F) or 3 d p.i. (Figure 78 G and H).

Similar results were obtained for pre-treatment of Vero cells with 0.1mg/mL kino extract followed by RRV infection. Viral load as determined by $TCID_{50}$ assay showed virus levels below the calculation minimum at 1 d p.i. for Vero cells pre-treated with 0.1 mg/mL KE (Figure 79). No active virus was detected in any of the KE pre-treated samples at 3 d p.i.

Visual observation of the cells under a light microscope showed again progressive CPE for RRV-infected samples without KE-pre-treatment at 1 and 3 d p.i. (Figure 80 B and D) compared to mock-infected control (A and C). Pre-exposure to 0.1 mg/mL KE shows morphological changes with cells forming vacuoles within the cytoplasm (Figure 80 E-H). This effect was observed for all samples pre-treated with aqueous KE. RRV infection shows reduced cytopathic effect and cytolysis in pre-treated samples as compared to samples without prior KE exposure. This is especially noticeable at 3 d p.i. (Figure 80 D and H).

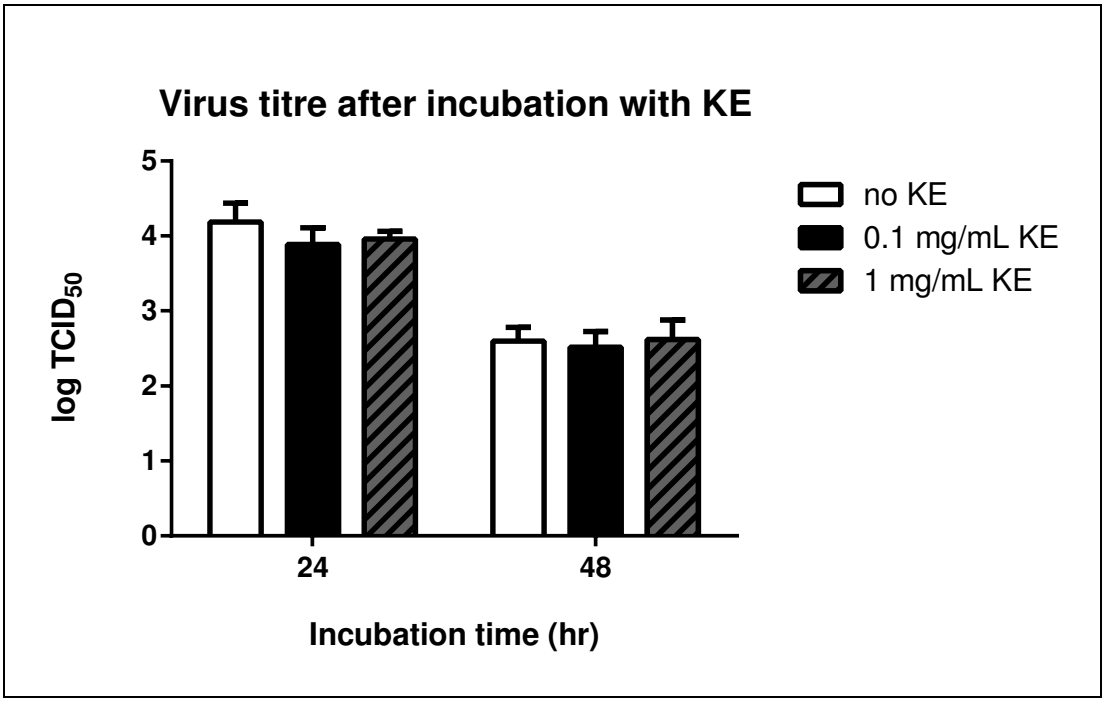

Figure 76: Virus titres after incubation of RRV T48 with various concentrations of KE

RRV T48 stock solution (TCID50 = 106.801) was incubated with or without KE (0.1 and 1 mg/mL) for 24 and 48 hrs and virus titres were determined as previously by TCID50 assay. Data shown above is graphed as mean values ± SEM (n=3). Statistical analysis by two-way ANOVA showed no significant differences between RRV that had been exposed to KE and the respective non treated sample.

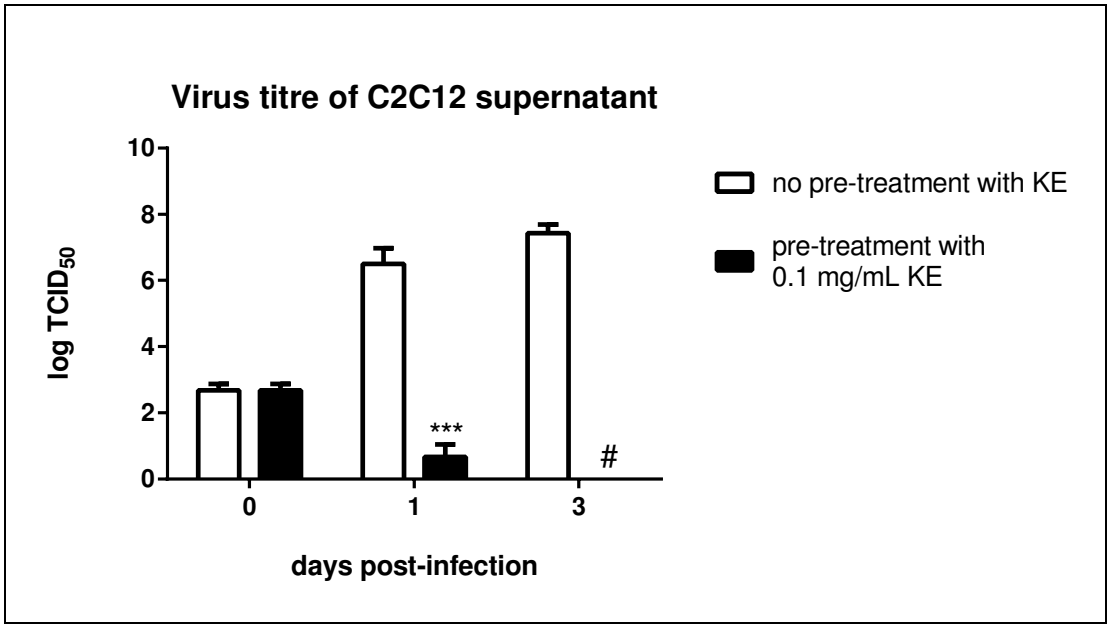

Figure 77: Virus titre in the supernatant of C2C12 myoblasts pre-treated with kino extract upon RRV infection

C2C12 myoblasts were exposed to 0.1 mg/mL aqueous kino extract (KE) for 24 hr prior to infection with RRV T48. Viral load in the supernatant was determined by TCID50 assay and graphed as log TCID50. # (no virus detected at day 3 p.i. for C2C12 pre-treated with KE). Data is shown as mean value ± SEM (n=3). Statistical analysis was performed by two-way ANOVA and compared to non-treatment infection. ***($p \leq 0.001$)

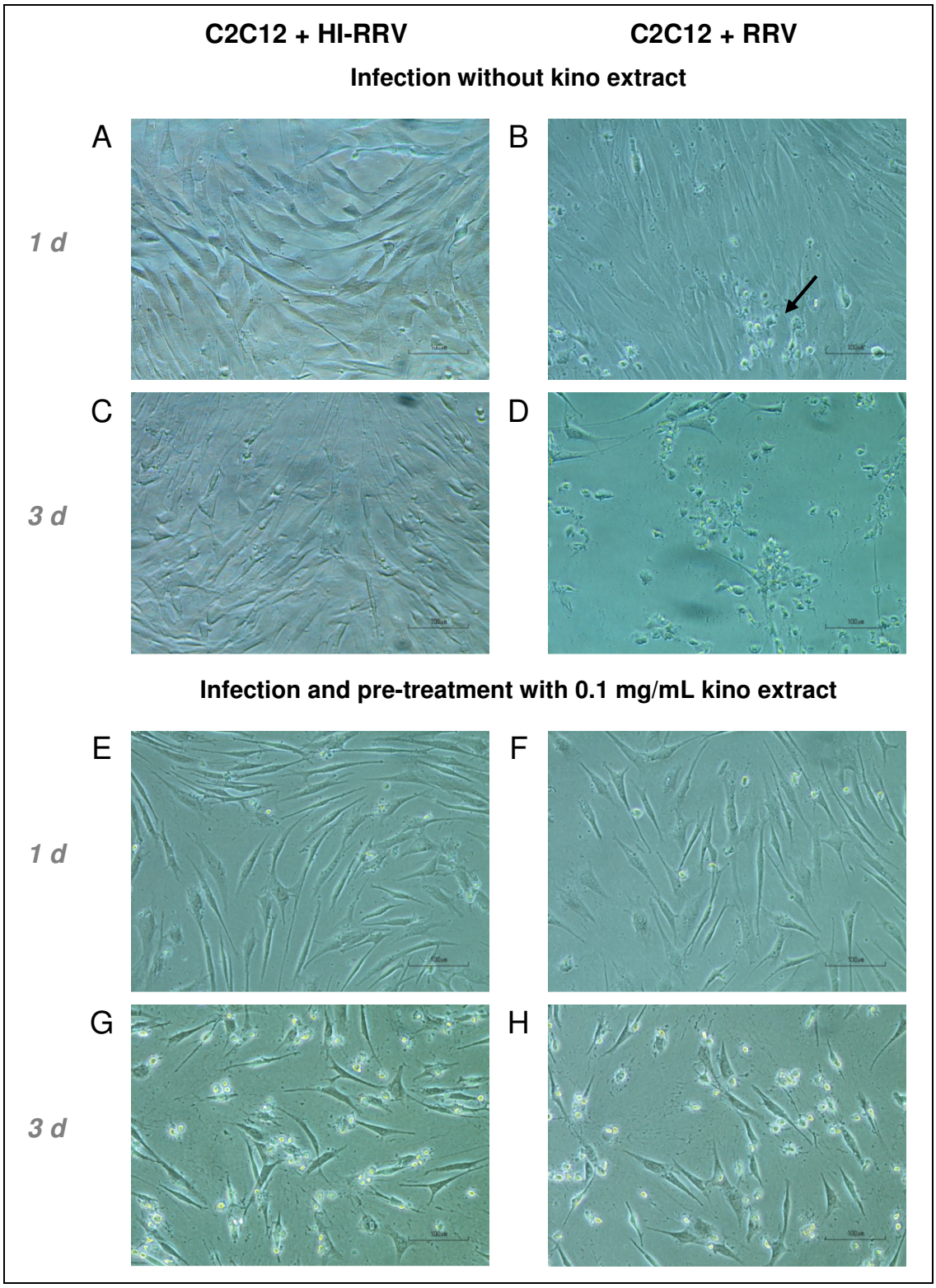

Figure 78: RRV infection of C2C12 cells after pre-treatment with kino extract

C2C12 were exposed to 0.1 mg/mL aqueous kino-extract (E-H) or R-2 (A-D) for 24 hr. The supernatant was replaced with R-2 prior to inoculation with RRV T48 (MOI of 1) (B,D,F,H) or HI-RRV (A,C,E,G). (B) shows characteristic CPE foci as indicated by the arrow.

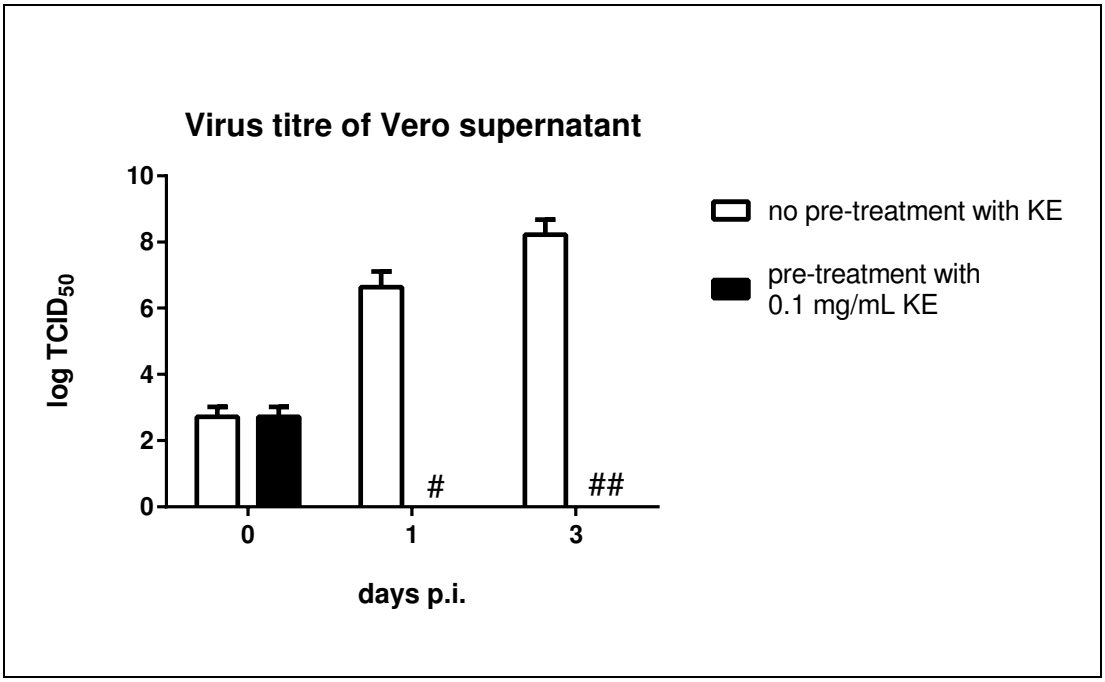

Figure 79: Viral load in the supernatant of RRV-infected Vero cells after pre-treatment with 0.1 mg/mL aqueous kino extract

Vero cells were exposed to 0.1 mg/mL kino extract (KE) for 24 hr prior to infection with RRV T48 at an MOI of 1. Viral titres in the supernatant samples were determined by TCID50 assay and graphed as log TCID50. Data is shown as mean values ± SEM (n=3). # (number of infected wells for pre-treated KE samples at 1 d p.i. below calculation limit), ## (no virus detected at day 3 p.i. for C2C12 pre-treated with KE).

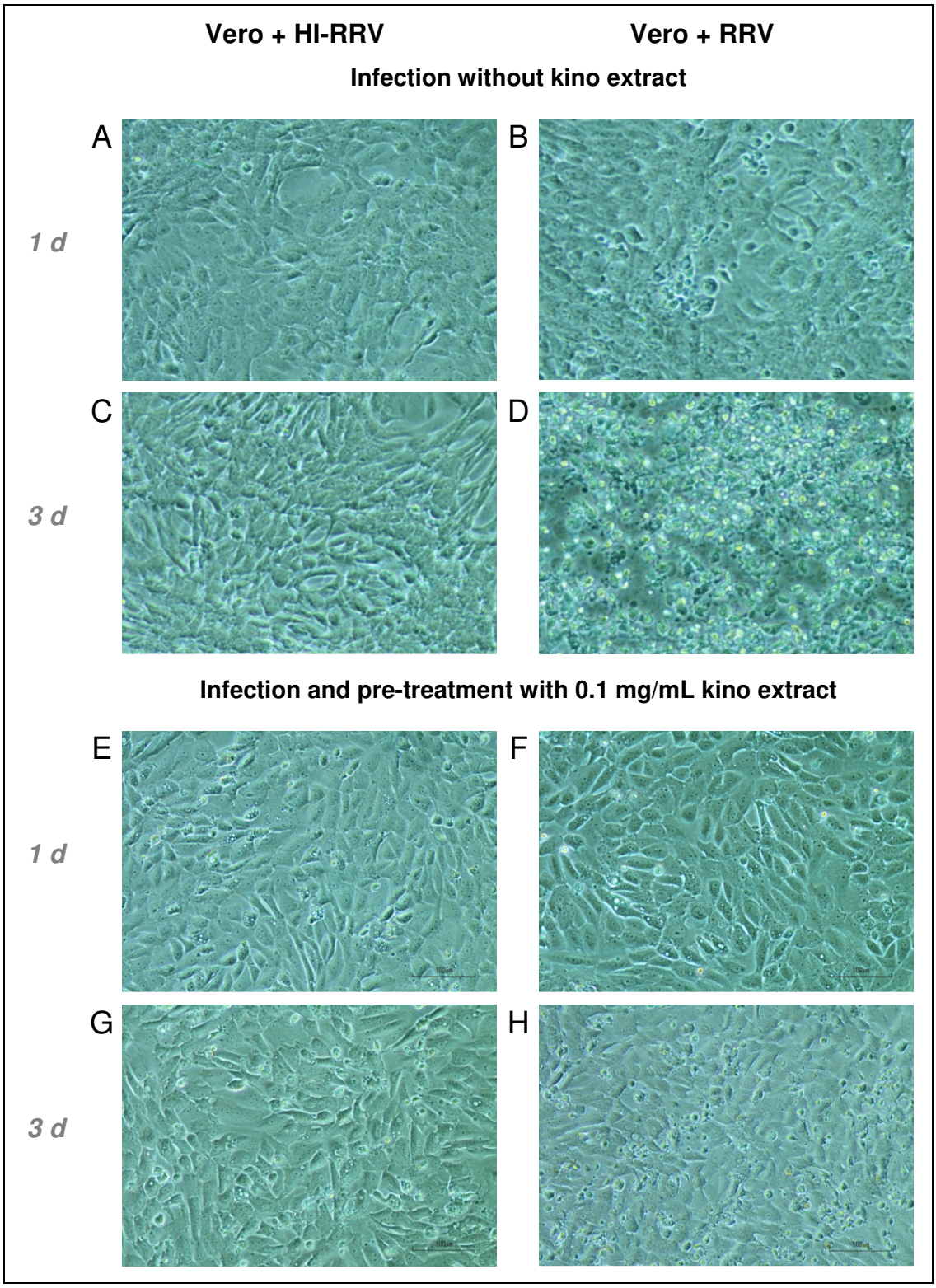

Figure 80: RRV infection in Vero cells after pre-treatment with kino extract

Vero cells were exposed to 0.1 mg/mL aqueous kino-extract (E-H) or R-2 (A-D) for 24 hr prior to inoculation with RRV T48 (MOI of 1) (B,D,F,H) or HI-RRV (A,C,E,G). Cells were observed daily for morphological changes and CPE. Formation of vacuoles was observed in all samples pre-treated with 0.1 mg/mL KE (E-H).

5.6 Discussion of C2C12 results

The role of muscle cells during RRV infection has still not been fully identified. Initial reports gave varying cellular responses for *in vivo* and *in vitro* infections and it was concluded, that other host factors must be contributing to the necrotic muscle pathology in infected mice (Lidbury et al., 2000).

We were able to show that RRV can undergo a replication cycle in C2C12 mouse myoblasts which leads to significantly increased viral numbers and lysis of infected cells. Only recently another study was published independently with similar reports of C2C12 being suitable cells for RRV propagation (Stoermer Burrack et al., 2014). We believe, and our findings support this idea, that the initial spike in viral titres and the tissue destruction found in muscles during acute infections are partially caused by exponential cytolytic virus replication in muscle cells. With these necrotic processes during initial infection, the symptomatic myalgia and myositis would be expected. It is however also important to emphasize that we do not doubt the significant role of infiltrating macrophages and other leukocytes into the muscle during RRVD. Numerous studies have shown that various immune responses such as macrophage cytokines or complement activation contribute to the inflammatory myopathy of infected mice (Morrison et al., 2007; Morrison et al., 2006) and a recent study by Burrack et al. (K. S. Burrack et al., 2015) has highlighted the regulatory function of T-cells on virus infection and inflammation in the skeletal muscle tissue.

We could show that initial infection of C2C12 muscle cells with RRV triggers the production of a variety of cytokines. The transcription and/or secretion of the pro-inflammatory mediators TNFα, MIF, IL-6, IL-18 and IL-33 were clearly up-regulated after exposure to RRV. This could explain early macrophage migration and activation into the muscle as observed in RRV infected mice. Early research (G. Williams et al., 1994) has suggested that LPS alone is not able to induce nitrite release from C2C12 myoblasts and a combination of TNFα and IFNγ was required for successful induction of NO secretion. Frost et al. (Frost et al., 2004) however reported of increased iNOS production and nitrite secretion in LPS challenged C2C12 myoblasts. Similar to these results we could show that iNOS mRNA was transcribed in both LPS- and RRV-challenged myoblast cells. Despite induction of iNOS however, no elevation in supernatant nitrite levels was detected in infected C2C12 cells. Initially the increasing lysis of RRV infected cells was considered to be a contributing factor to this phenomenon as cell destruction may occur before detectable levels of nitrite are synthesised. LPS stimulation however showed similar

induction of iNOS mRNA transcription without elevated nitrite levels. It remains to be determined whether iNOS is translated in insufficient amounts or if the NO response is delayed compared to iNOS induction. Due to excessive cytolysis no time points past 24 hr post-infection were analysed for cytokine secretion.

Inhibitors that were previously trialled in macrophages were tested for their effect on IL-6 secretion in infected C2C12 myoblasts. IL-6 is recognized as one of the major regulatory cytokines released from muscle cells and it has been shown previously that IL-6 contributes to macrophage activation (Chomarat et al., 2000; Mark A. Febbraio & Pedersen, 2002). Of the tested compounds, little or no inhibitory effect was detected for CLA, RXM, EP and RVT. ERY showed some inhibition on IL-6 release in muscle cells. This together with the results from macrophage experiments makes ERY an interesting compound for further investigation as a treatment option for RRVD.

It should be noted that cytokines released from muscle cells function as regulatory mediators likely only within the first 12 to 24 hr of infection. Increasing cytolysis could result in uncontrolled release of various cytoplasmic compounds and therefore macrophage infiltration and activation would be inevitable.

A second set of experiments focused on the biological effects of aqueous *Eucalyptus calophylla* kino extract (KE) in RRV infected muscle cells. We were able to show that treatment with kino extract reduced virus propagation in both C2C12 as well as Vero cells. Pre-treatment with KE seemed to completely inhibit the replication cycle in both cell lines. KE does not have any direct antiviral properties on RRV but chemical analysis has revealed large amounts of tannins in the kino exudate (Locher & Currie, 2010). These astringent compounds may precipitate surface proteins including integrins, which are considered crucial for successful virus adhesion to the cell (La Linn et al., 2005). At the correct KE concentration virus entry may be inhibited without impairing cell viability.

While kino extract seems not suitable as a therapy option in the treatment of RRV infections, it does highlight the importance of cell surface structures for alphavirus infections, which could potentially offer a target for treatment or prevention of RRV disease. It remains to be determined whether KE interacts with specific surface structures to interfere with virus adhesion or whether the effects are non-specific due to the astringent properties of the extract. Due to its physicochemical properties KE is poorly absorbed (Locher & Currie, 2010). A possible future research project could however examine the astringent effect in the gastro-intestinal tract and

investigate KE as a possible protective agent against enteric virus infections. It also remains to be investigated whether the astringent effect is reversible in C2C12 cells or whether cell viability is impaired after prolonged periods of time. The formation of vacuoles in the cytoplasm, similar to what we could observe, has previously been linked to statin-induced cell damage and apoptotic processes in muscle cells (Sakamoto & Kimura, 2013) and therefore more long term viability experiments are needed to fully assess cytotoxicity.

Future research projects could focus on following questions:

- Are macrophages attracted to infected muscle tissue due to the active release of chemokines or due to necrotic processes after infection of RRV?
- Does the avirulent strain RRV DC5692 show similar cytolytic effects on C2C12 myoblast cells? Does it induce the same cytokine response?
- Is the vacuolisation caused by KE in C2C12 cells a reversible effect? Does KE show cytotoxicity upon prolonged exposure to C2C12 cells?

6. Results IV: Cytokine production of 3T3-L1 adipocytes after exposure to Ross River Virus T48

6.1 Introduction

Previous studies on the pathogenesis of murine RRV infections in various tissues found extensive viral growth in brown adipose tissue (Murphy et al., 1973). Despite these findings, no further investigations were undertaken to investigate RRV infection in adipocyte cells. Adipocytes are known to produce a wide array of cytokines upon stimulation – often labelled adipokines – and their role in many inflammatory conditions has been acknowledged (Berg & Scherer, 2005; Coppack, 2001). A review of the involvement of adipose tissue in rheumatoid arthritis (Tarner et al., 2007) has highlighted a possible role of adipokines as targets for future treatments. Considering these findings we decided to investigate a potential role of adipocytes in RRV infection. The fibroblast-like pre-adipose cell line 3T3-L1 can be differentiated to adipocytes as outlined previously and is commonly used in adipocyte research (Poulos et al., 2010). We therefore decided to use differentiated 3T3-L1 adipocytes in our infection experiments.

6.2 Infection of 3T3-L1 adipocytes with RRV T48

6.2.1 3T3-L1 pre-adipocytes do not show CPE upon exposure to RRV

Even in optimized conditions, differentiation rates of 3T3-L1 pre-adipocytes to adipocytes are not likely to reach 100% (Mehra et al., 2007). Hence preliminary experiments were conducted to examine the effect of RRV on 3T3-L1 pre-adipocytes first. To ensure sufficient viral loading the concentration of virus dilution was adjusted to MOI = 4 since culture vessel surface was increased. Non-differentiated 3T3-L1 cells were exposed to RRV T48 (MOI of 4) and observed daily for up to 4 d. No cytopathic effect was visible and no morphological changes were detected by day 4 (Figure 81 A). Supernatant taken immediately after addition of RRV as well as 2 and 4 d p.i. was examined for viral titres by $TCID_{50}$ assay (Figure 81 B). Viral load in the supernatant expressed as log $TCID_{50}$ dropped from 4.88 ± 0.08 to 2.35 ± 0.55 by day 2 p.i. and no virus could be detected by day 4 p.i. This indicates that RRV does not undergo a cytolytic replication cycle in 3T3-L1 pre-adipocytes within the first 4 days of infection.

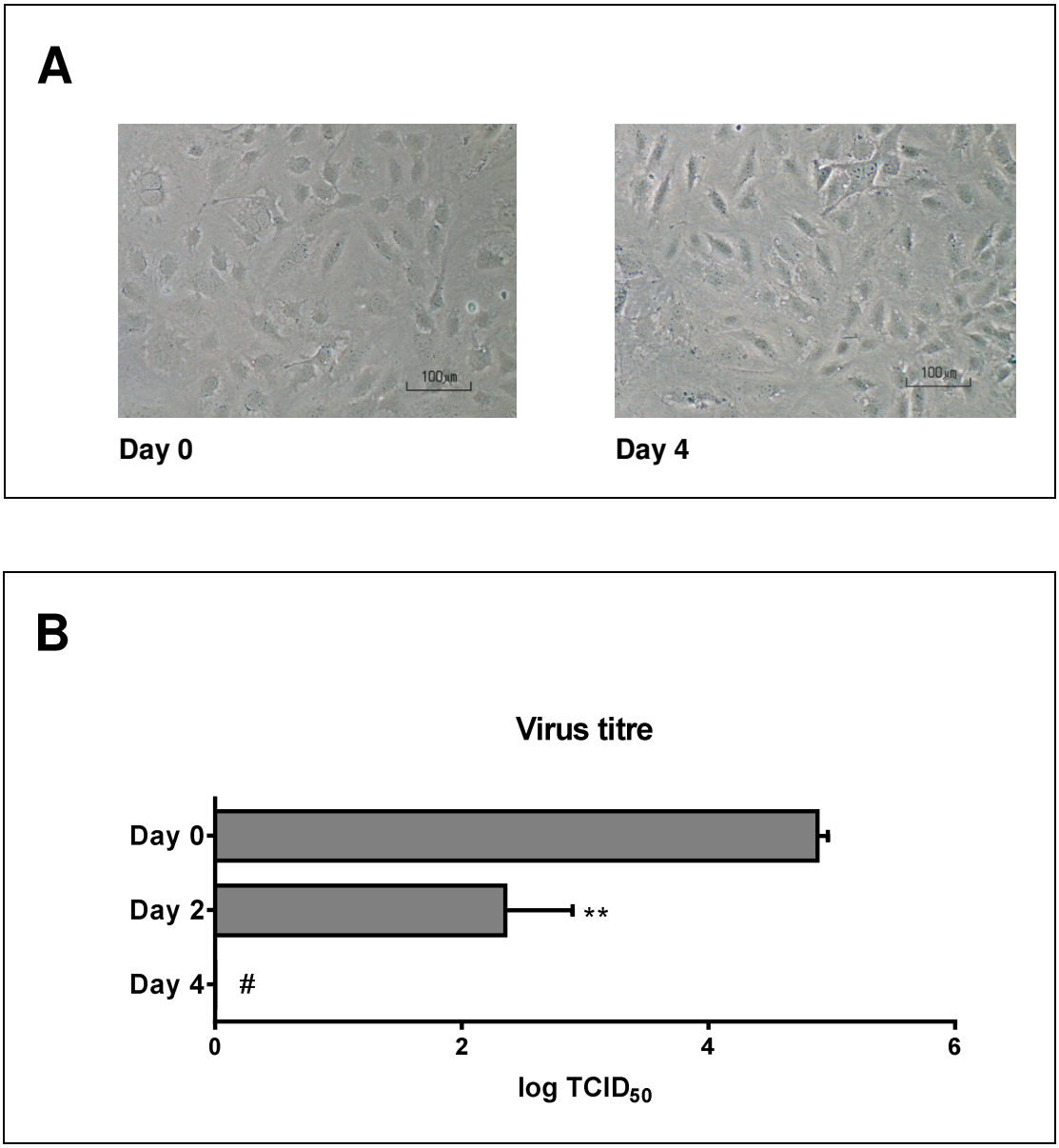

Figure 81: 3T3-L1 pre-adipocytes exposed to RRV T48

3T3-L1 pre-adipocytes were exposed to RRV for up to 4 d and examined under a light microscope for CPE or morphological changes. Shown in (A) are representative photographs of 3T3-L1 pre-adipocytes immediately after infection (Day 0) and 4 d p.i. (Day 4). Viral titres of the supernatant were determined as usual and graphed as log $TCID_{50}$ values. All data shown is expressed as mean values ± SEM (n=3). Statistical analysis was performed by one-way ANOVA and compared to Day 0. **($p \leq 0.01$); # (no virus detected).

6.2.2 3T3-L1 adipocytes do not show CPE upon exposure to RRV

The next aim was to investigate if RRV does infect 3T3-L1 adipocytes and cause cytolysis upon virus replication, similar to Vero or C2C12 cells. In order to test this, 3T3-L1 pre-adipocytes were differentiated into adipocytes as outlined in Methods and exposed to RRV T48 (MOI of 4). Photographs were taken at 36 hr p.i. and adipocytes were examined for cytopathic effect. None of the infected cells showed cytolysis or any other morphological changes (Figure 82).

6.2.3 RRV mRNA is expressed in 3T3-L1 adipocytes upon exposure to RRV

In light of the initial findings that RRV does not immediately undergo a replication cycle that leads to lysis of the host cell, we examined if RRV can enter adipocytes in a non-cytolytic infection as reported for synovial cells previously (Journeaux et al., 1987). Differentiated 3T3-L1 adipocytes were exposed to RRV T48 at an MOI of 4 and RNA was extracted at various time points post-infection. A conventional RT-PCR was performed to investigate if RRV RNA (viral RNA coding the entire region of the viral E2 protein) can be detected within the first 36 hr post-infection. As shown in Figure 83, at 18 hr p.i. a very faint band could be detected for adipocytes exposed to RRV but not in controls. The amplicon appeared more prominent at 36 hr post-infection.

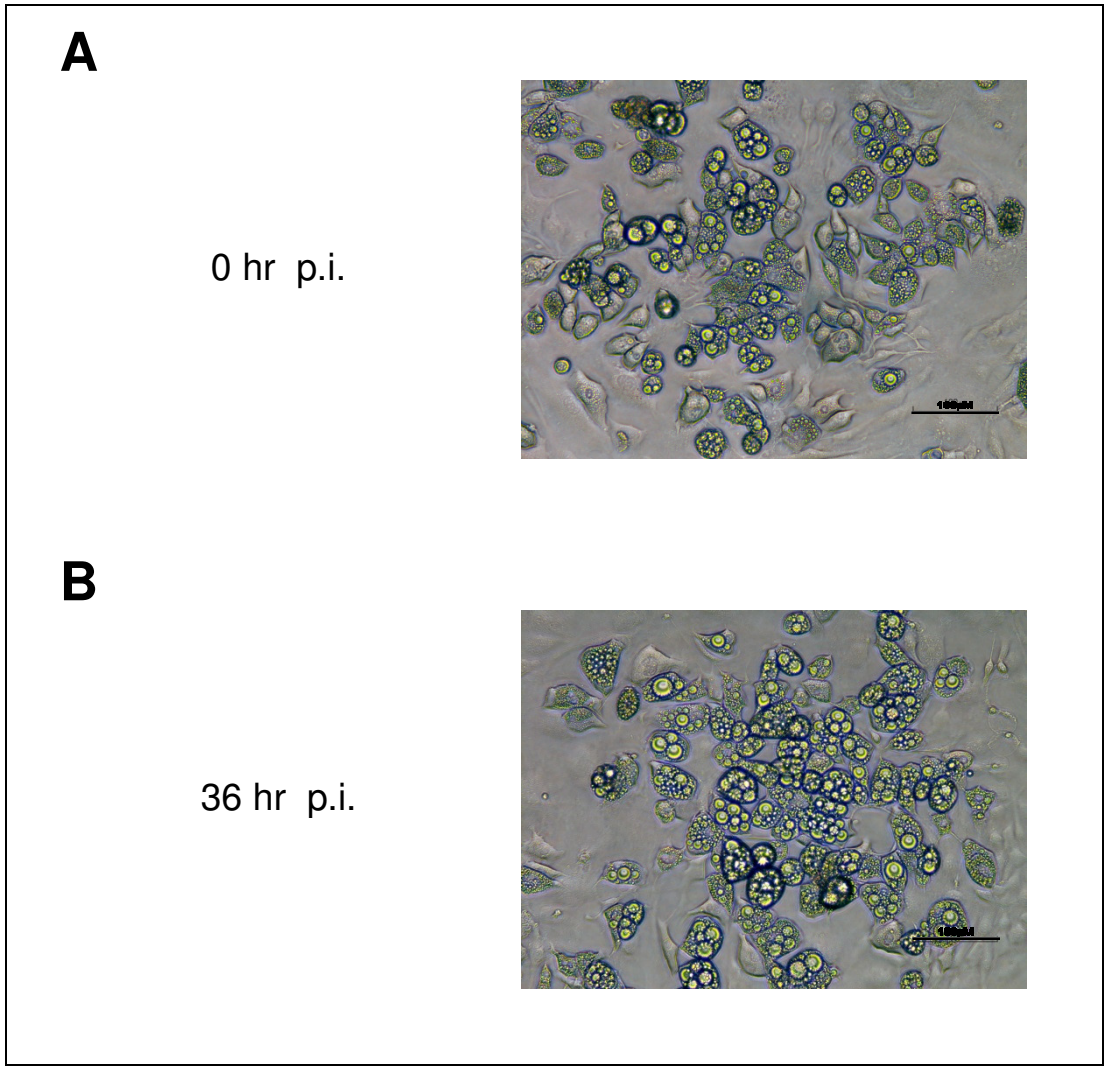

Figure 82: 3T3-L1 adipocytes after exposure to RRV T48

3T3-L1 adipocytes were exposed to RRV T48 (MOI of 4) and examined for CPE. Shown are representative photographs of the adipocytes at 0 hr (A) and 36 hr (B) post-infection. Photographs were taken with an inverse phase contrast microscope at 25x magnification.

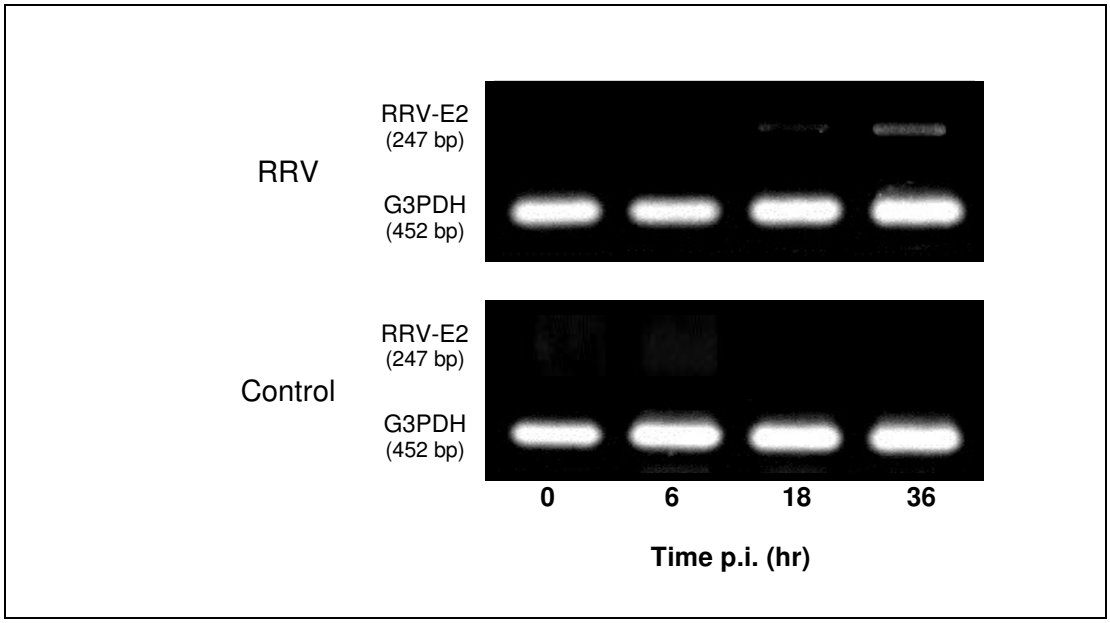

Figure 83: RRV RNA can be detected in 3T3-L1 adipocytes post exposure

3T3-L1 adipocytes were exposed to RRV T48 (MOI of 4) and RNA was extracted at various time points post-infection and transcribed into a first strand cDNA as outlined in Methods. A PCR was performed to evaluate the expression of viral E2 RNA with G3PDH used as control gene on the same samples. Shown above are representative photographs of the agarose gels under UV light stained with GelRed®.

6.3 Cytokine production in 3T3-L1 adipocytes in RRV infection

6.3.1 Neither RRV nor LPS induce TNF-α release in 3T3-L1 adipocytes

After confirming that RRV does enter 3T3-L1 adipocytes we explored the cellular response of infected cells in regards to cytokine production. To examine if RRV induces secretion of TNFα in adipocytes we infected differentiated 3T3-L1 with RRV T48 and analysed the supernatant by ELISA. Samples taken at any time point p.i. did not show increased levels of TNFα (Figure 84). LPS successfully induces TNFα secretion in macrophages and was trialled as alternative stimulant, however failed to induce TNFα secretion in 3T3-L1 adipocytes. It has previously been reported that LPS stimulation induces several pro-inflammatory cytokines in human adipocytes but not TNFα (Hoch et al., 2008). RNA extracted at the same time points was screened for TNFα mRNA but did not show gene expression in RRV samples or LPS samples (data not shown) despite previous reports of LPS induced TNFα transcription in 3T3-L1 (Ajuwon & Spurlock, 2005).

6.3.2 RRV does not induce secretion of NO however induces transcription of iNOS mRNA in 3T3-L1 adipocytes

3T3-L1 adipocytes were exposed to RRV T48 (MOI of 4) and supernatant samples were taken after 0, 6, 18 and 36 hr post-infection and examined by Griess-assay for nitrite, a stable oxidation product of biologically released NO. Neither LPS-stimulated nor RRV-infected 3T3-L1 adipocytes showed increased levels of nitrite in the supernatant at any time (Figure 85). RNA extracted at the same time was reverse transcribed and analysed by PCR with gene-specific primers for inducible iNOS. Transcription of iNOS mRNA was significantly induced in RRV ($p \leq 0.05$) and LPS ($p \leq 0.01$) samples by 6 hr post exposure and gene expression continued in both samples by 18 hr p.i., however decreased thereafter (Figure 86).

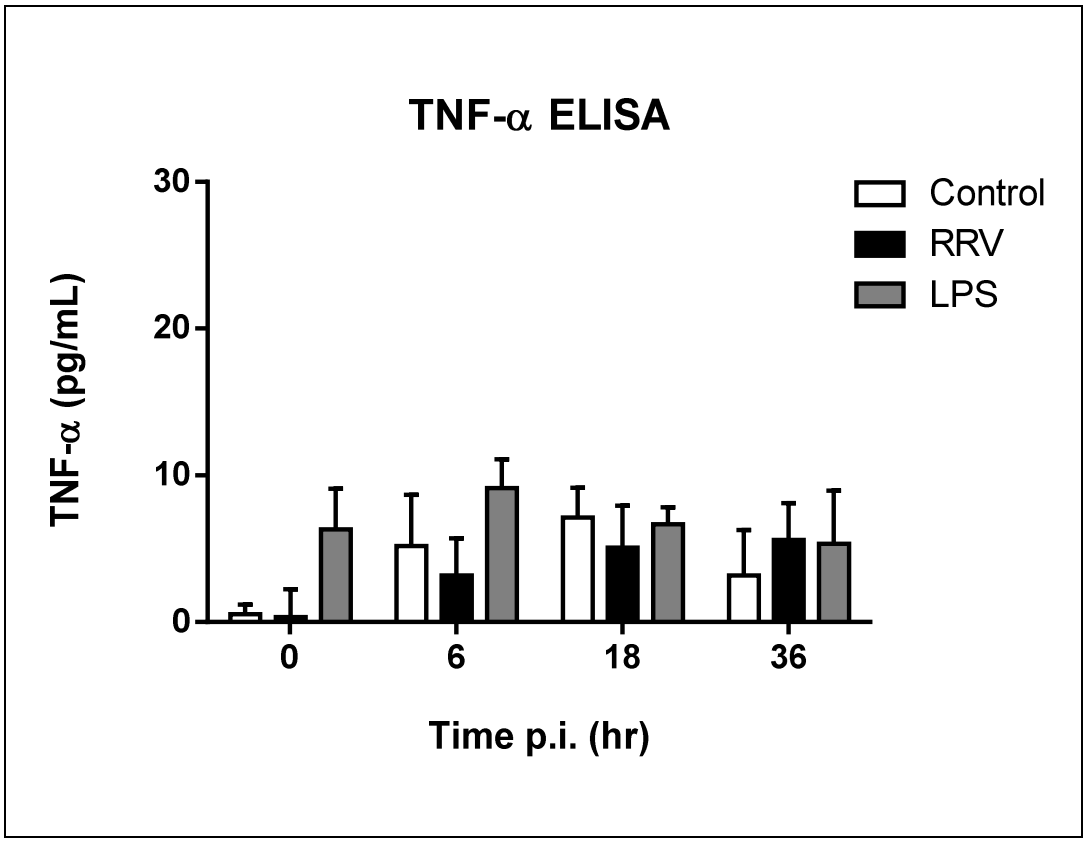

Figure 84: TNFα secretion of 3T3-L1 adipocytes post RRV infection

3T3-L1 adipocytes were exposed to RRV T48 (MOI of 4) and supernatant samples taken at appropriate time points p.i. were tested for TNFα concentration by ELISA. Data shown are mean values ± SEM (n=4). Statistical analysis was performed by two-way ANOVA. No significant change in TNFα levels was detected.

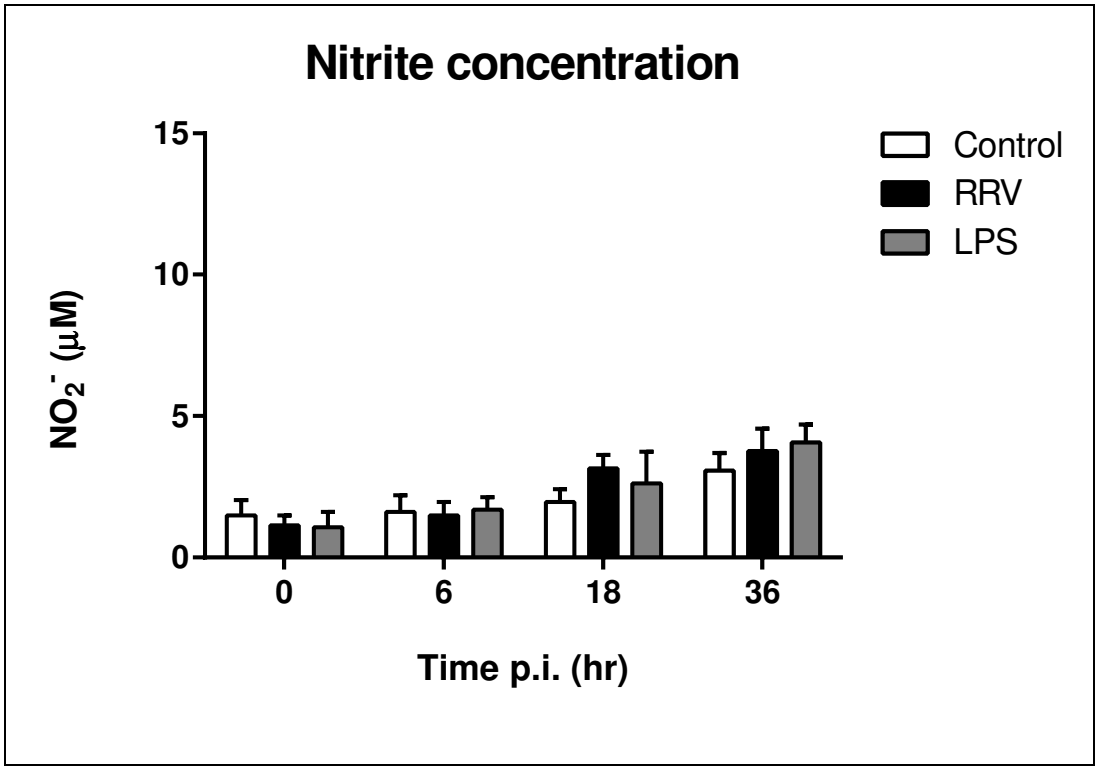

Figure 85: NO production of 3T3-L1 adipocytes upon RRV infection or LPS stimulation

3T3-L1 adipocytes were exposed to RRV at an MOI of 4, LPS (1 μg/mL) or culture media and supernatant samples were taken at appropriate time points. Nitrite concentration was determined by Griess assay as outlined in Methods. Data above is expressed in mean values ± SEM (n=4). No significant change in nitrite concentration could be detected.

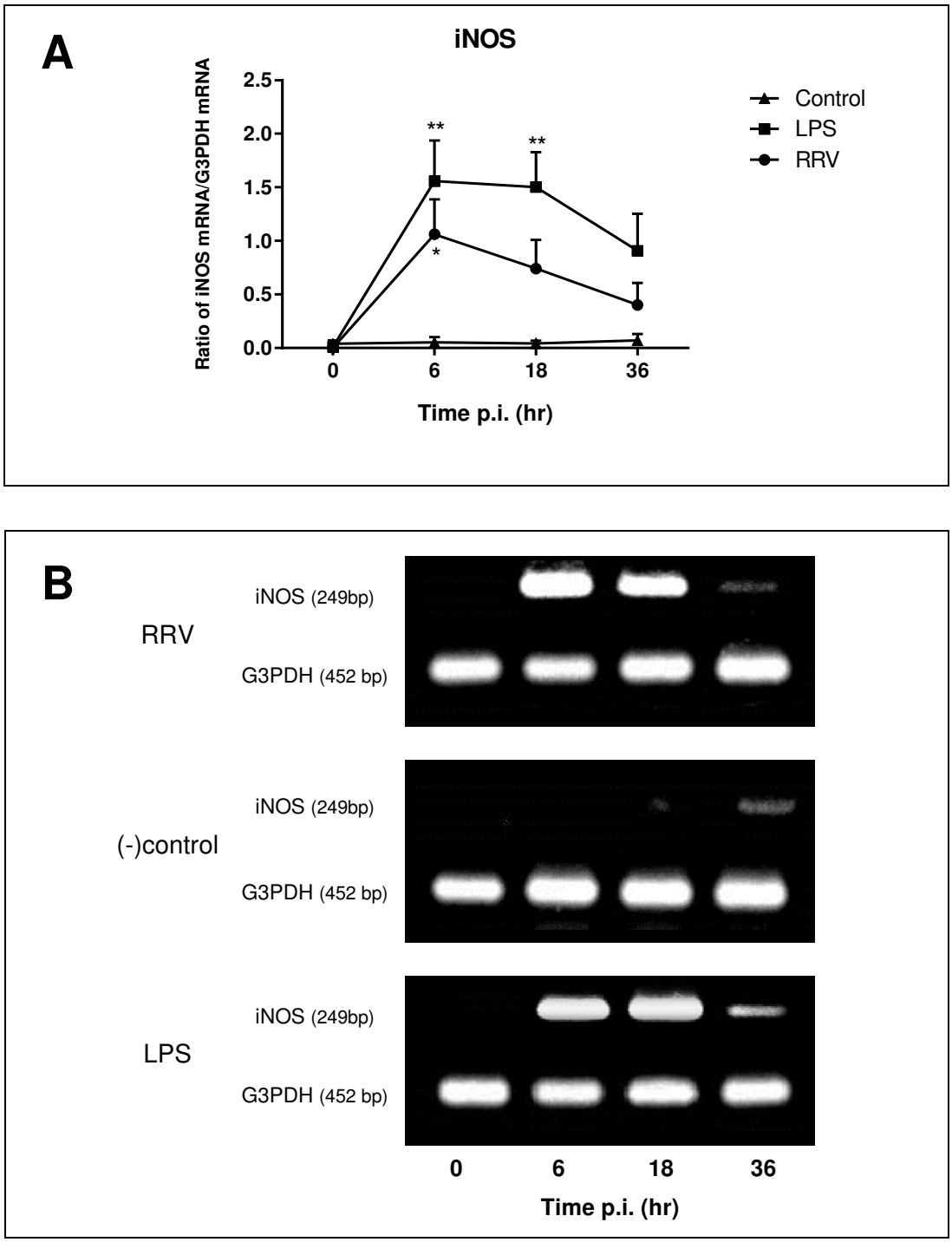

Figure 86: iNOS mRNA expression in 3T3-L1 adipocytes after exposure to RRV or LPS

3T3-L1 adipocytes were exposed to RRV T48 an MOI of 4 or LPS (1 µg/ml) and mRNA was extracted at various times. The mRNA expression of iNOS and G3PDH was determined by semi-quantitative densiometric analysis and the ratio of cytokine mRNA over G3PDH mRNA was graphed (A). Data shown are mean values ± SEM (n=3 for RRV, LPS, control, n=4 for G3PDH). (B) shows representative photographs of agarose gels. *($p \leq 0.05$), **($p \leq 0.01$) as determined by two-way ANOVA.

6.3.3 3T3-L1 adipocytes secrete IL-6 after infection with RRV

Previous reports (Fasshauer et al., 2003) have shown that 3T3-L1 adipocytes secrete IL-6 upon LPS challenge. To investigate if this pro-inflammatory cytokine is also released in RRV infection we exposed adipocytes to RRV T48 and examined supernatant samples at different times for IL-6 by ELISA (Figure 87). IL-6 could be detected in significant concentrations as early as 6 hr post stimulation with levels increasing in a time-dependent manner to 1464 ± 194 pg/mL by 36 hr p.i. ($p \leq 0.001$). LPS at 1 µg/mL induced IL-6 in a similar way with levels reaching 1575 ± 177 by 36 hr post stimulation.

6.3.4 RRV induces expression of IL-6 mRNA in 3T3-L1 adipocytes

To further investigate the increase of IL-6 secretion, 3T3-L1 adipocytes were exposed to RRV or LPS and RNA was extracted at various times post stimulation. A RT-PCR with IL-6 specific primers was performed and the obtained gel blots were analysed densiometrically as outlined in Methods. Expression of IL-6 mRNA can be detected in RRV at 6 hr p.i. increasing in a time-dependent manner (Figure 88 A). LPS stimulation similarly shows a significant induction of IL-6 mRNA by 6 hr ($p \leq 0.05$) with expression still strongly increased after 36 hrs. The semi-quantitative densiometric analysis did not show a significantly higher level of expression for RRV samples, however photographs of the agarose gels clearly visualised an increase in IL-6 mRNA expression (Figure 88 B).

6.3.5 IL-18 mRNA expression in 3T3-L1 is not influenced by RRV or LPS

It was previously reported (Sun et al., 2009) that 3T3-L1 adipocytes can secrete IL-18 and considering the role of IL-18 as one of the pro-inflammatory cytokines in rheumatoid arthritis we investigated a possible increase in IL-18 expression during RRV infection (Gracie et al., 1999). In order to examine IL-18 mRNA expression, 3T3-L1 adipocytes were infected with RRV or stimulated with LPS and RNA was extracted at various time points. A PCR with IL-18 specific primers was performed after reverse transcription and agarose gels were photographed and analysed as previously. IL-18 was expressed in RRV-, LPS- as well as non-treated control-samples equally and no significant change in gene expression was detected over time (Figure 89).

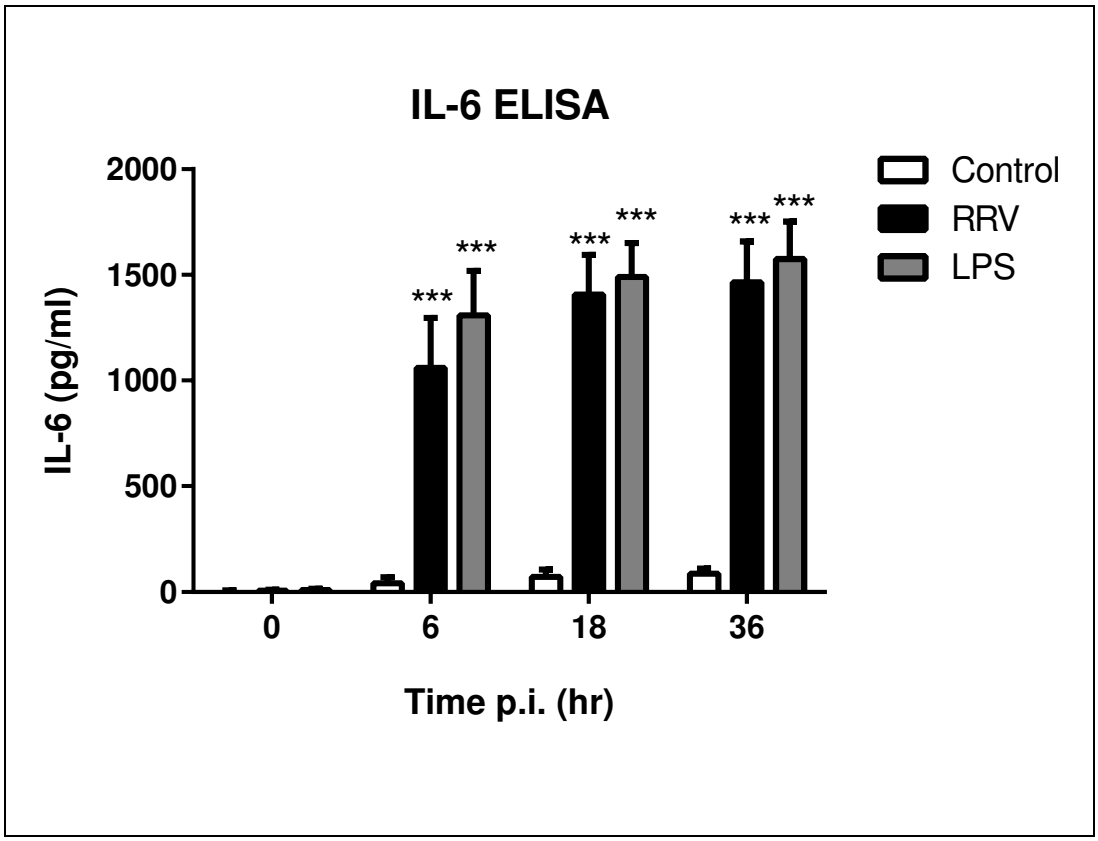

Figure 87: IL-6 concentration in supernatant of 3T3-L1 adipocytes exposed to RRV

3T3-L1 adipocytes were exposed to RRV an MOI of 4, LPS (1 µg/mL) or culture media and supernatant samples taken at 0, 6, 18 and 36 hr p.i. were tested for IL-6 by ELISA. Data above is expressed in mean values ± SEM (n=4). ***(p≤0.001) as determined by two-way ANOVA compared to non-treatment control.

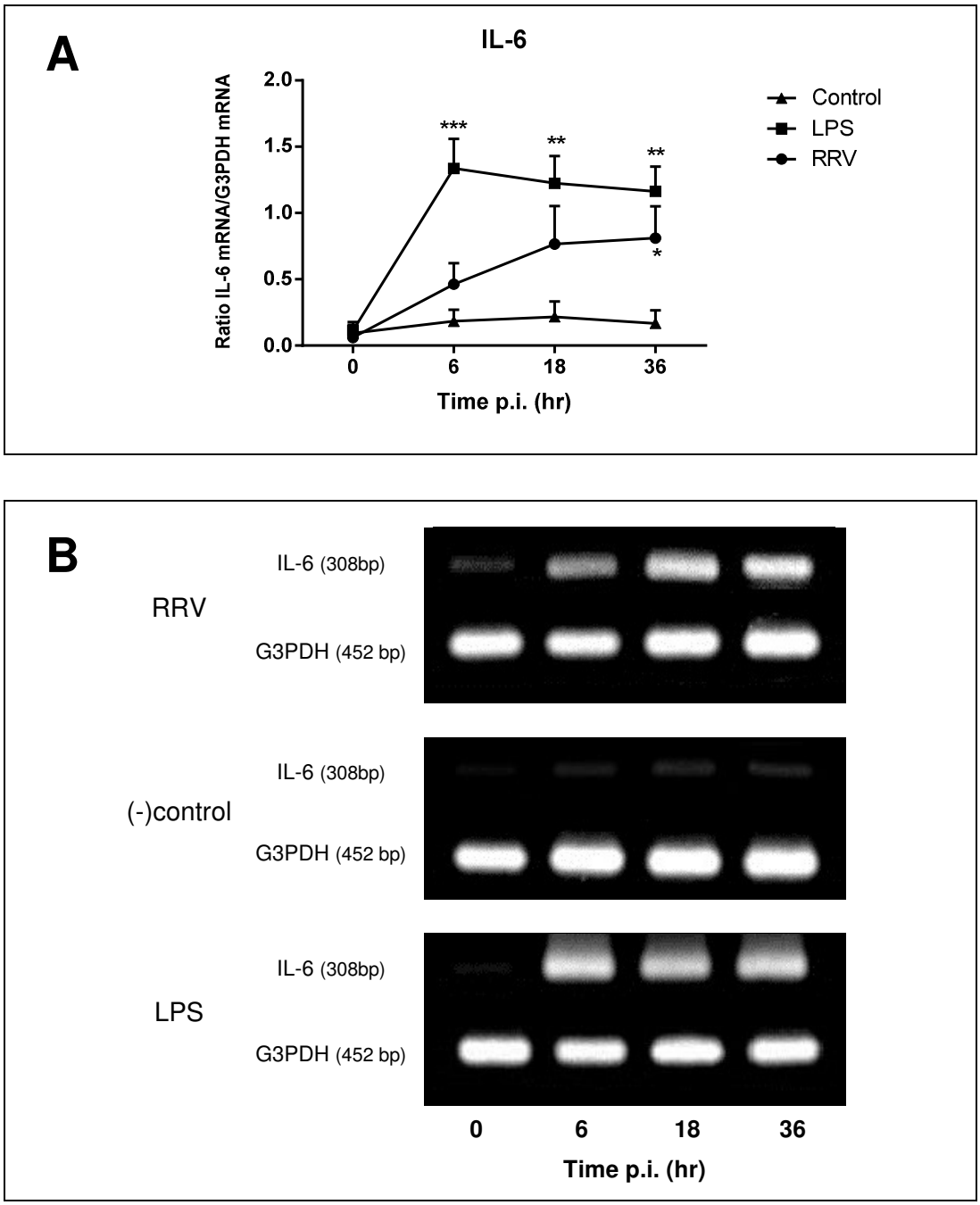

Figure 88: IL-6 mRNA expression in 3T3-L1 adipocytes after exposure to RRV or LPS

3T3-L1 adipocytes were exposed to RRV T48 an MOI of 4 or LPS (1 µg/ml) and mRNA was extracted at various times. The mRNA expression of the cytokine IL-6 and G3PDH were determined by densiometric analysis and the ratio of cytokine mRNA over G3PDH mRNA is graphed in (A). Data shown are mean values ± SEM (n=3 for RRV, LPS and control, n=4 for G3PDH). *(p≤0.05),**(p≤0.01),***(p≤0.001) as determined by two-way ANOVA compared to control. (B) shows representative photographs of agarose gels .

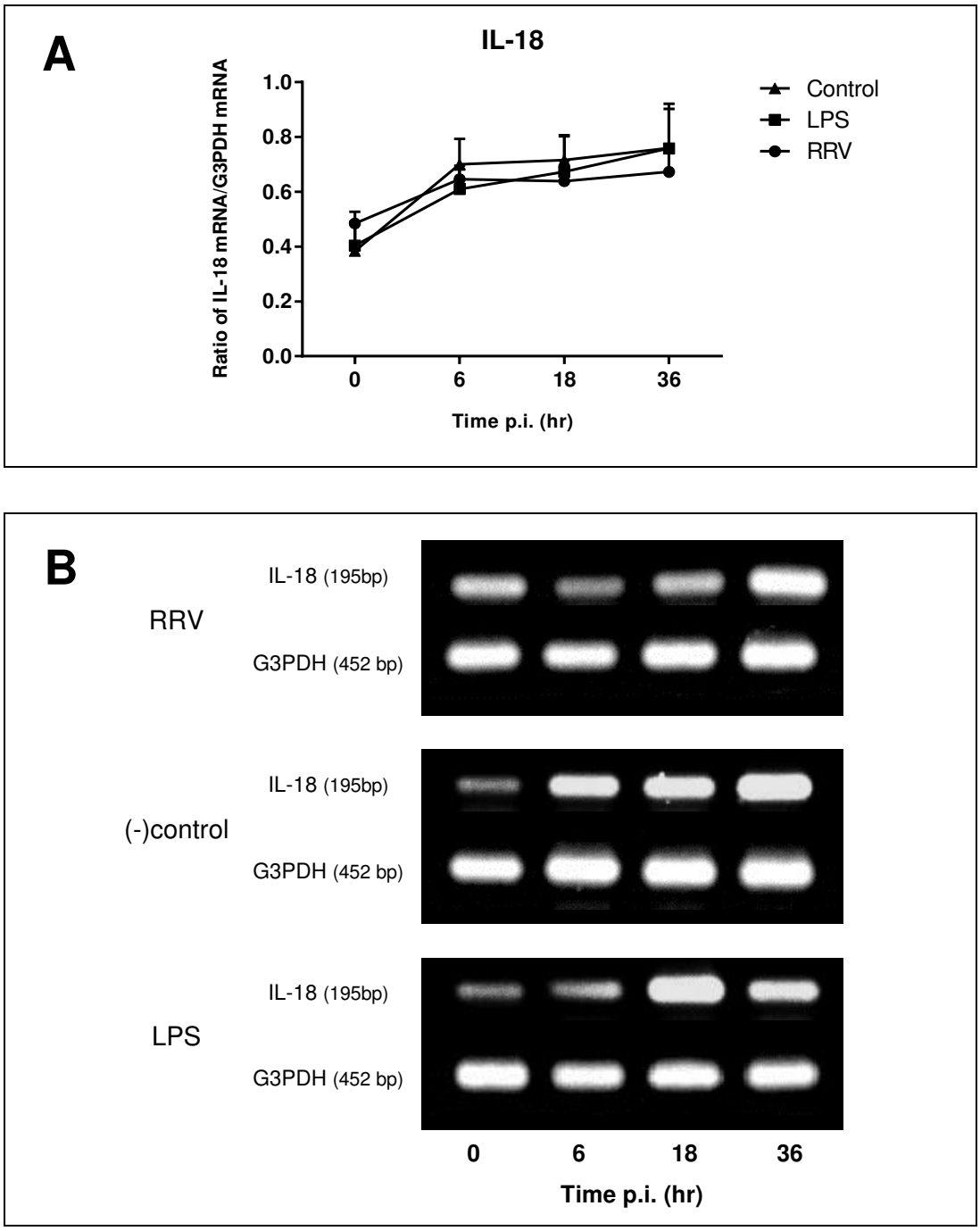

Figure 89: IL-18 mRNA expression in 3T3-L1 adipocytes after exposure to RRV or LPS

3T3-L1 adipocytes were exposed to RRV T48 an MOI of 4 or LPS (1 µg/mL) and mRNA was extracted at various times. mRNA expression of IL-18 and G3PDH was determined by densiometric analysis and the ratio of IL-18 mRNA over G3PDH mRNA is graphed in (A). Data is expressed in mean values ± SEM (n=4 for RRV and G3PDH, n=3 for LPS and control). Analysis by two-way ANOVA compared to controls showed no significant change. (B) shows representative photographs of agarose gels.

6.3.6 RRV induces transcription of IL-33 mRNA in 3T3-L1 adipocytes in a time dependent manner

IL-33 has been investigated as a possible contributing factor in rheumatoid arthritis and it is known that adipose tissue can release IL-33 (Schaffler & Scholmerich, 2010; D. Xu et al., 2008). To examine if RRV infection increases expression of this cytokine, 3T3-L1 adipocytes were infected with RRV T48 or challenged with LPS as previousl and RNA was extracted at several time points post-infection. Transcription levels of IL-33 mRNA were determined by RT-PCR and densiometric analysis of gel photographs was performed with ImageJ. As shown in Figure 90 B, RRV induces IL-33 mRNA by 6 hr p.i. and expression increases in a time-dependent manner. At 18 hr ($p \leq 0.05$) and 36 hr ($p \leq 0.01$) p.i. the levels of IL-33 mRNA were significantly higher compared to non-treated controls. LPS also seems to stimulate IL-33 mRNA transcription, however levels were considerably lower compared to RRV samples (Figure 90 B).

6.3.7 HMGB1 mRNA transcription in 3T3-L1 adipocytes during RRV infection

As mentioned earlier in this thesis, the function of HMGB1 as a cytokine has been recognised and it has recently been shown that pre-adipocytes can release HMGB1 upon stimulation (Nativel et al., 2013). HMGB1 has been identified as a novel adipokine that induces IL-6 secretion in SW872 pre-adipocytes and contributes to inflammatory processes in adipose tissue. To investigate the role of HMGB1 in RRV-infected adipocytes we exposed differentiated 3T3-L1 cells to RRV T48 (MOI of 4) and extracted RNA at various times post-infection. RT-PCR was performed with primers specific for HMGB1 and agarose gels were photographed and analysed with ImageJ as previously. There was a small decrease in HMGB1 transcription for RRV-infected samples as compared to control samples, which was however not statistically significant as determined by two-way ANOVA (Figure 91). Exposure to LPS (1 µg/mL) induced transcription of the HMGB1 gene in 3T3-L1 adipocytes, which reached significance by 36 hrs post-infection ($p \leq 0.05$) as compared to mock infected control.

6.3.8 Basal HMGB2 expression in 3T3-L1 adipocytes exposed to RRV or LPS

Similar to HMGB1 we analysed expression of HMGB2 mRNA upon exposure of 3T3-L1 adipocytes to RRV or LPS. A RT-PCR of extracted RNA samples with HMGB2 specific primers indicated a basal HMGB2 expression in 3T3-L1 adipocytes. This expression was however not influenced by RRV or LPS (Figure 92).

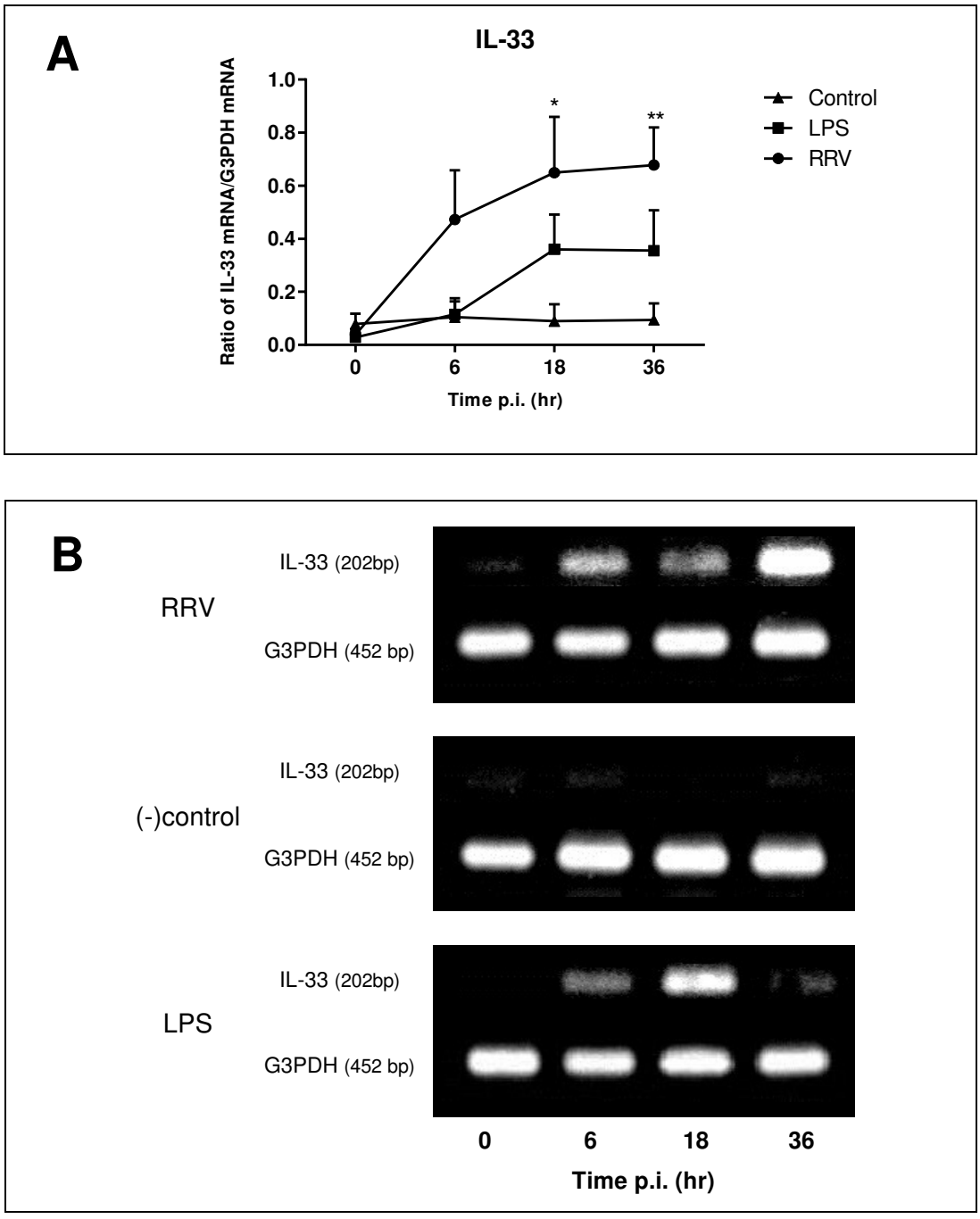

Figure 90: IL-33 mRNA expression in 3T3-L1 adipocytes after exposure to RRV or LPS

3T3-L1 adipocytes were exposed to RRV T48 (MOI of 4) or LPS (1 µg/mL) and RNA extracted at various times. Expression of IL-33 and G3PDH mRNA was determined by densiometric analysis and the ratio of IL-33 over G3PDH mRNA was graphed in (A). Data shown are mean values ± SEM (n=3 for RRV, LPS and control, n=4 for G3PDH). *($p \leq 0.05$), **($p \leq 0.01$) as determined by two-way ANOVA. (B) shows representative photographs of agarose gels. Contrast for IL-33 gel photographs was adjusted differently to G3PDH gels, therefore ratio is given in arbitrary values.

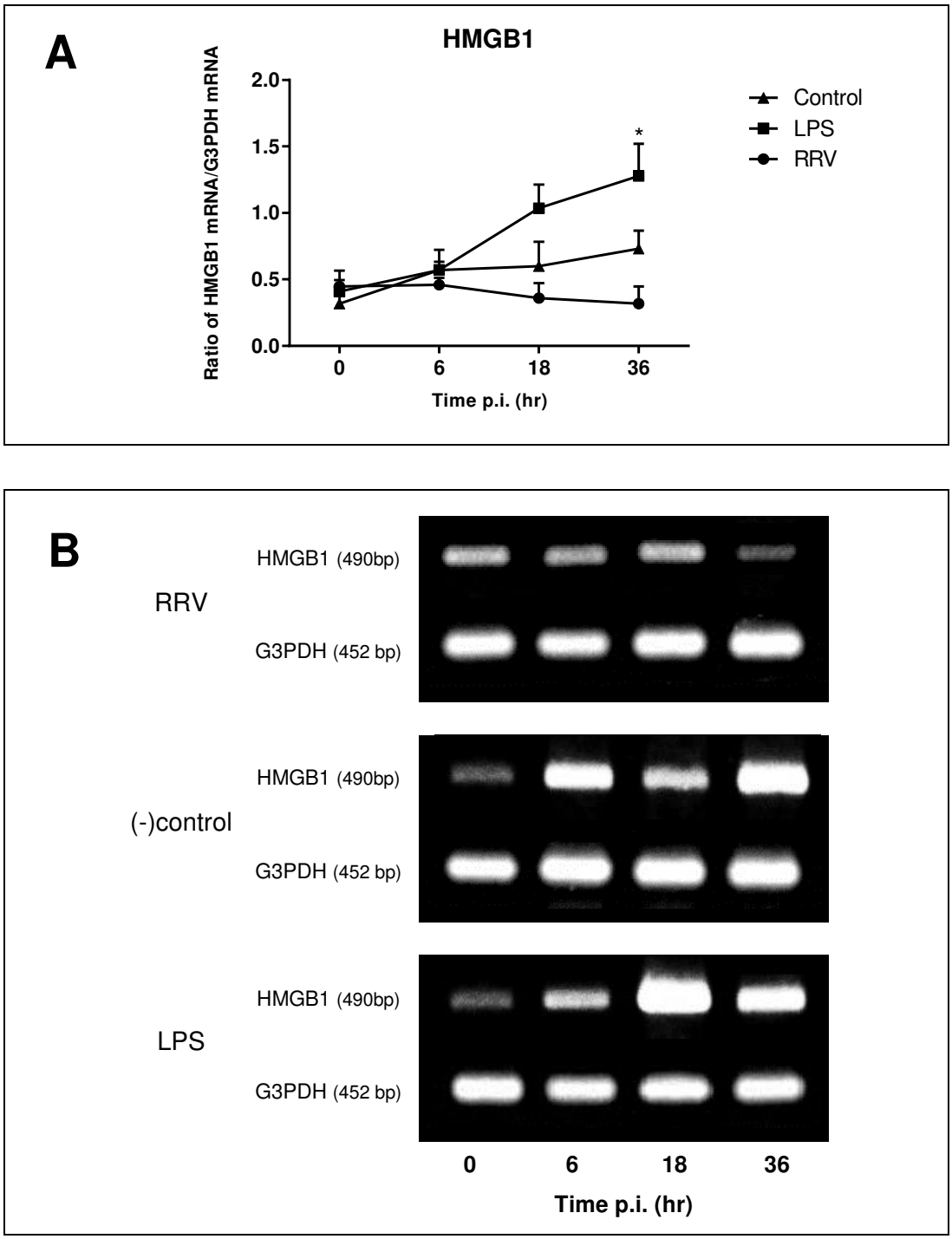

Figure 91: HMGB1 mRNA expression in 3T3-L1 adipocytes after exposure to RRV or LPS

3T3-L1 adipocytes were exposed to RRV T48 an MOI of 4 or LPS (1 µg/mL) and mRNA was extracted at various times. The mRNA expression of HMGB1 and G3PDH were determined by densiometric analysis and the ratio of HMGB1 mRNA over G3PDH mRNA was graphed in (A). Data is shown in mean values ± SEM (n=3 for RRV, LPS and control, n=4 for G3PDH). *($p \leq 0.05$) as determined by two-way ANOVA. (B) shows representative photographs of agarose gels.

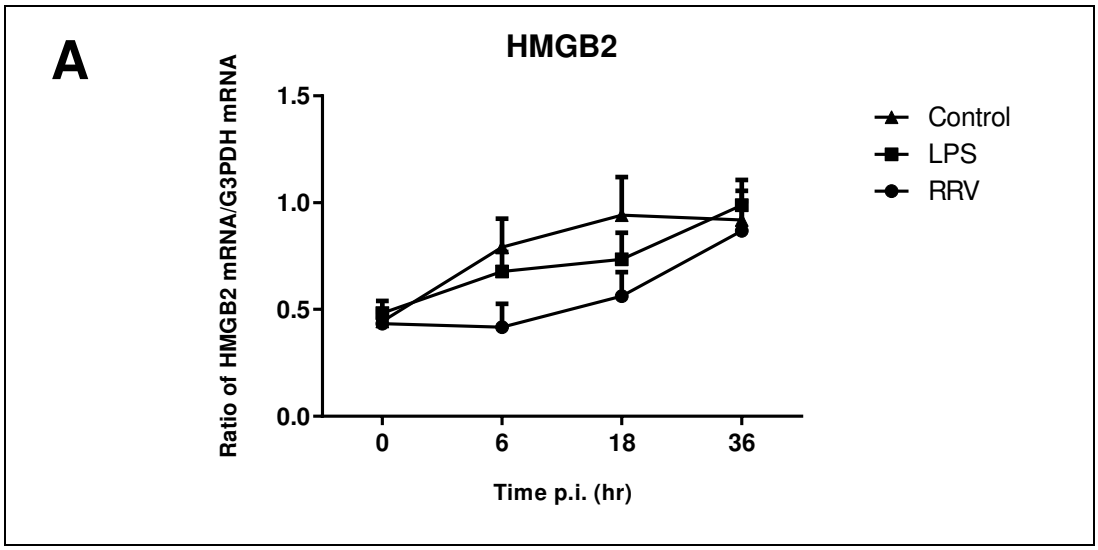

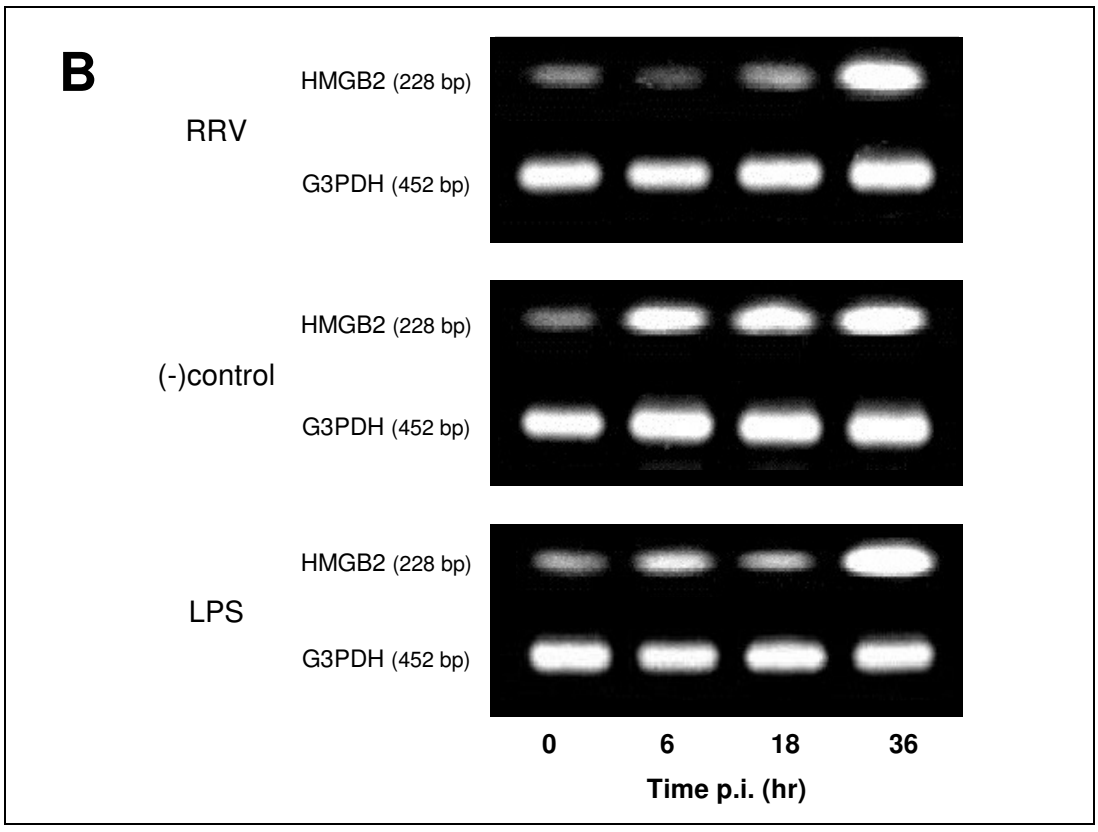

Figure 92: HMGB2 mRNA expression in 3T3-L1 adipocytes after exposure to RRV or LPS

3T3-L1 adipocytes were exposed to RRV T48 an MOI of 4 or LPS (1 µg/mL) and mRNA was extracted at various times. The mRNA expression of HMGB2 and G3PDH was determined by densiometric analysis and the ratio of HMGB2 mRNA over G3PDH mRNA is graphed in (A). Data shown are mean values ± SEM (n=3 for all samples). (B) shows representative photographs of agarose gels.

6.3.9 RRV reduces transcription of HMGB3 mRNA in 3T3-L1 adipocytes

Further investigations examined the influence of RRV on HMGB3 transcription in 3T3-L1 adipocytes. Previously obtained cDNA samples were tested for HMGB3 mRNA with specific primers. As graphed in Figure 93, densiometric analysis showed reduction of HMGB3 mRNA expression in a timely manner in RRV-infected cells compared to controls and reached statistical significance by 18 hr p.i. ($p \leq 0.05$). Exposure of 3T3-L1 adipocytes to LPS did not change the rate of HMGB3 mRNA expression.

6.3.10 MIF mRNA is not expressed in 3T3-L1 adipocytes and neither LPS nor RRV induce MIF gene transcription or MIF release

Increased MIF secretion from 3T3-L1 adipocytes upon TNFα challenge has been reported previously (Hirokawa et al., 1997) and more recentrly the crucial role of MIF in RRV induced arthritis was established (Herrero et al., 2011). To investigate MIF mRNA transcription in adipocytes we exposed 3T3-L1 cells to RRV or LPS and extracted mRNA at various time points post exposure. A RT-PCR with MIF specific primers was performed on samples and agarose gels were photographed as previously. In our conditions, 3T3-L1 adipocytes did not show basal MIF mRNA expression and transcription was neither induced by RRV nor by LPS (Figure 94). MIF expression in human adipocytes has been examined previously and it was reported that basal expression of MIF is not influenced by exposure to LPS (Skurk et al., 2005). An ELISA on supernatant samples confirmed that no MIF was secreted by 3T3-L1 adipocytes upon exposure to RRV (data not shown).

6.3.11 LPS and RRV induce MCP-1 gene expression in 3T3-L1 adipocytes

Inflammatory stimulation has been reported to induce MCP-1 secretion from 3T3-L1 adipocytes (Sun et al., 2009) and since MCP-1 is a regulatory cytokine in RRV infection (Mateo et al., 2000) we investigated its expression in RRV-infected adipocytes. RNA was extracted from 3T3-L1 adipocytes at various times post exposure to RRV or LPS and RT-PCR was performed with primers specific to the MCP-1 gene. Photographs of PCR amplicons were analysed and plotted as shown in Figure 95. There was no detectable expression of the MCP-1 gene in control samples. LPS-challenged 3T3-L1 adipocytes showed induced transcription of MCP-1 as early as 6 hr p.s. ($p \leq 0.05$), with transcription levels increasing in a time-dependent manner. Similarly, MCP-1 expression increased in RRV-infected 3T3-L1 and reached significant levels by 18 hr p.i. ($p \leq 0.05$).

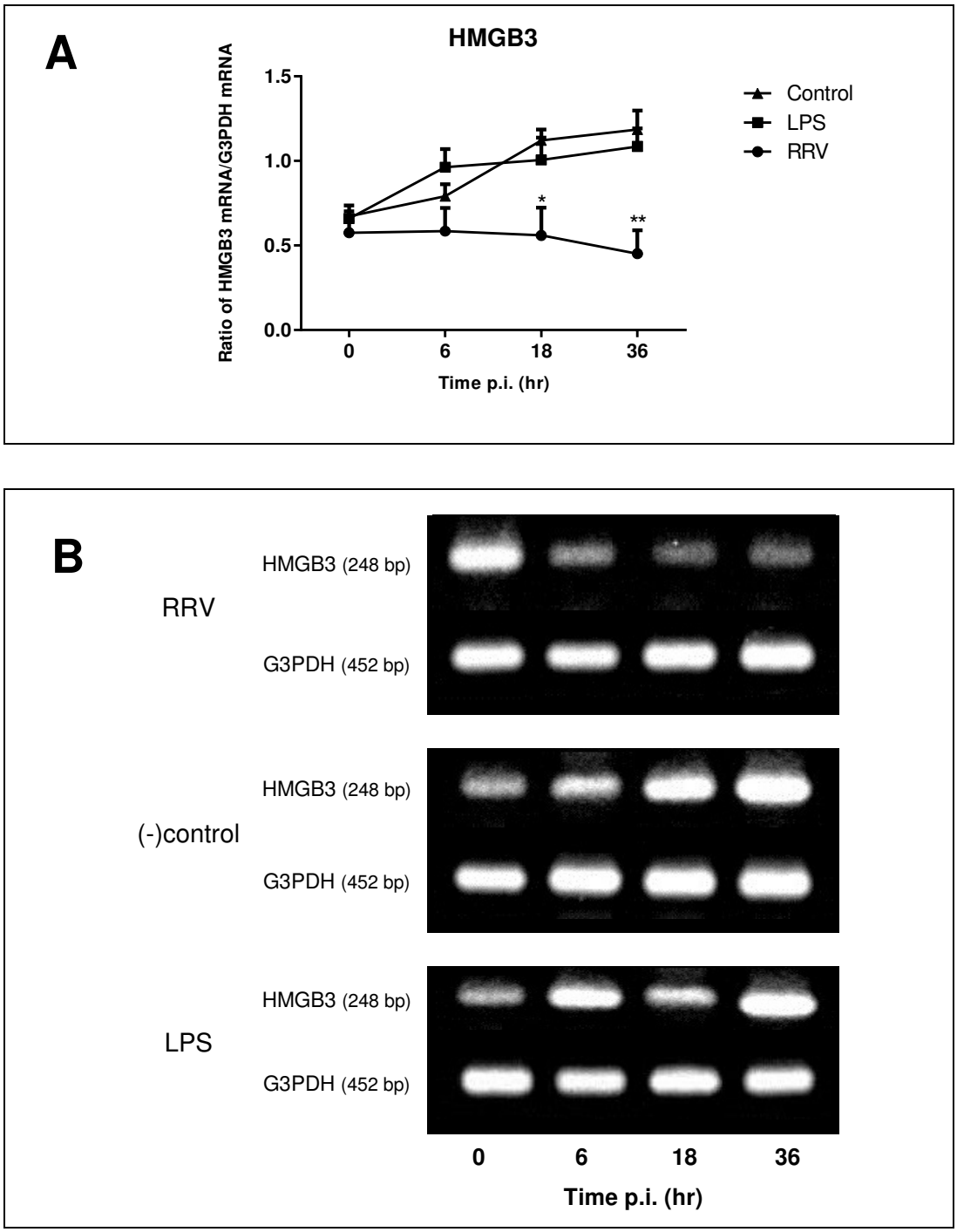

Figure 93: HMGB3 mRNA expression in 3T3-L1 adipocytes after exposure to RRV or LPS

3T3-L1 adipocytes were exposed to RRV T48 an MOI of 4 or LPS (1 µg/mL) and mRNA was extracted at various times. The mRNA expression was determined by densiometric analysis and the ratio of cytokine mRNA over G3PDH mRNA was graphed in (A). Data shown are mean values ± SEM (n=4 G3PDH, n=3 for RRV, LPS and control). (B) shows representative photographs of agarose gels. *($p \leq 0.05$), **($p \leq 0.01$) as determined by two-way ANOVA compared to control.

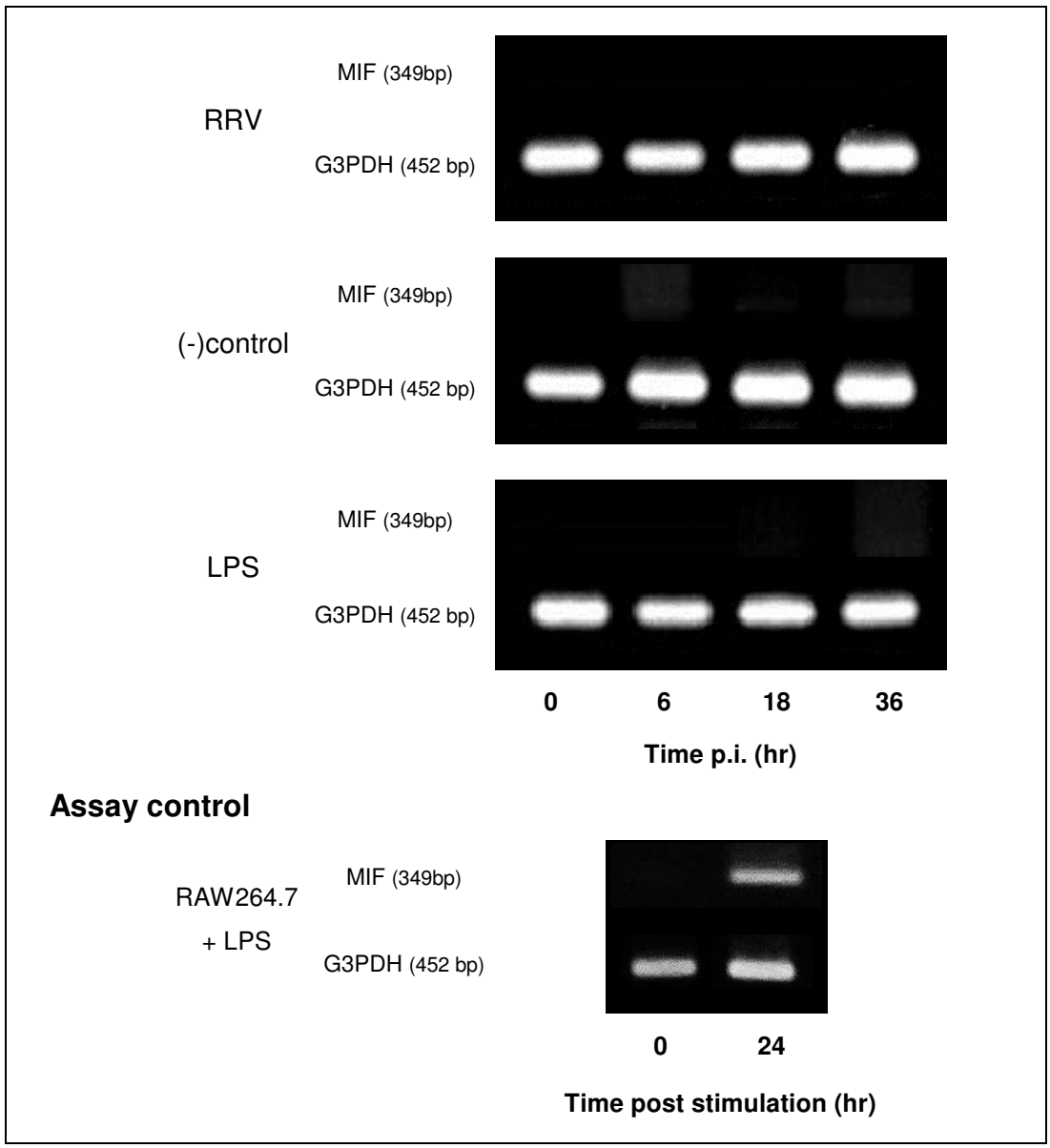

Figure 94: MIF mRNA expression in 3T3-L1 adipocytes after exposure to RRV or LPS

3T3-L1 adipocytes were exposed to RRV T48 an MOI of 4 or LPS (1 µg/mL) and mRNA was extracted at various periods of time. A RT-PCR with specific primers was performed and PCR amplicons were photographed. No MIF mRNA was detected in any sample in 3 independent experiments. MIF positive samples from RAW264.7 cells treated with LPS were included in the PCR to verify assay (RAW264.7+LPS). Shown are representative photographs of agarose gels.

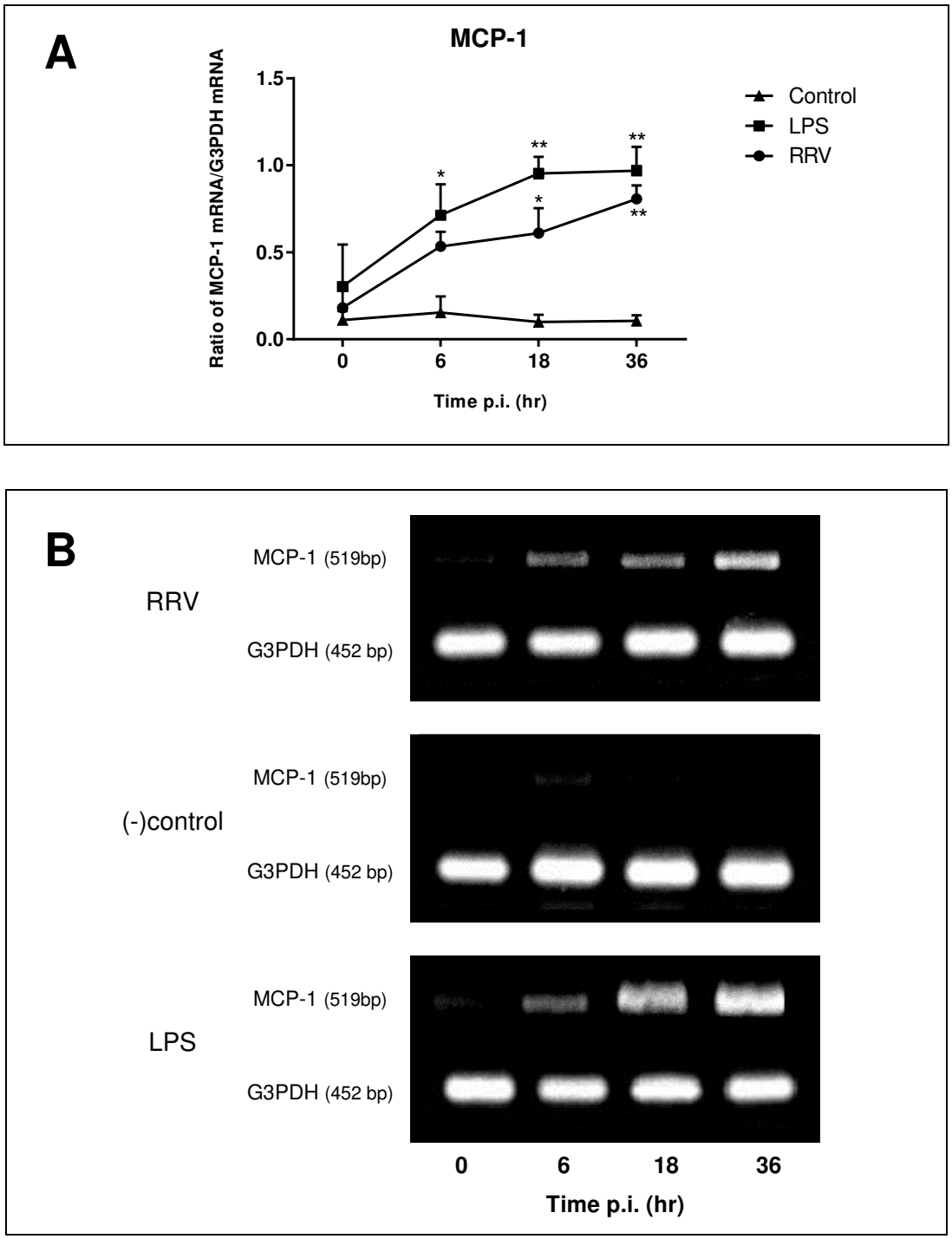

Figure 95: MCP-1 mRNA expression in RAW264.7 macrophages after exposure to RRV or LPS

3T3-L1 adipocytes were exposed to RRV T48 an MOI of 4 or LPS (1 µg/mL) and mRNA was extracted at various times. The mRNA expression of MCP-1 and G3PDH were determined by densiometric analysis and graphed as the ratio of cytokine mRNA over G3PDH mRNA (A). Data shown are mean values ± SEM (n=4 for RRV and G3PDH, n=3 for LPS and control). (B) shows representative photographs of agarose gels.

6.4 Discussion of 3T3-L1 results

As mentioned in the literature review, only Murphy et al. (Murphy et al., 1973) have previously described the cytolytic replication cycle of RRV in adipose tissue of infected mice. Apart from these early findings, no further information is available on the effect of RRV or CHIKV on adipocytes. With our experiments we have shown that RRV successfully infects 3T3-L1 adipocytes in a non-cytolytic way *in vitro*, similar to the non-destructive infection previously reported for RRV in human synovial cells (Journeaux et al., 1987). These observations seem to stand in contrast to previous reports of severe necrosis and cytolysis found in adipose tissue of RRV-infected mice (Murphy et al., 1973). The differences in the pathological mechanisms of infection and replication however may be caused by various other host factors that initiate the cytolytic processes *in vivo*. Previous studies on RRV infected muscle cells have similarly given conflicting reports for *in vivo* and *in vitro* experiments and it is now recognised that involvement of the complement and infiltrating macrophages contribute to the pathological processes in the host response (Lidbury et al., 2000; Morrison et al., 2007).

Our experiments showed that viral mRNA was expressed for more than 6 d p.i. without any noticeable cytopathic effect or visible morphological changes. This indicates a persistent asymptomatic infection of RRV in adipocytes, comparable to the persistent infection found in macrophages (Linn et al., 1996). Whether the infection persists over longer periods of time in adipose tissue (e.g. weeks or months) is still to be determined. Considering the prolonged duration of RRVD with serum viral titres dropping below detection levels these results could indicate a possible role of adipocytes as reservoir cells that harbour the virus.

The potential of adipocytes to release pro-inflammatory cytokines has been reported extensively and adipose tissue is considered to be an important contributor to inflammatory processes (Berg & Scherer, 2005). Our experiments could show that RRV induces various inflammatory and immune mediators in 3T3-L1 adipocytes upon infection. An increase in transcription or secretion of the pro-inflammatory cytokines IL-6, IL-33 and MCP-1 was observed. Especially the latter has been shown to facilitate the recruitment of monocytes and macrophages into the tissue and could possibly be a contributing mediator to macrophage infiltration in RRV infection as hypothesized earlier (Mateo et al., 2000). IL-18 was not induced in 3T3-L1 adipocytes after exposure to RRV T48, despite previous reports of its important role in alphavirus infection (Chirathaworn et al., 2010). Basal expression of IL-18

mRNA was detected in all samples but there was no significant difference between RRV samples and mock infected samples. Adipocytes may therefore not be the primary sources for systemic IL-18 in alphavirus infections.

Continuous low level expression of MIF has previously been reported in adipocytes (Hirokawa et al., 1997) and a more recent study showed the crucial role of MIF in alphavirus infections (Herrero et al., 2011). Despite these findings we could not detect any basal or induced transcription of MIF mRNA in 3T3-L1 adipocytes or secretion of MIF into the supernatant. It is possible, although unlikely, that basal expression of MIF mRNA was below our detection level for conventional PCR. It appears that adipose tissue does not release MIF upon RRV infection.

Neither RRV nor LPS induced transcription or secretion of TNFα in 3T3-L1 adipocytes. Previous reports indicated that LPS-challenge alone does not stimulate release of TNFα from adipocytes and our experiments confirmed this. It must be noted at this point that no suitable positive stimulator was available at the time of our adipocyte experiments and LPS was only trialled as it has previously been shown to induce the transcription and release of various cytokines in an array of cells and cell types. Future experiments need to include a suitable positive control. Similarly the induction of NO-release was not confirmed by positive control stimulation. Neither RRV nor LPS induced significant release of nitric oxide from 3T3-L1 adipocytes, despite increased transcription of iNOS as detected by RT-PCR. As summarised in the literature review, iNOS is an enzyme with a high throughput catalysing production of NO and considering the early onset of iNOS induction, an increase of nitrite in the supernatant was expected. A similar pattern of early increase in iNOS transcription but delayed release of nitric oxide into the supernatant was observed for RAW264.7 macrophages. It remains to be investigated if iNOS itself is fully synthesized after transcription and whether nitric oxide is produced and released at a later stage.

Basal expression of HMGB1 and HMGB2 were detected as expected but did not change upon LPS or RRV stimulation whereas HMGB3 mRNA transcription appeared down-regulated in RRV infected adipocytes. The release of HMGB proteins as potential extracellular cytokines in RRV infection was investigated, however it seems that adipocytes do not show increased synthesis of these mediators.

It is noteworthy that conventional RT-PCR blots were used for semi-quantitative densiometric measurement of mRNA transcription. Each sample was calculated

against its corresponding G3PDH blot to normalise the value. The data derived should however only be used to visualize an increase or decrease of transcription. It is strictly semi-quantitative and would require quantitative real-time PCR for confirmation. In order to save time and cost we decided not to proceed with real-time analysis as the initial focus was on identifying genes that are influenced during RRV infection. Further experiments with possible inhibitors should include quantitative real time PCR analysis.

Future investigations for RRV infection in adipocytes should focus on following questions:

- Can persistent infection be confirmed with detection of viral mRNA in 3T3-L1 adipocytes even after longer periods of times (e.g. weeks or months)?
- Do 3T3-L1 adipocytes show CPE after longer periods of time or with higher MOIs?
- Can Western blots or similar assays detect the transcription of viral proteins in 3T3-L1 adipocytes post exposure to RRV?
- Do adipose tissue samples from RRV mouse models show signs of infection? Can the virus be reactivated from adipose tissue or adipocyte cell lines if persistent infection was confirmed?
- Why is iNOS transcription induced within hours after infection with RRV without increasing nitrite levels in the supernatant? Is nitric oxide released from 3T3-L1 adipocytes at a delayed stage? Is iNOS synthesized after transcription of iNOS mRNA?
- Can these results be repeated with primary adipocytes?
- Do different viral strains have the same effect on 3T3-L1 adipocytes?

7. General discussion

RRV is the most common arbovirus in Australia with up to 5000 infections recorded annually. While this number may seem to be small in comparison to the country's population, the impact on people's health as well as the economy is substantial. In addition, case numbers appeared to have increased in the last few years and a recent report by the Queensland Health Department (Queensland Health, 2015) confirms this trend. By March 2015, Queensland alone recorded more than 3000 cases which is 8.1 times the five year mean.

Furthermore, alphaviruses such as RRV or CHIKV present a considerable risk for larger outbreaks in the future. A variation in the gene sequence of the viral nsP1 and pE2 has been reported to be the cause of the difference in virulence between RRV DC5692 and RRV T48 (Jupille et al., 2011). In accordance with these findings our preliminary experiments confirmed a significantly reduced cytokine response from RRV DC5692-infected macrophages as compared to infection with RRV T48. RRV DC7294 showed similar virulence to the T48 strain and it can be assumed that there is no or very little difference in the gene sequence coding the nsP1 and pE2. Small mutations in these regions however could turn a previously avirulent or asymptomatic strain into a virulent strain causing severe symptoms in infection. Thus the number of affected patients would increase drastically as current non-symptomatic infections are generally not noticed and recorded.

Mutations in the genome of an alphavirus have previously also facilitated vector-specific adaption. A change in the sequence of the viral E1 gene of CHIKV resulted in increased infectivity to the vectors *Aedes albopictus* and *Aedes aegypti* and thereby contributed to the rapid global spread of CHIKV (Tsetsarkin et al., 2007), with outbreaks affecting up to 1.5 million people, such as the 2006 outbreak in India. It can be assumed that similar mutations in the genome of RRV may potentially cause vector adaption to a wider spectrum of mosquito species or more efficient transmission, as reported for CHIKV (de Lamballerie et al., 2008), which would undoubtedly increase the risk of large outbreaks in Australia. A recent review (Claflin & Webb, 2015) has highlighted the increasing range of suitable RRV vectors within Australia, which now includes several brackish and fresh water mosquitoes.

Lastly, with increasing global travel the risk of introducing CHIKV to Australia is growing. Between 2002 and 2012, 168 cases of CHIKVD have been reported in

travellers returning from affected areas (Viennet et al., 2013) and with suitable mosquito vectors such as *Aedes alpopictus* present throughout the country, it appears inevitable that CHIKV will be introduced and established in Australia. In this case, the impact on health and economy would be considerably larger as disease symptoms are generally more severe and longer lasting. Similar circumstances have previously led to a small CHIKV outbreak in Italy in 2007 (Rezza et al., 2007). The virus was introduced by a visiting traveller from India and had quickly spread in a small region through established mosquito vectors.

In light of these possible threats and a lack of antiviral therapy it is necessary to investigate alternative treatment options for the management of alphavirus infections, such as RRVD or CHIKVD. Current treatment options only target symptomatic relief with NSAID and analgesic drugs but often lead to severe adverse effects when used long term (Suhrbier et al., 2012). It is therefore important to further investigate the pathological processes during alphavirus infections and to find more effective and economic treatment options. This study aimed to investigate the pathogenesis in alphavirus infection and identify targets for pharmacotherapeutic intervention. It has previously been suggested that findings in RRV research may contribute to the understanding of CHIKV disease (Srivastava et al., 2008) and we have therefore decided to use RRV in our experiments, as it poses a lower safety hazard compared to CHIKV. The results obtained in this study are however possibly applicable to other alphavirus infections, such as CHIKV or BFV.

After the initial replication and distribution within the host, alphaviruses are known to infect a variety of cells and tissues triggering pathological and inflammatory processes. Most research has focused on the infection of macrophages and their role in the pathogenesis of RRV arthritis is undisputed (Atkins, 2013). Macrophages have been shown to migrate into the synovial lining and secrete various cytokines during RRV infection which contribute to the local joint inflammation (Lidbury et al., 2008). To understand the regulatory processes, we investigated which cytokines are altered during infection.

In accordance with other reports we could detect an increase in TNFα (Lidbury et al., 2008) and MIF (Herrero et al., 2011) secretion in RRV infected macrophages. Our experiments showed induction of iNOS expression, however without increasing supernatant NO levels. RRV has been reported to inhibit the iNOS/NO pathway previously (Lidbury & Mahalingam, 2000b) but more research is needed to highlight the regulatory processes. In accordance to these findings we could however confirm

reduced NO secretion from LPS-challenged macrophages after 48 hr pre-exposure to RRV. Similar results were reported previously in infections with the Venezuelan equine encephalitis virus, which further suggests the interference of alphaviruses with the NO pathway (Schoneboom et al., 2000).

The role of IL-6 in CHIKVD has been highlighted before and a correlation between IL-6 plasma levels and the severity of arthritic symptoms had been reported (Ng et al., 2009). It appears however that the role of IL-6 in RRV infection has not been fully investigated yet and we could show increased IL-6 secretion from macrophages during infection. Similarly, the role of IL-18 has been recognised in CHIKV (Chirathaworn et al., 2010) and we were able to also show increased IL-18 mRNA transcription in RRV-infected macrophages respectively. To our knowledge this study has for the first time shown that transcription of IL-33 mRNA is increased in RRV infected macrophages, indicating a contributing role in the pathogenesis. Further we were able to show that PGE_2 secretion is not altered in RRV infection. HMGB-1 levels in the supernatant were increased, however more research is necessary to investigate its role in RRV infection, including more long term infection assays to assess whether HMGB1 acts as a possible late mediator in the host's response to the virus. Lastly, in accordance to previous reports (Mahalingam & Lidbury, 2002) we could show an increased secretion of IL-10 from RRV-infected macrophages.

With this more detailed knowledge of cytokine expression and secretion from RRV-infected macrophages we were able to test several compounds for their ability to alter cytokine expression and thereby possibly reduce inflammatory responses. Apart from non-specific macrophage depletion (Lidbury et al., 2008) or anti-TNFα therapy (Zaid et al., 2011) only few other cytokine inhibitors have been trialled previously in RRV infection, such as the MCP-1 inhibitor Bindarit (Rulli et al., 2009) and more recently the glycosaminoglycan-like molecule Pentosan Polysulfate (Herrero et al., 2015).

As outlined in section 4.4, we tested the macrolide antibiotics erythromycin, clarithromycin and roxithromycin as well as ethyl pyruvate, pentoxifylline and resveratrol for their ability to reduce pro-inflammatory cytokine expression in RRV-infected macrophages. Especially ERY and EP showed promising results which warrant further investigation. ERY reduced secretion or transcription of TNFα, MIF, IL-6 and IL-18, but did not alter the IL-10 response from RRV-infected macrophages. Inhibition of IL-10 secretion has been suggested to reduce disease

symptoms as it inhibits excessive host responses to clear the virus (Rulli et al., 2005). It is however not known whether the anti-inflammatory effect of IL-10 would outbalance these properties and reduce symptom manifestation during infection. Our results suggest a possible role for ERY in the treatment of RRV or other alphavirus infections. The highest concentration used in the experiments was similar to peak plasma levels in humans treated with a standard antibiotic therapy of 4 times 500 mg ERY per day (Krasniqi et al., 2012). The safety of ERY has been established at this dose and a small clinical trial could assess whether ERY reduces the inflammatory symptoms during acute RRV infection. In addition, the results from chapter 4.4 indicate a possible role of EP in the treatment of inflammatory symptoms during RRV-infection. Treatment with EP reduced the release of TNFα, IL-6 and MIF and inhibited transcription of IL-18 mRNA in infected macrophages. A dose-independent inhibitory effect of EP on IL-6 production has been reported previously and our results indicated a similar effect on TNFα during RRV infection (Nativel et al., 2013). Further investigations are needed to identify the molecular mechanisms of inhibition.

It should be noted that the results from the inhibitor experiments were derived from *in vitro* conditions only. It remains to be investigated if the inhibitory effect on various cytokines does occur *in vivo*. It has previously been shown that, apart from macrophages, many other factors are involved in the progression of RRVD. The activation of complement during the host immune response is undoubtedly a major contributor to the disease pathology (Morrison et al., 2008) and recent research in a RRV mouse model has revealed an important role of T-cells in the control of RRV infection in muscle tissue (K. S. Burrack et al., 2015).

The inhibitors in these experiments have been tested on RRV-infected macrophages and their pharmacological effect on other cells during infection is largely unknown. We have suggested the involvement of muscle cells in the pathogenesis of RRV and several experiments of this study focused on muscle cells as possible target for pharmacotherapy intervention in RRV.

After an incubation period of approximately 3-11 days patients generally start to develop symptoms of RRV infection in an initial acute phase with flu like symptoms, fever and severe myalgia, mostly lasting for around 4-10 days (Assuncao-Miranda et al., 2013). This time frame coincides with a spike in viral titres found in the plasma of infected patients (Suhrbier et al., 2012), indicating that rapid viral propagation occurs during the acute phase. It has so far however not been investigated whether this

virus propagation involves specific cell types. We believe that RRV undergoes a cytolytic replication cycle in muscle cells, which may explain the exponential increase in viral numbers as well as the severe myalgia during the acute phase of infection. Necrosis of the muscle has been reported previously in RRV infections, however infiltrating macrophages or activation of complement has been suggested as the causative factor (Lidbury et al., 2008; Morrison et al., 2008). Our experiments show a rapid cytolytic replictation of RRV in muscle myoblast cells, which may contribute to the intial phase myopathies concurrent with peak virus titres.

To further investigate the role of muscle cells in RRV infection we focused on a possible involvement of myokines, such as IL-6. Our experiments showed that several cytokines are released by C2C12 muscle cells during RRV infection, including TNFα, MIF and IL-6 and in addition, the transcription of the pro-inflammatory cytokines IL-18 and IL-33 was induced. Considering the early onset of cytokine release it can be assumed that these mediators are actively secreted rather than passively released from necrotic or apoptotic cells. We believe that these cytokines contribute to the local inflammation and possibly initiate the excessive infiltration of macrophages into the muscle tissue.

This may offer an interesting therapeutic target and we therefore tested the inhibitors from previous macrophage experiments on C2C12 cells, focussing on the myokine IL-6. The role of muscle derived IL-6 in inflammatory conditions has been reviewed previously and the IL-6 signalling pathway has been suggested as a possible therapeutic target in anti-inflammatory treatment (M. A. Febbraio et al., 2010).

Of the tested compounds only ERY showed an inhibitory effect on IL-6 secretion during RRV infection. This effect was however not statistically significant and further investigations are necessary to evaluate a possible therapeutic role of ERY. Our experiments showed increasing cytolysis of muscle cells within 24 hr of infection *in vitro* and therefore cytokine levels were only analysed for up to 24 hr p.i. The inhibitory effect of ERY might however reach significance at a later stage during infection, which possibly progresses slower in muscle tissue *in vitro* due to antiviral host response mechanisms. Our data further supports a possible role of ERY in the treatment of RRV infection and warrants the use of ERY in a mouse model of RRVD.

In a separate set of experiments the anti-inflammatory effect of kino extract (Martha Y Mungkaje, personal communication) was investigated on RRV-infected C2C12

myoblasts. Concurrent exposure of C2C12 and Vero cells to KE and RRV showed a reduction of cytolysis and virus titres in the supernatant. Pre-treatment of both C2C12 and Vero cells appeared to completely inhibit viral replication, with virus titres falling below detectable levels by 3 d post-infection. RRV requires certain cell surface proteins, such as integrins, for successful binding and possibly to facilitate virus entry. It is possible that the tannins found in kinos precipitate surface structures including these proteins and therefore inhibit binding of the virus to the cell surface. Unbound RRV would then slowly degrades into an inactivated form over time, possibly involving oxidative processes. High concentrations of KE showed cytotoxicity on C2C12 myoblasts but at concentrations of 0.125 mg/mL and below it appeared that the astringent effect was sufficient to inhibit virus entry without affecting cell viability. As previously described, long term experiments are necessary to assess prolonged viability of C2C12. Prolonged exposure to 0.125 mg/mL KE initiated the formation of vacuoles in the cytoplasm of both Vero cells as well as C2C12 cells. It has previously been shown that similar vacuolisation can indicate apoptotic processes in muscle cells (Sakamoto & Kimura, 2013), however it remains to be investigated whether this is also true for KE treated cells. As mentioned previously, initial cytotoxicity assays showed no reduced viability at the given concentrations within 3 days.

The final part of this study briefly investigated a possible involvement of adipocytes in RRVD. Early investigations (Murphy et al., 1973) reported of necrotic lesions in the fat tissue of RRV-infected mice, but to our knowledge no further study considered a possible involvement of adipose tissue or adipocytes in the pathogenesis of RRVD. Our experiments indicate that RRV can infect differentiated 3T3-L1 adipocytes *in vitro* inducing a non-cytolytic replication, with viral RNA detectable for more than 6 days post-infection in the adipocytes. No morphological changes or cytolytic foci were visible, in contrast to the observed necrosis in the adipose tissue of mice within days of infection with RRV (Murphy et al., 1973). It appears that host-mediated immune responses contribute to the severe destruction of adipose tissue *in vivo*, similar to how it was suggested for muscle tissue previoulsy (Rulli et al., 2005). Infiltrating immune cells such as macrophages might further exacerbate the immune reaction and possibly initiate the necrotic tissue destruction. Due to the non-cytolytic infection, adipocytes may act as reservoir cells for RRV *in vivo* and therefore possibly contribute to the prolonged infection. A recent study (Couturier et al., 2015) has reported of similar mechanisms with adipose tissue being able to harbour the HIV-1 virus and therefore act as a reservoir. Long

term studies are necessary to clarify whether cytolysis occurs at a later stage during infection or whether virus replication subsides without lysis of the cell.

In addition, it has previously been reported that numerous viruses such as cytomegalovirus and respiratory syncitial virus can infect human adipocytes and induce secretion of pro-inflammatory cytokines such as IL-6 (Bouwman et al., 2008). In line with these reports we could show that RRV initiated the transcription and expression of numerous cytokines in 3T3-L1 adipocytes *in vitro*. Both transcription of IL-6 mRNA as well as secretion of IL-6 into the supernatant were significantly induced in RRV infection. Similarly, the expression of IL-33 mRNA was induced in adipocytes exposed to RRV or LPS. Contrary to the cytokine response from infected macrophages we could not detect increased transcription of IL-18, MIF, HMGB1 or HMGB2 mRNA, it appeared however that expression of HMGB3 mRNA was down-regulated in RRV-infected adipocytes. MCP-1 has previously been recognised as a regulatory cytokine in RRV infection (Mateo et al., 2000) and we could show for the first time that adipocytes also exhibited increased transcription of MCP-1 mRNA when challenged with LPS or RRV. TNFα secretion and transcription was neither induced by RRV- nor by LPS-stimulation. Due to limited availability of other inflammatory stimulants LPS was trialled as a possible inducer of TNFα but failed to initiate secretion or transcription. This set of experiments was therefore lacking a positive control. Each assay did however include an internal control with TNFα-positive samples from experiments with other cell lines in order to validate the assay procedure. Similarly, nitrite was below the detectable level in RRV-treated samples, despite increased transcription of iNOS mRNA. These findings are consistent with previous experiments in in RAW264.7 and C2C12 cells and further suggest that RRV interferes with NO production. More long term experiments are needed to investigate whether the NO response is delayed or otherwise inhibited.

In conclusion, this study could uncover the contribution of several macrophage-derived cytokines in the pathogenesis or RRV infections. We have shown that several compounds were able to inhibit cytokine expression from macrophages and especially ERY and EP may be suitable alternatives for the treatment of RRVD. The therapeutic potential of these compounds however needs to be further evaluated in a RRV mouse model. A recent review has concluded that numerous models of alphaviral disease adequately mimic the pathological processes observed in alphavirus infections in humans (Taylor et al., 2014) and could therefore examine the effects to these compounds beyond macrophages. The involvement of muscle cells in disease progression has been investigated and we propose an initial

replication cycle in muscle cells to be a contributory factor to the development of myalgia during RRV infection. We were able to show for the first time that RRV can infect adipocytes in what appears to be a non-cytolytic way *in vitro* and induce secretion of pro-inflammatory cytokines and chemokines. The non-cytolytic infection indicates a possible role of adipose tissue as a reservoir and further investigations are necessary to confirm these suggestions.

8. Bibliography

Aaskov, J., Doherty, R., Beran, G., & Steele, J. (1994). Arboviral zoonoses of Australasia (pp. 289-306): CRC Press Boca Raton, Florida.

Ajuwon, K. M., & Spurlock, M. E. (2005). *Adiponectin inhibits LPS-induced NF-κB activation and IL-6 production and increases PPARγ2 expression in adipocytes* (Vol. 288).

Al-Abed, Y., Dabideen, D., Aljabari, B., Valster, A., Messmer, D., Ochani, M., . . . Tracey, K. J. (2005). ISO-1 binding to the tautomerase active site of MIF inhibits its pro-inflammatory activity and increases survival in severe sepsis. *J Biol Chem, 280*(44), 36541-36544. doi:10.1074/jbc.C500243200

Alam, A., Haldar, S., Thulasiram, H. V., Kumar, R., Goyal, M., Iqbal, M. S., . . . Bandyopadhyay, U. (2012). Novel anti-inflammatory activity of epoxyazadiradione against macrophage migration inhibitory factor: inhibition of tautomerase and proinflammatory activities of macrophage migration inhibitory factor. *The Journal of biological chemistry, 287*(29), 24844-24861. doi:10.1074/jbc.M112.341321

Allonso, D., Vázquez, S., Guzmán, M. G., & Mohana-Borges, R. (2013). High Mobility Group Box 1 Protein as an Auxiliary Biomarker for Dengue Diagnosis. *The American Journal of Tropical Medicine and Hygiene, 88*(3), 506-509. doi:10.4269/ajtmh.2012.12-0619

Altavilla, D., Squadrito, F., Bitto, A., Polito, F., Burnett, B. P., Di Stefano, V., & Minutoli, L. (2009). Flavocoxid, a dual inhibitor of cyclooxygenase and 5-lipoxygenase, blunts pro-inflammatory phenotype activation in endotoxin-stimulated macrophages. *British journal of pharmacology, 157*(8), 1410-1418. doi:10.1111/j.1476-5381.2009.00322.x

Amvros'eva, T. V., Votiakov, V. I., Andreeva, O. T., Vladyko, G. V., Nikolaeva, S. N., Orlova, S. V., . . . Zgirovskaia, A. A. (1993). [New properties of trental as an inhibitor of viral activity with a wide range of activity]. *Vopr Virusol, 38*(5), 230-233.

Andersson, U., Antoine, D. J., & Tracey, K. J. (2014). The functions of HMGB1 depend on molecular localization and post-translational modifications. *Journal of Internal Medicine, 276*(5), 420-424. doi:10.1111/joim.12309

Andersson, U., & Erlandsson-Harris, H. (2004). HMGB1 is a potent trigger of arthritis. *J Intern Med, 255*(3), 344-350. doi:1303 [pii]

Andersson, U., Erlandsson-Harris, H., Yang, H., & Tracey, K. J. (2002). HMGB1 as a DNA-binding cytokine. *J Leukoc Biol, 72*(6), 1084-1091.

Arend, W. P., Palmer, G., & Gabay, C. (2008). IL-1, IL-18, and IL-33 families of cytokines. *Immunological Reviews, 223*(1), 20-38. doi:10.1111/j.1600-065X.2008.00624.x

Assinger, A., Kral, J. B., Yaiw, K. C., Schrottmaier, W. C., Kurzejamska, E., Wang, Y., . . . Söderberg-Naucler, C. (2014). Human Cytomegalovirus–Platelet Interaction Triggers Toll-Like Receptor 2–Dependent Proinflammatory and Proangiogenic Responses. *Arteriosclerosis, Thrombosis, and Vascular Biology, 34*(4), 801-809. doi:10.1161/atvbaha.114.303287

Assuncao-Miranda, I., Bozza, M. T., & Da Poian, A. T. (2010). Pro-inflammatory response resulting from sindbis virus infection of human macrophages: implications for the pathogenesis of viral arthritis. *J Med Virol, 82*(1), 164-174. doi:10.1002/jmv.21649

Assuncao-Miranda, I., Cruz-Oliveira, C., & Da Poian, A. T. (2013). Molecular mechanisms involved in the pathogenesis of alphavirus-induced arthritis. *Biomed Res Int, 2013*, 973516. doi:10.1155/2013/973516

Atkins, G. J. (2013). The Pathogenesis of Alphaviruses. *ISRN Virology, 2013*, 22. doi:10.5402/2013/861912

Bailly, S., Pocidalo, J. J., Fay, M., & Gougerot-Pocidalo, M. A. (1991). Differential modulation of cytokine production by macrolides: interleukin-6 production is increased by spiramycin and erythromycin. *Antimicrobial Agents and Chemotherapy, 35*(10), 2016-2019.

Bandyopadhyay, B., Bandyopadhyay, D., Bhattacharya, R., De, R., Saha, B., Mukherjee, H., & Hati, A. K. (2009). Death due to chikungunya. *Trop Doct, 39*(3), 187-188. doi:10.1258/td.2008.080382

Baur, J. A., & Sinclair, D. A. (2006). Therapeutic potential of resveratrol: the in vivo evidence. *Nat Rev Drug Discov, 5*(6), 493-506. doi:http://www.nature.com/nrd/journal/v5/n6/suppinfo/nrd2060_S1.html

Benigni, F., Atsumi, T., Calandra, T., Metz, C., Echtenacher, B., Peng, T., & Bucala, R. (2000). The proinflammatory mediator macrophage migration inhibitory factor induces glucose catabolism in muscle. *The Journal of Clinical Investigation, 106*(10), 1291-1300. doi:10.1172/JCI9900

Berg, A. H., & Scherer, P. E. (2005). Adipose tissue, inflammation, and cardiovascular disease. *Circ Res, 96*(9), 939-949. doi:10.1161/01.RES.0000163635.62927.34

Beutler, B. A., Milsark, I. W., & Cerami, A. (1985). Cachectin/tumor necrosis factor: production, distribution, and metabolic fate in vivo. *The Journal of Immunology, 135*(6), 3972-3977.

Bi, X. L., Yang, J. Y., Dong, Y. X., Wang, J. M., Cui, Y. H., Ikeshima, T., . . . Wu, C. F. (2005). Resveratrol inhibits nitric oxide and TNF-alpha production by lipopolysaccharide-activated microglia. *International immunopharmacology, 5*(1), 185-193. doi:10.1016/j.intimp.2004.08.008

Biron, C. A. (1998). Role of early cytokines, including alpha and beta interferons (IFN-alpha/beta), in innate and adaptive immune responses to viral infections. *Semin Immunol, 10*(5), 383-390. doi:10.1006/smim.1998.0138

Bogdan, C. (2015). Nitric oxide synthase in innate and adaptive immunity: an update. *Trends in Immunology, 36*(3), 161-178. doi:http://dx.doi.org/10.1016/j.it.2015.01.003

Bonilauri, P., Bellini, R., Calzolari, M., Angelini, R., Venturi, L., Fallacara, F., . . . Dottori, M. (2008). Chikungunya virus in Aedes albopictus, Italy. *Emerg Infect Dis, 14*(5), 852-854.

Borde, C., Barnay-Verdier, S., Gaillard, C., Hocini, H., Maréchal, V., & Gozlan, J. (2011). Stepwise Release of Biologically Active HMGB1 during HSV-2 Infection. *PLoS ONE, 6*(1), e16145. doi:10.1371/journal.pone.0016145

Bouwman, J. J. M., Visseren, F. L. J., Bouter, K. P., & Diepersloot, R. J. A. (2008). Infection-induced inflammatory response of adipocytes in vitro. *Int J Obes, 32*(6), 892-901.

Boyd, A. M., & Kay, B. H. (2000). Vector competence of Aedes aegypti, Culex sitiens, Culex annulirostris, and Culex quinquefasciatus (Diptera: Culicidae) for Barmah Forest virus. *J Med Entomol, 37*(5), 660-663.

Brennan, F. M., & McInnes, I. B. (2008). Evidence that cytokines play a role in rheumatoid arthritis. *J Clin Invest, 118*(11), 3537-3545. doi:10.1172/JCI36389

Bucala, R. (2012). MIF, MIF Alleles, and the Regulation of the Host Response. *The MIF Handbook*, 1.

Burmester, G. R., Stuhlmuller, B., Keyszer, G., & Kinne, R. W. (1997). Mononuclear phagocytes and rheumatoid synovitis. Mastermind or workhorse in arthritis? *Arthritis Rheum, 40*(1), 5-18.

Burrack, K., Her, Z., Gill, R., Ng, L., & Morrison, T. (2014). Myeloid cell Arg1 and iNOS inhibit control of arthritogenic alphavirus infection by suppressing anti-

viral T cells (VIR1P.965). *The Journal of Immunology, 192*(1 Supplement), 74.77.

Burrack, K. S., Montgomery, S. A., Homann, D., & Morrison, T. E. (2015). CD8+ T Cells Control Ross River Virus Infection in Musculoskeletal Tissues of Infected Mice. *The Journal of Immunology, 194*(2), 678-689. doi:10.4049/jimmunol.1401833

Caglioti, C., Lalle, E., Castilletti, C., Carletti, F., Capobianchi, M. R., & Bordi, L. (2013). Chikungunya virus infection: an overview. *New Microbiol, 36*(3), 211-227.

Campagna, M., & Rivas, C. (2010). Antiviral activity of resveratrol. *Biochem Soc Trans, 38*(Pt 1), 50-53. doi:10.1042/bst0380050

Capiralla, H., Vingtdeux, V., Zhao, H., Sankowski, R., Al-Abed, Y., Davies, P., & Marambaud, P. (2012). Resveratrol mitigates lipopolysaccharide- and Aβ-mediated microglial inflammation by inhibiting the TLR4/NF-κB/STAT signaling cascade. *Journal of Neurochemistry, 120*(3), 461-472. doi:10.1111/j.1471-4159.2011.07594.x

Chandler, D., Woldu, A., Rahmadi, A., Shanmugam, K., Steiner, N., Wright, E., . . . Munch, G. (2010). Effects of plant-derived polyphenols on TNF-alpha and nitric oxide production induced by advanced glycation endproducts. *Mol Nutr Food Res, 54 Suppl 2*, S141-150. doi:10.1002/mnfr.200900504

Chen, D., Nie, M., Fan, M. W., & Bian, Z. (2008). Anti-inflammatory activity of curcumin in macrophages stimulated by lipopolysaccharides from Porphyromonas gingivalis. *Pharmacology, 82*(4), 264-269. doi:10.1159/000161127

Chen, W., Foo, S.-S., Rulli, N. E., Taylor, A., Sheng, K.-C., Herrero, L. J., . . . Mahalingam, S. (2014). Arthritogenic alphaviral infection perturbs osteoblast function and triggers pathologic bone loss. *Proceedings of the National Academy of Sciences of the United States of America, 111*(16), 6040-6045. doi:10.1073/pnas.1318859111

Chirathaworn, C., Rianthavorn, P., Wuttirattanakowit, N., & Poovorawan, Y. (2010). Serum IL-18 and IL-18BP Levels in Patients with Chikungunya Virus Infection. *Viral Immunology, 23*(1), 113-117. doi:10.1089/vim.2009.0077

Cho, Y., Crichlow, G. V., Vermeire, J. J., Leng, L., Du, X., Hodsdon, M. E., . . . Lolis, E. J. (2010). Allosteric inhibition of macrophage migration inhibitory factor revealed by ibudilast. *Proc Natl Acad Sci U S A, 107*(25), 11313-11318. doi:10.1073/pnas.1002716107

Chomarat, P., Banchereau, J., Davoust, J., & Palucka, A. K. (2000). IL-6 switches the differentiation of monocytes from dendritic cells to macrophages. *Nature immunology, 1*(6), 510-514.

Chow, A., Her, Z., Ong, E. K., Chen, J. M., Dimatatac, F., Kwek, D. J., . . . Ng, L. F. (2011). Persistent arthralgia induced by Chikungunya virus infection is associated with interleukin-6 and granulocyte macrophage colony-stimulating factor. *J Infect Dis, 203*(2), 149-157. doi:10.1093/infdis/jiq042

Chuang, Y.-C., Chen, H.-R., & Yeh, T.-M. (2015). Pathogenic Roles of Macrophage Migration Inhibitory Factor during Dengue Virus Infection. *Mediators Inflamm, 2015*, 7. doi:10.1155/2015/547094

Claflin, S. B., & Webb, C. E. (2015). Ross River Virus: Many Vectors and Unusual Hosts Make for an Unpredictable Pathogen. *PLoS Pathog, 11*(9), e1005070. doi:10.1371/journal.ppat.1005070

Clarke, P. A. (2011). *Aboriginal People and their Plants*. Sydney: Sydney : Rosenberg Publishing.

Coppack, S. W. (2001). Pro-inflammatory cytokines and adipose tissue. *Proc Nutr Soc, 60*(3), 349-356. doi:S0029665101000386 [pii]

Couturier, J., Suliburk, J. W., Brown, J. M., Luke, D. J., Agarwal, N., Yu, X., . . . Lewis, D. E. (2015). Human adipose tissue as a reservoir for memory CD4+ T cells and HIV. *AIDS, 29*(6), 667-674. doi:10.1097/qad.0000000000000599

D'Hellencourt, C. L., Diaw, L., Cornillet, P., & Guenounou, M. (1996). Differential regulation of TNFα, IL-1β, IL-6, IL-8, TNFβ, and IL-10 by pentoxifylline. *International Journal of Immunopharmacology, 18*(12), 739-748. doi:http://dx.doi.org/10.1016/S0192-0561(97)85556-7

Dave, S. H., Tilstra, J. S., Matsuoka, K., Li, F., DeMarco, R. A., Beer-Stolz, D., . . . Plevy, S. E. (2009). Ethyl pyruvate decreases HMGB1 release and ameliorates murine colitis. *J Leukoc Biol, 86*(3), 633-643. doi:10.1189/jlb.1008662

de Lamballerie, X., Leroy, E., Charrel, R. N., Ttsetsarkin, K., Higgs, S., & Gould, E. A. (2008). Chikungunya virus adapts to tiger mosquito via evolutionary convergence: a sign of things to come? *Virol J, 5*, 33. doi:10.1186/1743-422X-5-33

Dinarello, C. A., Novick, D., Kim, S., & Kaplanski, G. (2013). Interleukin-18 and IL-18 Binding Protein. *Frontiers in Immunology, 4*, 289. doi:10.3389/fimmu.2013.00289

Doherty, G. M., Jensen, J. C., Alexander, H. R., Buresh, C. M., & Norton, J. A. (1991). Pentoxifylline suppression of tumor necrosis factor gene transcription. *Surgery, 110*(2), 192-198.

Doherty, R., Whitehead, R., Gorman, B., & O'gower, A. (1963). The isolation of a third group A arbovirus in Australia, with preliminary observations on its relationship to epidemic polyarthritis. *Aust J Sci, 26*, 183-184.

Eaton, B. T., & Hapel, A. J. (1976). Persistent noncytolytic togavirus infection of primary mouse muscle cells. *Virology, 72*(1), 266-271. doi:http://dx.doi.org/10.1016/0042-6822(76)90329-9

Economopoulou, A., Dominguez, M., Helynck, B., Sissoko, D., Wichmann, O., Quenel, P., . . . Quatresous, I. (2009). Atypical Chikungunya virus infections: clinical manifestations, mortality and risk factors for severe disease during the 2005-2006 outbreak on Reunion. *Epidemiol Infect, 137*(4), 534-541. doi:10.1017/S0950268808001167

Elmali, N., Baysal, O., Harma, A., Esenkaya, I., & Mizrak, B. (2007). Effects of Resveratrol in Inflammatory Arthritis. *Inflammation, 30*(1-2), 1-6. doi:10.1007/s10753-006-9012-0

Evans, T. J. (2000). Bioassay for tumor necrosis factors-alpha and -beta. *Mol Biotechnol, 15*(3), 243-248. doi:10.1385/MB:15:3:243

Faragher, S. G., Meek, A. D. J., Rice, C. M., & Dalgarno, L. (1988). Genome sequences of a mouse-avirulent and a mouse-virulent strain of ross river virus. *Virology, 163*(2), 509-526. doi:http://dx.doi.org/10.1016/0042-6822(88)90292-9

Fasshauer, M., Klein, J., Lossner, U., & Paschke, R. (2003). Interleukin (IL)-6 mRNA Expression is Stimulated by Insulin, Isoproterenol, Tumour Necrosis Factor Alpha, Growth Hormone, and IL-6 in 3T3-L1 Adipocytes. *Horm Metab Res, 35*(03), 147-152. doi:10.1055/s-2003-39075

Febbraio, M. A., & Pedersen, B. K. (2002). Muscle-derived interleukin-6: mechanisms for activation and possible biological roles. *The FASEB Journal, 16*(11), 1335-1347. doi:10.1096/fj.01-0876rev

Febbraio, M. A., Rose-John, S., & Pedersen, B. K. (2010, Apr). Is interleukin-6 receptor blockade the Holy Grail for inflammatory diseases? *Clin Pharmacol Ther.* Retrieved from http://www.ncbi.nlm.nih.gov/pubmed/20305672

Fink, M. P. (2007). Ethyl pyruvate: a novel anti-inflammatory agent. *J Intern Med, 261*(4), 349-362. doi:10.1111/j.1365-2796.2007.01789.x

Firestein, G. S. (2003). Evolving concepts of rheumatoid arthritis. *Nature, 423*(6937), 356-361.

Flaujac, C., Boukour, S., & Cramer-Borde, E. (2010). Platelets and viruses: an ambivalent relationship. *Cell Mol Life Sci, 67*(4), 545-556. doi:10.1007/s00018-009-0209-x

Franssila, R., & Hedman, K. (2006). Infection and musculoskeletal conditions: Viral causes of arthritis. *Best Pract Res Clin Rheumatol, 20*(6), 1139-1157. doi:10.1016/j.berh.2006.08.007

Fraser, C., Lousberg, E. L., Kumar, R., Hughes, T. P., Diener, K. R., & Hayball, J. D. (2009). Dasatinib inhibits the secretion of TNF-alpha following TLR stimulation in vitro and in vivo. *Exp Hematol, 37*(12), 1435-1444. doi:10.1016/j.exphem.2009.09.007

Fraser, J. R. (1986). Epidemic polyarthritis and Ross River virus disease. *Clinics in rheumatic diseases, 12*(2), 369-388.

Frost, R. A., Nystrom, G. J., & Lang, C. H. (2002). Lipopolysaccharide regulates proinflammatory cytokine expression in mouse myoblasts and skeletal muscle. *Am J Physiol Regul Integr Comp Physiol, 283*(3), R698-709. doi:10.1152/ajpregu.00039.2002

Frost, R. A., Nystrom, G. J., & Lang, C. H. (2003). Lipopolysaccharide and proinflammatory cytokines stimulate interleukin-6 expression in C2C12 myoblasts: role of the Jun NH2-terminal kinase. *Am J Physiol Regul Integr Comp Physiol, 285*(5), R1153-1164. doi:10.1152/ajpregu.00164.2003

Frost, R. A., Nystrom, G. J., & Lang, C. H. (2004). Lipopolysaccharide stimulates nitric oxide synthase-2 expression in murine skeletal muscle and C(2)C(12) myoblasts via Toll-like receptor-4 and c-Jun NH(2)-terminal kinase pathways. *Am J Physiol Cell Physiol, 287*(6), C1605-1615. doi:10.1152/ajpcell.00010.2004

Gallucci, S., Provenzano, C., Mazzarelli, P., Scuderi, F., & Bartoccioni, E. (1998). Myoblasts produce IL-6 in response to inflammatory stimuli. *Int Immunol, 10*(3), 267-273.

Garai, J., & Lorand, T. (2009). Macrophage migration inhibitory factor (MIF) tautomerase inhibitors as potential novel anti-inflammatory agents: current developments. *Curr Med Chem, 16*(9), 1091-1114.

Gardella, S., Andrei, C., Ferrera, D., Lotti, L. V., Torrisi, M. R., Bianchi, M. E., & Rubartelli, A. (2002). The nuclear protein HMGB1 is secreted by monocytes via a non-classical, vesicle-mediated secretory pathway. *EMBO reports, 3*(10), 995-1001. doi:10.1093/embo-reports/kvf198

Girard, J. P. (2007). A direct inhibitor of HMGB1 cytokine. *Chem Biol, 14*(4), 345-347. doi:10.1016/j.chembiol.2007.04.001

Gracie, J. A., Forsey, R. J., Chan, W. L., Gilmour, A., Leung, B. P., Greer, M. R., . . . McInnes, I. B. (1999). A proinflammatory role for IL-18 in rheumatoid arthritis. *J Clin Invest, 104*(10), 1393-1401. doi:10.1172/JCI7317

Gracie, J. A., Robertson, S. E., & McInnes, I. B. (2003). Interleukin-18. *J Leukoc Biol, 73*(2), 213-224.

Green, L. C., Wagner, D. A., Glogowski, J., Skipper, P. L., Wishnok, J. S., & Tannenbaum, S. R. (1982). Analysis of nitrate, nitrite, and [15N]nitrate in biological fluids. *Anal Biochem, 126*(1), 131-138. doi:0003-2697(82)90118-X [pii]

Green, S., Vaughn, D. W., Kalayanarooj, S., Nimmannitya, S., Suntayakorn, S., Nisalak, A., . . . Ennis, F. A. (1999). Elevated plasma interleukin-10 levels in acute dengue correlate with disease severity. *J Med Virol, 59*(3), 329-334.

Guidotti, L. G., & Chisari, F. V. (2001). Noncytolytic control of viral infections by the innate and adaptive immune response. *Annu Rev Immunol, 19*, 65-91. doi:10.1146/annurev.immunol.19.1.65

Haas, R. (2004). *Asynchronies in synchronous baculovirus infections.* The University of Queensland.

Han, J., Thompson, P., & Beutler, B. (1990). Dexamethasone and pentoxifylline inhibit endotoxin-induced cachectin/tumor necrosis factor synthesis at separate points in the signaling pathway. *J Exp Med, 172*(1), 391-394.

Haraguchi, T., Takasaki, K., Naito, T., Hayakawa, K., Katsurabayashi, S., Mishima, K., . . . Fujiwara, M. (2009). Cerebroprotective action of telmisartan by inhibition of macrophages/microglia expressing HMGB1 via a peroxisome proliferator-activated receptor gamma-dependent mechanism. *Neurosci Lett, 464*(3), 151-155. doi:10.1016/j.neulet.2009.08.043

Haraldsen, G., Balogh, J., Pollheimer, J., Sponheim, J., & Kuchler, A. M. (2009). Interleukin-33 - cytokine of dual function or novel alarmin? *Trends Immunol, 30*(5), 227-233. doi:10.1016/j.it.2009.03.003

Harasawa, R., Mizusawa, H., Fujii, M., Yamamoto, J., Mukai, H., Uemori, T., . . . Kato, I. (2005). Rapid detection and differentiation of the major mycoplasma contaminants in cell cultures using real-time PCR with SYBR Green I and melting curve analysis. *Microbiol Immunol, 49*(9), 859-863.

Hardy, D. J., Hensey, D. M., Beyer, J. M., Vojtko, C., McDonald, E. J., & Fernandes, P. B. (1988). Comparative in vitro activities of new 14-, 15-, and 16-membered macrolides. *Antimicrob Agents Chemother, 32*(11), 1710-1719.

Harris, H. E., Andersson, U., & Pisetsky, D. S. (2012). HMGB1: a multifunctional alarmin driving autoimmune and inflammatory disease. *Nature reviews. Rheumatology, 8*(4), 195-202. doi:10.1038/nrrheum.2011.222

Haskó, G., Szabó, C., Németh, Z. H., Kvetan, V., Pastores, S. M., & Vizi, E. S. (1996). Adenosine receptor agonists differentially regulate IL-10, TNF-alpha, and nitric oxide production in RAW 264.7 macrophages and in endotoxemic mice. *The Journal of Immunology, 157*(10), 4634-4640.

Hennigan, S., & Kavanaugh, A. (2008). Interleukin-6 inhibitors in the treatment of rheumatoid arthritis. *Therapeutics and Clinical Risk Management, 4*(4), 767-775.

Herrero, L. J., Foo, S. S., Sheng, K. C., Chen, W., Forwood, M. R., Bucala, R., & Mahalingam, S. (2015). Pentosan Polysulfate: a Novel Glycosaminoglycan-Like Molecule for Effective Treatment of Alphavirus-Induced Cartilage Destruction and Inflammatory Disease. *J Virol, 89*(15), 8063-8076. doi:10.1128/JVI.00224-15

Herrero, L. J., Nelson, M., Srikiatkhachorn, A., Gu, R., Anantapreecha, S., Fingerle-Rowson, G., . . . Mahalingam, S. (2011). Critical role for macrophage migration inhibitory factor (MIF) in Ross River virus-induced arthritis and myositis. *Proceedings of the National Academy of Sciences of the United States of America, 108*(29), 12048-12053. doi:10.1073/pnas.1101089108

Hidaka, S., Iwasaka, H., Hagiwara, S., & Noguchi, T. (2011). Gabexate mesilate inhibits the expression of HMGB1 in lipopolysaccharide-induced acute lung injury. *J Surg Res, 165*(1), 142-150. doi:10.1016/j.jss.2009.05.039

Higgs, S., & Vanlandingham, D. (2015). Chikungunya Virus and Its Mosquito Vectors. *Vector Borne Zoonotic Dis*. doi:10.1089/vbz.2014.1745

Hirokawa, J., Sakaue, S., Tagami, S., Kawakami, Y., Sakai, M., Nishi, S., & Nishihira, J. (1997). Identification of macrophage migration inhibitory factor in adipose tissue and its induction by tumor necrosis factor-alpha. *Biochem Biophys Res Commun, 235*(1), 94-98. doi:10.1006/bbrc.1997.6745

Hoad, V. C., Speers, D. J., Keller, A. J., Dowse, G. K., Seed, C. R., Lindsay, M. D., . . . Pink, J. (2015). First reported case of transfusion-transmitted Ross River virus infection. *Med J Aust, 202*(5), 267-269.

Hoch, M., Eberle, A. N., Peterli, R., Peters, T., Seboek, D., Keller, U., . . . Linscheid, P. (2008). LPS induces interleukin-6 and interleukin-8 but not tumor necrosis factor-α in human adipocytes. *Cytokine, 41*(1), 29-37. doi:http://dx.doi.org/10.1016/j.cyto.2007.10.008

Hogan, M. M., & Vogel, S. N. (1988). Production of tumor necrosis factor by rIFN-gamma-primed C3H/HeJ (Lpsd) macrophages requires the presence of lipid A-associated proteins. *J Immunol, 141*(12), 4196-4202.

Hogan, M. M., & Vogel, S. N. (2001). Measurement of tumor necrosis factor alpha and beta. *Curr Protoc Immunol, Chapter 6*, Unit 6 10. doi:10.1002/0471142735.im0610s37

Holland, R., Barnsley, L., & Barnsley, L. (2013). Viral arthritis. *Aust Fam Physician, 42*(11), 770-773.

Hollenbach, M., Hintersdorf, A., Huse, K., Sack, U., Bigl, M., Groth, M., . . . Birkenmeier, G. (2008). Ethyl pyruvate and ethyl lactate down-regulate the production of pro-inflammatory cytokines and modulate expression of immune receptors. *Biochem Pharmacol, 76*(5), 631-644. doi:10.1016/j.bcp.2008.06.006

Hou, X. Q., Qin, J. L., Zheng, X. X., Wang, L., Yang, S. T., Gao, Y. W., & Xia, X. Z. (2014). Potential role of high-mobility group box 1 protein in the pathogenesis of influenza H5N1 virus infection. *Acta virologica, 58*(1), 69-75. doi:10.4149/av_2014_01_69

Huang, W., Tang, Y., & Li, L. (2010). HMGB1, a potent proinflammatory cytokine in sepsis. *Cytokine, 51*(2), 119-126. doi:http://dx.doi.org/10.1016/j.cyto.2010.02.021

Ianaro, A., Ialenti, A., Maffia, P., Sautebin, L., Rombola, L., Carnuccio, R., . . . Di Rosa, M. (2000). Anti-inflammatory activity of macrolide antibiotics. *J Pharmacol Exp Ther, 292*(1), 156-163.

Ignarro, L. J., Fukuto, J. M., Griscavage, J. M., Rogers, N. E., & Byrns, R. E. (1993). Oxidation of nitric oxide in aqueous solution to nitrite but not nitrate: comparison with enzymatically formed nitric oxide from L-arginine. *Proc Natl Acad Sci U S A, 90*(17), 8103-8107.

Iino, Y., Toriyama, M., Kudo, K., Natori, Y., & Yuo, A. (1992). Erythromycin inhibition of lipopolysaccharide-stimulated tumor necrosis factor alpha production by human monocytes in vitro. *Ann Otol Rhinol Laryngol Suppl, 157*, 16-20.

Iwamoto, T., Okamoto, H., Toyama, Y., & Momohara, S. (2008). Molecular aspects of rheumatoid arthritis: chemokines in the joints of patients. *FEBS J, 275*(18), 4448-4455. doi:10.1111/j.1742-4658.2008.06580.x

Jacups, S. P., Whelan, P. I., & Currie, B. J. (2008). Ross River virus and Barmah Forest virus infections: a review of history, ecology, and predictive models, with implications for tropical northern Australia. *Vector Borne Zoonotic Dis, 8*(2), 283-297. doi:10.1089/vbz.2007.0152

Jiang, W. L., Chen, X. G., Qu, G. W., Yue, X. D., Zhu, H. B., Tian, J. W., & Fu, F. H. (2009). Rosmarinic acid protects against experimental sepsis by inhibiting proinflammatory factor release and ameliorating hemodynamics. *Shock, 32*(6), 608-613. doi:10.1097/SHK.0b013e3181a48e86

Journeaux, S. F., Brown, W. G., & Aaskov, J. G. (1987). Prolonged infection of human synovial cells with Ross River virus. *J Gen Virol, 68 (Pt 12)*, 3165-3169.

Jupille, H. J., Medina-Rivera, M., Hawman, D. W., Oko, L., & Morrison, T. E. (2013). A tyrosine-to-histidine switch at position 18 of the Ross River virus E2 glycoprotein is a determinant of virus fitness in disparate hosts. *J Virol, 87*(10), 5970-5984. doi:10.1128/JVI.03326-12

Jupille, H. J., Oko, L., Stoermer, K. A., Heise, M. T., Mahalingam, S., Gunn, B. M., & Morrison, T. E. (2011). Mutations in nsP1 and PE2 are critical determinants of Ross River virus-induced musculoskeletal inflammatory disease in a mouse model. *Virology, 410*(1), 216-227. doi:10.1016/j.virol.2010.11.012

Kalinski, P. (2012). Regulation of immune responses by prostaglandin E2. *The Journal of Immunology, 188*(1), 21-28.

Kamau, E., Takhampunya, R., Li, T., Kelly, E., Peachman, K. K., Lynch, J. A., . . . Palmer, D. R. (2009). Dengue virus infection promotes translocation of high mobility group box 1 protein from the nucleus to the cytosol in dendritic cells, upregulates cytokine production and modulates virus replication. *Journal of General Virology, 90*(8), 1827-1835. doi:10.1099/vir.0.009027-0

Kerr, J. R., Cunniffe, V. S., Kelleher, P., Coats, A. J. S., & Mattey, D. L. (2004). Circulating cytokines and chemokines in acute symptomatic parvovirus B19 infection: Negative association between levels of pro-inflammatory cytokines and development of B19-associated arthritis. *Journal of Medical Virology, 74*(1), 147-155. doi:10.1002/jmv.20158

Keystone, E., Wherry, J., & Grint, P. (1998). IL-10 AS A THERAPEUTIC STRATEGY IN THE TREATMENT OF RHEUMATOID ARTHRITIS. *Rheumatic Disease Clinics of North America, 24*(3), 629-639. doi:http://dx.doi.org/10.1016/S0889-857X(05)70030-2

Kikuchi, K., Kawahara, K., Biswas, K. K., Ito, T., Tancharoen, S., Morimoto, Y., . . . Maruyama, I. (2009). Minocycline attenuates both OGD-induced HMGB1 release and HMGB1-induced cell death in ischemic neuronal injury in PC12 cells. *Biochem Biophys Res Commun, 385*(2), 132-136. doi:10.1016/j.bbrc.2009.04.041

Kim, D. C., Lee, W., & Bae, J. S. (2011). Vascular anti-inflammatory effects of curcumin on HMGB1-mediated responses in vitro. *Inflammation research : official journal of the European Histamine Research Society ... [et al.], 60*(12), 1161-1168. doi:10.1007/s00011-011-0381-y

Kim, H. R., Park, M. K., Cho, M. L., Yoon, C. H., Lee, S. H., Park, S. H., . . . Kim, H. Y. (2007). Macrophage migration inhibitory factor upregulates angiogenic factors and correlates with clinical measures in rheumatoid arthritis. *J Rheumatol, 34*(5), 927-936.

Kinne, R. W., Brauer, R., Stuhlmuller, B., Palombo-Kinne, E., & Burmester, G. R. (2000). Macrophages in rheumatoid arthritis. *Arthritis Res, 2*(3), 189-202.

Klimstra, W. B., Nangle, E. M., Smith, M. S., Yurochko, A. D., & Ryman, K. D. (2003). DC-SIGN and L-SIGN can act as attachment receptors for alphaviruses and distinguish between mosquito cell- and mammalian cell-derived viruses. *J Virol, 77*(22), 12022-12032.

Klimstra, W. B., Ryman, K. D., Bernard, K. A., Nguyen, K. B., Biron, C. A., & Johnston, R. E. (1999). Infection of Neonatal Mice with Sindbis Virus Results in a Systemic Inflammatory Response Syndrome. *Journal of Virology, 73*(12), 10387-10398.

Kobayashi, Y. (2010). The regulatory role of nitric oxide in proinflammatory cytokine expression during the induction and resolution of inflammation. *Journal of Leukocyte Biology, 88*(6), 1157-1162. doi:10.1189/jlb.0310149

Kohri, K., Tamaoki, J., Kondo, M., Aoshiba, K., Tagaya, E., & Nagai, A. (2000). Macrolide antibiotics inhibit nitric oxide generation by rat pulmonary alveolar macrophages. *Eur Respir J, 15*(1), 62-67.

Krasniqi, S., Matzneller, P., Kinzig, M., Sörgel, F., Hüttner, S., Lackner, E., . . . Zeitlinger, M. (2012). Blood, Tissue, and Intracellular Concentrations of Erythromycin and Its Metabolite Anhydroerythromycin during and after Therapy. *Antimicrobial Agents and Chemotherapy, 56*(2), 1059-1064. doi:10.1128/aac.05490-11

Kuchler, A. M., Pollheimer, J., Balogh, J., Sponheim, J., Manley, L., Sorensen, D. R., . . . Haraldsen, G. (2008). Nuclear interleukin-33 is generally expressed in resting endothelium but rapidly lost upon angiogenic or proinflammatory activation. *Am J Pathol, 173*(4), 1229-1242. doi:10.2353/ajpath.2008.080014

Kuhn, R. J., Niesters, H. G., Hong, Z., & Strauss, J. H. (1991). Infectious RNA transcripts from Ross River virus cDNA clones and the construction and

characterization of defined chimeras with Sindbis virus. *Virology, 182*(2), 430-441.
Kwon Ii, J., Chung, Y., & Benveniste, E. N. (1993). Cloning and sequence analysis of the rat tumor necrosis factor-encoding genes. *Gene, 132*(2), 227-236. doi:http://dx.doi.org/10.1016/0378-1119(93)90200-M
Kwon, W. Y., Suh, G. J., Kim, K. S., Jo, Y. H., Lee, J. H., Kim, K., & Jung, S. K. (2010). Glutamine attenuates acute lung injury by inhibition of high mobility group box protein-1 expression during sepsis. *Br J Nutr, 103*(6), 890-898. doi:10.1017/S0007114509992509
La Linn, M., Eble, J. A., Lubken, C., Slade, R. W., Heino, J., Davies, J., & Suhrbier, A. (2005). An arthritogenic alphavirus uses the alpha1beta1 integrin collagen receptor. *Virology, 336*(2), 229-239. doi:10.1016/j.virol.2005.03.015
Labro, M. T. (1998). Anti-inflammatory activity of macrolides: a new therapeutic potential? *Journal of Antimicrobial Chemotherapy, 41*(suppl 2), 37-46. doi:10.1093/jac/41.suppl_2.37
Leung, J. Y.-S., Ng, M. M.-L., & Chu, J. J. H. (2011). Replication of Alphaviruses: A Review on the Entry Process of Alphaviruses into Cells. *Advances in Virology, 2011*, 9. doi:10.1155/2011/249640
Lidbury, B. A., & Mahalingam, S. (2000a). A role for chemokine activity in Alphavirus pathogenesis: Evidence from the analysis of polyarthritis and myalgia post-Ross river virus infection.
Lidbury, B. A., & Mahalingam, S. (2000b). Specific ablation of antiviral gene expression in macrophages by antibody-dependent enhancement of Ross River virus infection. *J Virol, 74*(18), 8376-8381.
Lidbury, B. A., Rulli, N. E., Suhrbier, A., Smith, P. N., McColl, S. R., Cunningham, A. L., . . . Mahalingam, S. (2008). Macrophage-derived proinflammatory factors contribute to the development of arthritis and myositis after infection with an arthrogenic alphavirus. *J Infect Dis, 197*(11), 1585-1593. doi:10.1086/587841
Lidbury, B. A., Simeonovic, C., Maxwell, G. E., Marshall, I. D., & Hapel, A. J. (2000). Macrophage-induced muscle pathology results in morbidity and mortality for Ross River virus-infected mice. *J Infect Dis, 181*(1), 27-34. doi:10.1086/315164
Liew, F. Y., Pitman, N. I., & McInnes, I. B. (2010). Disease-associated functions of IL-33: the new kid in the IL-1 family. *Nat Rev Immunol, 10*(2), 103-110. doi:10.1038/nri2692
Lim, T. K. (2014). Corymbia calophylla *Edible Medicinal and Non Medicinal Plants* (pp. 456-459): Springer Netherlands.
Lindsay, M. D., Coelen, R. J., & Mackenzie, J. S. (1993). Genetic heterogeneity among isolates of Ross River virus from different geographical regions. *J Virol, 67*(6), 3576-3585.
Linn, M. L., Aaskov, J. G., & Suhrbier, A. (1996). Antibody-dependent enhancement and persistence in macrophages of an arbovirus associated with arthritis. *J Gen Virol, 77 (Pt 3)*, 407-411.
Locher, C., & Currie, L. (2010). Revisiting kinos—An Australian perspective. *Journal of Ethnopharmacology, 128*(2), 259-267. doi:http://dx.doi.org/10.1016/j.jep.2010.01.028
Loftis, L. L., Meals, E. A., & English, B. K. (1997). Differential effects of pentoxifylline and interleukin-10 on production of tumor necrosis factor and inducible nitric oxide synthase by murine macrophages. *The Journal of infectious diseases, 175*(4), 1008-1011.
Lu, X., Ma, L., Ruan, L., Kong, Y., Mou, H., Zhang, Z., . . . Le, Y. (2010). Resveratrol differentially modulates inflammatory responses of microglia and astrocytes. *Journal of neuroinflammation, 7*, 46. doi:10.1186/1742-2094-7-46
Lutter, R., Loman, S., Snoek, M., Roger, T., Out, T. A., & Jansen, H. M. (2000). IL-6 PROTEIN PRODUCTION BY AIRWAY EPITHELIAL(-LIKE) CELLS

DISABLED IN IL-6 mRNA DEGRADATION. *Cytokine, 12*(8), 1275-1279. doi:http://dx.doi.org/10.1006/cyto.1999.0728

Mahalingam, S., & Lidbury, B. A. (2002). Suppression of lipopolysaccharide-induced antiviral transcription factor (STAT-1 and NF-kappa B) complexes by antibody-dependent enhancement of macrophage infection by Ross River virus. *Proc Natl Acad Sci U S A, 99*(21), 13819-13824. doi:10.1073/pnas.202415999

Mahy, B. W., & Kangro, H. O. (1996). *Virology methods manual* (Vol. 32): Academic Press London, UK.

Maksymowych, W. P., Avina-Zubieta, A., Luong, M. H., & Russell, A. S. (1995). An open study of pentoxifylline in the treatment of severe refractory rheumatoid arthritis. *J Rheumatol, 22*(4), 625-629.

Marques, L. J., Zheng, L., Poulakis, N., Guzman, J., & Costabel, U. (1999). Pentoxifylline inhibits TNF-alpha production from human alveolar macrophages. *American journal of respiratory and critical care medicine, 159*(2), 508-511. doi:10.1164/ajrccm.159.2.9804085

Mateo, L., La Linn, M., McColl, S. R., Cross, S., Gardner, J., & Suhrbier, A. (2000). An arthrogenic alphavirus induces monocyte chemoattractant protein-1 and interleukin-8. *Intervirology, 43*(1), 55-60. doi:int43055 [pii]

Matsuyama, Y., Okazaki, H., Tamemoto, H., Kimura, H., Kamata, Y., Nagatani, K., . . . Minota, S. (2010). Increased levels of interleukin 33 in sera and synovial fluid from patients with active rheumatoid arthritis. *J Rheumatol, 37*(1), 18-25. doi:10.3899/jrheum.090492

McInnes, I. B., & Schett, G. (2007). Cytokines in the pathogenesis of rheumatoid arthritis. *Nat Rev Immunol, 7*(6), 429-442. doi:10.1038/nri2094

McInnes, I. B., & Schett, G. (2011). The pathogenesis of rheumatoid arthritis. *N Engl J Med, 365*(23), 2205-2219. doi:10.1056/NEJMra1004965

Mehra, A., Macdonald, I., & Pillay, T. S. (2007). Variability in 3T3-L1 adipocyte differentiation depending on cell culture dish. *Analytical Biochemistry, 362*(2), 281-283. doi:http://dx.doi.org/10.1016/j.ab.2006.12.016

Mencarelli, A., Distrutti, E., Renga, B., Cipriani, S., Palladino, G., Booth, C., . . . Fiorucci, S. (2011). Development of non-antibiotic macrolide that corrects inflammation-driven immune dysfunction in models of inflammatory bowel diseases and arthritis. *European Journal of Pharmacology, 665*(1–3), 29-39. doi:http://dx.doi.org/10.1016/j.ejphar.2011.04.036

Miller, A. M. (2011). Role of IL-33 in inflammation and disease. *J Inflamm (Lond), 8*(1), 22. doi:10.1186/1476-9255-8-22

Molnar, V., & Garai, J. (2005). Plant-derived anti-inflammatory compounds affect MIF tautomerase activity. *International immunopharmacology, 5*(5), 849-856. doi:10.1016/j.intimp.2004.12.017

Morand, E. F. (2005). New therapeutic target in inflammatory disease: macrophage migration inhibitory factor. *Intern Med J, 35*(7), 419-426. doi:10.1111/j.1445-5994.2005.00853.x

Morrison, T. E., Fraser, R. J., Smith, P. N., Mahalingam, S., & Heise, M. T. (2007). Complement contributes to inflammatory tissue destruction in a mouse model of Ross River virus-induced disease. *J Virol, 81*(10), 5132-5143. doi:10.1128/JVI.02799-06

Morrison, T. E., Oko, L., Montgomery, S. A., Whitmore, A. C., Lotstein, A. R., Gunn, B. M., . . . Heise, M. T. (2011). A mouse model of chikungunya virus-induced musculoskeletal inflammatory disease: evidence of arthritis, tenosynovitis, myositis, and persistence. *Am J Pathol, 178*(1), 32-40. doi:10.1016/j.ajpath.2010.11.018

Morrison, T. E., Simmons, J. D., & Heise, M. T. (2008). Complement receptor 3 promotes severe ross river virus-induced disease. *J Virol, 82*(22), 11263-11272. doi:10.1128/JVI.01352-08

Morrison, T. E., Whitmore, A. C., Shabman, R. S., Lidbury, B. A., Mahalingam, S., & Heise, M. T. (2006). Characterization of Ross River virus tropism and virus-induced inflammation in a mouse model of viral arthritis and myositis. *J Virol, 80*(2), 737-749. doi:10.1128/JVI.80.2.737-749.2006

Mosmann, T. R. (1994). Properties and functions of interleukin-10. *Adv Immunol, 56*, 1-26.

Moulin, D., Donze, O., Talabot-Ayer, D., Mezin, F., Palmer, G., & Gabay, C. (2007). Interleukin (IL)-33 induces the release of pro-inflammatory mediators by mast cells. *Cytokine, 40*(3), 216-225. doi:10.1016/j.cyto.2007.09.013

Muller, S., Scaffidi, P., Degryse, B., Bonaldi, T., Ronfani, L., Agresti, A., . . . Bianchi, M. E. (2001). New EMBO members' review: the double life of HMGB1 chromatin protein: architectural factor and extracellular signal. *EMBO J, 20*(16), 4337-4340. doi:10.1093/emboj/20.16.4337

Muñoz-Cánoves, P., Scheele, C., Pedersen, B. K., & Serrano, A. L. (2013). Interleukin-6 myokine signaling in skeletal muscle: a double-edged sword? *FEBS Journal, 280*(17), 4131-4148. doi:10.1111/febs.12338

Murphy, F. A., Taylor, W. P., Mims, C. A., & Marshall, I. D. (1973). Pathogenesis of Ross River Virus Infection in Mice.: II. Muscle, Heart, and Brown Fat Lesions. *Journal of Infectious Diseases, 127*(2), 129-138. doi:10.1093/infdis/127.2.129

Mylonas, A. D., Brown, A. M., Carthew, T. L., McGrath, B., Purdie, D. M., Pandeya, N., . . . Suhrbier, A. (2002). Natural history of Ross River virus-induced epidemic polyarthritis. *Med J Aust, 177*(7), 356-360. doi:myl10636_fm [pii]

Mylonas, A. D., Harley, D., Purdie, D. M., Pandeya, N., Vecchio, P. C., Farmer, J. F., & Suhrbier, A. (2004). Corticosteroid therapy in an alphaviral arthritis. *J Clin Rheumatol, 10*(6), 326-330. doi:10.1097/01.rhu.0000147052.11190.36

Nagy, G., Koncz, A., Telarico, T., Fernandez, D., Érsek, B., Buzás, E., & Perl, A. (2010). Central role of nitric oxide in the pathogenesis of rheumatoid arthritis and sysemic lupus erythematosus. *Arthritis Research and Therapy, 12*(3), 210.

Nakaya, H. I., Gardner, J., Poo, Y. S., Major, L., Pulendran, B., & Suhrbier, A. (2012). Gene profiling of Chikungunya virus arthritis in a mouse model reveals significant overlap with rheumatoid arthritis. *Arthritis & Rheumatism, 64*(11), 3553-3563.

Nathan, C. F. (1987). Secretory products of macrophages. *J Clin Invest, 79*(2), 319-326. doi:10.1172/JCI112815

Nativel, B., Marimoutou, M., Thon-Hon, V. G., Gunasekaran, M. K., Andries, J., Stanislas, G., . . . Viranaicken, W. (2013). Soluble HMGB1 Is a Novel Adipokine Stimulating IL-6 Secretion through RAGE Receptor in SW872 Preadipocyte Cell Line: Contribution to Chronic Inflammation in Fat Tissue. *PLoS ONE, 8*(9), e76039. doi:10.1371/journal.pone.0076039

Naugler, W. E., & Karin, M. (2008). The wolf in sheep's clothing: the role of interleukin-6 in immunity, inflammation and cancer. *Trends Mol Med, 14*(3), 109-119. doi:10.1016/j.molmed.2007.12.007

Neighbours, L. M., Long, K., Whitmore, A. C., & Heise, M. T. (2012). Myd88-Dependent Toll-Like Receptor 7 Signaling Mediates Protection from Severe Ross River Virus-Induced Disease in Mice. *Journal of Virology, 86*(19), 10675-10685. doi:10.1128/jvi.00601-12

Ng, L. F., Chow, A., Sun, Y. J., Kwek, D. J., Lim, P. L., Dimatatac, F., . . . Leo, Y. S. (2009). IL-1beta, IL-6, and RANTES as biomarkers of Chikungunya severity. *PLoS ONE, 4*(1), e4261. doi:10.1371/journal.pone.0004261

Nogueira-Machado, J. A., & de Oliveira Volpe, C. M. (2012). HMGB-1 as a target for inflammation controlling. *Recent Pat Endocr Metab Immune Drug Discov, 6*(3), 201-209.

Noman, A. S., Koide, N., Hassan, F., I, I. E.-K., Dagvadorj, J., Tumurkhuu, G., . . . Yokochi, T. (2009). Thalidomide inhibits lipopolysaccharide-induced tumor necrosis factor-alpha production via down-regulation of MyD88 expression. *Innate Immun, 15*(1), 33-41. doi:10.1177/1753425908099317

Ogrendik, M. (2014). Antibiotics for the treatment of rheumatoid arthritis. *International Journal of General Medicine, 7*, 43-47. doi:10.2147/IJGM.S56957

Okamura, H., Tsutsi, H., Komatsu, T., Yutsudo, M., Hakura, A., Tanimoto, T., . . . et al. (1995). Cloning of a new cytokine that induces IFN-gamma production by T cells. *Nature, 378*(6552), 88-91. doi:10.1038/378088a0

Onda, H., Kasuya, H., Takakura, K., Hori, T., Imaizumi, T.-a., Takeuchi, T., . . . Takeda, J. (1999). Identification of Genes Differentially Expressed in Canine Vasospastic Cerebral Arteries After Subarachnoid Hemorrhage. *J Cereb Blood Flow Metab, 19*(11), 1279-1288.

Ong, S. P., Lee, L. M., Leong, Y. F., Ng, M. L., & Chu, J. J. (2012). Dengue virus infection mediates HMGB1 release from monocytes involving PCAF acetylase complex and induces vascular leakage in endothelial cells. *PLoS ONE, 7*(7), e41932. doi:10.1371/journal.pone.0041932

Oppenheim, J. J., Feldmann, M., & Durum, S. K. (2001). *Cytokine Reference: A Compendium of Cytokines and Other Mediators of Host Defense. Ligands*: Academic Press.

Ouertatani-Sakouhi, H., El-Turk, F., Fauvet, B., Roger, T., Le Roy, D., Karpinar, D. P., . . . Lashuel, H. A. (2009). A new class of isothiocyanate-based irreversible inhibitors of macrophage migration inhibitory factor. *Biochemistry, 48*(41), 9858-9870. doi:10.1021/bi900957e

Ozden, S., Huerre, M., Riviere, J.-P., Coffey, L. L., Afonso, P. V., Mouly, V., . . . Ceccaldi, P.-E. (2007). Human Muscle Satellite Cells as Targets of Chikungunya Virus Infection. *PLoS ONE, 2*(6), e527. doi:10.1371/journal.pone.0000527

Parashar, D., & Cherian, S. (2014). Antiviral Perspectives for Chikungunya Virus. *Biomed Res Int, 2014*, 11. doi:10.1155/2014/631642

Paredes, A. M., Ferreira, D., Horton, M., Saad, A., Tsuruta, H., Johnston, R., . . . Brown, D. T. (2004). Conformational changes in Sindbis virions resulting from exposure to low pH and interactions with cells suggest that cell penetration may occur at the cell surface in the absence of membrane fusion. *Virology, 324*(2), 373-386. doi:10.1016/j.virol.2004.03.046

Pattrick, M., Luckett, J., Yue, L., & Stover, C. (2009). Dual role of complement in adipose tissue. *Molecular Immunology, 46*(5), 755-760. doi:http://dx.doi.org/10.1016/j.molimm.2008.09.013

Paulukat, J., Bosmann, M., Nold, M., Garkisch, S., Kämpfer, H., Frank, S., . . . Mühl, H. (2001). Expression and Release of IL-18 Binding Protein in Response to IFN-γ. *The Journal of Immunology, 167*(12), 7038-7043. doi:10.4049/jimmunol.167.12.7038

Pautz, A., Art, J., Hahn, S., Nowag, S., Voss, C., & Kleinert, H. (2010). Regulation of the expression of inducible nitric oxide synthase. *Nitric Oxide, 23*(2), 75-93. doi:http://dx.doi.org/10.1016/j.niox.2010.04.007

Pedersen, B. K., Åkerström, T. C. A., Nielsen, A. R., & Fischer, C. P. (2007). Role of myokines in exercise and metabolism. *J Appl Physiol (1985), 103*(3), 1093-1098.

Pham, T. N. Q., Rahman, P., Tobin, Y. M., Khraishi, M. M., Hamilton, S. F., Alderdice, C., & Richardson, V. J. (2003). Elevated serum nitric oxide levels in patients with inflammatory arthritis associated with co-expression of inducible nitric oxide synthase and protein kinase C-eta in peripheral blood monocyte-derived macrophages. *J Rheumatol, 30*(12), 2529-2534.

Phillips, D. A., Murray, J. R., Aaskov, J. G., & Wiemers, M. A. (1990). Clinical and subclinical Barmah Forest virus infection in Queensland. *Med J Aust, 152*(9), 463-466.

Pialoux, G., Gauzere, B. A., Jaureguiberry, S., & Strobel, M. (2007). Chikungunya, an epidemic arbovirosis. *Lancet Infect Dis, 7*(5), 319-327. doi:10.1016/S1473-3099(07)70107-X

Piper, R. C., Slot, J. W., & Li, G. (1994). Recombinant Sindbis Virus as an Expression System for Cell Biology. *Protein Expression in Animal Cells, 43*, 55.

Poulos, S. P., Dodson, M. V., & Hausman, G. J. (2010). Cell line models for differentiation: preadipocytes and adipocytes. *Exp Biol Med (Maywood), 235*(10), 1185-1193. doi:10.1258/ebm.2010.010063

Powers, A. M., Brault, A. C., Tesh, R. B., & Weaver, S. C. (2000). Re-emergence of chikungunya and o'nyong-nyong viruses: evidence for distinct geographical lineages and distant evolutionary relationships. *Journal of General Virology, 81*(2), 471-479.

Queensland Health. (2015). *Department of Health, Queensland - Statewide Weekly Communicable Diseases Surveillance Report, 08/03/2015*. Retrieved from http://www.health.qld.gov.au/ph/documents/cdb/weeklyrprt-150308.pdf

Queiroz-Junior, C. M., Bessoni, R. L. C., Costa, V. V., Souza, D. G., Teixeira, M. M., & Silva, T. A. (2013). Preventive and therapeutic anti-TNF-α therapy with pentoxifylline decreases arthritis and the associated periodontal co-morbidity in mice. *Life Sci, 93*(9–11), 423-428. doi:http://dx.doi.org/10.1016/j.lfs.2013.07.022

Qureshi, A. A., Guan, X. Q., Reis, J. C., Papasian, C. J., Jabre, S., Morrison, D. C., & Qureshi, N. (2012). Inhibition of nitric oxide and inflammatory cytokines in LPS-stimulated murine macrophages by resveratrol, a potent proteasome inhibitor. *Lipids Health Dis, 11*, 76. doi:10.1186/1476-511X-11-76

Reed, L. J., & Muench, H. (1938). A simple method of estimating fifty per cent endpoints. *American Journal of Epidemiology, 27*(3), 493-497.

Reiss, C. S., & Komatsu, T. (1998). Does Nitric Oxide Play a Critical Role in Viral Infections? *Journal of Virology, 72*(6), 4547-4551.

Rezza, G., Nicoletti, L., Angelini, R., Romi, R., Finarelli, A. C., Panning, M., . . . group, C. s. (2007). Infection with chikungunya virus in Italy: an outbreak in a temperate region. *Lancet, 370*(9602), 1840-1846. doi:10.1016/S0140-6736(07)61779-6

Riveiro-Naveira, R. R., Loureiro, J., Valcárcel-Ares, M. N., López-Peláez, E., Centeno-Cortés, A., Vaamonde-García, C., . . . López-Armada, M. J. (2014). Anti-inflammatory effect of resveratrol as a dietary supplement in an antigen-induced arthritis rat model. *Osteoarthritis and Cartilage, 22*, S290. doi:10.1016/j.joca.2014.02.539

Robinson, M. C. (1955). An epidemic of virus disease in Southern Province, Tanganyika territory, in 1952–1953. *Transactions of the Royal Society of Tropical Medicine and Hygiene, 49*(1), 28-32. doi:http://dx.doi.org/10.1016/0035-9203(55)90080-8

Rooijen, N. V., & Sanders, A. (1994). Liposome mediated depletion of macrophages: mechanism of action, preparation of liposomes and applications. *Journal of Immunological Methods, 174*(1–2), 83-93. doi:http://dx.doi.org/10.1016/0022-1759(94)90012-4

Rubinstein, E. (2001). Comparative safety of the different macrolides. *Int J Antimicrob Agents, 18, Supplement 1*(0), 71-76. doi:http://dx.doi.org/10.1016/S0924-8579(01)00397-1

Rulli, N. E., Guglielmotti, A., Mangano, G., Rolph, M. S., Apicella, C., Zaid, A., . . . Mahalingam, S. (2009). Amelioration of alphavirus-induced arthritis and myositis in a mouse model by treatment with bindarit, an inhibitor of

monocyte chemotactic proteins. *Arthritis Rheum, 60*(8), 2513-2523. doi:10.1002/art.24682

Rulli, N. E., Melton, J., Wilmes, A., Ewart, G., & Mahalingam, S. (2007). The molecular and cellular aspects of arthritis due to alphavirus infections: lesson learned from Ross River virus. *Ann N Y Acad Sci, 1102*, 96-108. doi:10.1196/annals.1408.007

Rulli, N. E., Suhrbier, A., Hueston, L., Heise, M. T., Tupanceska, D., Zaid, A., . . . Mahalingam, S. (2005). Ross River virus: molecular and cellular aspects of disease pathogenesis. *Pharmacol Ther, 107*(3), 329-342. doi:10.1016/j.pharmthera.2005.03.006

Ryman, K. D., & Klimstra, W. B. (2014). Closing the gap between viral and noninfectious arthritis. *Proceedings of the National Academy of Sciences, 111*(16), 5767-5768. doi:10.1073/pnas.1404206111

Sakamoto, K., & Kimura, J. (2013). Mechanism of Statin-Induced Rhabdomyolysis. *Journal of Pharmacological Sciences, 123*(4), 289-294. doi:10.1254/jphs.13R06CP

Salgado, D., Zabaleta, T. E., Hatch, S., Vega, M. R., & Rodriguez, J. (2012). Use of Pentoxifylline in Treatment of Children With Dengue Hemorrhagic Fever. *The Pediatric Infectious Disease Journal, 31*(7), 771-773. doi:10.1097/INF.0b013e3182575e6a

Salhiyyah, K., Senanayake, E., Abdel-Hadi, M., Booth, A., & Michaels, J. A. (2012). Pentoxifylline for intermittent claudication. *Cochrane Database Syst Rev, 1*, CD005262. doi:10.1002/14651858.CD005262.pub2

Salvemini, D., Misko, T. P., Masferrer, J. L., Seibert, K., Currie, M. G., & Needleman, P. (1993). Nitric oxide activates cyclooxygenase enzymes. *Proceedings of the National Academy of Sciences, 90*(15), 7240-7244.

Sammels, L. M., Coelen, R. J., Lindsay, M. D., & Mackenzie, J. S. (1995). Geographic distribution and evolution of Ross River virus in Australia and the Pacific Islands. *Virology, 212*(1), 20-29. doi:10.1006/viro.1995.1449

Sane, J., Kurkela, S., Desdouits, M., Kalimo, H., Mazalrey, S., Lokki, M.-L., . . . Vapalahti, O. (2012). Prolonged myalgia in Sindbis virus infection: case description and in vitro infection of myotubes and myoblasts. *Journal of Infectious Diseases*. doi:10.1093/infdis/jis358

Santoro, M. G., Rossi, A., & Amici, C. (2003). NF-kappaB and virus infection: who controls whom. *EMBO J, 22*(11), 2552-2560. doi:10.1093/emboj/cdg267

Santos, L. L., & Morand, E. F. (2006). The role of macrophage migration inhibitory factor in the inflammatory immune response and rheumatoid arthritis. *Wiener Medizinische Wochenschrift, 156*(1-2), 11-18. doi:10.1007/s10354-005-0243-8

Saraiva, M., & O'Garra, A. (2010). The regulation of IL-10 production by immune cells. *Nat Rev Immunol, 10*(3), 170-181. doi:10.1038/nri2711

Sato, Y., Kaneko, K., & Inoue, M. (2007). Macrolide antibiotics promote the LPS-induced upregulation of prostaglandin E receptor EP2 and thus attenuate macrolide suppression of IL-6 production. *Prostaglandins, Leukotrienes and Essential Fatty Acids, 76*(3), 181-188. doi:http://dx.doi.org/10.1016/j.plefa.2006.12.005

Schäffler, A., Müller-Ladner, U., Schölmerich, J., & Büchler, C. (2006). Role of Adipose Tissue as an Inflammatory Organ in Human Diseases. *Endocrine Reviews, 27*(5), 449-467. doi:doi:10.1210/er.2005-0022

Schaffler, A., & Scholmerich, J. (2010). Innate immunity and adipose tissue biology. *Trends Immunol, 31*(6), 228-235. doi:10.1016/j.it.2010.03.001

Schandené, L., Vandenbussche, P., Crusiaux, A., Alègre, M. L., Abramowicz, D., Dupont, E., . . . Goldman, M. (1992). Differential effects of pentoxifylline on the production of tumour necrosis factor-alpha (TNF-alpha) and interleukin-6 (IL-6) by monocytes and T cells. *Immunology, 76*(1), 30-34.

Scheller, J., Chalaris, A., Schmidt-Arras, D., & Rose-John, S. (2011). The pro- and anti-inflammatory properties of the cytokine interleukin-6. *Biochimica et Biophysica Acta (BBA) - Molecular Cell Research, 1813*(5), 878-888. doi:http://dx.doi.org/10.1016/j.bbamcr.2011.01.034

Schmitz, J., Owyang, A., Oldham, E., Song, Y., Murphy, E., McClanahan, T. K., . . . Kastelein, R. A. (2005). IL-33, an Interleukin-1-like Cytokine that Signals via the IL-1 Receptor-Related Protein ST2 and Induces T Helper Type 2-Associated Cytokines. *Immunity, 23*(5), 479-490. doi:http://dx.doi.org/10.1016/j.immuni.2005.09.015

Schoneboom, B. A., Lee, J. S., & Grieder, F. B. (2000). Early expression of IFN-alpha/beta and iNOS in the brains of Venezuelan equine encephalitis virus-infected mice. *J Interferon Cytokine Res, 20*(2), 205-215. doi:10.1089/107999000312621

Schuffenecker, I., Iteman, I., Michault, A., Murri, S., Frangeul, L., Vaney, M.-C., . . . Brisse, S. (2006). Genome Microevolution of Chikungunya Viruses Causing the Indian Ocean Outbreak. *PLoS Medicine, 3*(7), e263. doi:10.1371/journal.pmed.0030263

Schwartz, O., & Albert, M. L. (2010). Biology and pathogenesis of chikungunya virus. *Nature Reviews. Microbiology, 8*(7), 491-500. doi:http://dx.doi.org/10.1038/nrmicro2368

Sebastian, L., Desai, A., Madhusudana, S. N., & Ravi, V. (2009). Pentoxifylline inhibits replication of Japanese encephalitis virus: a comparative study with ribavirin. *Int J Antimicrob Agents, 33*(2), 168-173. doi:http://dx.doi.org/10.1016/j.ijantimicag.2008.07.013

Semple, J. W., Italiano, J. E., Jr., & Freedman, J. (2011). Platelets and the immune continuum. *Nat Rev Immunol, 11*(4), 264-274. doi:10.1038/nri2956

Shabman, R. S., Morrison, T. E., Moore, C., White, L., Suthar, M. S., Hueston, L., . . . Heise, M. T. (2007). Differential induction of type I interferon responses in myeloid dendritic cells by mosquito and mammalian-cell-derived alphaviruses. *J Virol, 81*(1), 237-247. doi:10.1128/JVI.01590-06

Shang, G. H., Lin, D. J., Xiao, W., Jia, C. Q., Li, Y., Wang, A. H., & Dong, L. (2009). Ethyl pyruvate reduces mortality in an endotoxin-induced severe acute lung injury mouse model. *Respir Res, 10*, 91. doi:10.1186/1465-9921-10-91

Sharkey, C. M., North, C. L., Kuhn, R. J., & Sanders, D. A. (2001). Ross River Virus Glycoprotein-Pseudotyped Retroviruses and Stable Cell Lines for Their Production. *Journal of Virology, 75*(6), 2653-2659. doi:10.1128/JVI.75.6.2653-2659.2001

Shepherd, P. R., Nave, B. T., & Siddle, K. (1995). Insulin stimulation of glycogen synthesis and glycogen synthase activity is blocked by wortmannin and rapamycin in 3T3-L1 adipocytes: evidence for the involvement of phosphoinositide 3-kinase and p70 ribosomal protein-S6 kinase. *Biochem J, 305 (Pt 1)*, 25-28.

Shimony, N., Elkin, G., Kolodkin-Gal, D., Krasny, L., Urieli-Shoval, S., & Haviv, Y. S. (2009). Analysis of adenoviral attachment to human platelets. *Virol J, 6*, 25. doi:10.1186/1743-422X-6-25

Skurk, T., Herder, C., Kräft, I., Müller-Scholze, S., Hauner, H., & Kolb, H. (2005). Production and Release of Macrophage Migration Inhibitory Factor from Human Adipocytes. *Endocrinology, 146*(3), 1006-1011. doi:10.1210/en.2004-0924

Soden, M., Vasudevan, H., Roberts, B., Coelen, R., Hamlin, G., Vasudevan, S., & La Brooy, J. (2000). Detection of viral ribonucleic acid and histologic analysis of inflamed synovium in Ross River virus infection. *Arthritis Rheum, 43*(2), 365-369. doi:10.1002/1529-0131(200002)43:2<365::aid-anr16>3.0.co;2-e

Song, M., Kellum, J. A., Kaldas, H., & Fink, M. P. (2004). Evidence That Glutathione Depletion Is a Mechanism Responsible for the Anti-Inflammatory Effects of

Ethyl Pyruvate in Cultured Lipopolysaccharide-Stimulated RAW 264.7 Cells. *Journal of Pharmacology and Experimental Therapeutics, 308*(1), 307-316. doi:10.1124/jpet.103.056622

Srivastava, U., Nelson, M., Su, Y.-C., & Mahalingam, S. (2008). Mechanisms of Chikungunya virus disease informed by Ross River virus research. *Future Virology, 3*(6), 509-511. doi:10.2217/17460794.3.6.509

Steer, S. A., & Corbett, J. A. (2003). The Role and Regulation of COX-2 during Viral Infection. *Viral Immunology, 16*(4), 447-460. doi:10.1089/088282403771926283

Stein, M. (2003). *The Encyclopedia of Arthritis*. New York: New York : Infobase Publishing.

Stoermer Burrack, K. A., Hawman, D. W., Jupille, H. J., Oko, L., Minor, M., Shives, K. D., . . . Morrison, T. E. (2014). Attenuating mutations in nsP1 reveal tissue-specific mechanisms for control of Ross River virus infection. *J Virol, 88*(7), 3719-3732. doi:10.1128/JVI.02609-13

Strauss, J. H., & Strauss, E. G. (1994). The alphaviruses: gene expression, replication, and evolution. *Microbiological Reviews, 58*(3), 491-562.

Stros, M. (2010). HMGB proteins: interactions with DNA and chromatin. *Biochim Biophys Acta, 1799*(1-2), 101-113. doi:10.1016/j.bbagrm.2009.09.008

Stros, M., Launholt, D., & Grasser, K. D. (2007). The HMG-box: a versatile protein domain occurring in a wide variety of DNA-binding proteins. *Cell Mol Life Sci, 64*(19-20), 2590-2606. doi:10.1007/s00018-007-7162-3

Strüßmann, T., Tillmann, S., Wirtz, T., Bucala, R., von Hundelshausen, P., & Bernhagen, J. (2013). Platelets are a previously unrecognised source of MIF. *Thromb Haemost, 110*(11), 1004-1013. doi:10.1160/TH13-01-0049

Suhrbier, A., Jaffar-Bandjee, M. C., & Gasque, P. (2012). Arthritogenic alphaviruses--an overview. *Nature reviews. Rheumatology, 8*(7), 420-429. doi:10.1038/nrrheum.2012.64

Suhrbier, A., & La Linn, M. (2004). Clinical and pathologic aspects of arthritis due to Ross River virus and other alphaviruses. *Curr Opin Rheumatol, 16*(4), 374-379.

Suhrbier, A., & Mahalingam, S. (2009). The immunobiology of viral arthritides. *Pharmacol Ther, 124*(3), 301-308. doi:10.1016/j.pharmthera.2009.09.005

Sun, J., Xu, Y., Dai, Z., & Sun, Y. (2009). Intermittent high glucose stimulate MCP-l, IL-18, and PAI-1, but inhibit adiponectin expression and secretion in adipocytes dependent of ROS. *Cell Biochemistry and Biophysics, 55*(3), 173-180. doi:10.1007/s12013-009-9066-3

Tamaoki, J., Kadota, J., & Takizawa, H. (2004). Clinical implications of the immunomodulatory effects of macrolides. *The American Journal of Medicine Supplements, 117*(9, Supplement 1), 5-11. doi:http://dx.doi.org/10.1016/j.amjmed.2004.07.023

Tang, D., Kang, R., Xiao, W., Zhang, H., Lotze, M. T., Wang, H., & Xiao, X. (2009). Quercetin prevents LPS-induced high-mobility group box 1 release and proinflammatory function. *Am J Respir Cell Mol Biol, 41*(6), 651-660. doi:10.1165/rcmb.2008-0119OC

Taniguchi, N., Kawahara, K., Yone, K., Hashiguchi, T., Yamakuchi, M., Goto, M., . . . Maruyama, I. (2003). High mobility group box chromosomal protein 1 plays a role in the pathogenesis of rheumatoid arthritis as a novel cytokine. *Arthritis Rheum, 48*(4), 971-981. doi:10.1002/art.10859

Tarkowski, A. (2006). Infectious arthritis. *Best Practice & Research Clinical Rheumatology, 20*(6), 1029-1044. doi:http://dx.doi.org/10.1016/j.berh.2006.08.001

Tarner, I. H., Muller-Ladner, U., & Gay, S. (2007). Emerging targets of biologic therapies for rheumatoid arthritis. *Nat Clin Pract Rheumatol, 3*(6), 336-345. doi:10.1038/ncprheum0506

Taylor, A., Herrero, L. J., Rudd, P. A., & Mahalingam, S. (2014). Mouse models of alphavirus-induced inflammatory disease. *Journal of General Virology*. doi:10.1099/vir.0.071282-0

Taylor, A., Sheng, K.-C., Herrero, L. J., Chen, W., Rulli, N. E., & Mahalingam, S. (2013). Methotrexate Treatment Causes Early Onset of Disease in a Mouse Model of Ross River Virus-Induced Inflammatory Disease through Increased Monocyte Production. *PLoS ONE, 8*(8), e71146. doi:10.1371/journal.pone.0071146

Tkalcevic, V. I., Bosnjak, B., Pasalic, I., Hrvacic, B., Situm, K., Kramaric, M. D., . . . Erakovic Haber, V. (2008). The anti-inflammatory activity of clarithromycin inhibits TNFalpha production and prolongs survival following lipopolysaccharide administration in mice. *Int J Antimicrob Agents, 32*(2), 195-196. doi:10.1016/j.ijantimicag.2008.03.016

Toda, K., Kumagai, N., Kaneko, F., Tsunematsu, S., Tsuchimoto, K., Saito, H., & Hibi, T. (2009). Pentoxifylline prevents pig serum-induced rat liver fibrosis by inhibiting interleukin-6 production. *Journal of Gastroenterology and Hepatology, 24*(5), 860-865. doi:10.1111/j.1440-1746.2008.05749.x

Tone, M., Thompson, S. A., Tone, Y., Fairchild, P. J., & Waldmann, H. (1997). Regulation of IL-18 (IFN-gamma-inducing factor) gene expression. *J Immunol, 159*(12), 6156-6163.

Tong, Z., Dai, H., Chen, B., Abdoh, Z., Guzman, J., & Costabel, U. (2003). Inhibition of cytokine release from alveolar macrophages in pulmonary sarcoidosis by pentoxifylline: comparison with dexamethasone. *Chest, 124*(4), 1526-1532.

Trinchieri, G. (1997). Cytokines acting on or secreted by macrophages during intracellular infection (IL-10, IL-12, IFN-gamma). *Curr Opin Immunol, 9*(1), 17-23.

Tsetsarkin, K. A., Vanlandingham, D. L., McGee, C. E., & Higgs, S. (2007). A single mutation in chikungunya virus affects vector specificity and epidemic potential. *PLoS Pathog, 3*(12), e201. doi:10.1371/journal.ppat.0030201

Ueki, Y., Miyake, S., Tominaga, Y., & Eguchi, K. (1996). Increased nitric oxide levels in patients with rheumatoid arthritis. *J Rheumatol, 23*(2), 230-236.

Ulloa, L., Batliwalla, F. M., Andersson, U., Gregersen, P. K., & Tracey, K. J. (2003). High mobility group box chromosomal protein 1 as a nuclear protein, cytokine, and potential therapeutic target in arthritis. *Arthritis Rheum, 48*(4), 876-881. doi:10.1002/art.10854

Ulloa, L., Ochani, M., Yang, H., Tanovic, M., Halperin, D., Yang, R., . . . Tracey, K. J. (2002). Ethyl pyruvate prevents lethality in mice with established lethal sepsis and systemic inflammation. *Proc Natl Acad Sci U S A, 99*(19), 12351-12356. doi:10.1073/pnas.192222999

Urasaki, Y., Nori, M., Iwata, S., Sasaki, T., Hosono, O., Kawasaki, H., . . . Morimoto, C. (2005). Roxithromycin specifically inhibits development of collagen induced arthritis and production of proinflammatory cytokines by human T cells and macrophages. *J Rheumatol, 32*(9), 1765-1774.

van Dartel, S. A., Fransen, J., Kievit, W., Flendrie, M., den Broeder, A. A., Visser, H., . . . van Riel, P. L. (2012). Difference in the risk of serious infections in patients with rheumatoid arthritis treated with adalimumab, infliximab and etanercept: results from the Dutch Rheumatoid Arthritis Monitoring (DREAM) registry. *Annals of the rheumatic diseases*, annrheumdis-2012-201338.

van den Hurk, A. F., Hall-Mendelin, S., Pyke, A. T., Smith, G. A., & Mackenzie, J. S. (2009). Vector Competence of Australian Mosquitoes for Chikungunya Virus. *Vector-Borne and Zoonotic Diseases, 10*(5), 489-495. doi:10.1089/vbz.2009.0106

Viennet, E., Knope, K., Faddy, H. M., Williams, C. R., & Harley, D. (2013). Assessing the threat of chikungunya virus emergence in Australia. *Commun Dis Intell Q Rep, 37*(2), E136-143.

Vitali, R., Palone, F., Cucchiara, S., Negroni, A., Cavone, L., Costanzo, M., . . . Stronati, L. (2013). Dipotassium Glycyrrhizate Inhibits HMGB1-Dependent Inflammation and Ameliorates Colitis in Mice. *PLoS ONE, 8*(6), e66527. doi:10.1371/journal.pone.0066527

von Martius, S., Hammer, K. A., & Locher, C. (2012). Chemical characteristics and antimicrobial effects of some Eucalyptus kinos. *Journal of Ethnopharmacology, 144*(2), 293-299. doi:http://dx.doi.org/10.1016/j.jep.2012.09.011

Waage, A., Sorensen, M., & Storrdal, B. (1990). Differential effect of oxpentifylline on tumour necrosis factor and interleukin-6 production. *The Lancet, 335*(8688), 543. doi:http://dx.doi.org/10.1016/0140-6736(90)90779-5

Wadsworth, T. L., & Koop, D. R. (1999). Effects of the wine polyphenolics quercetin and resveratrol on pro-inflammatory cytokine expression in RAW 264.7 macrophages. *Biochem Pharmacol, 57*(8), 941-949.

Wahlfors, J. J., Zullo, S. A., Loimas, S., Nelson, D. M., & Morgan, R. A. (2000). Evaluation of recombinant alphaviruses as vectors in gene therapy. *Gene Ther, 7*(6), 472-480. doi:10.1038/sj.gt.3301122

Walzl, G., Matthews, S., Kendall, S., Gutierrez-Ramos, J. C., Coyle, A. J., Openshaw, P. J. M., & Hussell, T. (2001). Inhibition of T1/St2 during Respiratory Syncytial Virus Infection Prevents T Helper Cell Type 2 (Th2)-but Not Th1-Driven Immunopathology. *The Journal of Experimental Medicine, 193*(7), 785-792. doi:10.1084/jem.193.7.785

Wang, H., Bloom, O., Zhang, M., Vishnubhakat, J. M., Ombrellino, M., Che, J., . . . Tracey, K. J. (1999). HMG-1 as a late mediator of endotoxin lethality in mice. *Science, 285*(5425), 248-251. doi:7585 [pii]

Wang, H., Liao, H., Ochani, M., Justiniani, M., Lin, X., Yang, L., . . . Ulloa, L. (2004). Cholinergic agonists inhibit HMGB1 release and improve survival in experimental sepsis. *Nat Med, 10*(11), 1216-1221. doi:10.1038/nm1124

Wang, H., Ward, M. F., Fan, X. G., Sama, A. E., & Li, W. (2006). Potential role of high mobility group box 1 in viral infectious diseases. *Viral Immunol, 19*(1), 3-9. doi:10.1089/vim.2006.19.3

Wang, H., Ward, M. F., & Sama, A. E. (2009). Novel HMGB1-inhibiting therapeutic agents for experimental sepsis. *Shock, 32*(4), 348-357. doi:10.1097/SHK.0b013e3181a551bd

Wang, H., Xu, T., & Lewin, M. R. (2009). Future possibilities for the treatment of septic shock with herbal components. *Am J Emerg Med, 27*(1), 107-112. doi:10.1016/j.ajem.2008.08.003

Wang, H., Zhu, S., Zhou, R., Li, W., & Sama, A. E. (2008). Therapeutic potential of HMGB1-targeting agents in sepsis. *Expert Rev Mol Med, 10*, e32. doi:10.1017/S1462399408000884

Wang, J. (2009). SM905, an artemisinin derivative, inhibited NO and pro-inflammatory cytokine production by suppressing MAPK and NF-κB pathways in RAW 264.7 macrophages. *Acta pharmacologica Sinica (monthly), 30*(10), 1428.

Wang, Q., Ding, Q., Zhou, Y., Gou, X., Hou, L., Chen, S., . . . Xiong, L. (2009). Ethyl pyruvate attenuates spinal cord ischemic injury with a wide therapeutic window through inhibiting high-mobility group box 1 release in rabbits. *Anesthesiology, 110*(6), 1279-1286. doi:10.1097/ALN.0b013e3181a160d6

Wang, W., Vernon, P., Li, G., Sampath, P., Stephen, T., Liang, X., & Lotze, M. (2014). Depletion of high mobility group box 1(HMGB1) in dendritic cells (DCs) suppresses tumorigenesis and promotes viral clearance. *Journal for Immunotherapy of Cancer, 2*(Suppl 3), P64. doi:10.1186/2051-1426-2-s3-p64

Way, S. J., Lidbury, B. A., & Banyer, J. L. (2002). Persistent Ross River virus infection of murine macrophages: an in vitro model for the study of viral

relapse and immune modulation during long-term infection. *Virology, 301*(2), 281-292. doi:S0042682202915874 [pii]

Wesselingh, S. L., Levine, B., Fox, R. J., Choi, S., & Griffin, D. E. (1994). Intracerebral cytokine mRNA expression during fatal and nonfatal alphavirus encephalitis suggests a predominant type 2 T cell response. *J Immunol, 152*(3), 1289-1297.

Williams, C. R. (2012). The Asian Tiger Mosquito (Aedes Albopictus) Invasion into Australia: A Review of Likely Geographic Range and Changes to Vector-Borne Disease Risk. *Transactions of the Royal Society of South Australia, 136*(2), 128-136. doi:10.1080/03721426.2012.10887167

Williams, G., Brown, T., Becker, L., Prager, M., & Giroir, B. P. (1994). Cytokine-induced expression of nitric oxide synthase in C2C12 skeletal muscle myocytes. *Am J Physiol, 267*(4 Pt 2), R1020-1025.

Woodruff, R., & Bambrick, H. (2008). Climate change impacts on the burden of Ross River virus.

Wressnigg, N., van der Velden, M. V., Portsmouth, D., Draxler, W., O'Rourke, M., Richmond, P., . . . Aichinger, G. (2014). An inactivated Ross River Virus vaccine is well-tolerated and immunogenic in an adult population: a randomized phase 3 trial. *Clin Vaccine Immunol*. doi:10.1128/CVI.00546-14

Wu, C., He, L., Guo, H., Tian, X., Liu, Q., & Sun, H. (2014). Inhibition Effect of Glycyrrhizin in Lipopolysaccharide Induced HMGB1 Releasing and Expression from RAW264.7 Cells. *Shock, Publish Ahead of Print*. doi:10.1097/SHK.0000000000000309

Xiao, X., Yang, M., Sun, D., & Sun, S. (2012). Curcumin protects against sepsis-induced acute lung injury in rats. *J Surg Res, 176*(1), e31-39. doi:10.1016/j.jss.2011.11.1032

Xie, X. H., Zang, N., Li, S. M., Wang, L. J., Deng, Y., He, Y., . . . Liu, E. M. (2012). Resveratrol Inhibits respiratory syncytial virus-induced IL-6 production, decreases viral replication, and downregulates TRIF expression in airway epithelial cells. *Inflammation, 35*(4), 1392-1401. doi:10.1007/s10753-012-9452-7

Xu, D., Jiang, H. R., Kewin, P., Li, Y., Mu, R., Fraser, A. R., . . . Liew, F. Y. (2008). IL-33 exacerbates antigen-induced arthritis by activating mast cells. *Proc Natl Acad Sci U S A, 105*(31), 10913-10918. doi:10.1073/pnas.0801898105

Xu, L., Li, Y., Sun, H., Zhen, X., Qiao, C., Tian, S., & Hou, T. (2013). Current developments of macrophage migration inhibitory factor (MIF) inhibitors. *Drug Discovery Today, 18*(11–12), 592-600. doi:http://dx.doi.org/10.1016/j.drudis.2012.12.013

Yanai, H., Ban, T., & Taniguchi, T. (2012). High-mobility group box family of proteins: ligand and sensor for innate immunity. *Trends in Immunology, 33*(12), 633-640. doi:10.1016/j.it.2012.10.005

Yanai, H., Ban, T., Wang, Z., Choi, M. K., Kawamura, T., Negishi, H., . . . Taniguchi, T. (2009). HMGB proteins function as universal sentinels for nucleic-acid-mediated innate immune responses. *Nature, 462*(7269), 99-103. doi:10.1038/nature08512

Yang, R., Gallo, D. J., Baust, J. J., Uchiyama, T., Watkins, S. K., Delude, R. L., & Fink, M. P. (2002). Ethyl pyruvate modulates inflammatory gene expression in mice subjected to hemorrhagic shock. *American Journal of Physiology - Gastrointestinal and Liver Physiology, 283*(1), G212-G221.

Yuksel, M., Okajima, K., Uchiba, M., & Okabe, H. (2003). Gabexate mesilate, a synthetic protease inhibitor, inhibits lipopolysaccharide-induced tumor necrosis factor-alpha production by inhibiting activation of both nuclear factor-kappaB and activator protein-1 in human monocytes. *J Pharmacol Exp Ther, 305*(1), 298-305. doi:10.1124/jpet.102.041988

Zaid, A., Rulli, N. E., Rolph, M. S., Suhrbier, A., & Mahalingam, S. (2011). Disease exacerbation by etanercept in a mouse model of alphaviral arthritis and myositis. *Arthritis Rheum, 63*(2), 488-491. doi:10.1002/art.30112

Zapata, J. C., Cox, D., & Salvato, M. S. (2014). The Role of Platelets in the Pathogenesis of Viral Hemorrhagic Fevers. *PLoS neglected tropical diseases, 8*(6), e2858. doi:10.1371/journal.pntd.0002858

Zarogoulidis, P., Papanas, N., Kioumis, I., Chatzaki, E., Maltezos, E., & Zarogoulidis, K. (2012). Macrolides: from in vitro anti-inflammatory and immunomodulatory properties to clinical practice in respiratory diseases. *European Journal of Clinical Pharmacology, 68*(5), 479-503. doi:10.1007/s00228-011-1161-x

Zebisch, K., Voigt, V., Wabitsch, M., & Brandsch, M. (2012). Protocol for effective differentiation of 3T3-L1 cells to adipocytes. *Anal Biochem, 425*(1), 88-90. doi:10.1016/j.ab.2012.03.005

Zhang, Z., Zhang, L., Zhou, C., & Wu, H. (2014). Ketamine inhibits LPS-induced HGMB1 release in vitro and in vivo. *International immunopharmacology, 23*(1), 14-26. doi:10.1016/j.intimp.2014.08.003

Zhang, Z., Zhang, Q. Y., Zhou, M. T., Liu, N. X., Chen, T. K., Zhu, Y. F., & Wu, L. (2009). Antioxidant Inhibits HMGB1 Expression and Reduces Pancreas Injury in Rats with Severe Acute Pancreatitis. *Dig Dis Sci*. doi:10.1007/s10620-009-1073-0

Zhong, M., Cheng, G. F., Wang, W. J., Guo, Y., Zhu, X. Y., & Zhang, J. T. (1999). Inhibitory effect of resveratrol on interleukin 6 release by stimulated peritoneal macrophages of mice. *Phytomedicine, 6*(2), 79-84. doi:http://dx.doi.org/10.1016/S0944-7113(99)80039-7